

**A 2D Finite Volume Model for Groundwater Flow  
Simulations: Integrating Non-Orthogonal Grid  
Capability into MODFLOW**

**Dalila Loudyi**

Thesis submitted for the degree of  
Doctor of Philosophy

Division of Civil Engineering, Cardiff School of Engineering  
Cardiff University

May 2005

UMI Number: U584707

All rights reserved

INFORMATION TO ALL USERS

The quality of this reproduction is dependent upon the quality of the copy submitted.

In the unlikely event that the author did not send a complete manuscript and there are missing pages, these will be noted. Also, if material had to be removed, a note will indicate the deletion.



UMI U584707

Published by ProQuest LLC 2013. Copyright in the Dissertation held by the Author.  
Microform Edition © ProQuest LLC.

All rights reserved. This work is protected against  
unauthorized copying under Title 17, United States Code.



ProQuest LLC  
789 East Eisenhower Parkway  
P.O. Box 1346  
Ann Arbor, MI 48106-1346

## DECLARATION

This work has not previously been accepted in substance for any degree and is not concurrently being submitted in candidature for any degree.

Signed



(Dalila Loudyi)

Date

06/05/2005

## STATEMENT 1

This thesis is the result of my own investigations, except where otherwise stated. Other sources are acknowledged by footnotes giving explicit references. A bibliography is appended.

Signed



(Dalila Loudyi)

Date

06/05/2005

## STATEMENT 2

I hereby give consent for my thesis, if accepted to be available for photocopying and for interlibrary loan, and for the title and summary to be made available to outside organisations.

Signed



(Dalila Loudyi)

Date

06/05/2005

# Abstract

The modular finite-difference groundwater flow model MODFLOW is one of the most widely used groundwater modelling programs, and is applicable to most types of flow problems in its field. However, its finite difference formulation decreases its ability to simulate accurately natural aquifer geometries. To enhance its capability in simulating such boundaries, a finite volume scheme has been developed for inclusion in MODFLOW.

In this study, the two-dimensional formulation has been considered. Three discretisations of the two-dimensional diffusion equation, governing groundwater flow and for use with structured quadrilateral meshes, have been developed. The three methods rely on a cell-centred finite volume approach, but show distinct differences in the choice of: gradient approximation, head interpolations and control volume. A time implicit formulation has been used in each model. The sparse system of linear equations that result from the implicit formulation has been solved by using an iterative solver, based on the strongly implicit procedure. Five test examples have been undertaken to compare the performance of the newly developed methods against MODFLOW predictions and analytical results. The accuracy of the results obtained was found to depend on the spatial and temporal discretisations. One of the three developed methods proved its robustness, with regard to mesh non-orthogonality and skewness, and was called the GWFV method. In a second step of studies, a field case study was used to test the preferred model. A mesh generator using a structured quadrilateral grid was used to produce the finite volume mesh of the simulated area. The results of MODFLOW and the GWFV model simulations were compared against field observations. A discussion about the performance of the new developed model has been included and the model has been shown to perform well in comparison with MODFLOW.

**Keywords:** numerical models, finite volume discretisations, groundwater flow models, MODFLOW, non-orthogonal grid.

# Acknowledgements

I would like to express my sincere gratitude to my supervisors, Prof. Roger A. Falconer and Dr. Binliang Lin for their continuous interest, support and guidance during this study.

I am also indebted to my friends in the Hydroenvironmental Research Centre, particularly to Dr. Catherine Wilson and Dr. Bettina Bockelmann for the arrangement of many technical matters and continuous support.

I would like to thank all my teachers, present and past, for instilling the proper knowledge in me, which has enabled me to pursue this path.

Finally, I owe a great deal to my family for their encouragement and support, which has made it all possible.

*Dedicated to my Father*

# Contents

<b>Abstract</b>	<b>i</b>
<b>Acknowledgments</b>	<b>ii</b>
<b>Dedication</b>	<b>iii</b>
<b>Contents</b>	<b>iv</b>
<b>List of Figures</b>	<b>x</b>
<b>List of Tables</b>	<b>xiv</b>
<b>1 Introduction</b>	<b>1</b>
1.1 Background .....	1
1.2 Aims of the Study .....	2
1.3 Outline of the Thesis .....	3
<b>2 Review of Groundwater Modelling Methods</b>	<b>5</b>
2.1 Groundwater Models .....	5
2.1.1 Physical Models .....	5
2.1.2 Mathematical Models .....	9
2.1.2.1 Analytical Models .....	9
2.1.2.2 Numerical Models .....	10
2.1.2.3 Stochastic Models .....	10
2.1.2.4 Assumptions .....	11
2.2 Model Development Procedures .....	13

---

2.2.1 Code Development Procedure .....	13
2.2.1.1 Code Objectives .....	14
2.2.1.2 Mathematical Model .....	14
2.2.1.3 Solution Technique .....	15
2.2.1.4 Code Testing .....	15
2.2.1.5 Code Reporting .....	15
2.2.2 Model Application Procedure .....	16
2.2.2.1 Model Objectives .....	16
2.2.2.2 Data Analysis .....	17
2.2.2.3 Conceptual Model .....	17
2.2.2.4 Code Selection .....	19
2.2.2.5 Calibration and Sensitivity Analysis .....	19
2.2.2.6 Model Validation .....	19
2.2.2.7 Predictive Runs .....	21
2.2.2.8 Uncertainty Analysis .....	21
2.3 Mathematical Statement of Groundwater Flow .....	22
2.3.1 Governing Equations .....	22
2.3.1.1 The Fluid .....	22
2.3.1.2 The Aquifer .....	24
2.3.1.3 Mass Conservation Equation .....	25
2.3.1.4 Darcy's Law .....	26
2.3.1.5 Groundwater Flow Equation .....	27
2.3.1.6 External Sources .....	30
2.3.2 Boundary and Initial Conditions .....	31
2.4 Review of Analytical Solutions and Limits .....	32
2.4.1 Existing Analytical Solutions .....	32
2.4.2 Limits .....	39
2.4.3 Analytic Element Methods .....	39
2.5 Review of Numerical Methods and Limits .....	41
2.5.1 Existing Numerical Techniques .....	42
2.5.1.1 Finite Difference Method .....	43
2.5.1.2 Finite Element Method .....	44

---

2.5.1.3	Integrated Finite Difference Method .....	45
2.5.1.4	Boundary Element Method .....	46
2.5.1.5	Finite Volume Method .....	47
2.5.1.6	Time Stepping .....	47
2.5.1.7	Matrix Solvers .....	48
2.5.2	Comparison and Discussion .....	50
2.5.3	Limits .....	51
2.6	Existing Codes and Limitations .....	53
2.6.1	Existing Codes .....	53
2.6.2	Accuracy of Numerical Models .....	56
2.6.3	Codes Limitations .....	57
2.7	Conclusions and Relevance to Present Research .....	58
<b>3</b>	<b>Review of MODFLOW</b> .....	<b>59</b>
3.1	Introduction .....	59
3.2	MODFLOW Description .....	59
3.2.1	Development History .....	59
3.2.2	MODFLOW Mathematical Model .....	62
3.2.2.1	Assumptions, Equation and Boundary Conditions .....	62
3.2.2.2	Spatial and Temporal Discretisation .....	63
3.2.3	MODFLOW Solution Technique .....	63
3.2.4	Code Design .....	64
3.2.5	Code Usability .....	67
3.2.5.1	Data Requirement – Input .....	67
3.2.5.2	Code Output .....	70
3.2.5.3	Pre-Processing and Post-Processing Facilities .....	70
3.2.6	Related Programs .....	71
3.2.7	Source Code Availability and Cost .....	72
3.2.8	Hardware and Software Requirements .....	72
3.2.9	MODFLOW Capabilities and Maintenance .....	73

---

3.2.10 MODFLOW Applications .....	74
3.2.11 MODFLOW Testing and Reporting: Quality Assurance .....	75
3.2.12 History of Use and References .....	75
3.3 MODFLOW Limitations .....	76
3.4 MODFLOW Critics and Improvements .....	78
3.4.1 MODFLOW Popularity .....	78
3.4.2 MODFLOW Accuracy .....	79
3.4.3 Finite Volume and MODFLOW .....	82
<b>4 Finite Volume Discretisation</b> .....	<b>83</b>
4.1 Introduction .....	83
4.2 Finite Volume Method .....	83
4.3 Finite Volume Discretisations of Groundwater Flow Equation .....	85
4.3.1 Diffusion term .....	88
4.3.1.1 Gradient Approximation on a Control Volume Face: Review .....	88
4.3.1.2 Approximating the Permeability on a Control Volume Face .....	104
4.3.2 Implementation of Boundary Conditions .....	107
4.3.3 Source Term .....	108
4.3.4 Transient Term – Temporal Discretisation .....	108
4.4 Formulation of Linear Equations .....	109
4.5 Matrix Properties and Solution Method .....	111
4.5.1 Matrix Properties .....	111
4.5.2 Solution Technique .....	112
4.6 Accuracy Issues of the Selected Scheme .....	114
4.6.1 Numerical Errors in the Discretisation Procedure .....	114
4.6.1.1 Numerical Diffusion from Temporal Discretisation .....	114
4.6.1.2 Mesh-Induced Errors .....	116
4.6.2 Error Estimation .....	117
4.6.3 Accuracy Analysis .....	118

---

<b>5 Numerical Tests</b>	<b>120</b>
5.1 Introduction .....	120
5.2 Model Testing and Evaluation .....	121
5.2.1 Numerical Tests Selection .....	121
5.2.2 Evaluation Methods .....	121
5.3 Numerical Tests .....	122
5.3.1 Test 1: Accuracy .....	122
5.3.2 Test 2 : Numerical Error – Sensitivity to Mesh Size .....	128
5.3.3 Test 3: Grid Shape Effect: Non-orthogonality and Skewness .....	132
5.3.4 Test 4: Accuracy at Irregular Boundaries .....	135
5.3.5 Test 5: Permeability - Heterogeneity .....	137
5.4 Discussion .....	140
5.5 Finite Volume- Based Changes in MODFLOW .....	141
<b>6 A Field Application: Case Study</b>	<b>142</b>
6.1 Introduction .....	142
6.2 Site Presentation .....	143
6.2.1 Land Description .....	143
6.2.2 Site Geology .....	145
6.2.3 Site Hydrogeology .....	147
6.3 Data Availability and Site Investigation .....	147
6.4 MODFLOW Three-Dimensional Simulations .....	149
6.4.1 Model Domain and Boundaries .....	149
6.4.1.1 Northern and Eastern Boundaries .....	150
6.4.1.2 Swansea Canal .....	151
6.4.1.2 Western and Southern Boundaries .....	151
6.4.1.4 Tawe River .....	152
6.4.1.5 General Head Boundaries .....	152
6.4.1.6 Constant Head Boundaries .....	153
6.4.1.7 Recharge Data .....	153
6.4.2 Model Calibration .....	155
6.4.2.1 Calibration Programme .....	155

---

6.4.2.2 Calibration Results for Steady State Simulations .....	155
6.4.2.3 Calibration Results for Transient State Simulations .....	158
6.4.2.4 Calibrated Conceptual Model .....	161
6.4.3 Sensitivity Analysis .....	162
6.5 MODFLOW Two-Dimensional Simulation .....	165
6.6 GWFV Two-Dimensional Simulation .....	169
6.6.1 Discretisation .....	169
6.6.2 Data Generation .....	169
6.6.3 Program Runs .....	169
6.7 Comparisons and Discussion .....	170
6.8 Conclusion .....	172
<b>7 Conclusions and Recommendations</b> .....	<b>175</b>
7.1 Review and Conclusions .....	175
7.2 Recommendations for Further Work .....	177
7.2.1 Two-Dimensional Finite Volume Extension to Other Processes .....	177
7.2.2 Extension to 3-D and Implementation in MODFLOW Recommendations .....	178
7.2.2.1 Three-Dimensional Finite Volume Discretisation .....	178
7.2.2.2 Implementation in MODFLOW .....	179
7.2.2.3 Three-Dimensional Finite Volume Model Testing .....	180
<b>Appendices</b> .....	<b>182</b>
<b>Bibliography</b> .....	<b>207</b>

# List of Figures

Figure 2.1	Model code development process .....	14
Figure 2.2	Model application process .....	16
Figure 2.3	Schematic approach to the construction of a conceptual groundwater model .....	18
Figure 2.4	Mass conservation for a control volume .....	25
Figure 2.5	A one-dimensional hypothetical flow problem .....	36
Figure 2.6	Mathematical model of the regional flow system described by Toth (1962) .....	36
Figure 2.7	Finite difference grid conventions in two dimensions .....	44
Figure 2.8	Example of finite element grid in two dimensions .....	45
Figure 2.9	Example of integrated finite difference element grid in two dimensions .....	46
Figure 2.10	Example of a boundary element discretisation .....	47
Figure 3.1	Discretisation convention in MODFLOW .....	63
Figure 3.2	Flowchart of MODFLOW-2000 four processes: Global (GLO), Ground-Water Flow (GWF), Observation (OBS), Sensitivity (SEN), and Parameter Estimation (PES) .....	68
Figure 4.1	Different two-dimensional finite volume mesh concepts: (a) cell-structured FV; (b) cell-unstructured FV mesh; (c) cell-centred FV mesh; (d) cell- vertex FV mesh .....	84
Figure 4.2	Space discretisation convention in MODFLOW and its equivalent finite volume discretisation .....	86
Figure 4.3	A quadrilateral cell with normal surface vectors .....	87
Figure 4.4	Two adjacent orthogonal control volumes in finite difference method .....	89

Figure 4.5	Secondary mesh and related element used in finite element method .....	90
Figure 4.6	Quadrilateral element in physical space .....	90
Figure 4.7	Non-orthogonal control volumes .....	93
Figure 4.8	Skewness correction through surface $S_{AP}$ for non-orthogonal mesh .....	95
Figure 4.9	Representative control-volume face .....	96
Figure 4.10	Neighbouring nodes involved in surface flux calculation .....	99
Figure 4.11	Auxiliary cell used to calculate diffusive balance in model V .....	100
Figure 4.12	Staggered grid for face $AB$ in model S .....	101
Figure 4.13	Volumes used in head interpolation at vertex $B$ .....	102
Figure 4.14	Geometrical weight factors for permeability interpolation in MODFLOW .....	105
Figure 4.15	Typical boundary control volume and related point values .....	108
Figure 4.16	A nine-node stencil reduced to five-node stencil .....	110
Figure 4.17	Estimation of a function at one corner of a quadrilateral in terms of the function values at remaining corners .....	110
Figure 5.1	A $41 \times 41$ random quadrilateral mesh used with the three models ...	123
Figure 5.2	Head contours obtained using: (a) analytical solution; (b) MODFLOW; (c) model GWFV; (d) model S; (e) model V.....	124
Figure 5.3	Variation of drawdown with time at different distances in Test 1 .....	126
Figure 5.4	Plot of drawdown values versus time for the well test, computed by MODFLOW for different time steps using various matrix solvers at a distance of 1000 m from the pumping well : (a) SIP solver, (b) PCG solver, (c) SOR solver , (d) WHS solver .....	127
Figure 5.5	Error on the overall test area versus number of time steps in each stress period for the four solvers .....	128
Figure 5.6	Example 1: Random grids, (a): $5 \times 5$ ; (b): $10 \times 10$ ; (c): $20 \times 20$ ; (d): $40 \times 40$ ; and (e): $80 \times 80$ .....	130
Figure 5.7	The $10 \times 10$ Kershaw mesh .....	132
Figure 5.8	Isolines on the $10 \times 10$ Kershaw mesh for the four models .....	133
Figure 5.9	The $20 \times 20$ Kershaw grid, (a) The mesh; (b), (c) and (d) Isolines resulting from the three new models .....	134

Figure 5.10	The aquifer and grid used in Test 2 .....	135
Figure 5.11	The aquifer mesh in test 4: (a) orthogonal mesh; (b) non-orthogonal mesh .....	136
Figure 5.12	Head isolines for Test 4 from application of (a) MODFLOW, (b) GWFFV, (c) model S, (d) model V .....	137
Figure 5.13	Drawdown for test 4 from application of (a) MODFLOW, (b) GWFFV, (c) model S, (d) model V on non-orthogonal grid .....	139
Figure 6.1	Site location plan (courtesy of ExCal Ltd) . .....	144
Figure 6.2	Site geological map (courtesy of ExCal Ltd.) .....	146
Figure 6.3	Borehole and trial pit locations (courtesy of ExCal Ltd.).....	148
Figure 6.4	Plan view of the model and boundary conditions .....	150
Figure 6.5	Three-dimensional view of the final model input .....	151
Figure 6.6	River stage upstream river Tawe in year 2000 .....	152
Figure 6.7	Monthly rainfall in mm/year in 2000 .....	154
Figure 6.8	Recharge model zones distribution .....	154
Figure 6.9	Locations of observation boreholes used for model calibration .....	155
Figure 6.10	Steady state calibration results: (a) Statistical measure of Predictions, and (b) calibration residuals histogram .....	157
Figure 6.11	Predicted steady state groundwater levels (equipotentials at 0.5 m intervals) .....	158
Figure 6.12	Observed and predicted groundwater levels for transient simulation at different boreholes .....	159
Figure 6.13	Calibrated model permeability distribution in layer 2 .....	161
Figure 6.14	Increasing flow velocities toward the river .....	164
Figure 6.15	Flow direction in the fourth layer in the three-dimensional 100 × 100 MODFLOW simulation in vertical cut along row 50 ....	166
Figure 6.16	Recharge input for two-dimensional simulation of MODFLOW ....	167
Figure 6.17	Predicted hydraulic heads from the 2D steady state MODFLOW simulation on the 100 × 100 mesh (equipotentials at 0.5 m intervals) .....	167
Figure 6.18	Calibration of the two-dimensional MODFLOW simulation: (a) error for the overall observation boreholes, (b) error for the river observation boreholes .....	168
Figure 6.19	The non-orthogonal 50 × 50 mesh .....	169

---

Figure 6.20	Head results from MODFLOW (50 × 50 mesh).....	172
Figure 6.21	Head results from GWFV on non-orthogonal grid (50 × 50 mesh) .....	172
Figure 6.22	Comparison of head results from MODFLOW and the GWFV model for non-orthogonal with observed heads, for different observations well groups .....	173
Figure 6.23	Steady state calculated vs. observed heads on 35 observation boreholes .....	174

## List of Tables

Table 2.1	Analogy between groundwater processes and other processes (Spitz and Moreno, 1996, p. 17) .....	7
Table 2.2	Applicability of models and analogs (after Bear 1972) .....	7
Table 2.3	Code selection criteria for groundwater flow modelling .....	20
Table 2.4	Main processes in groundwater modelling (USEPA, 1993) .....	29
Table 3.1	A summary of MODFLOW versions history from 12/1983 to 04/2005 .....	60
Table 3.2	MODFLOW packages versus versions .....	66
Table 3.3	Organisation of modules by processes, packages and procedures ....	69
Table 3.4	Packages interconnection and process-independent packages (MODFLOW-2000 1.15.01) .....	69
Table 5.1	Test2: Errors on random grids .....	131
Table 6.1	Steady state water balance .....	156
Table 6.2	Root mean squared error for sensitivity runs .....	163
Table 6.3	Root mean squared error results comparison .....	170

# Chapter 1

## Introduction

### 1.1 Background

The amount of water available on earth is as important as its quality. In recent years, both the quantity and quality of water have been known to change dramatically. Increasing water demand and intensification of industry, agriculture and urban activities are the main anthropogenic factors of this degradation. Statistics show that groundwater, in particular, is the main source of drinking water in poor countries and the most at risk resource in industrialised countries. A necessary step into the management of this precious resource is an understanding of the behaviour of groundwater systems. Therefore, hydrologists are often called upon to predict groundwater flow in a range of scenarios related to this resource. So far, this task has essentially been fulfilled by using a groundwater model. Researchers have developed basically two kinds of models: physical and mathematical models. Among the later, numerical models have become the most widely used due to the increasing development and availability of high-performance computers. These models solve the governing equations of the groundwater processes, as a special case of the mass conservation law systems, and as solved using Computational Fluid Dynamics (CFD) numerical methods. The complexity of practical flow situations has emerged alongside the development of numerous numerical techniques. At an early stage in the history of CFD, the finite difference method dominated the solution procedures, and applications of this method to various types of flow problems were widely developed. In the 80s, the U.S. Geological Survey developed a three-dimensional

(3D), finite-difference groundwater flow model, commonly referred to as MODFLOW. Later, this programme became one of the most popular models used by government agencies and consulting firms for groundwater flow applications worldwide. One of the reasons for its success was the use of the relatively straightforward finite difference method to solve the groundwater flow equation. As a matter of fact, this technique presented user-wise advantages of ease of meshing the domain and solving in a straightforward manner the resulting system of discretised equations. This numerical method is known to have many strengths, but has the shortcoming of its rigidity in conforming to boundary geometries, doubled by a loss of accuracy in predicting hydraulic heads along and near these boundaries (USEPA, 1994, Anderson and Woessner, 1992, p. 21).

## **1.2 Aims of the Study**

The main aim of this study has therefore been to include the finite volume method in MODFLOW using a boundary-fitted computational grid that will enhance the model flexibility in representing complex boundary geometries and improve the accuracy of results based on the premise that the finite volume method has the inherent advantage of being unconditionally mass conservative. However, it was also desirable to introduce the minimum number of changes that would affect users familiarity with this widely used model. The principal changes were relevant to recent versions of MODFLOW and recent design changes. The new MODFLOW-2000 structure was oriented towards accommodating the solutions of the new equations, such as transport or parameter estimation. This new design concept provides another valuable basis to modify MODFLOW with the aim being to implement the changes as additional options for solving the flow equation by the finite volume technique.

Numerous solutions have been obtained for CFD equations using a variety of finite volume methods. However, a judicious choice of the appropriate finite volume discretisation approach for the groundwater flow equation used in MODFLOW has been considered where the main aim has been to minimise the changes required to the code.

The merits of the selected finite volume model have been assessed with respect to its potential impact on the accuracy and code additional change requirements. Thus, another goal of the present work has been to test and evaluate the new developed code by running a suite of test cases, including results generated by analytical solutions and/or by MODFLOW. The main feature of the new programme is its use of an irregular mesh, with this study giving an insight into the strengths and weaknesses of this particular feature. A field case study was also desirable as an efficient opportunity to assess the performance of MODFLOW and the newly developed model. Therefore, a suitable field case study for validating the new finite volume approach has also been sought and used.

### **1.3 Outline of the Thesis**

This research study employs one of the recently developed numerical methods, namely the finite volume method, for modelling a specific case of groundwater problems. Therefore in Chapter 2 groundwater model concepts and development procedures are summarised, along with the mathematical description of groundwater problems, including the flow, solute transport, temperature and Darcy equations. A review of existing mathematical models for groundwater flow was then undertaken, particularly with regard to analytical solutions and numerical techniques, wherein a comparison of the strengths and the shortcomings of each approach was undertaken.

As one of the aims of this study was to improve the modelling performance of MODFLOW, Chapter 3 gives a thorough description of this very widely used code, along with a discussion of its shortcomings and potential for improvement. Particular focus was made on the mathematical model of MODFLOW based on the popular finite difference numerical technique.

Within the framework of MODFLOW, the groundwater flow equation has been discretised using the finite volume method in different ways and arising from various options for approximating the hydraulic gradient for a control volume face and manipulating the resulting linear equations. In Chapter 4, these options have been

reviewed, and their merits are assessed with respect to the resulting matrix properties, accuracy and impact on the MODFLOW code.

In Chapter 5, the proposed solution procedures are applied for five selected test cases. The accuracy of the methods has been examined for transient-state two-dimensional (2D) flow to a discharging well using the Theis analytical solution for this problem. The sensitivity of the procedures to the mesh size was also examined. A 2D Kershaw mesh has been selected to examine the effects of the grid non-orthogonality and skewness on the overall performance of these procedures. The accuracy at irregular boundaries has also been examined. Finally, a heterogeneity test has been carried out to check the effectiveness of the selected equivalent permeability formulation. A comparison of the test results for the different selected schemes is provided, with one procedure proving to perform better than the others. A brief description about the implementation of this procedure within MODFLOW is also presented.

The new code has been applied to a field case model for validation purposes in Chapter 6. The observation results have been compared with the new model results and details are provided in this chapter.

Finally, a review of the results obtained from the tests carried out in Chapters 5 and 6 has been outlined in Chapter 7, along with future recommendations for research.

# **Chapter 2**

## **Review of Groundwater Modelling**

### **Methods**

#### **2.1 Groundwater Models**

A model is a tool designed to represent a simplified version of a complex physical process. A groundwater model, if properly constructed, can be a valuable predictive tool for the management of groundwater resources (Anderson and Woessner, 1992). The modelling effort in this sense can have three important objectives:

- predicting the effect of certain actions given the field conditions,
- interpreting system dynamics by gaining insight into controlling parameters and, if data are insufficient, guiding data collection activities,
- generating geological conditions to analyse flow in hypothetical hydrological systems and to formulate regulatory guidelines for a specific region.

Several types of models have been developed to meet these objectives. They can generally be classified into two categories namely physical and mathematical models.

##### **2.1.1 Physical Models**

Physical models are used to understand the flow and transport processes in groundwater by means of experiments. They are more likely to be used to meet the second modelling objective and they include such models as the sand box and analog models.

**The Sand box model** is a reduced scale representation of the natural porous medium domain. The water is induced to flow through a tank filled with an unconsolidated porous medium. This type of model has many applications in groundwater, varying from studying transport phenomena to validating other model results. Oswald and Kinzelbach (2000) used a series of laboratory experiments to study variable-density flow in a saturated porous medium and used their results to verify the reliability of some existing numerical codes. In this sense, laboratory experiments can be performed to obtain data required for the elaboration of benchmarking examples. Sand box models can also be used to study some groundwater phenomena such as the movement of a plume under different field conditions (Hoopes and Harleman, 1967, and Ishaq and Ajward, 1993). They offer a three dimensional representation of groundwater processes, particularly when a two-dimensional flow assumption may induce simulation errors (Turner et al., 1994) or where the assumptions of homogeneity and isotropy rarely, if ever, apply (Simmons et al., 2001). In fact, a sand model is a true model as it involves the real porous medium. However, considerable differences between phenomena measured at the scale of a sand tank model and conditions observed in the field may occur due to the scaling down of a field situation to the dimensions of a laboratory model. Therefore, conclusions drawn from such models should be re-examined when translated to a field situation.

**Analog models** are used to replicate an aquifer system and its behaviour by using a set of partial differential equations. Similarities between these equations and those governing other processes, such as: (i) the flow of an electrical current through a resistive medium, (ii) the flow of a viscous liquid in the narrow space between two parallel planes, or (iii) the flow of heat through a solid, have given rise to analog models. Some of these techniques have been in use since the late 1800s. The physical analogy between these processes is given in Table 2.1 (Spitz and Moreno, 1996, p. 17). Among these types of models the most renowned are: the electrical analog model, the Hele-Shaw analog or parallel-plate model (synonyms to a viscous fluid model), and the membrane analog (Bear, 1972). Applicability of these analogs and other models is shown in Table 2.2. It should be noted that analog models have very restricted applicability regarding the model tasks. These types of physical model are regarded as a simulator of the flow regime in the

Physical Process	Law	Conservation Law	Quantity	Potential	Proportionality Factor
Groundwater Flow	Darcy $q = -K\nabla h$	$\nabla^2 h = 0$	Darcy flux $q$	Potentiometric head $h$	Hydraulic conductivity $K$
Viscous fluid flow	Poiseuille $v = -f_r \nabla h$	$\nabla^2 h = 0$	Velocity $v$	Potentiometric head $h$	Conductivity of fracture $f_r$
Electricity flow	Ohm $I = -\sigma E$	$\nabla^2 E = 0$	Current $I$	Voltage $E$	Electrical conductivity $\sigma$
Heat flow	Fourier $Q_\theta = -\lambda \nabla \theta$	$\nabla^2 \theta = 0$	Heat flow $Q_\theta$	Temperature $\theta$	Thermal conductivity $\lambda$
Force field	Newton $f = m \nabla U$	$\nabla^2 U = 0$	Force $f$	Potential $U$	Mass $m$
Diffusion	Fick $q_c = -D_0 \nabla c$	$\nabla^2 c = 0$	Diffusive flux $q_c$	Concentration $c$	Diffusion coefficient $D_0$
Incompressible flow of a frictionless fluid	$v = -\nabla \phi$	$\nabla^2 \phi = 0$	Velocity $v$	Velocity potential $\phi$	1

Table 2.1 Analogy between groundwater processes and other processes (Spitz and Moreno, 1996, p. 17).

Model Task \ Model Type	Sand Box model	Hele-Shaw analog	Electric analogs		Membrane analogs
			Electrolytic	RC-Network	
<b>DIMENSIONALITY</b>					
two-dimensional	●	●	●	●	●
three-dimensional	●	○	●	●	○
<b>FLOW PROBLEM</b>					
steady	●	●	●	●	●
unsteady	●	●	○	●	○
phreatic	●	●	●	○	○
Leaky formation	●	●	●	●	○
anisotropy	●	●	●	●	●
heterogeneity	●	●	●	●	○
variably saturated	●	●	○	○	○
immiscible fluids	●	○	○	○	○
<b>TRANSPORT PROBLEM</b>					
stream/pathlines	●	●	○	○	○
advection	●	●	○	○	○
dispersion	●	○	○	○	○
sorption	●	○	○	○	○
decay/reactions	●	○	○	○	○
● Yes      ● With certain constraints      ○ No					

Table 2.2 Applicability of models and analogs (after Bear 1972).

aquifer. Each laboratory model or analog is designed to solve a specific problem (Alley and Emery, 1986). It is based on the analogy between a set of mathematical equations that describe the behaviour of the real aquifer system and those describing the behaviour of the physical model. Another approach to model an aquifer system is to solve directly or approach the solution of the mathematical equations that have been stated using a mathematical model (see section 2.1.2).

Other laboratory experiments have been developed for specific applications, such as seepage face and water infiltration (Hall, 1955, and Haverkamp et al., 1977). They are generally used to develop the mathematical formulation to obtain an accurate model representation and to analyse model sensitivity for physical parameters and numerical formulations (Burns, 1983).

*Field experiments* are used for measuring head and/or concentration values through field sampling or monitoring, or for the acquisition of groundwater flow and transport parameters. The most classical investigation methods are pumping tests and borehole geophysics. Other methods, such as cone penetrometers, surface geophysics, and isotopic analysis, are less used due to their relatively high cost. Monitoring wells are used to provide an access point for measuring groundwater levels and access to accurate groundwater point samples. Geologic logging gives valuable information about underlying formations. Transmissivity, hydraulic conductivity, storage coefficients and specific yield are typically obtained using traditional pumping tests (Walton, 1987, Boonstra and Kselik, 2001). Slug tests are used to determine point values for hydraulic conductivity (Bouwer, 1989). Physical parameters of the rock and the fluids contained in that rock can be obtained by mean of geophysical logging techniques (Keys and MacCary, 1971). Effective porosity may be estimated by tracer experiments (De Marsily, 1986). Measuring local groundwater flow or studying the mechanism of a solute transport under natural conditions can also be performed by introducing tracers into the ground (Courtois et al., 2000). It should be noted that the results of many of these tests are obtained by use of mathematical codes (e.g. aquifer test analysis, tracer test analysis). They are often used in analytical or numerical model development processes (e.g. model calibration, validation or benchmarking). Groundwater techniques, such as artificial

recharge, air sparging, are not considered as field experiments and thus will not be addressed in this chapter.

### **2.1.2 Mathematical Models**

These models are based on the fact that the aquifer system and its behaviour are represented in the form of a set of mathematical expressions, such as partial differential equations or linear algebraic equations. Mathematical models of groundwater flow have been in use since the late 1800s. They can broadly be classified as either deterministic or stochastic.

Deterministic methods assume that a system operates such that the occurrence of a given set of events leads to a unique definable outcome, while stochastic methods presuppose that the outcome is uncertain and are designated to account for this uncertainty. Deterministic methods are used more widely than stochastic methods even though there is a growing trend in research towards the development of stochastic methods, as will be discussed later in this section. Using a deterministic approach, the governing equations can be solved either analytically or numerically, depending upon the assumptions made when stating the flow problem in terms of partial differential equations, boundary conditions and initial conditions. These assumptions will subsequently be addressed in more detail.

#### **2.1.2.1 Analytical Models**

When the field situation can be described by a mathematical model under simplified assumptions, the flow equation can be solved analytically. In fact, fairly restrictive simplifications of the real world are required to use classical analytical solutions. However, these types of solutions are generally more efficient than other model types whenever analytical solutions for the investigated groundwater problem exist. A more detailed description of cases when analytical solutions exist is given in the next section.

### 2.1.2.2 Numerical Models

To deal with more realistic field situations, the solution of the constructed mathematical model for a regional flow is usually approximated by the use of numerical techniques. This kind of model has been in continuous development since about the 1960s. They have become the preferred type of model to approach complex groundwater problems, especially with the wide availability of high-speed digital computers. Depending on the numerical techniques employed in solving the governing equations, there exist several types of numerical models, among them: finite-differences, finite elements, boundary elements, analytic elements, integrated finite differences and finite volume models. These schemes approach the solution of partial differential equations by giving values of state variables only at specified points in the space and time domains investigated, rather than provide a continuous function in these domains as is the case for analytical solutions. The partial differential equations representing water balances are replaced by a set of algebraic equations involving discrete values of the state variables at discrete points in space and time. These equations must be solved simultaneously and a computer program is often required. The solution is obtained for a specified set of numerical values of the various model coefficients. Section 2.5 gives more details of the different numerical techniques and their limitations in modelling practice.

### 2.1.2.3 Stochastic Models

In the first two approaches, expected values of hydraulic head or concentrations are considered as deterministic values. However, natural flow and transport systems are rarely described with certainty and predictions always account for risk. Much of the uncertainty associated with modelling is owed to the incomplete knowledge about the values of model coefficients and their spatial (and sometimes temporal) variation, hydrologic stresses, and head and concentration distributions. The stochastic modelling approach is often used to address uncertainty directly by assuming that the flow and transport parameters are random variables (Satish and Zhu, 1992 and 1994, Castelli, 1996, Harter and Yeh, 1998, and Li and Graham, 1998). The mean, variance, and correlation length are used to generate quantitative descriptions of the considered variable

field and results are given in the form of a probability density function (Figueiredo, 2000). Many techniques are used to perform such calculations. Monte Carlo simulation, Gaussian quadrature numerical integration, generalised likelihood uncertainty estimation method, and first-order second-moment analysis are the most widely used techniques in uncertainty analysis in groundwater problems. Recent advances in these models include the use of fuzzy mathematical methods to address the vague nature of uncertainties associated with hydrogeologic parameters (LaRue and Tyagi, 1998, Chen et al., 2003, Guan and Aral, 2004). Another new application in this field is the use of genetic algorithms for estimating groundwater parameters and how to extract information regarding the sensitivity of the model to these parameters (El Harrouni et al., 1996 and Giacobbo et al., 2002). Further research in this field are focusing on how to incorporate these techniques in a numerical model for self calibration (Capilla et al., 1998 and Katsifarakis et al., 1999), or to determine the relationship between random variables and deterministic parameters via a sensitivity analysis (Gau and Liu, 2000). Its feasibility could also be investigated in the framework of an expert system for groundwater model development, or selection, as the applicability of a numerical model is most commonly limited by uncertainty in both conceptual and mathematical models (Freeze and Reeves, 1996).

In the following sections, emphasis will be primarily on numerical and analytical models for their widespread use in groundwater applications and their particular use in this field. These types of models are based on sets of simplifying assumptions to different extents. Special attention needs to be paid to these assumptions as they form a decisive element in a model conception and an important criterion in model selection (see section 2.5).

#### **2.1.2.4 Assumptions**

Most aquifer systems are complicated beyond our capability to describe them and treat them exactly as is the case in reality. Therefore, the construction of a groundwater model is always made on the basis of a set of simplifying specific assumptions that should not be forgotten in the course of investigation whenever the model is being deployed. In fact,

three fundamental and common assumptions are typically used whenever we deal with groundwater flow and transport. They are:

- the continuum approach: the porous medium is considered as a continuum, thus the flow through the medium is treated at the macroscopic level, rather than the microscopic level. This assumption arises from the difficulty of taking measurements at this level in order to validate a model. The passage from the microscopic description to the macroscopic one is translated by introducing the concept of a representative elementary volume (REV) of the porous medium domain. A value at a point within this domain is interpreted as the average of the variable taken over the REV centred at that point. However, this phenomena at the microscopic level should first be examined to justify the validity of this assumption especially when dealing with variably saturated flow, multiple phase flow or contaminant transport. This assumption could be no more valid if changes in the flow or transport parameters are induced by external reactions and therefore may compromise the flow direction or cause a breakthrough of contaminants (Fryar and Schwartz, 1998). Special experiments should be undertaken to check the possibility of up scaling microscopic phenomena and representing them within an equivalent macroscale medium (Braun et al., 1998, and Ahmadi et al., 2001).
- the hydraulic approach: at regional scales, flow is considered to be essentially horizontal. This assumption is made on the basis that when the ratio of the aquifer saturated thickness to horizontal length is important, then the flow is particularly horizontal. The Dupuit assumption for a phreatic aquifer is based essentially on this approximation. The approach allows transforming a three-dimensional problem into a two-dimensional one. Model variables are averaged over the vertical thickness of the aquifer. The assumption fails in regions where the flow has a large vertical component, in leaky aquifers if the hydraulic conductivity of the semi-permeable layer is significant or when considering contaminant transport.
- Flow velocities in the continuum are considered low enough to justify the reduction of the momentum balance equation to the linear motion equation of Darcy (see section 2.3). This assumption should be verified in cases where the flow regime is not uniform or occurs at large Reynolds (Re) numbers (e.g. fractured or karstic aquifers and multiphase flow or in the immediate vicinity of outlets).

Depending on the case study, many others assumptions could be adopted to simplify the real field conditions to produce a reliable representation and reduce the computational effort for simulation. Assumptions on the distribution of parameters (classical, deterministic and bayesian approaches, see Loaiciga and Marino, 1987), model dimensionality (1D, 2D or 3D, one or multi-layers, aquifer thickness, etc.), aquifer areal extent, boundary conditions and various stresses are necessary to build the conceptual model of an aquifer. These assumptions are usually made in order to overcome the lack of information and uncertainties we regarding the aquifer system features. However, much research has been undertaken to quantify and reduce uncertainties in the conceptual, mathematical and parameter uncertainties using the sensitivity analysis method.

Therefore, one of the most important steps in the modelling process is the selection of a set of appropriate assumptions that simplify the aquifer and flow conditions with regard to the level of accuracy and objectives required.

## **2.2 Model Development Procedures**

In groundwater modelling, the term ‘model’ may refer to the generalised computer code designed for application to many different sites, or to the use of such codes at a particular site as an ‘operational model’ (Van der Heijde and Kanzer, 1997). This is why model development may refer to code development resulting in a software product (i.e. code development) or model development resulting in the application of such a product for a specific purpose (i.e. model application).

### **2.2.1 Code Development Procedure:**

A standard code development process involves the following main steps (Figure 2.1):

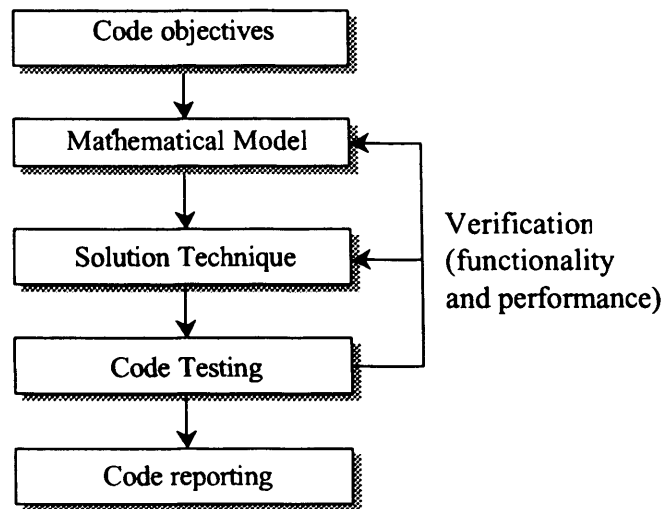


Figure 2.1 Model code development process.

### 2.2.1.1 Code Objectives

The first step in a groundwater modelling code development is the definition of its functionality. The code objectives are formulated in terms of a set of functions and features. This conceptual formulation includes: model framework geometry, simulated processes, boundary conditions, and analytical and operational capabilities.

### 2.2.1.2 Mathematical Model

The next step in the modelling process is to describe the groundwater system, specified in code objectives by a mathematical model. This consists of defining the geometry of the considered domain, specifying equations that describe the behaviour of the fluids involved, specifying equations that express the initial conditions and providing equations that define the boundary conditions. The mathematical model contains the same information as in the code's conceptual formulation, but expressed as a set of equations that are amenable to analytical or numerical solution. The complete mathematical statement of groundwater problems is detailed below.

### **2.2.1.3 Solution Technique**

The Partial Differential Equations (PDEs) formulated in the mathematical model must be solved or approximated using an analytical or numerical method. The selection of an appropriate solution technique for the class of problems treated depends on several factors including accuracy, efficiency and usability of a particular method (i.e. assumptions which may include simplifications, truncation, and round-off errors and modeller mathematical background). A more detailed comparison between the performance of analytical and numerical methods is given later in section 2.5.

### **2.2.1.4 Code Testing**

Code testing or code verification in groundwater modelling is defined as the process of demonstrating the consistency, completeness, correctness and accuracy of a groundwater modelling code with respect to its design criteria (ASTM, 1984). This evaluation is performed by mean of code tests. The three main objectives of these tests are:

- functionality analysis: which involves the verification of code functions with regard to predefined code objectives,
- performance evaluation: which involves checking the operational characteristics of the code in terms of its computational accuracy, limitations with respect to numerical convergence and stability, sensitivity for grid design and model parameters, algorithm efficiency and resources required for model setup,
- applicability assessment focuses on determining for which types of problems the code is particularly suited to.

### **2.2.1.5 Code Reporting**

Once the code has been developed and tested, a comprehensive documentation about its capabilities and limitations must be prepared. According to Van der Heijde and Elnawawy (1992) the code documentation should include a description of the theoretical framework of the model (i.e. assumptions, mathematical equations and treatment and limiting conditions), code structure and language (i.e. programmer's manual), and code

use instructions regarding model setup and code execution parameters (i.e. user's manual). Detailed guidelines for the preparation of comprehensive code documentation are given by the American Society for Testing and Materials (ASTM, 1997).

### 2.2.2 Model Application Procedure

A model application requires appropriate site characterisation. Figure 2.2 illustrates a simple diagram of a model application process.

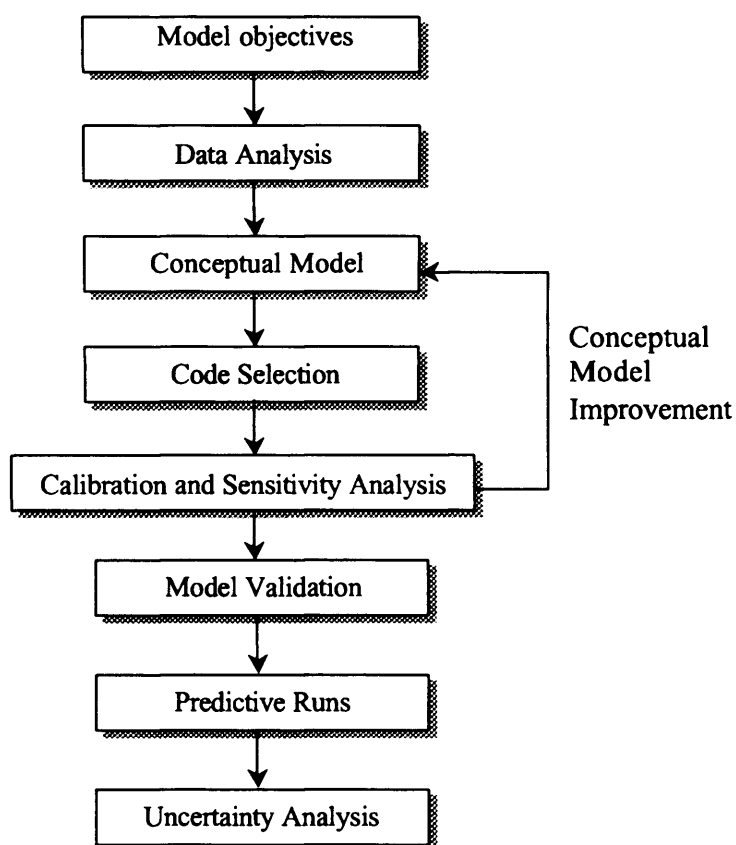


Figure 2.2 Model application process.

#### 2.2.2.1 Model Objectives

As stated above, modelling application objectives range from prediction (e.g. flow and transport models) to system interpretation (e.g. test analysis, parameter identification) and generic modelling (e.g. water budget, chemical mass balance). The purpose will

determine what governing equation will be solved (e.g. flow, transport), the size of the domain to be investigated (i.e. local or regional) and areas of particular interest (i.e. finer resolution for higher accuracy).

#### **2.2.2.2 Data Analysis**

Data analysis includes the collection of available site-specific data, and analysis and interpretation of the data. The data are usually acquired from public bodies, site investigations (previous studies or/and study-specific), and the literature. The quality of site-specific data should be analysed (e.g. sampling techniques and testing methods) and the source of all model input parameter values should be given and justified. Specific-site data interpretation gives information about spatial distribution of the model parameters (e.g. permeability, storativity), boundary and initial conditions and stresses on the system. Each data as outlined above are a determining factor in the formulation of a good representative conceptual model and the effort that will be spent in the model calibration and verification. Uncertainties associated with groundwater mechanisms and hydrogeological features are associated with the quantity and quality of these data.

#### **2.2.2.3 Conceptual Model**

The construction of a conceptual model consists of identifying a set of assumptions describing the system composition, the relevant medium properties and the flow process mechanism. To do so, extensive information on the natural system, compilation and interpretation of field data are essential to understand the natural system and have a clearer definition of the flow problems. The selection of an appropriate conceptual model and the level of simplification included in the model also rely on the objective of the management problem, in the sense that it dictates which features of the investigated problem should be represented in the model and to what level of accuracy. Figure 2.3 gives a schematic approach to the construction of a conceptual model. As can be noted, the assumptions made at this stage are generally related to the geometry of the boundaries, the kind of solid matrix, the flow mode and regime, the properties of the fluid, sources and sinks, and finally initial and boundary conditions.

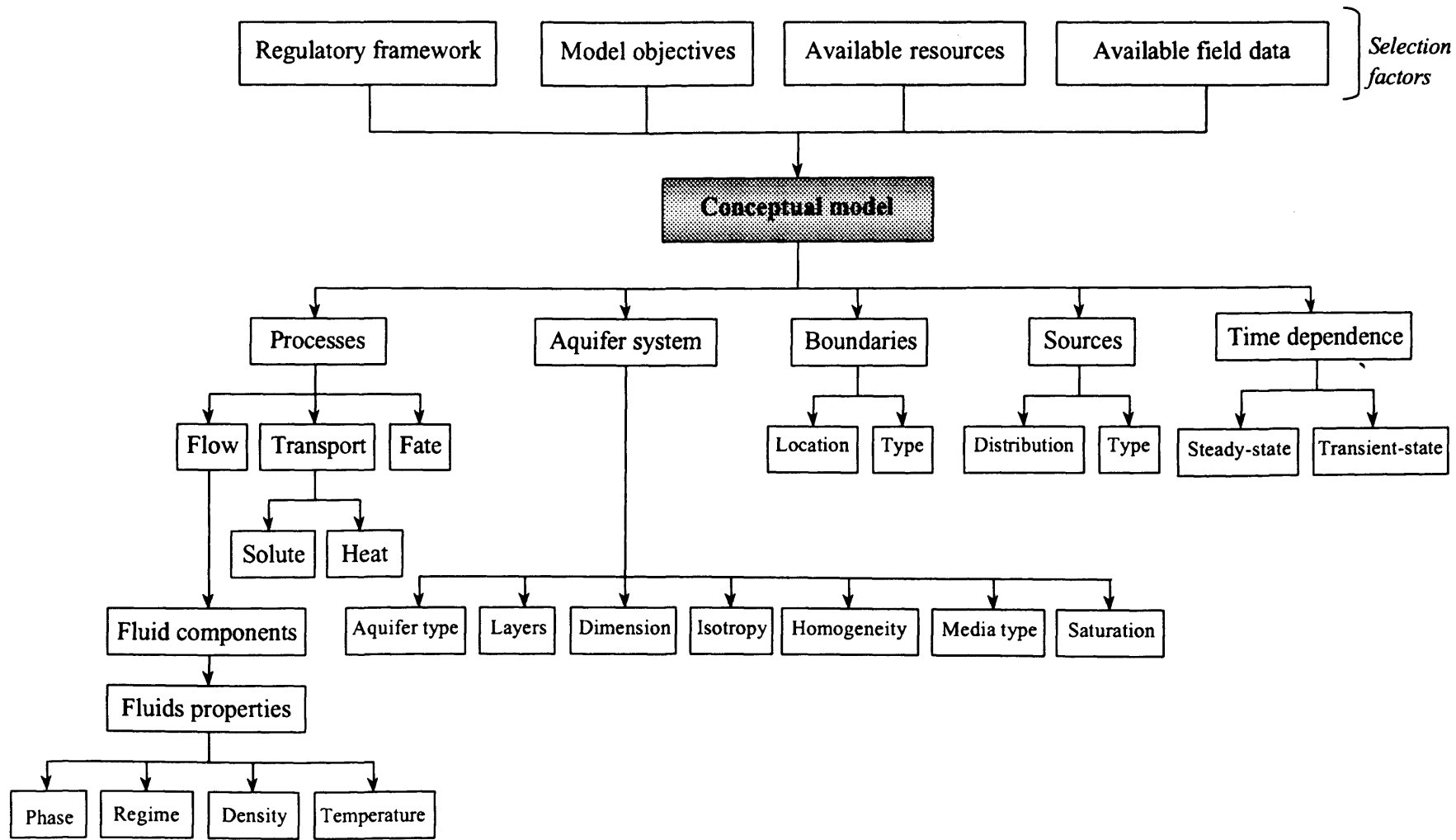


Figure 2.3 Schematic approach to the construction of a conceptual groundwater model.

More detailed models are more costly and require more sophisticated codes and larger computers. The model should be simple enough to facilitate model efforts, but not too simple so as to exclude features dominant to the groundwater problem being investigated. In summary, a good conceptual model is one that is suited to the need, cost and availability of data to develop and calibrate the model. At this stage, the conceptual model is not definitive as it can always be adjusted using the calibration results, as shall be highlighted later.

#### **2.2.2.4 Code Selection**

Once a decision to develop a model for a specific site has been made, a code must be selected that is appropriate for the given problem. The user checks the capabilities of existing codes and other code information of particular interest to the model objectives. In 1994 the USEPA has established a general classification of selection criteria for special cases of site contamination. A more general summary of selection criteria is given in Table 2.3. The selection of the appropriate code and appropriate level of complexity remains subjective and dependent upon the judgement and experience of the analysts, the objectives of the study, and the level of prior information on the system of interest.

#### **2.2.2.5 Calibration and Sensitivity Analysis**

A sensitivity analysis of a model application aims to quantify the effects of uncertainty in the estimates of model coefficients such as aquifer parameters, stresses, and boundary conditions on the calibrated model. Evaluating the importance of each factor helps determine which data must be defined more accurately and which data are already adequate.

#### **2.2.2.6 Model Validation**

The purpose of model validation is to demonstrate the credibility of code-based predictions by using the set of calibrated parameter values and stresses to reproduce well-monitored new set of field data (Van der Heijde and Kanzer, 1997).

<b>CRITERIA</b>	
<b>Administrative Data</b>	
	Objective of the model (simulation, parameter identification, aquifer test analysis)
	Available resources
	Available field data
	legal and regulatory framework applying to the situation
<b>Site-Related Criteria</b>	
	<b>Aquifer system characteristics</b>
	Confined aquifers
	unconfined aquifers (water-table)
	aquitards
	multiple aquifers
	convertible
	<b>Soil/Rock characteristics</b>
	heterogeneity in properties
	anisotropy in properties
	fractured
	macropores
	layered soils
	<b>Flow conditions</b>
	fully saturated
	variably saturated
	laminar flow
	linear/Darcian
	nonlinear/non-Darcian
	turbulent flow
	variable viscosity
	variable density
	steady-state flow
	transient flow
	<b>Multiphase fluid conditions</b>
	two-phase water/NAPL
	two-phase water/air
	three-phase water/NAPL/air
	<b>Boundary conditions</b>
	type I: (Dirichlet) prescribed head
	type II: (Neuman) prescribed flux
	type III: (Cauchy) head dependent flux
	Inflow/Outflow
	geometry (line, point, area)
	type (constant/variable)
<b>Code-related criteria</b>	
	Development objectives (research, general use, education)
	source code availability
	history of use
	code usability (pre-processing, post-processing, mathematical background required)
	quality assurance
	code documentation
	code testing
	hardware requirements
	solution methodology
	code output
	code dimensionality
	cost
	code language

Table 2.3 Code selection criteria for groundwater flow modelling.

### **2.2.2.7 Predictive Runs**

The code is run with the calibrated values for model parameters to simulate the response of the system to future events (i.e. predictive simulations). The justification and reasoning for these various runs is related to the model application objectives.

### **2.2.2.8 Uncertainty Analysis**

In a final model report, prediction results are presented. Ranges and uncertainties in these model results need to be indicated. An uncertainty analysis provides a means of taking account of the effects of uncertainty in input parameter values on the model results. A detailed description of uncertainty analysis is provided by the McMahon et al. (2001). When the predictions are related to a problem or system of continuing interest to society, uncertainty analysis roles include the improvement of the design of the observation network and prediction of the trends and direction of changes in the aquifer system. The model should then be periodically post-audited, or re-calibrated, to incorporate new information necessary for model validation, such as changes in imposed stresses or revisions in the assumed conceptual model. New field data are collected to determine whether the prediction was correct. If the accuracy of the predictions was sufficiently close in matching the field data, then the model was regarded as being satisfactorily validated for the studied area, otherwise changes in the conceptual model or in model parameters need to be made. The model final report should follow the Quality Assurance (QA) criteria associated with the documentation and organisation of records and computer files. Any decision made during the study (e.g. assumptions, data sources, calculations, simplifications, etc.) or changes made to the model during its development should be justified and recorded. These elements assure technically and scientifically adequate execution of all project tasks included in the study, and ensure that all modelling-based analyses are verifiable and defensible (Taylor, 1985).

## 2.3 Mathematical Statement of Groundwater Flow

A mathematical statement is an important step in the model development process. It is the translation of the conceptual model into a completed, well-posed mathematical one, which can be solved using a computer algorithm. A complete mathematical description of a model consists of a statement of the governing equations, the boundary conditions and the initial conditions if the problem is time dependent. Each of these elements is discussed in the following sections.

### 2.3.1 Governing Equations

In groundwater flow models, the environmental water manager is primarily concerned with fluids contained in the aquifer system. This supposes a good understanding of both the fluid and aquifer properties.

#### 2.3.1.1 The Fluid

The fluid is generally described by stating (Bredehoeft et al., 1982, p. 7):

1/ *the pressure of the fluid*: described by a partial differential equation for pressure which in certain simplifying instances can be reduced to an equation for the hydraulic head; this is commonly referred to as the flow equation:

$$\nabla \cdot \frac{\rho k}{\mu} (\nabla p + \rho g \nabla z) - q = \frac{\partial}{\partial t} (\rho n) \quad (2.1)$$

2/ *the composition of the fluid*: a partial differential equation for composition is set for each chemical constituent of interest within the fluid column; this is used for studying the solute transport distribution in groundwater:

$$\nabla \cdot \left( \rho C \frac{k}{\mu} (\nabla p + \rho g \nabla z) \right) + \nabla \cdot (\rho D) \cdot \nabla C - qC = \frac{\partial}{\partial t} (\rho n C) \quad (2.2)$$

3/ *the energy contained in the fluid*: generally either in the form of temperature or enthalpy of the fluid and described by a partial differential equation of the form:

$$\nabla \left( \frac{\rho k}{\mu} H (\nabla p + \rho g \nabla z) \right) + \nabla \cdot K_T \cdot \nabla T - q_L - q C_p T = \frac{\partial}{\partial t} [\rho n U + (1-n) (\rho C_p)_R T] \quad (2.3)$$

where:

- $C$ : concentration, mass fraction,  $ML^{-3}$ , ( $Kg/m^3$ );
- $C_p$ : specific heat of fluid at constant pressure,  $EM^{-1}T^{-1}$ , ( $J/Kg \cdot ^\circ C$ );
- $D$ : hydrodynamic dispersion coefficient,  $L^2t^{-1}$ , ( $m^2/s$ );
- $g$ : acceleration due to gravity,  $Lt^{-2}$ , ( $m/s^2$ );
- $H$ : enthalpy,  $EM^{-1}$ , ( $J/Kg$ ); ( $H=U+p/\rho$ )
- $k$ : permeability,  $L^2$ ;
- $K_T$ : thermal conductivity of the aquifer,  $EL^{-1}t^{-1}T^{-1}$  or  $Ft^{-1}T^{-1}$ , ( $W/m \cdot ^\circ C$ );
- $p$ : pressure,  $ML^{-1}t^{-2}$ ;  $F/L^2$ ; Pascal (Pa)
- $q$ : mass rate of production or injection of liquid per unit volume,  $ML^{-3}t^{-1}$ , ( $Kg/m^3 \cdot s$ );
- $q_L$ : rate of the heat loss per unit volume,  $EL^{-3}t^{-1}$ , ( $J/m^3 \cdot s$ );
- $R$ : refers to rock phase;
- $t$ : time,  $t$ , (s);
- $T$ : temperature,  $T$ , deg. Celsius ( $^\circ C$ );
- $U$ : internal energy,  $EM^{-1}$ , ( $J/Kg$ ); (Joule (J) or Watt-second (W-s));
- $z$ : elevation above a reference plane,  $L$ ; (m)
- $n$ : porosity, dimensionless;
- $\rho$ : density,  $ML^{-3}$ ; ( $Kg/m^3$ )
- $\mu$ : viscosity,  $ML^{-1}t^{-1}$ ; (Pa-s)
- $\nabla$ : gradient vector ( $\equiv grad$ );
- $\nabla \cdot ()$ : divergence ( $\equiv div$ ).

For the most general case and for a more complete and realistic representation of the flow mechanism in the aquifer, these three equations (or set of equations) are coupled and must be solved simultaneously. However, when the conceptual model is developed, the analysis of the fluid properties shows the terms and mechanisms that have a non-dominant effect and thus, should be deleted. Therefore, in many cases, the coupling of the equations may be negligible and the equations can be treated separately. For instance, in

many problems, the change in temperature is unimportant and the system is regarded as isothermal, dropping consideration of equations for the internal energy of the fluid. If no chemical constituent movement is of interest and has no effect on the fluid properties, then the only equation considered is the flow equation. In the following analysis the fluid composition and temperature will be neglected, as focus will be concentrated only on water flow problems and the assumptions that may simplify the corresponding equations.

### **2.3.1.2 The Aquifer**

As mentioned above, the flow equation that describes a porous media groundwater system involves parameters that describe certain properties of aquifers. A good understanding of the aquifer properties may enable considerable simplifications to be made to the mathematical flow model, with the aquifer properties depending on the type of aquifer. Therefore, a description of the existing classification of aquifers regarding their hydraulic behaviour is provided. The classic three types of aquifers are (Bear, 1972, p. 5):

*Confined aquifer*: the aquifer is bounded above and below by impervious formations. The saturated thickness is independent upon the flux or boundary conditions unless special stresses cause the aquifer to become unconfined. A special case of this category is an artesian aquifer where the elevations of the piezometric surface are above the ground surface.

*Leaky or semi-confined aquifer*: the aquifer can lose or receive water through adjacent semipervious formations laying above or below the aquifer. The aquifer can be fully or partially saturated (e.g. leaky confined aquifer, leaky phreatic aquifer).

*Unconfined or phreatic aquifer*: the aquifer has a free surface water table that serves as its upper boundary. For this case the saturated thickness is variable.

Aquifer parameters that affect the flow are porosity, permeability and storativity. They are usually combined with the fluid properties into new coefficients including: hydraulic

conductivity or transmissivity and specific yield or specific storage. Depending on the aquifer type, the flow equation can be written in terms of the hydraulic conductivity and specific yield (unconfined aquifers), or transmissivity and specific storage (confined aquifers) as it will be detailed in the next paragraph. The general flow Equation 2.1 is derived by mathematically combining a water balance equation with Darcy's law.

### 2.3.1.3 Mass Conservation Equation

Using the assumption of a continuum, the law of mass conservation is applied over a control volume of an aquifer situated in the flow field using an Eulerian approach. The net inflow into the volume must equal the rate at which water accumulates within the control volume (Bear, 1979, p. 90, Wang and Anderson, 1982, p. 12). Traditionally, the control volume used is a fixed in shape and position rectangular parallel-piped box of dimensions  $\Delta x$ ,  $\Delta y$ ,  $\Delta z$ , centred at some point  $P(x, y, z)$  inside the flow domain, as shown in Figure 2.4. The volume of the control volume is  $\Delta V$ .

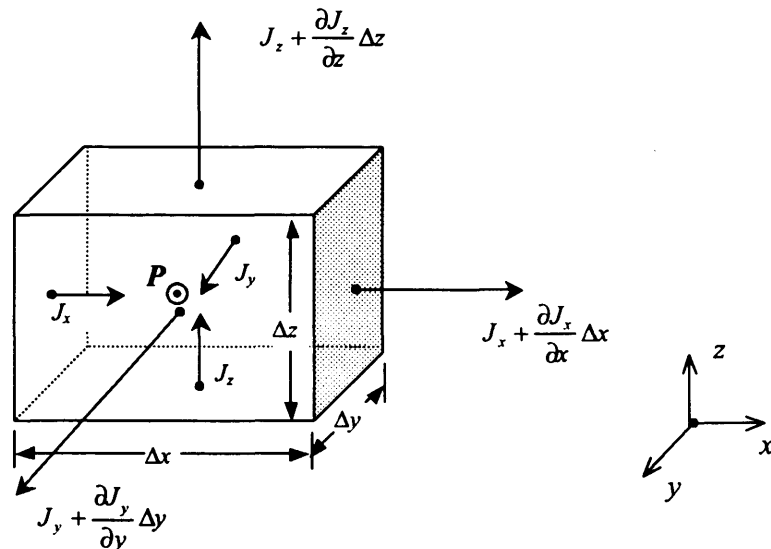


Figure 2.4 Mass conservation for a control volume.

The vector  $J$  denotes the mass flux (mass per unit area per unit time,  $ML^{-2}t^{-1}$ ) of water of density  $\rho$  at point  $P(x, y, z)$ . The mass balance is computed by summing the results from each component direction. For instance, the component  $J_x$  represents the mass flux through the left face of the control volume. The change in mass flux in the  $x$  direction is

the excess of inflow at the left face over outflow of mass during a short time  $\Delta t$ , which is equal to  $-(\partial J_x / \partial x) \Delta V \Delta t$ . Similar expressions can be written for the change in mass flux along the  $y$  and  $z$  axes. The total change in mass flux during  $\Delta t$  is expressed as:

$$-\left(\frac{\partial J_x}{\partial x} + \frac{\partial J_y}{\partial y} + \frac{\partial J_z}{\partial z}\right) \Delta V \Delta t = -\text{div} J \Delta V \Delta t \quad \text{where } J = \rho q \quad \text{and } \Delta V = \Delta x \Delta y \Delta z \quad (2.4)$$

where  $q$  is the specific discharge,  $LT^{-1}$ . By the principle of mass conservation, in the absence of sources and/or sinks of mass, the excess of mass expressed by Equation 2.4 must be equal to the change of mass  $m$ , during  $\Delta t$  within the control volume. Since  $m = \rho n \Delta V$ , this mass accumulation in the box during  $\Delta t$  can be expressed as:

$$m|_{t+\Delta t} - m|_t = [(\rho n)|_{t+\Delta t} - (\rho n)|_t] \Delta V \quad (2.5)$$

where  $n$  is the porosity of the porous medium. Stating the equality between Equations 2.4 and 2.5 the mass balance at  $P(x, y, z)$  can now be written as:

$$-\text{div}(\rho q) = \frac{\partial(\rho n)}{\partial t} \quad (2.6)$$

#### 2.3.1.4 Darcy's Law

According to Darcy's experiment in 1856, the groundwater motion with respect to the solid matrix can be described by:

$$q = -Ki = -K \text{grad} \phi ; \quad V = \frac{q}{n} \quad (2.7)$$

where  $V$  is the velocity vector [ $LT^{-1}$ ],  $q$  is the specific discharge vector [ $LT^{-1}$ ],  $i$  is the hydraulic gradient [1],  $K$  is the hydraulic conductivity tensor of the porous medium [ $LT^{-1}$ ] and  $\phi$  is the piezometric head [L]. Equation 2.7 is valid for a three-dimensional flow through an inhomogeneous anisotropic medium, with  $K$  representing the second rank tensor of hydraulic conductivity of an anisotropic medium (Bear, 1972, p. 137) and consisting of nine components that may vary in space in case of inhomogeneous medium. Symbolically,  $K$  is written as:

$$[K] = \begin{bmatrix} K_{xx} & K_{xy} & K_{xz} \\ K_{yx} & K_{yy} & K_{yz} \\ K_{zx} & K_{zy} & K_{zz} \end{bmatrix} \quad \text{where } K_{i,j} = K_{i,j}(x,y,z) \quad (2.8)$$

The hydraulic conductivity tensor is symmetric, thus in three-dimensional flow only six distinct components are needed to fully define the hydraulic conductivity. It is shown that it is always possible to find three mutually orthogonal directions, called the principal directions of the anisotropic medium, such that when these directions are used as the coordinate system, then the components  $K_{i,j}=0$  for all  $i \neq j$  and  $K_{i,j} \neq 0$  for  $i = j$ , and Equation 2.8 becomes (Bear, 1979, p. 72):

$$[K] = \begin{bmatrix} K_{xx} & 0 & 0 \\ 0 & K_{yy} & 0 \\ 0 & 0 & K_{zz} \end{bmatrix} \quad (2.9)$$

Darcy's law is valid only for small velocities through porous media. The linear relationship expressed in 2.7 between the specific discharge  $q$  and the hydraulic gradient  $J$  is applicable as long as the Reynolds number  $Re$  is within the range 1 and 10. A Reynolds number for flow through porous media is defined by  $Re = qd/\nu$  where  $d$  is a representative length of the porous matrix, traditionally taken as the main grain diameter and  $\nu$  is the kinematic viscosity of the fluid ( $= \mu/\rho$ ,  $L^2T^{-1}$ ). In an isotropic medium,  $K$  is reduced to a scalar ( $LT^{-1}$ ) which may be expressed as (Bear, 1972, p. 133):  $K = kg/\nu$  ( $k$  is the intrinsic permeability  $L^2$  of the porous matrix).

### 2.3.1.5 Groundwater Flow Equation

Substituting equation 2.7 into Equation 2.6 yields:

$$\text{div}(\rho K \text{grad} \phi) = \frac{\partial(\rho n)}{\partial t} \quad (2.10)$$

To write this equation in terms of one variable, one should choose the right variable that describes the flow problem. This is usually performed once the conceptual model is formulated (assumptions related to the dominating phenomena).

- When the flow is *density-dependent* and involves miscible fluids the flow equation must be written in terms of pressure  $p$  and permeability  $k$ , as the piezometric head  $\phi$  and the hydraulic conductivity  $K$  are both functions of the density  $\rho$  (Anderson and Woessner, 1992, p. 334):

$$\phi = z + \frac{p}{\rho g} \quad \text{and} \quad K = \frac{k\rho g}{\mu} \quad (2.11)$$

where  $\mu$  is the dynamic viscosity. In this case, Darcy's law takes the form:

$$q = -\frac{k}{\mu} (\nabla p + \rho g \nabla z) \quad (2.12)$$

which, when substituted into Equation 2.6 and considering the external fluid sources yields the flow equation as given in 2.1.

- When the flow occurs in *unsaturated zones*, also referred to as the "vadose zone", the flow equation may be written in terms of a piezometric head  $\phi$ , moisture content  $\theta$  [1], or pressure head  $p / \rho g$ . The hydraulic conductivity  $K$  is a function of the moisture content  $\theta$  which is a function of the pressure head  $p / \rho g$ .
- If the flow is *immiscible* then the governing equations that describe multiphase flow are formulated in terms of the pressure of each of the phases.

In general, when describing a groundwater system using a mathematical statement, two points are considered: the hydrogeological features and the processes to be modelled. According to the USEPA (1993) these two elements form the basis of groundwater model classifications. Table 2.4 summarises the different processes that are generally modelled in groundwater studies. Flow models simulate the movement of one or more fluids in porous or fractured rock. Classically, one such fluid is water, the others, if present, can be air, methane, or other vapours (in soil) or immiscible nonaqueous phase liquids (NAPLs), sometimes having a density distinct from water (LNAPLs, DNAPLs). A special case of multi-fluid flow occurs when layers of water of distinct density are separated by a relatively small transition zone, a situation often encountered when seawater intrusion occurs (although other conceptual approaches to this problem are used). For further details, see Bear and Verruijt (1987), National Research Council (1990), De Marsily (1986), Huyakorn and Pinder (1983), Javandel et al. (1984), and Wang and Anderson (1982).

<p><b>Flow</b></p> <ul style="list-style-type: none"> <li>* single fluid flow</li> <li>* multfluid flow               <ul style="list-style-type: none"> <li>* multicomponent</li> <li>* multiphase</li> </ul> </li> <li>* laminar flow               <ul style="list-style-type: none"> <li>* linear/Darcian</li> <li>* nonlinear/non-Darcian</li> </ul> </li> <li>* turbulent</li> </ul> <p><b>Transport</b></p> <ul style="list-style-type: none"> <li>* advection/convection</li> <li>* conduction (heat)</li> <li>* mechanical dispersion</li> <li>* molecular diffusion</li> <li>* radiation (heat)</li> </ul>	<p><b>Fate</b></p> <ul style="list-style-type: none"> <li>* hydrolysis/substitution</li> <li>* dissolution/precipitation</li> <li>* reduction/oxidation</li> <li>* complexation</li> <li>* radioactive decay</li> <li>* microbial decay/biotransformation</li> </ul> <p><b>Phase Transfers</b></p> <ul style="list-style-type: none"> <li>* solid - gas      * (vapor) sorption</li> <li>* solid - liquid   * sorption</li> <li>                          * ion exchange</li> <li>* liquid - gas    * volatization</li> <li>                          * condensation</li> <li>                          * sublimation</li> </ul> <p><b>Phase Changes</b></p> <ul style="list-style-type: none"> <li>* freezing/thawing</li> <li>* evaporation/condensation</li> </ul>
--	---

Table 2.4 Main processes in groundwater modelling (USEPA, 1993).

In the following discussion, we shall restrict our interest to standard flow mathematical models, which assume that the flowing fluid is water, with a constant density ( $\approx 1g/cm^3$ ), with no considerable changes in temperature or concentrations of other dissolved solids or solutes, and that the porous medium is saturated.

By definition, the specific storativity of the porous medium is the volume of water released from storage in a unit volume per unit change in the piezometric head (Bear, 1979, p. 86), thus:

$$\frac{\partial(\rho n)}{\partial t} = \rho S_0 \frac{\partial \phi}{\partial t} \quad (2.13)$$

Using these assumptions, and substituting equation 2.13 into 2.10 yields:

$$\text{div}(K \text{grad} \phi) = S_0 \frac{\partial \phi}{\partial t} \quad (2.14)$$

### 2.3.1.6 External Sources

External sources refer to the amount of water that may enter or leave the aquifer through sources or sinks other than the inflow through aquifer boundaries. They account for leakage from overlying or underlying aquifers, recharge or discharge through wells, infiltration from precipitation or irrigation and sewage, artificial recharge, evapotranspiration, streams and lakes - aquifer interactions including seepage or alimentation and springs. Their spatial distribution can be accommodated in the form of:

- Point sources, such as springs or recharge or discharge from wells,
- Line sources, such as stream or sewage inputs, and
- Area sources, such as lakes, recharge or precipitation.

The time variation of the source term needs special attention, since it is necessary to determine whether the source is continuously and steadily releasing into (or discharging from) the aquifer, or instantaneously stressing the system. This information is important in determining the way in which any sources are modelled with regard to the modelling objectives.

A general form of the governing flow equation, with respect to the inclusion of external sources is given as:

$$\frac{\partial}{\partial x} \left( K_x \frac{\partial \phi}{\partial x} \right) + \frac{\partial}{\partial y} \left( K_y \frac{\partial \phi}{\partial y} \right) + \frac{\partial}{\partial z} \left( K_z \frac{\partial \phi}{\partial z} \right) + Q = S_0 \frac{\partial \phi}{\partial t} \quad (2.15)$$

where  $K_x$ ,  $K_y$  and  $K_z$  are components of the hydraulic conductivity tensor,  $S_0$  is the specific storage and  $Q$  is a general sink/source term, which is positive for an inflow into the system per unit volume of aquifer per unit of time and negative for an outflow.

Under steady state conditions, if the hydraulic conductivity is constant (i.e. the aquifer is isotropic, homogeneous and incompressible) and no external sources affect the aquifer system, Equation 2.15 may be reduced to the well-known Laplace equation or elliptic equation:

$$\nabla^2 \phi = \frac{\partial^2 \phi}{\partial x^2} + \frac{\partial^2 \phi}{\partial y^2} + \frac{\partial^2 \phi}{\partial z^2} = 0 \quad (2.16)$$

Another useful form of Equation 2.15 is given by:

$$\frac{K}{S_0} \left[ \frac{\partial^2 \phi}{\partial x^2} + \frac{\partial^2 \phi}{\partial y^2} + \frac{\partial^2 \phi}{\partial z^2} \right] = \frac{\partial \phi}{\partial t} \quad \text{or} \quad a \nabla^2 \phi = \frac{\partial \phi}{\partial t} \quad (2.17)$$

This equation is the well-known diffusion (or parabolic) equation that generally describes groundwater flow in a homogenous and isotropic confined aquifers with no external sources.

### 2.3.2 Boundary and Initial Conditions

One of the key steps required in completing the mathematical statement of a groundwater flow problem is that of identifying the model area and its boundaries. The model boundary is identified by the interface between the investigated area and the adjacent groundwater system. Conditions at these boundaries have to be specified, and are generally classified into three mathematical conditions:

- Specified Head boundary, or Dirichlet condition for which the head is given as:

$$\phi(x, y, z, t) = \text{constant}$$

- Specified flow boundary, or Neumann condition, for which the groundwater flux across the boundary is given. A typical example for this category is a no-flow boundary condition given as:

$$\frac{d\phi(x, y, z, t)}{dn} = \text{constant}$$

where  $n$  is the directional coordinate normal to the boundary

- Head-dependent flow boundary, or Cauchy condition for which the flux across the boundary is calculated for a given boundary head value as:

$$\frac{d\phi}{dn} + c\phi = \text{constant}$$

where  $c$  is also a constant.

These classifications account for natural boundaries, such as streams, lakes and reservoirs, wetlands, springs, recharge at the water table, adjacent materials of low hydraulic permeability, inter-basin flow, evapotranspiration, spatial change in density of water and divides or for artificial boundaries. The mathematical designation of boundary conditions, established for modelling purposes, should be carefully formulated so that the

proposed model boundaries will have the same effect as the natural 'physical' system boundaries. This should be achieved through the model calibration.

When modelling flow problems, specification of initial conditions is sometimes required for the entire area. In transient simulations, they are a physical requirement and should be estimated if a measured head distribution at the simulation initial time is not available or not generated from a previous steady state run. For steady state simulations, they are a numerical requirement as their set is used to start the numerical calculations whenever iterative solvers are used.

## **2.4 Review of Analytical Solutions and Limits**

### **2.4.1 Existing Analytical Solutions**

When the partial differential equations describing groundwater flow or transport can be solved directly or by means of simplified solutions to the governing equations the solution is said to be analytical. Basically, these equations are second-order differential equations that can be classified as parabolic (i.e. transient flow and dispersion), elliptic (i.e. steady flow) or hyperbolic (i.e. advective transport), based on the nature and magnitude of the coefficients of the equation (Peaceman, 1977). They can be linear or nonlinear. For flow problems, the equations are generally nonlinear when the transmissivity is a function of the saturated thickness (e.g. water table aquifers) or hydraulic conductivity is a function of the moisture content (e.g. unsaturated zone). Nonlinear transport problems involve those where changes in concentration, pressure or temperature cause changes in the viscosity, effective porosity or density (e.g., multiphase fluid conditions). Similarities between the governing equations of groundwater flow and those governing other engineering disciplines, such as heat transfer and wave propagation, have proven useful in finding analytical solutions for groundwater flow and transport problems (Carslaw and Jaeger, 1959). Many analytical solutions in the groundwater field are duly studied and addressed in numerous references, such as Polubarinova-Kochina (1952), Bear (1979), Hunt (1983), and Walton (1989). There are generally three types of analytical methods:

*Approximate analytical:* typical analytical solutions are in the form of infinite series of algebraic terms or definite integrals. Because an infinite series cannot be solved for exact solutions, these expressions are approximated by truncating the series. Convergence of these equations should be examined carefully.

*Exact analytical:* if the analytical solutions can be expressed by equations that take a closed form (i.e. a finite number of terms), then the solution is exact. In general, exact analytical equations tend to require infinite domains and boundaries, which limit their applicability.

*Semi-analytical:* these techniques use concepts from fluid mechanics, with velocity potentials being extended using numerical tools to construct flow patterns. They may be used where complex boundaries do not allow analytical solutions to be formulated.

In general, obtaining an exact or approximate analytical solution requires that the properties and boundaries of the flow/transport system be highly simplified. In fact, most of these solutions are restricted to problems with homogeneous properties, simple geometries, and simple boundary conditions, limiting their application to field situations. However, more complicated problems can be described and solved analytically if reducing them to simpler flow problems can be conceptually justified or by applying the principle of superposition if these solutions are linear, or could be linearised (Bear, 1972 and Hunt, 1983). This technique allows the superimposition of a number of equations and enables their different analytical solutions to be combined by adding them together. This type of solution is also called semi-analytical.

Many authors have presented examples of classic analytical solutions. For example, the nonlinear Boussinesq equation describing unsteady free surface groundwater flow has been approximated by Polubarinova-Kochina (1962), Babu (1976) and Basak (1981). Exact analytical solutions to this equation are not known, except for some special cases (Remson et al., 1971). An approximate solution in one dimension was presented by Tolikas et al. (1984) and then by Sewa and Chauhan (1987). Moltyaner (1988) described in his report an approximate analytical method that combined analytical and numerical

methods for obtaining an approximate solution to the equations governing two-dimensional steady state groundwater flow. Zimmerman and Bodvarsson (1989) presented an approximate analytical solution for the problem of a Newtonian fluid infiltrating into a porous spherical block, which could be incorporated into double-porosity models for fractured reservoirs and aquifers. Exact solutions are known only for few cases such as uniform unconfined two-dimensional groundwater flow over a stepped base (Fitts and Strack, 1996), two-dimensional groundwater flow involving a semi-pervious boundary in a semiconfined aquifer (Van der Veer, 1994). Recent advances in research are targeting more complex problems such as flow in the unsaturated zone (including seepage through dams), solute and heat transport in the saturated and unsaturated zone, flow and transport in fractured rocks, and saltwater intrusion. The growth of such research fields is due to the advantages that analytical solutions present in terms of accuracy and cost, and also as a result of the parallel growth in numerical model development and the use of such cases benchmarks for testing these models. Many of the test problems based on analytical solutions developed in the 1970s and early 1980s have become 'classical' problems, used by other researchers to demonstrate the correctness of their modelling codes. Ségol (1994) describes many of these tests, as well as sample applications of these problems in the testing of computer codes. In the following section emphasis will be focused on analytical solutions to the groundwater flow equation, with particular relevance to the present work in testing the new code described herein.

Many analytical solutions have been developed for saturated flow problems, specifically with respect to well and drain hydraulics (Bear, 1979, De Wiest, 1965, Edelman, 1972, Huisman, 1972, Marino and Luthin, 1982). A compilation of analytical drain solutions has been prepared by Beljin and Murdoch (1994). Many of these analytical solutions pertain to one dimensional or radial-symmetric flow problems with different flow conditions, including steady-state and transient flow, single and multiple aquifers, confined, leaky-confined, and unconfined aquifers, anisotropy, partial penetration of production and observation wells and drains, and time-varying boundary conditions or aquifer stresses. In well hydraulics, analytical models are used for the analysis of pumping test data or preliminary estimates of complicated well and contaminant source impacts. Appropriate use of the superposition principle enhances the utility of these analytical solutions, especially for two and three-dimensional numerical models testing.

Their independent results offer a valuable tool to check the correctness and accuracy of numerical solutions and insight into the sensitivity of the results to key parameters (Burns 1983). Examples of some classical analytical solutions are presented in the following.

**(i) One –dimensional plane symmetric flow**

In practice, many cases involving two-dimensional flow in the vertical plane can be reduced to a one-dimensional flow when the assumptions of essentially horizontal flow in an aquifer are justified. Considering the cross section shown in Figure 2.5, it can be assumed that the geometry is such that the flow is essentially horizontal and is in the  $x$  direction. The solutions of the three different regimes that can occur are as follows (Spitz and Morenao, 1996, p. 89):

- *Steady state:*

$$\text{Confined flow:} \quad \phi = Ax + B \quad (2.18)$$

$$\text{Leaky flow:} \quad \phi = Ae^{x/\lambda} + Be^{-x/\lambda} \quad (2.19)$$

$$\text{Unconfined flow:} \quad \phi = -\frac{N}{K}x^2 + Ax + B \quad (2.20)$$

where  $\phi$  is head at distance  $x$  [L],  $x$  is distance [L],  $K$  is hydraulic conductivity [L/T],  $\lambda$  is leakage factor [L],  $N$  is natural groundwater recharge [L/T], and  $A$  and  $B$  are constants to be determined from boundary conditions.

- *Unsteady state:*

One-dimensional unsteady flows are governed by the continuity equation such as

$$T \frac{\partial^2 \phi}{\partial x^2} = S \frac{\partial \phi}{\partial t} \text{ for a confined aquifer, or a phreatic surface given } T = Kh = \text{const.}, \text{ and}$$

$$T \frac{\partial^2 \phi}{\partial x^2} - \frac{\phi}{\lambda^2} = S \frac{\partial \phi}{\partial t} \text{ for a leaky aquifer. With respect to initial and boundary conditions,}$$

solutions of similar equations in other areas of physics can be found in the literature (Carslaw and Jaeger, 1959).

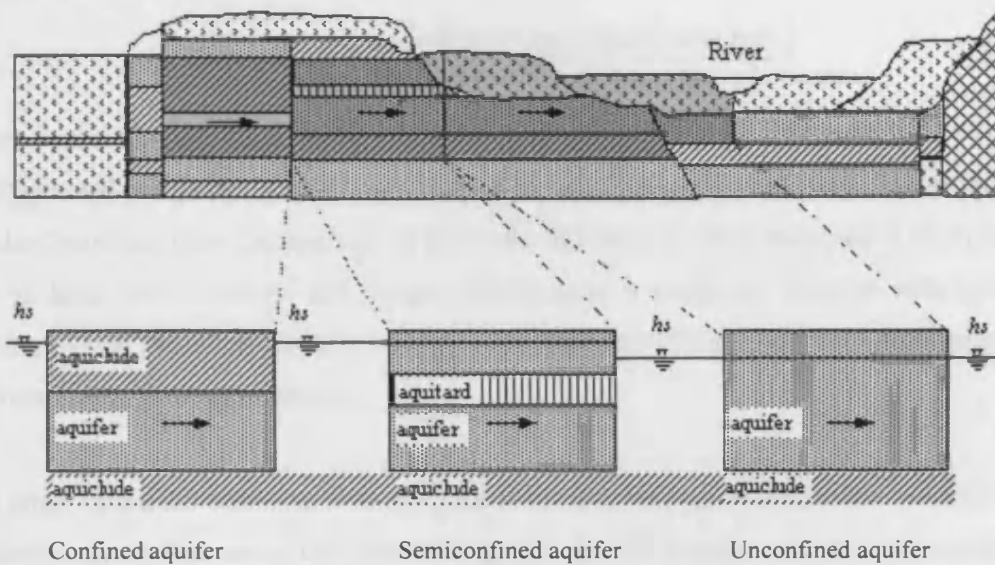


Figure 2.5 A one-dimensional hypothetical flow problem.

**(ii) Two-dimensional flows in vertical plane**

Toth (1962) derived an analytical solution to for two-dimensional steady regional groundwater flow system where the aquifer is assumed to be homogenous and isotropic. The aquifer domain is represented by a rectangle where the vertical sides and the lower boundary satisfy the Neumann conditions (i.e. no-flow) and the upper boundary is of Cauchy type, with a linear variation of heads as shown in Figure 2.6.

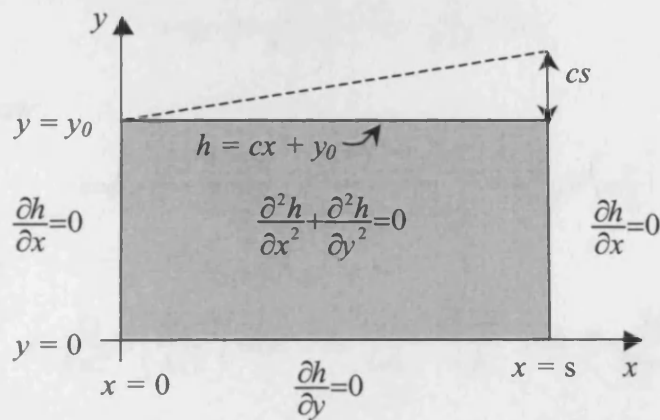


Figure 2.6 Mathematical model of the regional flow system described by Toth (1962).

The solution for these conditions is:

$$\phi(x,y) = y_0 + \frac{cs}{2} \frac{4cs}{\pi^2} \sum_{m=0}^{\infty} \frac{\cos[(2m+1)\pi x/s] \cosh[(2m+1)\pi y/s]}{(2m+1)^2 \cosh[(2m+1)\pi y_0/s]} \quad (2.21)$$

As can be noted, this problem is governed by Laplace's equation. This equation has been largely treated in mathematics (Crank, 1956). A wide range of boundary-value problems has also benefited from the analogy of flow and diffusion to other phenomena in physics, such as heat flow. Carslaw and Jaeger (1959) gave a complete range of solutions to boundary-value problems for heat conduction, with many of these solutions being applied to groundwater flow applications.

To a large extent 2D transient flow methods have been utilised to determine the hydraulic properties of aquifers using the permeability and specific storage pumping test methods. Walton (1970) compiled many illustrative case studies of pumping test analysis, with the practical aspects of pumping tests and well hydraulics also being summarized by Driscoll (1986).

### (iii) Radially converging flow

For an infinite homogenous isotropic aquifer, transient solutions for flow to a single perfect well with Dupuit assumption are given for:

Confined flow:

$$s = \phi_0 - \phi = \frac{Q}{4\pi T} \int_u^{\infty} \frac{e^{-y}}{y} dy = \frac{Q}{4\pi T} W(u) \quad (2.22)$$

Semi-confined flow:

$$s = \phi_0 - \phi = \frac{Q}{4\pi T} \int_u^{\infty} \frac{1}{y} \exp\left(-y \frac{r^2}{4\lambda^2 y}\right) dy = \frac{Q}{4\pi T} W\left(u, \frac{r}{\lambda}\right) \quad (2.23)$$

Unconfined flow:

$$s' = \frac{Q}{4\pi T} W\left(\frac{S'r^2}{4Tt}\right) \text{ with } s' = s - \frac{s^2}{2\phi_0} = \frac{\phi_0^2 - \phi^2}{2\phi_0} \text{ and } S' = \frac{S\phi_0}{(\phi_0 - s)} \quad (2.24)$$

where  $s$  is the drawdown [L], defined as the difference between a constant initial piezometric head  $\phi_0$  and the piezometric head  $\phi$  at a radial distance  $r$  and time  $t$ .  $Q$  is a constant well discharge or recharge,  $T$  is transmissivity [ $L^2/T$ ], and  $\lambda$  is a leakage factor [L].  $W(u)$  is the well function of  $u=r^2S/(4Tt)$  for a confined aquifer.  $W(u,r/\lambda)$  is the Hantush well function for a leaky aquifer. Tables of both mathematical functions can be found in the literature related to well hydraulics (Bear, 1979). Equation 2.22 is the well-known formula of Theis (1935).

Due to the linearity of the flow equation in the confined and semiconfined aquifer cases, further solutions can be constructed from the single well solutions by superposition, provided that boundary conditions can also be superimposed. This principle allows numerous solutions to be obtained for multiple-well flows in confined aquifers. A linearised approximation can be used for the equation for the phreatic aquifer in  $s'$ , if we substitute  $\phi$  with  $\phi_0 - s$  and  $S$  with  $S'$  allowing the superimposition of drawdown with respect to  $\phi^2$ . Examples of the analytical solutions for flow to wells for different hydrogeologic conditions can be found in Hantush (1960), Walton (1962), Papadopoulos (1965), Lohman (1972), Reed (1980), and Benett et al. (1982). Analytical solutions for well flow are used mostly in analysing pumping test analyses. The aquifer response in terms of drawdown is used to calculate the missing aquifer parameters, most often storativity and transmissivity. This technique is used basically to solve so-called inverse problems aiming to identify missing aquifer parameters. Ready-made computer programs that analyse pumping tests can be obtained from several sources such as Boonstra and Keselik (2001). More generally, models based on analytical solutions are listed in Table A.1 in Appendix A. They simulate the flow process for different hydrological conditions, with the list not being exhaustive and not describing all of the model capabilities (e.g. transport process, heat, graphical capacities, etc.). These features and other details such as: availability, cost, proprietary, user, hardware requirements, etc., can be found in the relevant references.

### 2.4.2 Limits

Where possible, preference should always be given to analytical solutions over numerical modelling. This will rely on the simplifications that can be made to approach the groundwater problem without substantial loss of accuracy. If a chosen analytical method is consistent with the hydrogeological controls, then analytical solutions can be more beneficial. They are numerically stable, readily obtained and are cheaply applied. This type of solution is generally also more efficient and accurate than other model types, if analytical solutions for the investigated groundwater problem exist. They usually involve approximate or exact solutions to simplified forms of the differential equations for water movement and their results are often used as a reference in simple test cases for the verification of newly developed numerical models. However, the number of simplifying assumptions regarding the flow system that are necessary to obtain analytical solutions represents a serious restriction to the real world representation by these models type and therefore limit their use. Hence, in certain complex modelling exercises, analytical models can only be used as a screening tool to conduct a rapid preliminary analysis of the behaviour of an aquifer system, to perform sensitivity analyses or to scope the problem to determine data needs. For example, one advantage of this practice is that the solution can be applied to different values of the parameters ( $K$ ,  $S$ ) and inputs (i.e. geometrical dimensions) involved and that it clearly shows the influence of each parameter. Analytical solutions are also judged more appropriate in field situations where few data are available, as use of complex numerical models would be very limited. To overcome some of the limitations of analytical solutions, a relatively new and useful extension of analytical models is the 'analytical element models'. Unlike the first type, these models can incorporate moderate levels of layering, inhomogeneity, and boundary conditions. They are more complex to use than analytical models, but are simpler than numerical models.

### 2.4.3 Analytic Element Methods

Analytic element models were first introduced by Strack and Haitjema (1981a, 1981b). The theoretical basis for the method is presented in Strack (1989). Application of the

method to groundwater flow problems is discussed in detail by Haitjema (1995). The method is based on the superposition of closed-form analytical solutions, referred to as analytic elements, to the governing differential equation to create an approximate but analytical solution to both local and regional flow. Hence, analytic element models do not require grid discretisation or specification of boundary conditions on the grid perimeter. There are specialised analytic elements that represent aquifer inhomogeneities, lakes, streams, wells, and spatially varying leakage and infiltration. The flow solution is written as the summation over harmonic functions and particular solutions to the Poisson equation. Analytic elements are not obtained by integration but instead by conformal mapping (Strack, 1989). Once the solution is calculated then the hydrogeological parameters can be obtained for any location in the aquifer. This method differs from classical analytical solutions in that the analytic elements are not restricted to a single boundary value problem, but possess degrees of freedom that allow the solutions to be combined.

The analytic element method is extensively applied for water management purposes (De Lange, 1991). A widely known application of this modelling technique is the delineation of wellhead protection areas (WHPAs) in a single layer or multi-layer setting (Wuolo et al., 1995). So far, the analytic element method has also been applied in groundwater flow to model special cases such as: steady flow in aquifers with properties that are piecewise constant and large aquifer system. In fact, one of the advantages of this method is that the model domain can be infinite, thus the user is not constrained by aquifer boundaries or by a grid mesh as for numerical methods. Moreover, regional scale as well as small-scale groundwater flow could be examined without changing parameters, boundary conditions, grid, or resolving the system of equations common to the implementation of numerical methods in groundwater models. This approach therefore saves time during model development and mass is always conserved (unlike finite methods). However, analytic element methods have shown limited capabilities for simulating transient flow conditions and restricted validity conditions for the case of unconfined aquifers. More complex local flow features are not easily handled. The latest advances in the application of the analytic element method to groundwater flow can be found in Bakker et al. (2000, 2003), Haitjema et al. (2000), Fredrick et al. (2004). Further developments of this method to large-scale applications, rotational flow and transient flow are still ongoing.

In conclusion, the complexity of real problems often involves conditions that are beyond the scope of analytical solutions. In fact, in most regional studies an analytical solution is not possible, mainly because of:

- irregularity of the shape of the aquifer boundaries (i.e. analytical solutions are available only for simple geometries such as rectangular or circular, or infinite dimensions,
- variations in the type of boundary conditions,
- nonhomogeneity in the transmissivity and storativity properties, and their distribution cannot be generated within analytical expression, and
- variations in the initial conditions and for the various inputs and outputs (natural recharge, artificial recharge and pumping).

Therefore, problems related to boundary conditions and inhomogeneities make analytical models seldom applied to the solution of regional flow studies. Phreatic aquifers, multilayer systems and anisotropy are subject to complex patterns of development because of the nature of the PDEs that describe these processes. Numerical methods are more widely used to tackle these kinds of problems when sufficient data have been collected. Analytical models should be viewed as a useful complement to numerical models. In the present work, specific analytical solutions will be invoked as benchmark examples for code testing and verification.

## **2.5 Review of Numerical Models and Limits:**

Compared to analytical models, numerical models offer many advantages, which include the ability to:

- simulate more complex physical systems (including non-linear problems);
- simulate multidimensional systems;
- incorporate complex boundary conditions;
- accommodate spatial variability of input parameters;
- accommodate both steady-state and transient conditions; and
- simulate both spatial and temporal distributions of model output.

Therefore, numerical models are better suited to simulating real flow field problems. In fact, once the conceptual model has been translated into a mathematical model in the form of governing equations, with associated boundary and initial conditions, the formulation could be more complex than that for an analytical solution. A solution can only be obtained by transforming the mathematical model into a numerical model and then writing a computer code to solve the numerical model. Different existing numerical techniques and codes are discussed in this chapter.

### **2.5.1 Existing Numerical Techniques**

Many numerical methods have been developed for general CFD applications. They are used to solve the different combinations of diffusion – advection problems. Groundwater problems can generally be described by the pure diffusion equation (i.e. flow problems), or by the diffusion-advection equation (solute transport, variable density flow). In this study, emphasis has been focused on flow problems that are generally dominated by diffusion and hence research has been restricted to an investigation of techniques used for this type of mechanism. The principal methods currently in use for similar equations in CFD applications are as follows (Abott, 1989):

- Finite difference method
- Finite element method
- Integrated finite difference method
- Boundary element method
- Finite volume method

All of these methods have already been discussed in groundwater applications, and some of the corresponding codes have been developed and used successfully. The first two methods are the most extensively reported for groundwater flow problems. The widespread use of classic codes based on these techniques has proven their strength for certain applications, but also their weaknesses for others. The three latter methods are newer and the extent of their application to groundwater flow problems is still being investigated. Recent advances of these techniques in the solution of special case problems

have contributed to the understanding of how these methods can be expanded to other groundwater flow applications. A description of each method and a comparison between their performances are provided.

Unlike analytical methods, numerical models are used as an approximate method of solving the partial differential equations stated in the flow mathematical model. The resulting hydraulic head is no more given as a continuous function of space, but as a set of numerical values of the variables at specified points in the space and time domains defined for the problem. The partial differential equations are replaced by a set of algebraic equations in terms of discrete values of the piezometric head at discrete points. Therefore, the first step in the solution process using a numerical method is the discretisation of the spatial and temporal terms within the model domain. The numerical methods mentioned above are used as discretisation methods for the spatial terms, whereas time-stepping methods are used to discretise the temporal term.

#### **2.5.1.1 Finite Difference Method**

Finite-difference approximations were first introduced in the classic paper of Richardson (1910). Applications of the method for solving partial differential equations have since been the subject of many books (Forsythe and Wasow, 1960, Smith, 1965, and Richtmeyer and Morton, 1967). The basic idea of the finite difference method is to replace the derivatives at a point by the ratio of changes in the appropriate variables over a small but finite interval using the Taylor series expansion. The problem domain is divided into a rectangular grid in which solutions are calculated in discrete points called nodes. In the finite difference method, nodes may be located at cell centre (i.e. the block centred formulation) or at the intersection of grid lines (i.e. the mesh centred formulation). Figure 2.7 illustrates, in two dimensions, these two cell conventions. The system parameters, such as permeability, natural groundwater recharge and length, are assumed to be constant within each cell. Water heads are calculated as discrete values at the grid nodes, or at the centre points of the cells, depending on the grid convention. The continuity equation is then written in terms of each nodal point, regardless of the representation. Time step sizes are specified over the simulated time of interest, and the mathematical expressions are solved successively for each individual time step. The

mathematical problem is then reduced to a linear system of equations that could be solved using matrix algebra. Comprehensive treatments of the application of this numerical method to groundwater problems can be found in Remson et al. (1971), and Wang and Anderson (1982).

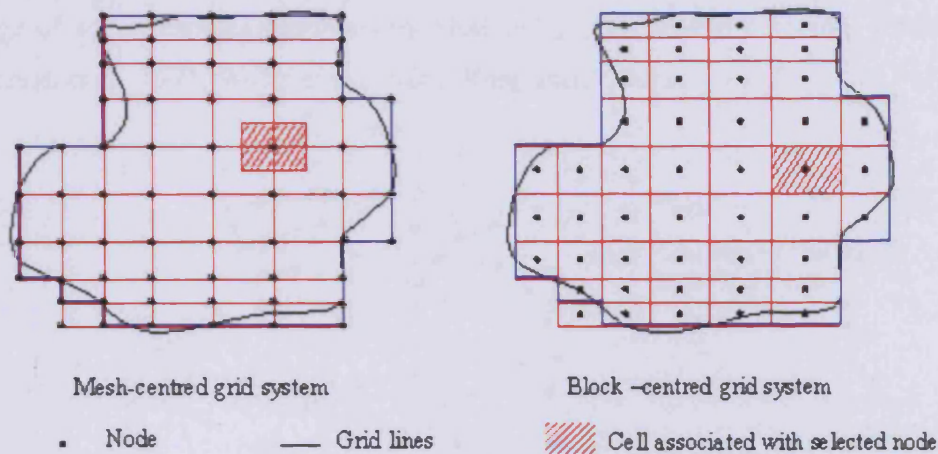


Figure 2.7 Finite difference grid conventions in two dimensions.

### 2.5.1.2 Finite Element Method

Zienkiewicz (1977) gave a detailed mathematical description of the Finite Element Method (FEM). Particular applications of this technique to fluid mechanics are available in numerous books, such as Fletcher (1984), Chung (1978), Connor and Brebbia (1976). While approximations to a continuous solution are defined at isolated points by finite differences, the approximate solution in FEM is defined over the entire domain by interpolation functions, although solutions to the functions are calculated only at the element nodes. In this sense the finite element approach differs from the finite difference method by approximating the flow equation by integration rather than differentiation. The model domain is subdivided into elements that could have any shape (e.g. triangular, quadrilateral; etc., see Figure 2.8). Hence the head distribution for each element is approximated by a linear interpolating function, such as piecewise linear functions or other higher-order interpolation functions (Pinder and Gray, 1977). When this approximate solution is substituted into the governing differential equation, an error or

residual occurs at each node. The weighted residual method of Galerkin is the commonly used approach to minimize the error between the approximate and actual solution for each node, by forcing the weighted average of the residuals for each node to equate to zero. A set of algebraic equations is formed for the unknown groundwater heads. The solution of the system will depend on the chosen time discretisation with treatment of a range of water resource problems by FEM being presented in numerous references (e.g. Remson et al., 1971, Wang et al., 1980, Wang and Anderson, 1982).

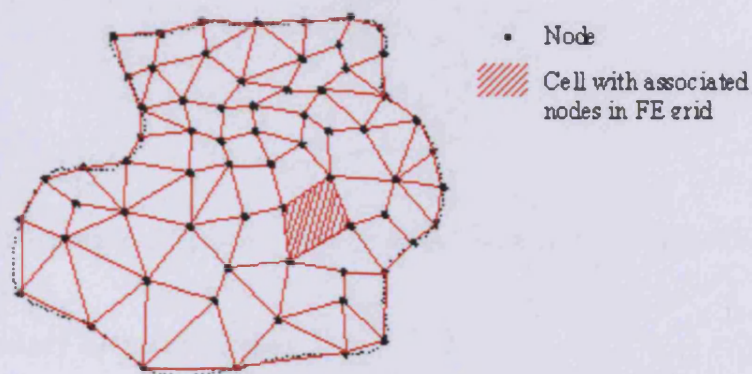


Figure 2.8 Example of finite element grid in two dimensions.

### 2.5.1.3 Integrated Finite Difference Method

The integrated finite difference method (IFD) has been used for investigation of water flow in soils, inter alia by Todd (1959), Cooley (1971) and Narasimhan and Whitherspoon, (1976). The method was first devised by Mac Neal (1953), who implemented the finite-difference method with an asymmetric grid. In this method, the domain is subdivided into elements of an arbitrary shape, implying that a quadratic or rectangular grid in the FD context can be substituted by a more complex system of triangles, trapezoids, polygons, etc. However, to secure the maximum accuracy, then each segment of the sub-area should be perpendicular to lines joining the adjacent nodes (Figure 2.9). The basic set of algebraic equations is obtained by considering the mass balance of each element by integration of the governing equation over their volume. The unknown variable is most conveniently defined at the centroid of each element with the

fluxes through to each elements interface being computed by a FD approximation. Application of IFD method in groundwater flow can be found in many references (e.g. Voss, 1984, Pruess, 1987, Ferraresi and Marinelli, 1996).

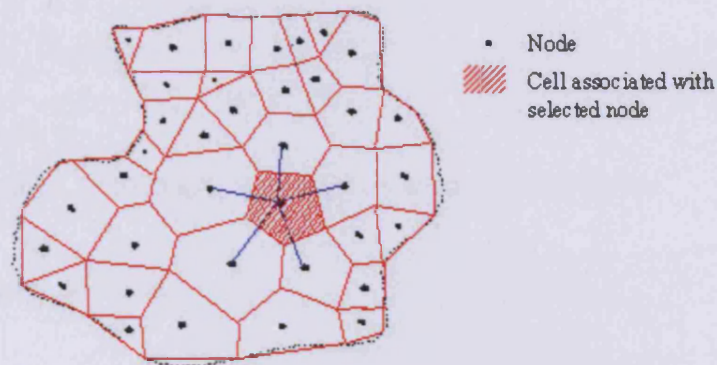


Figure 2.9 Example of integrated finite difference element grid in two dimensions.

#### 2.5.1.4 Boundary Element Method

The boundary element method (BEM) is also known as the boundary integral equation method (BIEM), with Brebbia and Walker (1980) first giving a general introduction to this method. The approach consists of dividing the external surface of the boundary into a series of elements, over which the functions under consideration are assumed to vary in much the same way as for the finite element method (Figure 2.10). This approach produces a series of nodal unknowns on the surface of the domain, rather than for the whole domain as for the finite element discretisation. The nodal unknowns are then related through the influence functions requiring boundary conditions to be satisfied at nodes along boundaries. This leads to a system of  $N$  equations with  $N$  unknowns and with these equations being usually linear. The number  $N$  relates to the number of points or nodes along the boundary and not, as in FD and FE methods, the number of points in the interior of the domain and along its boundary. If the solution is also explicitly required inside an element, then its value is calculated by numerical integration within the element. Illustrative applications of the BEM to groundwater flow problems have been given by Isaacs and Hunt (1981), Liggett and Liu (1983), Cheng and Ouazar (1993) and Archer (2000).

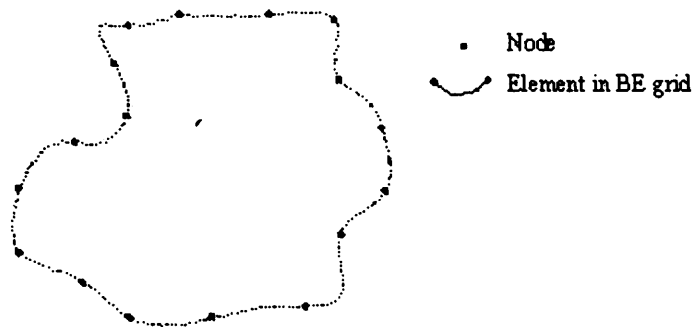


Figure 2.10 Example of a boundary element discretisation.

### 2.2.1.5 Finite Volume Method

In the Finite volume method (FV), or control-volume method, the problem domain is divided into discrete control volumes of any shape (e.g. triangles, polygons) with associated grid points. The conservation statement is applied in an integral form of the PDE across the control volume. The resulting discretised equation at a nodal point accounts for the cross-sectional fluxes and the properties that may be approximated by linear interpolations or other forms of the approximations. The finite volume procedure can in fact, be considered as a variant of the finite-element method (Hirsch, 1988, p. 223), although, from another point of view, it is just a particular type of finite difference scheme (Tannehill et al., 1997, p. 72). A detailed description of this method is provided in chapter four.

### 2.2.1.6 Time Stepping

Once the spatial domain is discretised with one of these methods, and when the governing equation is time dependent, then the temporal term is usually approximated by a time- stepping technique. This approximation is generally carried out in some finite difference way and is similarly employed in finite difference, finite element, boundary element or finite volume transient models. Four of the most commonly used time-stepping schemes include: Explicit, Implicit, Mixed Explicit-Implicit, and Alternating Direction Implicit (ADI) procedures. The application of any one of these schemes

dictates how the nodal variables in the system of space-discretised equations are plotted against time (i.e. both for backward or forward time levels). The end result is a system of multiple equations with multiple unknowns for each node. The number of unknowns in each equation depends upon the time-stepping scheme, which defines the type of matrix describing the resulting equations system. As a consequence, the choice of a time-stepping method influences the model run-times as well as the results. Explicit methods are simple but conditionally stable (i.e. in terms of time steps size), and they often require an excessive number of time steps. Implicit scheme produces unconditionally stable numerical solution and is much more flexible and robust than the explicit scheme (Kinzelbach, 1986, p. 36). However, the matrix formulation and solution procedure require substantial additional computational effort. Mixed Explicit-Implicit methods can be weighted in favour of either method, using a factor that ranges from 0 to 1. This usually produces an unconditionally stable solution which is more robust than explicit schemes, and generally more efficient. The ADI procedure also produces unconditionally stable numerical solutions for flow and transport, but is limited to rectangular finite-difference grids. Some of these schemes will be used and tested in this work during the treatment of the groundwater flow equation.

### 2.2.1.7 Matrix Solvers

The partial differential equations outlined above may be replaced by a set of algebraic equations in terms of discrete values of the unknowns (i.e. piezometric head or solute concentration) at discrete points. The resulting set of equations can be expressed as a matrix equation that can be solved using direct or iterative techniques, developed in matrix algebra.

In *direct methods*, a sequence of operations is performed only once to solve the matrix equation, thereby providing a solution that is exact, except for machine round-off error. These methods include three types of solutions, namely:

- solution by determinants,
- solution by successive elimination of the unknowns, and
- solution by matrix inversion.

These methods, however, have two key disadvantages: computer resource requirements (i.e. large storage and long computational times for large problems) and round-off error due to the large number of arithmetic operations performed.

*Iterative methods* avoid the need for storing large matrices. They arrive at a solution by a process of successive approximations. They involve making an initial guess at the solution, then improving this guess by some iterative process until an error criterion is satisfied. Therefore, in these techniques, convergence and efficiency are of concern. They may be less efficient than direct methods in terms of CPU time if a large core is available, but they are less sensitive to round-off errors (De Marsily, 1986). They are therefore very much still in use, especially with micro- or minicomputers. The most common iterative schemes used in groundwater numerical models include the following:

- Iterative Alternating Direction Implicit Procedure (IADIP)
- Successive Over-Relaxation Techniques (SOR)
- Strongly Implicit Procedure
- Preconditioned Conjugate Gradient techniques (PCG)

Each method presents qualities and limitations inherent to accuracy, convergence and the number of unknowns for each type of numerical model. Likewise, familiarity with the capabilities of these solvers provides a general recognition of the technical terms and also gives some indication as to the potential hardware requirements. These requirements are rarely part of the deciding factor in the code selection process but are very important in the code development process as the code numerical capabilities, and therefore limitations, will strongly depend upon the robustness of the solver. A description of these techniques along with their performances can be found in Varga (1962). Their implementation for solving linear systems in groundwater flow modelling is described by Remson et al. (1971) with the choice of the appropriate matrix solver for this work and its performances being addressed in Chapter 4.

### 2.5.2 Comparison and Discussion

Many numerical groundwater models have been developed over the past thirty years or so to simulate flow and contaminant transport. These models vary in terms of the assumptions, governing equations, numerical techniques, data requirements and outputs. In this section emphasis will be focused on the importance of the numerical method used to approximate groundwater flow equations. The choice between the different numerical models in this type of application depends upon the equations to be solved and on the preference of the user. The five numerical techniques outlined in the previous differ in their capabilities and in the way they handle special features, such as boundary conditions, flow regime, heterogeneities, anisotropy, sources, time- or potential-dependent changes in parameters etc.

The finite difference method has been extensively used in a range of engineering problems related to groundwater flow, especially with saturated zone (e.g. MODFLOW). Its relatively simple formulation and accuracy in tackling diffusion-dominated problems are its major assets. However, the use of a rectangular grid to discretise the problem domain necessitates a stepwise approximation of irregular boundary and aquifer zoning. Therefore, the mesh has to be refined along boundaries of interest to obtain the satisfying accuracy, which unnecessarily increases the computational effort in other areas of the domain. The IFD method offers more flexible approximations to the model domain and a balance is always conserved. However, for accuracy reasons, surface of elements should remain perpendicular to the lines joining adjacent nodes. From this viewpoint, the relevant characteristics of the finite element method, in comparison with the finite difference method, is its capability of designing an arbitrary grid. This allows a much greater flexibility in handling irregular domain geometries, material heterogeneities, anisotropy, meandering stream channels and wells, etc. However, boundary conditions are frequently imperfectly known in standard modelling approaches using the finite difference or finite element method, especially when simulating local flow conditions. In this sense, analytic element models are ideally suited for use in solving the regional flow problems as screening models and thereby developing boundary conditions for the local flow problem. Thus, inaccuracies related to the location of boundaries and their

conditions can be sensitively reduced and flux calibration of finite difference and finite element models simply improved. An example of improved finite-difference groundwater flow model using the results from an analytic element model can be found in Hunt et al. (1998). This example can be verified for a finite-element groundwater flow model. The incorporation of the analytic element method in finite difference or finite element models may be a potential field of research for improving calibration procedures for regional groundwater flow applications.

Finite element results are usually accurate for the original variable (i.e. hydraulic head) but when this variable is differentiated to obtain fluxes then the results are much less accurate and are usually discontinuous between elements. The problem is aggravated further if regions of high fluxes occur in the continuum. In this case, the boundary element method offers more accurate solutions with relatively simpler input data, especially for three-dimensional problems (Brebbia, 1980). Another important advantage of the boundary element method, which is of particular importance in water resources, is its ability to model domains extending to infinity without defining arbitrarily truncated boundaries where specific conditions are applicable. Because of this advantage, the BEM is increasingly being used to model problems with infinite or semi-infinite domains such as those occurring in geomechanics, ocean engineering, aerodynamics, and many other related problems (Brebbia and Wrobel, 1991).

### 2.5.3 Limits

Common limitations of numerical models include:

- the requirement of more development time compared to an analytical model of the same process;
- the requirement of greater amounts of input information where, for many field situations, limited data are available which often narrow the use of complex numerical models; and
- the possibility of numerical instability, which may cause the numerical model to become difficult to implement without major modifications to the geometric layout of the model domain.

A major asset of the finite difference method is its relatively simple formulation as compared to other numerical methods. The method also has a big advantage in computer storage in that the method generally leads to a banded and symmetric system. However, the method includes many limitations, such as:

- the use of a rectangular grid system necessitates a staircase (or stepwise) approximation of irregular and/or aquifer material zoning (e.g. heterogeneity, anisotropy, aquifer layers);
- the sensitive predictions to grid orientation effects in solving 2D and 3D flow and transport problems; and
- the vulnerability of the method to numerical dispersion or oscillations in solving transport problems.

From the first limitation viewpoint, the IFD method offers a more flexible grid discretisation with a mass balance that is always conserved. However, the orthogonality condition still presents a considerable difficulty in the representation of the problem domain with well-fitted grid and grid generation techniques becoming a more complex task. The variant of this method is the finite volume approach where any grid shape may be used, and the simplicity of the mathematical formulation is still conserved.

The finite element method also allows great flexibility in handling irregularities. It is less sensitive to grid orientation and less prone to dispersion but needs more care to limit potential oscillation in solving transport problems. The limitations of the finite element method include:

- complex data requirements to run a FE programs;
- long computer coding; and
- greater computational effort and computer storage capability for the solution of the generated matrix.

The boundary element method has a key advantage over all the numerical models, in that the precision of its calculations is not a function of the size of the elements used. Thus, few element need to be used, which considerably reduces the size of the resulting matrix

and, therefore, the memory and computational time requirements. The main restrictions of the method are:

- its limitation to linear problems (Pęcher and Stanislav, 1997)
- the need for a large number of elements to describe heterogeneity of the medium, and thus lose its superiority over FD and FE methods.

None of these methods is known to be ideal for a range of groundwater problems. The numerical methods that work best for parabolic PDEs (i.e. governing the flow and dispersion-dominated transport equations) are not best for solving hyperbolic equations (i.e. governing advective transport), and vice versa. The choice of whether to use one method or another will generally be a matter of personal preference. There is currently still much research on developing better mixed or adaptative methods that aim to minimize numerical errors and combine the best features of alternative standard numerical approaches (Carrera and Melloni, 1987, Neuman, 1984, Celia et al., 1990, Gottardi and Venutelli, 1994, Osnes and Langtangen, 1998, Meerschaert and Tadjeran, 2004). The present work is one such example.

## **2.6 Existing Codes and Limitations:**

### **2.6.1 Existing Codes**

In recent years, codes have been developed for almost all classes of problems encountered in the management of groundwater. Some codes are very comprehensive and can handle a variety of specific problems as special cases, whilst others are tailor-made for particular problems. Many of these codes have been developed or adapted for microcomputers and have benefited from the increasing development of computer speed, memory storage and graphical capacities. In groundwater flow applications codes are structured around the numerical algorithms that can tackle fluid flow problems, and these algorithms are called solvers. In addition, many codes offer considerable easy access to the code solving power. In fact, nowadays, all commercial CFD packages include sophisticated user interfaces to input parameters and to examine results. Hence, most codes contain three main elements:

1/ *a pre-processor*: pre-processing consists of the input of the flow problem and the transformation of this input into a form suitable for use by the solver. A pre-processor is a computer program that assists the modeller in:

- \* Defining the geometry of the region of interest namely the computational domain.
- \* Generating the grid.
- \* Selecting the physical and chemical phenomena that need to be modelled.
- \* Defining the fluid properties.
- \* Specifying the appropriate boundary conditions.

Certain pre-processors also offer some data import facilities, linked to external databases or other codes.

2/ *a solver*: a computer code that performs the following steps:

- \* Approximates the unknown flow variables by means of simple functions.
- \* Discretises by substituting approximations into the governing flow equations and subsequent mathematical manipulations.
- \* Solving the algebraic equations.

3/ *a post-processor*: a computer program that offers graphic capabilities for data visualisation. These typically include:

- \* Domain geometry and grid display.
- \* Vector plots.
- \* Line and shaded contour plots.
- \* 2D and 3D surface plots.
- \* Particle tracking plots.
- \* View manipulation (i.e. translation, rotation, scaling etc.).
- \* Animation displaying results dynamically.
- \* Colour postscript output.
- \* Data export facilities for further manipulation external to the code.

Public domain programs have generally less user-friendly facilities and concentrate more on the solver performances. Such capabilities are part of the code-related selection criteria that users consider in groundwater flow applications.

A summary of some of the existing numerical codes for groundwater flow simulations in saturated zones is given in Table A.2 in Appendix A. The list is not exhaustive and does not describe the entire model capabilities, as in this study interest is restricted to flow modelling and the method used. Additional information about the performance of each code, and its functionality or applicability, can be found in the corresponding references. Specific technical characteristics concerning accuracy, stability, data preparation or execution can be analysed by using test problems (included in the programme documentation or elsewhere) or collecting previous user comments and criticisms.

It has been noticed that over 500 computer programs for analysing ground-water problems exist (Van der Heijde, 1996) and the number is increasing as many codes that have been developed primarily for research purposes are being further developed into readily useable computer programs. One problem, however, is that there is no commonly agreed methodology to evaluate ground water model applications. Faced with decision-making based on model applications in numerous water quality issues, regulatory personnel need guidance for objective model evaluation. An expert system for selecting appropriate computer programs for analysing groundwater problems could be a very helpful tool to promote their use among local communities. Some authors have already proposed such systems for specific objectives, such as pumping-test expert system (Ouazar et al., 1996), groundwater protection programs, wellhead protection program (Wang, 1997), or ground water management focused on hazardous waste site risk assessment and cleanup activities (Chowdhury and Canter, 1998). Some governmental bodies have published their guide to the selection and application of mathematical models of contaminant transport processes (NGWCL, 2001, USEPA, 1994). More generally, The selection of the appropriate model for a particular field problem depends upon the modelling objectives, the criteria that are site specific and other data that are code related, as presented in Table 2.3. Among the latter, model accuracy will be more detailed for its relevant importance to the present work.

### 2.6.2 Accuracy of Numerical Models

The accuracy and reliability of numerical models relies on the minimisation of errors and uncertainties. In groundwater model applications, there are three sources of errors (Konikow and Bredehoeft, 1992):

- conceptual errors: they are theoretical misconceptions about the basic processes that are incorporated in the model
- numerical errors: they arise in the equation-solving algorithm and include truncation errors, round-off errors, and numerical dispersion (in transport models);
- errors arising from uncertainties and inadequacies in the input data, which reflect our inability to describe comprehensively and uniquely the aquifer properties, stresses, and boundaries.

In most model applications conceptualisation problems and uncertainty are the most common sources of error. Recent research emphasises how to incorporate uncertainties into modelling studies. Yangxiao and Van Geer (1992) presented a stochastic program to quantify and reduce the uncertainty of the groundwater flow input data processed by the numerical model MODFLOW. Linking stochastic and numerical models has been suggested by many authors (Anderson and Woessner, 1992, Krakostas et al., 1998). Moreover, for complex flow process simulation, stochastic models are often more efficient alternatives for prediction than numerical models. Flows in unsaturated porous media (Harter and Yeh, 1998), fractured media (Selroos et al., 2002) and multiphase flow (Ghanem and Dham, 1998) are examples of such cases.

In model development, errors occur at the level of the mathematical treatment of the governing equations, generating accuracy, consistency, stability or convergence problems. In the present work, a new numerical model will be developed. Therefore it is of interest to improve the accuracy of modelling through the minimisation of these error types. As numerical models are about approximations, these errors are generated while approaching the domain by a set grid, while integrating or differentiating the governing equations (i.e. the mass balance), while interpolating the different model parameters and while solving the resulting system of equations. Many research papers have used different combinations of existing techniques of spatial and temporal discretisation,

interpolation and solvers to improve the accuracy and performance of the numerical models in different CFD applications.

Model accuracy can be measured by comparing the results of the model code with an independently derived value for the calculated entity, assuming that this latter code gives the correct result for the calculations (i.e., the benchmark). One other measure of model accuracy is how accurately the model conserves mass. This can be measured by comparing the net fluxes calculated or specified in the model (e.g. inflow and sources, minus outflow and sinks) with changes in storage (i.e. accumulation or depletion).

### **2.6.2 Codes Limitations**

Codes are the result of the implementation of a numerical technique on a computer by means of a programming language. Thus, technical code capabilities and, therefore, limitations depend upon the performance of the numerical method as well as the performance of the computer platform. Evaluation of these limitations is important for code selection or improvement, with code limitations being broadly classified as:

- conceptual model-related: hydrogeological features and process that can be simulated. This process relies on the assumptions made when developing the model (confined/unconfined, dimensions, boundary conditions, steady/transient, isotropy/anisotropy, transport considerations, heat considerations, etc.);
- mathematical solution-related: these limitations have been discussed in the previous paragraphs. If a numerical technique is used in the code, then the limitations will depend upon whether a FD, FE, FV, or BE scheme has been chosen. Therefore this type of limitation will affect the level of accuracy and efficiency of the code, along with the stability and affect conditions (i.e. grid and time spacing, size, shape, orientation);
- hardware (portability)-related: storage capacity (memory), the numerical precision of calculations and speed will limit the number of cells, time steps, model size and the amount of data that can be handled (i.e. programming language).

In this work, we will be primarily interested in the limitations related to numerical techniques.

## **2.7 Conclusions and Relevance to Present Research**

Groundwater flow models have been widely investigated by engineers, hydrogeologists and mathematicians. For higher accuracy considerations, more complex features have to be considered. Different deterministic, stochastic or heuristic techniques have been deployed, but not proven as the ultimate appropriate approach for a given class of problems. In this chapter existing techniques for groundwater flow modelling have been presented, along with their applicability and limitations. Numerical models have been the most intensively investigated techniques. The growth of this particular field of research is essentially due to the continuous development of more accurate solutions or approximations to the PDEs governing CFD applications and the more easy-to-use pre and post-processors, in parallel with the development and widespread availability of faster, larger memory, and less expensive computer systems. In the next chapter, one of the most popular groundwater flow models, namely MODFLOW, based on finite difference method, will be presented. Chapter four will discuss in detail one of the latest numerical techniques in CFD applications, namely the finite volume method and how this method can enlarge the capabilities of MODFLOW and eliminate one of the model's key limitations. Its implementation in MODFLOW is subject to accuracy, consistency, stability and convergence analysis. A discussion about the new discretisation method and its combination with different interpolation techniques and solvers is provided in chapter four. Various tests are carried out in chapter five, ranging from known analytical solutions, mentioned above, to hypothetical problems treated with selected codes that were designed to handle similar types of problems, and for which the numerical-based techniques have been treated in this chapter.

# **Chapter 3**

## **Review of MODFLOW**

### **3.1 Introduction**

Of all of the groundwater flow models widely available, the U.S. Geological Survey three-dimensional modular finite-difference, groundwater flow model, commonly referred to as MODFLOW, is regarded by many as the most widely used by government agencies and consultant firms. The main reasons for this popularity, a detailed description of the code, and a discussion of its features, weaknesses and refinements are given in this chapter.

### **3.2 MODFLOW Description**

#### **3.2.1 Development History**

McDonald and Harbaugh from the United States Geological Survey (USGS) first developed MODFLOW in 1984. The program was originally written using FORTRAN 66 and then modified in 1988 to use FORTRAN 77. Since then, many changes, updates and corrections were introduced to the program simultaneously with its growing use. A summary of the development of the different versions of MODFLOW, and their specific features and references, is given in Table 3.1.

Version Name	Date of release	Added features/changes	USGS report references
MODFLOW Version 83/12/28	1984	Code written in FORTRAN 66.	OFR 83-875
MODFLOW-88 Version 87/07/24	1988	FORTRAN 77 version.	TWRI 6-A1
MODFLOW-88 Version 93/08/30	30/8/1993	PCG2, BCF3, STR1, HFB1, IBS1, CHD1, and GFD1 packages.	WRIR 90-4048, OFR 91-536, WRI 92-4124, OFR 88-729, OFR 92-477, TWRI 6-A2, TWRI 6-A2, OFR 91-494.
MODFLOW-88 Version 2.4	15/6/1995	TLK1 package.	OFR 94-59
MODFLOW-88 Version 2.5	23/6/1995	DE45 package.	OFR 95-288
MODFLOW-88 Version 2.6	20/9/1996	RES1, IBS improvement.	OFR 96-364
MODFLOW-96 Version 3.0	3/12/1996	Overall model update.	OFR 96-485, OFR 96-486
MODFLOW-96 Version 3.1	11/3/1997	Correction of calls to the HFB package.	
MODFLOW-96 Version 3.2	9/1/1998	FHB1 package.	OFR 97-571
MODFLOW-96 Version 3.3	2/5/2000	Error fixed in IBS code.	
MODFLOW-96 Version 3.3h	7/3/2000	HYDM package.	OFR 98-564
MODFLOW-2000 Version 1.0	20/7/2000	Enhanced modular structure, new data input methods, LPF and ADV packages added, IBS, TLK, and GFD packages are not included.	OFR 00-92, OFR 97-14
MODFLOW-2000 Version 1.1	17/1/2001	IBS, HUF, LAK, ETS and DRT packages added, HYDMOD option, EVT package modification.	OFR 00-342, WRIR 00-4167, OFR 00-466
MODFLOW-2000 Version 1.2	12/4/2001	Added support for use of binary files, bug fixes, and clarification of output.	
MODFLOW-2000 Version 1.3	11/6/2001	Error fixed in LPF package.	
MODFLOW-2000 Version 1.4	10/7/2001	LMG package.	OFR 01-177
MODFLOW-2000 Version 1.5	16/8/2001	LMT package.	OFR 01-82
MODFLOW-2000 Version 1.6	19/10/2001	Problems related to sensitivities fixed, support for new options for the name file.	
MODFLOW-2000 Version 1.7	4/12/2001	Added support for use of time-varying parameters.	Time-varying-parameters.pdf, str6.pdf
MODFLOW-2000 Version 1.8	1/5/2002	Added support related to printing of cell lists, problems fixed in ADV, LPF, HUF, LMT and RES packages, and a bug relate to the OBS and PES processes use.	OFR 01-54
MODFLOW-2000 Version 1.9	15/7/2002	Updates of LAK, GAGE, and HUF packages.	
MODFLOW-2000 Version 1.10	26/7/2002	Bugs related to the compilation of the source code and a problem in the LMG package fixed.	

MODFLOW-2000 Version 1.11	10/4/2003	DAF and MNW packages. Modifying the PCG2 package and bugs fixed.	OFR 99-217, OFR 02-293
MODFLOW-2000 Version 1.12	8/9/2003	SUB package. Upgrading the HUF and ADV packages.	OFR 03-233, OFR 02-409
MODFLOW-2000 Version 1.12.01	3/10/2003	Bug-fix release.	
MODFLOW-2000 Version 1.13.00	22/1/2004	Revision of the LAK3 package and bugs fixes for the DRT, SUB, HUF2, and PCG2 packages.	OFR 03-347
MODFLOW-2000 Version 1.14.00	1/7/2004	SFR package.	OFR 2004-1042
MODFLOW-2000 Version 1.15.00	6/8/2004	GMG package, and modification to the SFR package.	OFR 2004-1261
MODFLOW-2000 Version 1.15.01	5/4/2005	Bug-fix release.	

Table 3.1 A summary of MODFLOW versions history from 12/1983 to 04/2005.

Broadly speaking, it can be said that, so far, MODFLOW is most likely known under three version names: MODFLOW-88, documented by McDonald and Harbaugh (1988), MODFLOW-96, documented by Harbaugh and McDonald (1996a and 1996b), and finally MODFLOW-2000, documented by Harbaugh et al. (2000).

### 3.2.2 MODFLOW Mathematical Model

#### 3.2.2.1 Assumptions, Governing Equation and Boundary Conditions

MODFLOW solves the partial differential equation that describes three-dimensional groundwater flow in a saturated porous media. The model assumes a flow process involving a single fluid, basically water, with constant parameters (density, viscosity and temperature), in a single phase (liquid). The phase flow is assumed to be laminar and linear, and Darcy's conditions are assumed to be applicable (see paragraph 2.3.1.4). The principal directions of the hydraulic conductivity are assumed to be parallel to the Cartesian co-ordinate axes and do not vary within the system. Using standard MODFLOW notation, the equation solved is given as (McDonald and Harbaugh, 1988):

$$\frac{\partial}{\partial x} \left( K_{xx} \frac{\partial h}{\partial x} \right) + \frac{\partial}{\partial y} \left( K_{yy} \frac{\partial h}{\partial y} \right) + \frac{\partial}{\partial z} \left( K_{zz} \frac{\partial h}{\partial z} \right) - W = S_s \frac{\partial h}{\partial t} \quad (3.1)$$

where

$K_{xx}, K_{yy}$  and  $K_{zz}$  are values of the hydraulic conductivity in the  $x$ ,  $y$  and  $z$  co-ordinate axes,  $[LT^{-1}]$ ;

$h$  is the potentiometric head  $[L]$ ;

$W$  is a volumetric flux per unit volume and includes sources and/or sinks  $[T^{-1}]$ ;

$S_s$  is the specific storage of the porous material  $[L^{-1}]$ ; and

$t$  is time  $[T]$ .

MODFLOW allows three types of boundary conditions to be simulated (see section 2.3.2). Equation 3.1, together with specification of flow and/or head conditions at the boundaries of an aquifer system and specification of initial-head conditions, forms the mathematical representation of a groundwater flow system solved by MODFLOW.

### 3.2.2.2 Spatial and Temporal Discretisation

MODFLOW uses the finite difference numerical method to solve the groundwater flow mathematical model stated above. The spatial domain of the aquifer system is discretised using a block-centred grid. Each cell of the mesh is located by its row, column, and layer. Therefore, an  $i, j, k$  indexing system is used to reference rows, columns, and layers respectively. Figure 3.1 shows the discretisation convention used in MODFLOW. An implicit formulation of the equation time-variables is used. The time derivative of the head is approximated using a backward-difference approach.

Following these discretisation conventions, Equation 3.1 yields a system of equations, which includes one equation for each variable-head cell in the mesh, and can be written in matrix form.

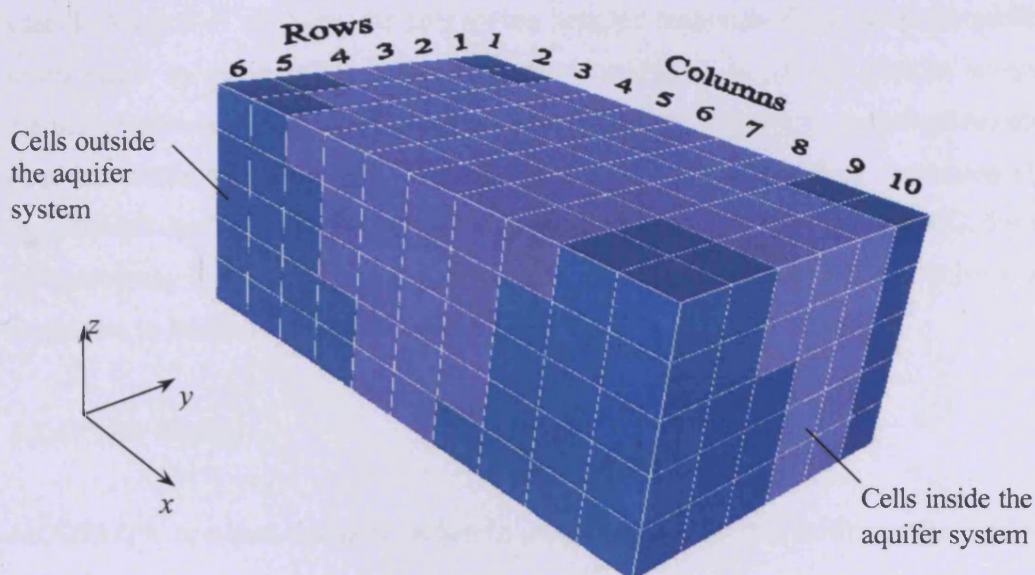


Figure 3.1 Discretisation convention in MODFLOW.

### 3.2.3 MODFLOW Solution Technique

The resulting matrix equation is solved by an iterative method. The MODFLOW-88 version incorporates the strongly implicit procedure (SIP) and the slice-successive over-relaxation (SOR) methods only (McDonald and Harbaugh, 1988). In MODFLOW-96, the preconditioned conjugate gradient (PCG) method was added as an alternative solver package (Hill, 1990). This version accounts also for a new direct solver (D4), based on

Gaussian elimination with the addition of Picard iterations when the flow equation is non-linear (Harbaugh, 1995). In the recent versions of MODFLOW-2000, another solver (AMG) was included using a linking package to MODFLOW, called LMG. AMG is an algebraic multigrid iterative solver for matrix equations that was developed by GMD (German National Research Center for Information Technology). The technique is fully described by Stüben (1999, 2001). Its implementation in MODFLOW-2000 by the LMG package is detailed in Mehl and Hill (2001). So far, the latest new technique for solving the finite difference matrix that has been added to MODFLOW-2000 is the GMG geometric multigrid solver, based in the preconditioned conjugate gradient algorithm and described in Wilson and Naff (2004).

The reason behind the incorporation of multiple solvers in MODFLOW is to give the user the chance of choosing the appropriate solution technique for a particular problem, as no single solver is well suited to all types of problems. It can also give an insight on the performances of each solver for the same application (accuracy, number of iterations, execution time, memory, convergence, and stability). A comparative discussion about the performance of MODFLOW iterative solvers SOR, SIP, PCG, and AMG, for two test problems, is provided by Mehl and Hill (2001). The AMG and GMG solvers were compared in Wilson and Naff (2004).

#### 3.2.4 Code Design

MODFLOW has been designed to have a modular structure that facilitates three primary objectives:

- ease of understanding;
- ease of enhancement; and
- minimisation of change that would impact existing MODFLOW users.

To meet these criteria, the program has been arranged according to a modularisation approach, consisting of the following basic entities: packages, procedures, modules and, in the latest MODFLOW version, processes.

**Packages** are entities that describe a hydrologic capability (either a flow component or a stress), or a solution method. The control of operations with these different packages is also included in a separate one, called Basic Package (BAS). Existing packages in MODFLOW-2000 are given in Table 3.2.

**Procedures** are pieces of the program that structure its logic in a simple way. Thus, the program flowchart is designed as a sequence of these procedures (see Figure 3.3). Each procedure is defined by the task that is achieved.

**Modules** or subroutines are smaller pieces of the programme that are combined within a single procedure for a single package. Calls of different modules, which belong to different packages, in the proper procedural sequence, are operated by the MAIN program.

**Processes** are more general entities as they define part of the code that solves a fundamental equation by a specified numerical method. This new modularisation concept has given a new dimension to the expansion of MODFLOW as it allows additional groundwater mechanisms to be modelled. In MODFLOW-2000, four processes are included:

- groundwater flow process (GWF): the original MODFLOW solves the groundwater flow equation using the finite difference method,
- observation process (OBS): which quantify statistically the difference between observed and simulated equivalent values and provides files to support graphical comparisons,
- sensitivity process (SEN): which calculates the sensitivity of hydraulic heads with respect to parameters of interest using the sensitivity equation method,
- parameter-estimation process (PES): which estimates selected parameters using non-linear regression.

Packages	MODFLOW-88	MODFLOW-98	MODFLOW-2000
	Version 2.6	Version 3.3 h	Version 1.15.01
Advective-Transport Observation Package (ADV)	-	-	ADV2
Basic Package (BAS)	BAS2	BAS5	BAS6
Block-Centered Flow Package (BCF)	BCF3	BCF5	BCF6
Time-Variant Specified-Head Package (CHD)	CHD1	CHD1	CHD6
Coupling DAFLOW Model to MODFLOW (DAF)	-	-	DAF1
Direct Solver (DE4)	DE45	DE45	DE45
Drain Package (DRN)	DRN1	DRN5	DRN6
Drains with Return Flow Package (DRT)	-	-	DRT1
Evapotranspiration with a Segmented Function Package (ETS)	-	-	ETS1
Evapotranspiration Package (EVT)	EVT1	EVT5	EVT6
Flow and Head Boundary Package (FHB)	-	FHB1	FHB1
Gaging Stations Package (GAGE)	-	-	GAGE5
General Finite Difference Flow Package (GFD)	GFD1	GFD1	-
General Head Boundary Package (GHB)	GHB1	GHB5	GHB6
Geometric Multigrid Solver (GMG)	-	-	GMG1
Horizontal Flow Barrier Package (HFB)	HFB1	HFB1	HFB6
Hydrogeologic-Unit Flow Package (HUF)	-	-	HUF1
Hydrograph Package (HYD)	-	HYD1	HYD1
Interbed Storage (subsidence) Package (IBS)	IBS1	IBS1	IBS6
Lake Package (LAK)	-	-	LAK3
Algebraic Multigrid Solver (LMG)	-	-	LMG1
Link to MT3DMS Contaminant-Transport Model (LMT)	-	-	LMT6
Layer-Property Flow Package (LPF)	-	-	LPF1
Drawdown-Limited Multi-Node Well Package (MNW)	-	-	MNW1
Preconditioned Conjugate Gradient (PCG)	PCG2	PCG2	PCG2
Recharge Package (RCH)	RCH1	RCH5	RCH6
Reservoir Package (RES)	RES1	RES1	RES1
River Package (RIV)	RIV1	RIV5	RIV6
Stream - Flow Routing Package (SFR)	-	-	SFR1
Strongly Implicit Procedure Package (SIP)	SIP1	SIP5	SIP5
Slice Successive Over-Relaxation Package (SOR)	SOR1	SOR5	SOR5
Streamflow-Routing Package (STR)	STR1	STR1	STR6
Subsidence and Aquifer System Compaction Package (SUB)	-	-	SUB1
Transient Leakage Package (TLK)	TLK1	TLK1	-
Utility Package (UTL)	UTL1	UTL5	UTL6
Well Package (WEL)	WEL1	WEL5	WEL6

Table 3.2 MODFLOW packages versus versions.

The overall program operation and data structure set-up used by these processes are controlled by a separate general process called the Global Process (GLO). Figure 3.3 shows a simplified flowchart of the GLO, GWF, OBS, SEN, and PES process combinations.

Another process for groundwater transport (GWT) modelling has also been constructed for MODFLOW-2000 as an optional package. The GWT process is activated by using an enhanced version of MODFLOW called MF2K\_GWT, that merges the MOC3D transport model and MODFLOW-2000, and adds solute calculations compatible with Lake and Gage packages. The program and its full description are available through the World Wide Web page at address:

[http://water.usgs.gov/nrp/gwsoftware/mf2k\\_gwt/mf2k\\_gwt.html](http://water.usgs.gov/nrp/gwsoftware/mf2k_gwt/mf2k_gwt.html)

Table 3.3 gives the relationship between the different procedures, packages and processes in MODFLOW-2000. The GWT process is not included as it integrates the code package MOC3D and its procedures with MODFLOW in a separate adapted version, namely MF2K\_GW. Note that solver packages and other packages are independent from processes and thus their related subroutines are organised only by procedures and/or packages as illustrated in Table 3.4.

If the finite volume method is to be used for solving the flow equation, a new separate process will have to be defined. This process will be called GWFV. Subsequent changes and additions, when necessary, have to be made to ensure compatibility with other MODFLOW-2000 packages. Consequently, modifications of the MAIN program to invoke the new modules of the new process are required.

### **3.2.5 Code Usability**

#### **3.2.5.1 Data Requirement – Input**

In order to run a MODFLOW application, the user must first specify grid dimensions; boundary and initial conditions, hydraulic properties, and stress parameters for every model cell in the finite-difference grid; and solver and output controls.

When processes other than GWF are used (OBS, SEN, PER or GWT), more input data are required. For instance, if the parameter estimation package (PES) is used, then an additional input file has to be prepared to define the estimated parameters and the observations used in the regression (existing independent estimates of parameter values,

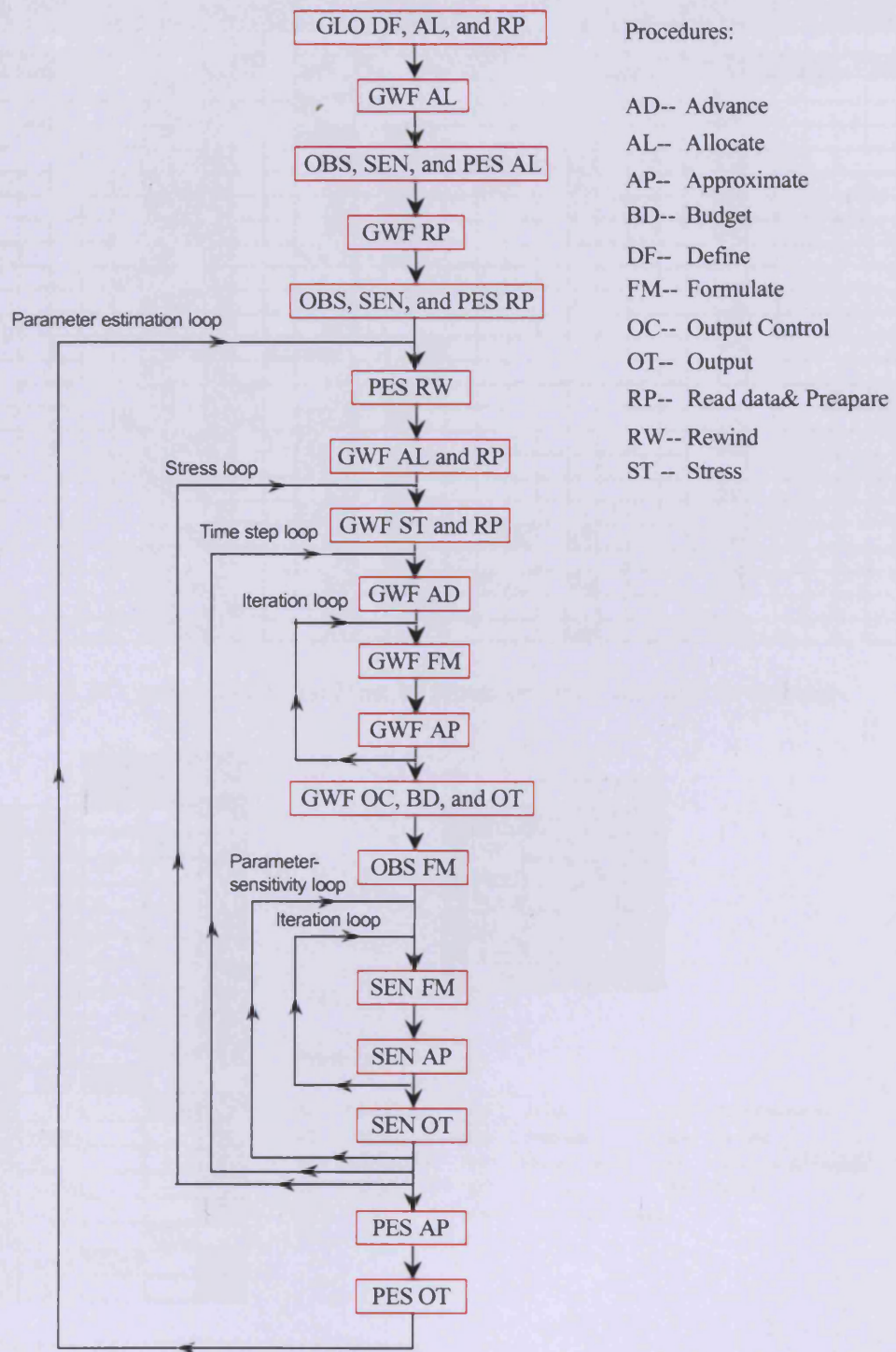


Figure 3.3 Flowchart of MODFLOW-2000 four processes: Global (GLO), Ground-Water Flow (GWF), Observation (OBS), Sensitivity (SEN), and Parameter Estimation (PES).



observed hydraulic heads or temporal changes in hydraulic heads, and observed gains and losses along head-dependent boundaries).

### 3.2.5.2 Code Output

The primary output is the head (or groundwater level) at every cell (except for those where head was specified as known in the input data sets) at specified time steps. Heads can be written to the listing file or into a separate file. Other output includes the complete listing of all input data, drawdown, and budget data. These latter output data are printed as a summary in the listing file, and detailed budget data for all model cells can be written into a separate file.

When other processes are invoked, more output files are generated. For instance, if the parameter estimation process (PES) is used, then the output includes tabular summaries of descriptive statistics and data for analysing the parameter estimates and the model reliability.

### 3.2.5.3 Pre-Processing and Post-Processing Facilities

#### *(i) Pre-Processors*

MODFLOW software, as it is distributed by the USGS, does not have any pre-processing facility. Yet, the USGS has separately developed two basic pre-processors to the MODFLOW program namely RADMOD, for the particular case of axisymmetric problems, and MFI2K, which assists in preparing input data for MODFLOW-2000. The two programmes can be downloaded for free from the USGS software home page. However, due to its growing use and development since its release, and the type of input files required for running a MODFLOW application, many pre-processors have been developed by other organisations and private companies to facilitate the use of the programme. These facilities include a mesh generator, CAD/GIS style tools and functionality, a graphical user interface, and importing and exporting data facilities. Commercial versions of the MODFLOW software allow most of these options. Table

B.1 in Appendix B gives a review of up-to-date available products pre-processing MODFLOW.

*(ii) Post-Processors*

The only post-processors distributed with the MODFLOW-2000 code by the USGS are:

- BEALE-2000 which calculates beale's measure of non-linearity,
- RESAN-2000 which performs residuals analysis,
- YCINT-2000 which calculates linear confidence intervals on simulated hydraulic heads and flows along head-dependent boundaries, and
- HYDFMT and HYDPOST which are post-processor packages that read a file containing unformatted output and write simulation times and head values (or other values) to a file that can be read into a graphing program.

The USGS has developed separately other programs, which perform other post-processing tasks (see Table B.1). More sophisticated post-processing capabilities for 3D views, animation, contour plots, colour postscript output, and vector plots are available within commercial software which process MODFLOW. Table B.1 summarises some of these post-processors. Most of these commercial software tools have their own in-built pre-and post-processors, as they bring other process simulation codes together (e.g. contaminant transport codes, surface water codes, particle tracking codes). Such functions are increasingly being improved as they represent a highly important criterion in software selection by modellers.

### **3.2.6 Related Programmes**

Since its establishment as a worldwide standard for groundwater flow modelling, many programs have been developed to link MODFLOW to other codes that use groundwater flow information in porous saturated media (e.g. heads, velocities, flow budget and fluxes). Processes such as solute transport, variable density flow, multiphase and unsaturated flow, integrated surface water and groundwater flow, parameter estimation, groundwater management and optimisation may be modelled using programs that solve a system combining the process governing equations with the groundwater flow equation

solved by MODFLOW. Table B.2 in Appendix B gives examples of MODFLOW related programmes.

### 3.2.7 Source Code Availability and Cost

MODFLOW is a public domain model. The source code for all MODFLOW versions (MAIN program as well as its subroutines) are distributed freely by the USGS. Self-extracting distribution files are available for electronic retrieval via the World Wide Web (WWW) at: <http://water.usgs.gov/software/>. The extracted files mostly contain compiled executables, the program packages source code, data sets for verification tests and their batch files, and information files (release notes or version history, files contained, user rights, the readme text, etc.).

### 3.2.8 Hardware and Software Requirements

MODFLOW (all versions) can be installed on three computer systems: Data General UNIX workstations, Sun SPARCstation and IBM compatibles personal computers. It can be used with UNIX, DOS or Windows operating systems. For MODFLOW-2000, the random-access memory (RAM) required is not less than 4 MB. This version can be run on an Intel 80386 based computer or higher with a math coprocessor or compatible.

The program has been written in Fortran 77 with few extensions (e.g. use of variable names longer than 6 characters and use of Fortran 90 statements in some parts of the code). The program compilation is made with the Lahey Fortran 95 extended memory, compiler version 5.60h. Thus a FORTRAN compiler is required for any modification and compilation of the code. The distributed source code of MODFLOW-2000 is compatible with standard Fortran 90 and FORTRAN 95 but can also be converted to standard Fortran 77 by modifying some aspects in the main program (Hill et al., 2000, p. 206).

The source code of the latest version offers a serial or parallel processing option for the sensitivity process. Parallel sensitivity distributes parameter related runs simultaneously across computer processors, i.e. network computing, thereby achieving enormous optimisation-time savings.

### 3.2.9 MODFLOW Capabilities and Maintenance

The code was originally developed to simulate three dimensional groundwater flow in saturated porous medium. This flow process involves a single fluid, basically water, with constant parameters (density, viscosity and temperature), in a single phase (liquid). The flow is assumed to be laminar and linear and Darcy's conditions are applicable (section 2.3.1.4). MODFLOW's recent modular design has provided a good foundation upon which substantial additions have occurred. Thus, in its latest versions, MODFLOW-2000 accommodates the simulation of new classes of problems in addition to saturated groundwater flow. This was achieved by incorporating other process codes into the MODFLOW code (e.g. PES, OBS processes), or linking the original programme to other simulators using linking packages (e.g. LMT package), or adding subroutines for coupling MODFLOW with other programs (e.g. DAF package). The two major recent extensions to MODFLOW have been calibration (i.e. the PES, SEN, OBS processes, and ADV package) and solute-transport modelling (i.e. the GWT process and the MT3DMS linking package LMT6). Other enhancements of the model incorporated in its latest versions include:

- new solver packages to improve accuracy and computational work (LMG and GMG packages),
- flexibility in simulating evapotranspiration and drains (ETS and DRT packages),
- interaction between lakes, and aquifers (LAK package),
- interaction between stream and aquifers (SFR)
- more flexibility in simulating boundary conditions (FHB and CHD packages) and aquifer heterogeneity and stratigraphy (LPF and HUF packages).

Each package of MODFLOW is prone to continuous maintenance to enhance its applicability. Thus, each package has an associated number that indicates its latest improved version, as shown in Table 3.3.

Using the USEPA method for evaluating a code (Van der Heijde and Kanzer, 1997), functionality checklists for MODFLOW-2000 version 1.15.01 are given in Appendix C. Other commercial MODFLOW products can offer additional capabilities, such as telescopic mesh refinement (Groundwater vistas), non-ponding or prescribed ponding

conditions for recharge/seepage face, simulation of a well that is screened across multiple model layers, and adaptive time-stepping and output control (MODFLOW-SURFACT). The SFWMD have developed several packages to integrate surface and ground water using MODFLOW (Restrepo et al., 1998), for example wetland (WTL1) and evapotranspiration-recharge (ET/RCH). Kiwa, a research and consultancy organisation in the Netherlands has developed the Density Package for simulating density driven flow in MODFLOW. Also, a package for simulating water movement in the unsaturated zone, called the Vadose module, was developed for MODFLOW by S.S Papadopoulos and Associates, Inc. (Blum et al., 2001).

### 3.2.10 MODFLOW Applications

MODFLOW has been extensively applied for different field situations, especially those where a relatively precise understanding of the flow system is needed to make a decision. Moreover, it is commonplace to see MODFLOW deployed in conjunction with one or more other models to simulate different hydraulic processes (e.g. surface water, recharge, etc). The class of problems where MODFLOW has been used and well-tested can be summarised as follows:

- Regional groundwater management which addresses planning for water demands and supply, the effects of natural or manmade stresses (e.g. drainage, withdrawal, artificial recharge) on groundwater system (Stamos et al., 2002, Hutson et al., 2002,) and more generally the impacts of urbanisation and land-use (Hunt and Steuer, 2001, Batelaan et al., 2003),
- groundwater contamination and remediation (e.g. pump and treat, soil vapor extraction, air sparging, bioremediation, and natural attenuation) in porous media (Wang and Zheng, 1997, Bumb et al., 1997, Bedard et al., 1997, Geistlinger et al., 2003),
- evaluation of pumping and tracer test data to determine hydraulic and transport properties of formations (Samani et al., 2004, Lemke et al., 2004),
- simulation of surface/groundwater interactions, such as river basins, wetlands and lakes (Grannemann et al., 2000, Krohelski et al, 2002), runoff, and evapotranspiration,

- Flow and transport optimisation of pumping by wells for dewatering, remediation or supply use (Manglik et al., 2004, Neville and Tonkin, 2004),
- uncertainty analysis and risk assessment (e.g. parameter estimation, delineation of well capture zones, contaminants fate and exposure pathways) as can be found in Heebner and Toran, 2000, and Jones et al., 2003.

### **3.2.11 MODFLOW Testing and Reporting: Quality Assurance**

Each simulation feature of MODFLOW has been extensively tested either through comparisons with analytical examples, benchmarks, field or laboratory test results or other similar program results. All initial packages are well documented, but no detailed report on their successive upgrades is available (just release notes to mention introduced changes). User and programmer's documentation exists for MODFLOW-88 and MODFLOW-96. User guides for the new MODFLOW-2000 are available whereas, at the time of this study, no programmer's documentation has yet been published. All of these documents contain a detailed description of the development history, theory, code structure, input instructions, and example simulations. A manual of instructional problems (Andersen, P.F., 1993) was developed by the United States Environmental Protection Agency to illustrate in a comprehensive way the model principles and options.

### **3.2.12 History of Use and References**

MODFLOW has been extensively used by different governmental bodies, companies (i.e. developers and user consultants) and public organisations such as universities and regulatory agencies. As of late 1992, the U.S. Geological Survey reported that MODFLOW had been used for 165 projects, significantly more than all of the other USGS models for simulating groundwater flow and water quality (Appel and Reilly, 1994). Many of these reports are published on the web for free consultation. One survey found that 73% of practicing hydrogeologists had used MODFLOW (Fetter, 1994). References and resources on the internet of MODFLOW-related freeware and shareware can be found in Winston (1999). In many court cases in the United States, the

programme has been accepted as a legitimate approach to analyse groundwater systems (see MODFLOW fact sheet FS-121-97). Examples of other MODFLOW official users include the U.S. Army Corps of Engineers (USACE), the U.S. Environment Protection Agency (USEPA), South Florida Water Management District (SFWMD) and the U.S. Department of Energy (DOE). As commercial effort was concentrated on making MODFLOW more user-friendly, the use of the model outside of the U.S. started develop worldwide. Private companies hold records of these international users.

### **3.3 MODFLOW Limitations**

If no other model is used in conjunction with MODFLOW-2000, then three types of limitations can be identified:

#### ***(i) Conceptual model-related limitations:***

As stated before, MODFLOW is formulated to simulate saturated groundwater flow in porous media. Accordingly its applicability is restricted to the simulation of this hydrogeological process. Thus, MODFLOW cannot be applied alone in several commonly occurring situations that involve other physical processes such as flow in the unsaturated and vadose zones, e.g. density dependent saltwater intrusions, multiphase flow and surface processes (e.g. overland runoff, surface water in hydraulic control structures, etc.).

MODFLOW also includes other limitations related to the representation of certain mechanisms within packages. Thus, the recharge package (RCH) provides unphysical predictions for unconfined systems, if the water table reaches, or is above land surface. Downward seepage from rivers (RIV), reservoirs (RES), streams (STR) and lakes (LAK) is limited to situations where the head in the underlying aquifer is always above the bottom elevation of the surface water feature and the bottom elevation of the layer containing the feature. The simulation of wells with the well package (WEL) is limited to withdrawal at a specified rate from individual cells, and short term transient effects between cells and wells, important in aquifer test analysis, are not simulated. The

calibration processes (PES, OBS and SEN) may not be compatible with TLK, IBS, and RES packages, and where transport processes are evolved (GWT).

***(ii) Mathematical solution-related limitations:***

Limitations related to finite difference formulations include the following:

- Rectilinear grids do not conform the model to geometric, topographic or lithologic features,
- Steep and rapid changes in the vicinity of hydraulic features, such as pumping/injection wells, lakes, rivers, drains, etc, cannot be captured accurately due to the relatively large distances between adjacent nodes,
- The geometry of hydraulic controls such as wells and canals, can be difficult to model with a rectilinear grid (Barrash et al., 1997).

Limitations related to the solution methods include the following:

- MODFLOW sometimes encounters difficulties, or fails to converge in drying/re-wetting situations,
- Solvers available in MODFLOW are efficient for small or straight forward problems, but become inefficient, or fail altogether, for large and complex problems, continuous effort is made to improve the code computational performance by integrating new solvers, but none of them has proved to be unconditionally efficient for applications with MODFLOW,
- MODFLOW's time stepping increases the step size in geometric progression indefinitely, thereby sacrificing robustness, efficiency, and efficient control of simulation output,
- Stability issues are limited when using packages such as the LAK package (Merritt and Konikow, 2000).

***(iii) Hardware and software-related limitations:***

The main hardware and software related limitations can be summarised as follows:

- pre and post-processing facilities are unavailable within MODFLOW-2000. In fact, data input/output, grid considerations, and simulation control have complex

data structures, particularly when several simulations are involved for calibration, and sensitivity analysis,

- for large, complex problems, simulation problem dimensions are limited by available computer memory or prohibitively long simulation times,

Some of these limitations have been overcome by the development of new packages and techniques that have not yet been included in the present version of MODFLOW-2000. The telescopic mesh refinement (TMR) procedures (Leake and Claar, 1999) and the drawdown-limited multi-node well (MNW) packages (Halford and Hanson, 2002) are examples of programs that have been developed by the USGS to improve on the model accuracy and applicability. The MNW has already been included in latest version of MODFLOW-2000, as other utility packages. Doherty (2001) proposed a number of adjustments to the BCF package to improve MODFLOW convergence when dewatered cells are included in the calculations. Osman and Bruen (2002) presented an improved technique to simulate stream-aquifer seepage in MODFLOW. The use of boundary representation method for solid models to generate an accurate grid-independent representation of complex hydrostratigraphy has been suggested by Jones et al., (2002). Modifications of the BCF package, in order to have additional flexibility in modelling spatially variable anisotropy in MODFLOW, were described in Kladias and Ruskauff (1997).

### **3.4 MODFLOW Critics and Improvements**

#### **3.4.1 MODFLOW Popularity**

In a comparative survey in 1992, MODFLOW was, by far, the most popular groundwater modelling programme (Geraghty and Miller Software Newsletter, 1992). In 1999-2000, 23000 copies of MODFLOW had been downloaded free from the USGS or purchased from others (Hill, 2002). With the additional functionality in MODFLOW-2000, the programme will by now be even more widely used. The programme's popular attributes account for its modular code design; including the good documentation of the programme theory and data input, and the free access and availability of these

documents as well as the source code. Moreover, the simple concept of finite differences, and the subsequent simplicity of the treatment of flow features, is one of the most attractive reasons why MODFLOW has become a very popular groundwater modelling tool around the world. Yet, the main simplifications lead to major limitations especially when complex modelling situations are involved. It is true that field situations are never simple enough to be simulated by simple models, however, the complexity level should be measured with the accuracy at which the model results are expected to be. The accuracy of MODFLOW has been subject to many research studies. The results have led to modifications or to the addition of new packages that tackle each complexity separately, whereas the data input structure has remained the same to keep users familiarity with new versions of MODFLOW. Thus, MODFLOW remains flexible in balancing between complexity and simplicity.

### 3.4.2 MODFLOW Accuracy

As stated in section 3.6.1, when developing a numerical model code, accuracy partly relies on the minimisation of errors generated by number of approximations. In MODFLOW, the approximations made at many levels include, in particular:

- the parabolic partial differential flow equation being discretised using a finite difference method. First order and second order spatial derivatives are approximated accordingly,
- the temporal derivative being approximated using a backward difference scheme and the flow equation being solved implicitly,
- the solution of the resulting set of equations system being approximated by different iterative matrix solver techniques,
- the hydraulic conductivity (or permeability) being approximated at cell surfaces using interpolations.

The accuracy of MODFLOW with regard to spatial discretisation was investigated by Haitjema et al. (2001). He found that an accurate flow field was obtained if the boundary conditions in the groundwater flow regime were represented accurately in MODFLOW with the appropriate cell sizes. In regions with singular velocities (e.g. near corners),

strongly converging or diverging flow or zones with a contrasting transmissivity level, then a large amount of cells are required. It should be noted that, given the nature of a finite difference grid, the cell sizes are restrictively dependent upon the number of cells (i.e. rectilinear rows and columns).

Barrash et al. (1997) found that the finite difference formulation used in MODFLOW underestimate large head gradients that can occur in the vicinity of pumping (or injection) wells. Generally, a detailed representation of the flow field in the vicinity of hydrologic features and through irregular hydrogeologic units (e.g. discontinuities, or very thin units) requires a relatively small grid spacing. Moreover, an accurate velocity field is critical to the accuracy of contaminant transport models, particularly for advection dominated transport, and model accuracy and stability are often conditional upon the use of small cell sizes. These limitations can be reduced or eliminated by refining the grid representing the system and by using a more flexible grid structure. Mehl and Hill (2002, 2004) presented a local grid refinement method for two-dimensional and then three-dimensional block-centred finite difference meshes using shared nodes. Leake and Claar (1999) developed three programmes (MODTMR, TMRDIFF and RIVGRID) that use telescopic mesh refinement method within MODFLOW. Another method for refining a model grid was presented by Spitz et al. (2001). The nested re-discretisation method is used to improve pathline resolution by eliminating weak sinks, representing wells in MODFLOW and MODPATH. However, fine grids can result in long execution times that prohibit the many model runs often needed to understand the system dynamics and calibrate the model. As an alternative to grid refinement for more accurate local modelling, Kelson (2002) suggested the use of an analytical element model where the boundary conditions, aquifer properties, and parameter values for the analytical element subregions were extracted from the MODFLOW regional model.

Jones (1997) presented a finite element package (NCF), analogous to the BCF package, as an alternative to solve the groundwater flow equation, using the finite element method within a model layer, while the vertical flow is simulated using the finite difference method. The input data input structure was kept consistent with other MODFLOW

modules, in addition to the capability for designing a non-rectangular grid. No other work on the flexibility of the grid structure in MODFLOW has been investigated so far as can be established from the main literature. Hill (2002) suggested that one of the future MODFLOW development axes would be to improve the local grid refinement and make grids less structured. Zheng (1990) developed a higher-order finite-volume TVD method, within the code MT3D, for transport simulation. Heberton et al. (2000) also have developed a finite volume Eulerian-Lagrangian method to solve the transport equation used in MOC3D. Both methods, however, are based on finite-difference cell and use MODFLOW to drive their interstitial fluid velocity components.

In the present work, emphasis has been focused on developing a non-orthogonal grid model version of MODFLOW. This has been achieved using the finite volume technique, and the accuracy gained using this scheme along with its performances and limitations, has been considered.

Performance and errors that can be generated by the different interpolation techniques used to approximate hydraulic parameters and gradient terms on cell surfaces in MODFLOW have not been investigated so far. Potential inaccuracies involving the matrix solvers SIP, SSOR and PCG2 were fully addressed by Osiensky and Williams (1997). A comparison with the recent added solver, AMG, was provided by Mehl and Hill (2001) for two simple tests. A comparison between the AMG solver and the latest integrated solver GMG, was also made by Wilson and Naff (2004). No detailed comparisons between all the MODFLOW solvers, namely SIP, SSOR, PCG2, DE4, AMG and GMG, have been undertaken to-date. An enhanced version of the preconditioned conjugate gradient solver, called PCG4, was developed by HydroGeologic.Inc within its product MODFLOW-SURFACT. It also offers a Newton-Raphson Linearisation and Backtracking package (NRB1) to stabilise the solution for highly non-linear conditions.

### 3.4.3 Finite Volume and MODFLOW

The accuracy of the results from solute-transport models relies heavily on the groundwater velocities calculated from flow models, such as MODFLOW. For advection dominated transport the accuracy of the velocity field is critical to the accuracy of the contaminant transport solution. Variable-density, ground-water models are even more dependent upon velocities because the groundwater velocities are, in turn affected by the solute concentrations. On the other hand, it is recognised that no single numerical technique has been shown to be effective for all transport conditions, each having its own strengths and limitations. However, it has been reported in many research publications that the finite volume method fits better with the transport problems than the finite difference method, which suffers, moreover, from the difficulty in reproducing boundary effects (Archer, 2000).

From these perspectives, and because MODFLOW is one of the most widely used groundwater models, the improvement in its accuracy will be investigated by implementing a finite volume discretisation method using a non-orthogonal grid. This will be achieved with respect to MODFLOW's popularity oriented objectives, by ensuring minimal changes that would impact existing code users and ease of understanding. The method can be subsequently used to discretise the transport equation used by MOC in conjunction with MODFLOW. The new formulation adds more features to the flow model, in particular a greater flexibility in the grid structure enabling irregular boundary geometries to be represented more accurately. Also, steep changes in the flow gradients can be represented more precisely, together with the benefits of unconditional mass conservation. The necessary tests and analyses will be conducted to check the method's performance relating to accuracy, stability, consistency and convergence issues, and comparisons with the finite difference method as used in MODFLOW.

# Chapter 4

## Finite Volume Discretisation

### 4.1 Introduction

In this chapter, the finite difference method used in MODFLOW will be replaced with the finite volume method. The major objective of this change is to enhance grid flexibility within MODFLOW and with minimal changes that could affect user familiarity with this popular model. Details of this technique are presented together with its implementation into the groundwater flow equation.

### 4.2 Finite Volume Method

The Finite volume method (FVM), also referred to as control volume method, was first introduced by MacDonald (1971) and MacCormack and Paullay (1972) as a special finite difference formulation for the solution of the Euler equations in fluid dynamics. From the viewpoint of other authors, the method is considered as a variant of the weighted residuals finite element method (Patankar, 1980, p. 30). The numerical technique is based on the integration of governing equations of fluid flow over a control volume. The continuous problem is discretised over a domain with a number of grid points associated with a number of non-overlapping control volumes (CVs) covering the whole domain. The mesh elements (or CVs) can have any shape with rectilinear sides, structured or unstructured and with flow variables associated with a point inside the cell

(i.e. the cell-centred finite volume) or attached to cell vertices (i.e. the cell-vertex finite volume). Figure 4.1 shows these different mesh concepts. A detailed description of the different discretisation options using the FVM can be found in many references, such as Hirsch (1988), Versteeg and Malalasekera (1995), and Tannehill et al. (1997).

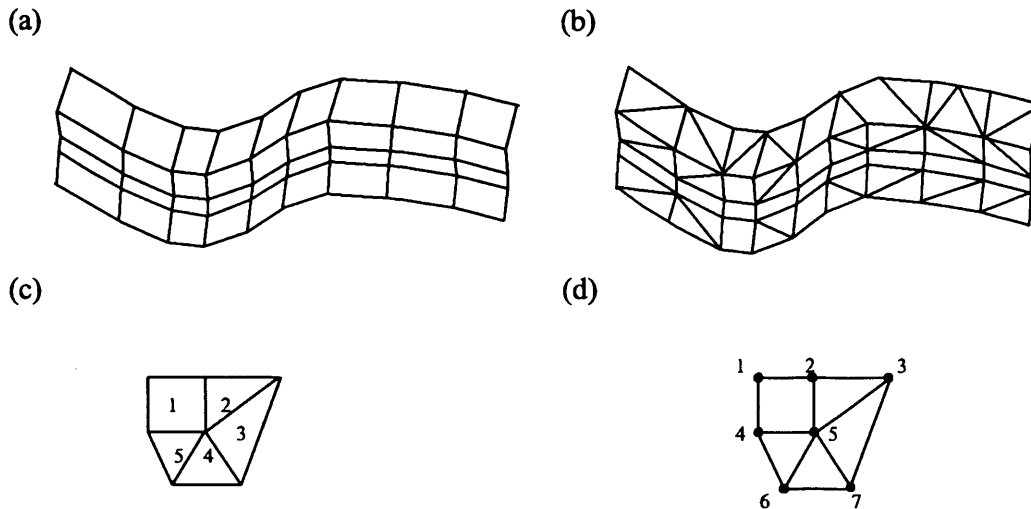


Figure 4.1 Different two-dimensional finite volume mesh concepts  
 (a) cell-structured FV; (b) cell-unstructured FV mesh;  
 (c) cell-centred FV mesh; (d) cell-vertex FV mesh.

Integration of the partial differential equations over all of the CVs of the solution domain involves substitution of a variety of finite-difference-type approximations (e.g. central, upwind) for the terms in the integrated equation representing the flow processes of convection, diffusion, source, etc. Fluxes through cell surfaces are evaluated in terms of the variables in adjacent cells. The integral equation is then converted into a system of algebraic equations. The nature of this system depends on the character of the problem posed by the PDE and the solution method is therefore carefully chosen. Consideration of truncation errors, consistency and stability, among other properties, determines the accuracy of the solution obtained.

The most attractive features of the FVM are that:

- The resulting solution implies the integral conservation of quantities such as mass, momentum, and energy over CVs. Therefore these quantities are conserved over the whole calculation domain, for any number of grid points, whereas in the finite

difference method the conservation principle is expressed only for infinitesimal CVs. The finite element method (FEM) does not conserve mass at the local level for certain schemes (Di Gimmarco et al., 1996).

- The mesh offers greater geometrical flexibility vis-à-vis the finite difference method and the integrated finite difference method, in the sense that the line joining two grid points does not necessarily have to be perpendicular to a given CV surface.

This chapter will focus on the two-dimensional formulation of the groundwater flow equation used in MODFLOW, as a preliminary step for the model expansion to three-dimensional problems. Three discretisations are derived for the two-dimensional diffusion equation and for use with structured quadrilateral meshes. The three methods rely on the cell-centred finite volume approach, but show distinct differences in the gradient approximation, head interpolation and matrix properties.

### 4.3 Finite Volume Discretisations of Groundwater Flow Equation

As described previously, and with reference to the 2D Cartesian co-ordinate system ( $x, y$ ), transient two-dimensional groundwater flow through porous material is governed by the elliptic partial differential equation:

$$\frac{\partial}{\partial x_i} \left( K_{ij} \frac{\partial h}{\partial x_j} \right) = S_s \frac{\partial h}{\partial t} + W \quad (4.1)$$

where  $K_{ij}$  is the hydraulic conductivity of the porous media (a second order tensor),  $L^2$ ;  $h$  is the potentiometric head,  $L$ ;  $S_s$  is the specific storage coefficient,  $L^{-1}$ ;  $t$  is time,  $T$ ;  $W$  is the volumetric flux per unit volume (positive for outflow and negative for inflow),  $T^{-1}$ ; and  $x_i$  are the Cartesian co-ordinates,  $L$ . The summation convention of Cartesian tensor analysis is implied in Equation 4.1.

In MODFLOW, a number of assumptions have been made in the development of the governing equation (McDonald and Harbaugh, 1988). The resulting 2D groundwater flow equation can be written as (see paragraph 3.2.2):

$$\frac{\partial}{\partial x} \left( K_{xx} \frac{\partial h}{\partial x} \right) + \frac{\partial}{\partial y} \left( K_{yy} \frac{\partial h}{\partial y} \right) - W = S_s \frac{\partial h}{\partial t} \quad (4.2)$$

where  $K_{xx}$ ,  $K_{yy}$  are values of hydraulic conductivity along the  $x$  and  $y$  coordinate axes,  $LT^{-1}$ .

MODFLOW uses an implicit, backward in time, finite difference method to calculate the head distribution for a given time step or steady state flow condition over a set of discrete points in space. The aquifer system is discretised with a mesh of block-centred orthogonal cells where head values are computed at the centre point of the cell called a 'node'. The finite volume method suggested in this work uses a structured, quadrilateral, non-orthogonal and cell-centred mesh for domain discretisation, to maintain conformity with the MODFLOW discretisation convention. In addition, for three-dimensional problems hexahedral elements are a natural choice and allow a greater flexibility in designing a grid. Therefore, the  $(i,j)$  indexing system used in MODFLOW has been kept (Figure 4.2). Each cell location is described in term of rows and columns. For a system consisting of ' $nrow$ ' rows and ' $ncol$ ' columns,  $i$  is the row index, i.e.  $i=1\dots nrow$ , and  $j$  is the column index, i.e.  $j=1\dots ncol$ . Thus in terms of Cartesian co-ordinates, increments in the row index  $i$ , would correspond to a decrease in  $y$ ; and increments in the column index  $j$  would correspond to an increase in  $x$ . The application of the model, however, differs from that used in MODFLOW in that it requires the designation of  $x$  and  $y$  co-ordinate axes as rows and columns that do not necessarily fall along their orthogonal directions.

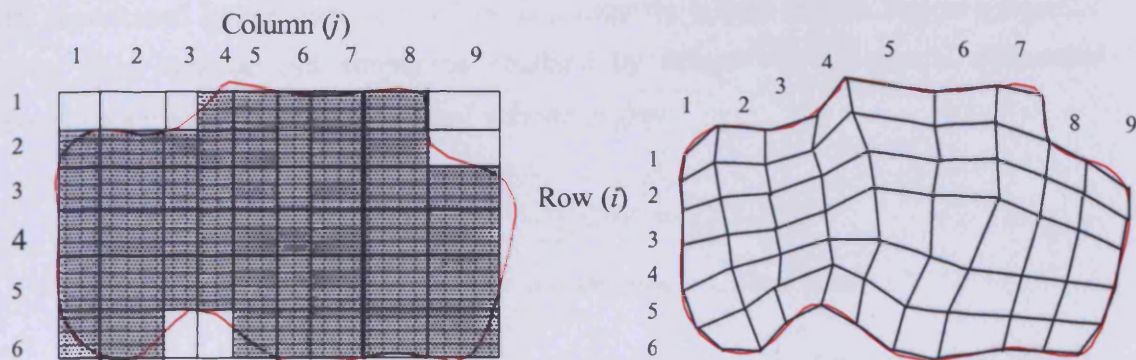


Figure 4.2 Space discretisation convention in MODFLOW and its equivalent finite volume discretisation.

Development of the groundwater flow equation in any form follows from the application of the continuity equation: the sum of all flows into and out of the cell must be equal the rate of change in storage within the cell (see section 2.3.1). In finite volume form, the

balance of flow for a given arbitrary control volume is ensured when all of the face contributions that surround a cell are accounted for in a way that is conservative. Therefore, the construction of an outward normal surface vector at each face is then summed for all face contributions to ensure that a mass conservation system is adopted for the control volume. Figure 4.3 shows the quadrilateral control volume used, together with its outward normal surface vectors.

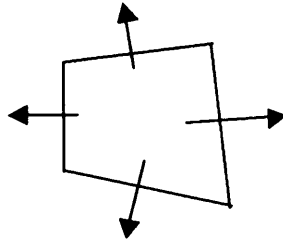


Figure 4.3 A quadrilateral cell with normal surface vectors.

The continuity equation expressing the balance of flow for a cell is given by:

$$\sum Q_i = S_s \frac{\Delta h}{\Delta t} \Delta V \quad (4.3)$$

where  $Q_i$  is a flow rate into the cell ( $L^3 T^{-1}$ ),  $S_s$  is the specific storage ( $L^{-1}$ ),  $\Delta V$  is the volume of the cell ( $L^3$ ),  $\Delta h$  is the change in head over a time interval of length  $\Delta t$ . Equation 4.3 is expressed in terms of the inflow and storage gain. The outflow and loss are represented by defining the outflow as a negative inflow and the loss as a negative gain. This equation can simply be obtained by integrating the general differential Equation 4.2 over an arbitrary control volume to give:

$$\underbrace{\iiint_V \left[ \frac{\partial}{\partial x} \left( K_{xx} \frac{\partial h}{\partial x} \right) + \frac{\partial}{\partial y} \left( K_{yy} \frac{\partial h}{\partial y} \right) \right] dV}_{\text{Diffusion term}} - \underbrace{\iiint_V W dV}_{\text{source term}} = \underbrace{\iiint_V S_s \frac{\partial h}{\partial t} dV}_{\text{transient term}} \quad (4.4)$$

where  $dV$  is volume of the considered element. The evaluation of the individual terms in Equation 4.4 is discussed separately.

### 4.3.1 Diffusion Term

The Gauss divergence theorem is used to simplify the diffusion term of Equation 4.4, thus:

$$\iiint_V \left[ \frac{\partial}{\partial x} \left( K_{xx} \frac{\partial h}{\partial x} \right) + \frac{\partial}{\partial y} \left( K_{yy} \frac{\partial h}{\partial y} \right) \right] dV = \iint_S K_i \frac{\partial h}{\partial x_i} dS \quad (4.5)$$

Discretising Equation 4.5 one can obtain:

$$\iiint_V \left[ \frac{\partial}{\partial x} \left( K_{xx} \frac{\partial h}{\partial x} \right) + \frac{\partial}{\partial y} \left( K_{yy} \frac{\partial h}{\partial y} \right) \right] dV \approx \sum_{f=1}^4 \iint_{S_f} \left( K_i \frac{\partial h}{\partial x_i} x_i \right) n_f dS \quad (4.6)$$

$$= \sum_{f=1}^4 K_{ij} \left( \frac{\partial h}{\partial x_i} \right) x_i S_f \quad (4.7)$$

where  $x_i$  ( $i = 1, 2$ ) forms the orthogonal co-ordinate system and  $n_f$  represents the outward normal area vector in a counter-clockwise traversal around the control volume boundary as shown in Figure 4.3.  $S_f$  is surface vector of a cell face  $f$  and  $f$  is a subscript denoting cell faces.

One of the main potential problems at this stage is the handling of the diffusion term. Its integration over a control volume leads to the necessity to estimate the derivative of  $h$  with respect to the face normal. This will be discussed in more detail in the following section.

#### 4.3.1.1 Gradient Approximation on a Control Volume Face: Review

In MODFLOW, the finite difference method approaches the gradient on a surface using a two-node backward difference scheme. In Figure 4.4, the gradient of  $h$  in the  $x$  direction from cell  $P$  to cell  $N$  is approximated by:

$$\left( \frac{\partial h}{\partial x} \right)_{S_{NP}} = \frac{h_N - h_P}{x_N - x_P} \quad (4.8)$$

In the  $y$  direction the derivative is null as the cells are orthogonal. With the finite volume method, the approximation of the gradient term for a common face presents more complexity as the grid is no longer orthogonal (see Figure 4.4). In fact, the accuracy of a control volume discretisation depends heavily on the order of approximation of the flux at the cell faces (Tukel, 1986).

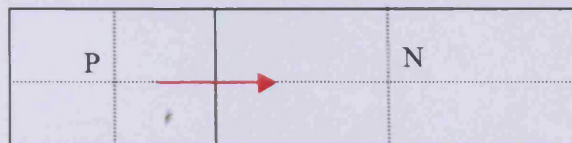


Figure 4.4 Two adjacent orthogonal control volumes in finite difference method.

Many methods have been proposed to approximate the gradient or fluxes along a control volume surface as the question has arisen from several CFD applications. In fact, the form of the diffusion term ruling the groundwater flow equation is common to a wide range of similar physical processes, such as heat, general diffusion occurring in continuum mechanics, magnetics, gas dynamics, petroleum reservoir simulation, etc (Hyman et al., 2002). From a review of the different articles on this subject, it can be seen that methods for approximating fluxes (and/or gradients) on cell faces within a finite volume discretisation scheme, can be broadly classified into five categories:

**(i) Control-Volume Mixed Finite Element Methods:**

This method is a hybrid of the cell-centred approach and the finite element method (Ferguson, 1998). It also considered by some authors as a synthesis of the integrated finite difference and finite element methods (Di Giammarco et al., 1996). The method allows the use of irregular grids while preserving many of the properties of block-centred finite difference methods for rectangular grids. In fact, on rectangular grids, the method can be even more accurate than finite differences in simulating flow in heterogeneous and anisotropic porous media (Cai et al., 1997). There is considerable literature for this method (Durlafsky, 1994, Di Giammarco et al., 1996, Turner and Ferguson, 1995).

The mass continuity equation is integrated over each control volume and the divergence theorem is used so that an equation similar to Equation 4.6 is obtained. Basis functions are then used to compute values at the points of integration (cell faces) by interpolating nodal values. In this study, the basis function has to be extracted from the four nodes forming the secondary cell (Figure 4.5), owing to the use of the quadrilateral element. The secondary mesh can be constructed by joining each four adjacent nodes. The gradient, and also head, at vertex  $A$ , is then approximated using an interpolation

function, such as piecewise bilinear polynomials, involving heads at the four nodes surrounding  $A$ .

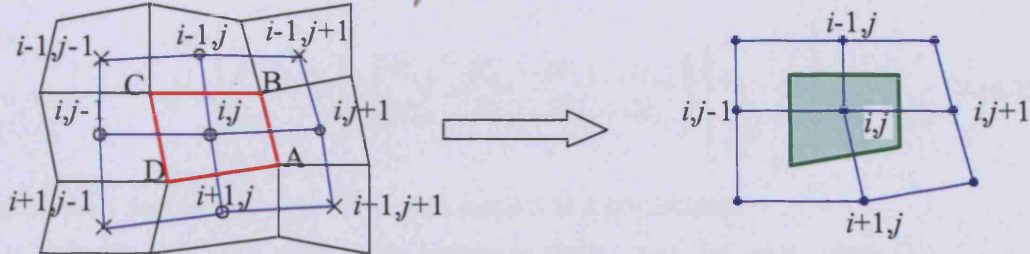


Figure 4.5 Secondary mesh and related element used in finite element method.

The head (or gradient) value inside the secondary element can be approximated by:

$$h(x,y) = \sum_{l=1}^4 h_l N_l(x,y) \tag{4.9}$$

where  $1 \sim (i+1, j)$ ;  $2 \sim (i+1, j+1)$ ;  $3 \sim (i, j+1)$  and  $4 \sim (i, j)$ .  $N_l$  is the interpolation function. For a bilinear quadrilateral element the appropriate choice of this function would be the piecewise bilinear polynomials, thus:

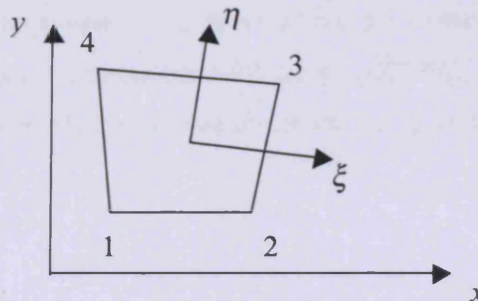


Figure 4.6 Quadrilateral element in physical space.

$$N_l(\xi,\eta) = \frac{1}{4}(1+\xi\xi_l)(1+\eta\eta_l) \quad \xi_l = \pm 1, \eta_l = \pm 1 \tag{4.10}$$

A co-ordinate transformation of the general type (Figure 4.6):

$$x = x(\xi,\eta) \quad \text{and} \quad y = y(\xi,\eta)$$

must be defined. The transformation rules require for the x-co-ordinate the approximation  $x = N_i x_i$ , and for the y-co-ordinate  $y = N_i y_i$ , where  $N_i$  are the same shape functions as used for the quadrilateral element. The Jacobi-matrix is defined in the following manner (Lahrman, 1992):

$$\begin{bmatrix} \partial_{,x} \\ \partial_{,y} \end{bmatrix} = J^{-1} \begin{bmatrix} \partial_{,\xi} \\ \partial_{,\eta} \end{bmatrix} \quad (4.11)$$

where

$$J = \begin{bmatrix} x_{,\xi} & y_{,\xi} \\ x_{,\eta} & y_{,\eta} \end{bmatrix} = \begin{bmatrix} N_{1,\xi} & N_{2,\xi} & N_{3,\xi} & N_{4,\xi} \\ N_{1,\eta} & N_{2,\eta} & N_{3,\eta} & N_{4,\eta} \end{bmatrix} \begin{bmatrix} x_1 & y_1 \\ x_2 & y_2 \\ x_3 & y_3 \\ x_4 & y_4 \end{bmatrix} \quad (4.12)$$

The comma denotes the derivative with respect to a co-ordinate.

Therefore, Equation 4.6 can now be written in the local co-ordinate system as:

$$\sum_{f=1}^4 \iint_{S_f} \left( K_i \frac{\partial h}{\partial x_i} x_i \right) n_f dS = \sum_{f=1}^4 \iint_{S_f} [K_{\xi} n_{\xi} K_{\eta} n_{\eta}]_f J^{-1T} J^{-1} \begin{bmatrix} N_{j,\xi} \\ N_{j,\eta} \end{bmatrix} dS \quad (4.13)$$

Unfortunately, the matrix associated with the head equations system is generally indefinite (Morel et al., 1998) or unsymmetric (Lahrmann, 1992) and thus difficult to solve. Also vertices ( $A$ ) of the finite element are not always an accurate representation of the potential  $h$  over the control volume when it does not coincide necessarily with the centre (Figure 4.5). This method is also often called the vertex-centred control volume method, and requires that control volumes are constructed around nodes, which means that the domain is firstly covered by a mesh where the vertices are actually at the nodal points. This approach is not compatible with the MODFLOW discretisation. Therefore, a cell-centred approach in the finite volume discretisation is to be sought.

### (ii) Support Operators:

Morel et al. (1998), have developed a local Support-Operators Method (SOM) to discretise the diffusion term on quadrilateral meshes. The underlying idea of the method is to develop a discrete operator calculus that faithfully reproduces selected properties of analytical calculus (Margolin et al., 2000). For diffusion problems, this is translated into developing finite difference approximations for the first-order spatial difference operators, namely divergence and gradient that *mimics* the fundamental properties of the physical problem, such as the conservation laws and symmetry in the solution. Therefore, these techniques are also called *mimetic* finite difference methods. The development of these discrete analogs proceeds in two steps. The first one is to define a 'prime' operator, which is the discrete form for one of the fundamental operators (e.g.

divergence). The second step is to construct the other fundamental operators (e.g. gradient) on the basis of the subset of analytical properties that one chooses to maintain (e.g. the accuracy order of energy conservation). The constructed operators are called 'derived' operators.

The advantage of the support operator theory is that it may be applied with equal effectiveness to regular, irregular, and unstructured meshes in both Eulerian and Lagrangian simulations.

Shashkov and Steinberg (1995) have also combined the method of support operators and the mapping method, where the original diffusion equations are transformed to a general curvilinear coordinate system and the resulting equations are then approximated on a rectangular grid in curvilinear coordinates. However, such schemes are usually satisfactory only for smooth grids (Shashkov and Steinberg, 1996).

**(iii) Flux Approximation using Decomposed Vectors (FADV):**

Turner and Ferguson (1995), found that the two-node approximation, expressed in Equation 4.8, is quite straightforward and provides simple discretisation formulation that reduces the computational time. However, its accuracy can be seriously affected by both orientation and orthogonality of the mesh. It provides reasonable results when the normal vector  $n$  and the vector  $v$  are approximately coincident (i.e. orthogonality) (see Figure 4.7) giving:

$$(\nabla h)_{f,n} \approx (\nabla h)_{f,v} = \frac{h_N - h_P}{\|v\|} \quad (4.14)$$

The symbol  $n$  is the unit normal to the cell face, and  $v$  is a unit nodal distance vector. To take account of the mesh non-orthogonality effect on this discretisation, Chow et al. (1996) integrated the diffusion term using the following expression:

$$\iint_S K_i \frac{\partial h}{\partial x_i} dS_i = \sum_{N=1}^4 \frac{h_N - h_P}{\sqrt{\delta x^2 + \delta y^2}} \times (K_x n_x \Delta y - K_y n_y \Delta x)_N + C_{diff} \quad (4.15)$$

where,  $N$  represents the node at the control volume that shares a common face with the control volume  $P$ , where  $\Delta x$  and  $\Delta y$  are the face surface area vector components and  $\delta x$  and  $\delta y$  are the distance vector components between the nodes  $N$  and  $P$  in Cartesian co-

ordinates. It is noted that  $D$  is the nodal distance vector with  $D = \delta x i + \delta y j$ , and  $S$  is the outward normal surface vector with  $S = \Delta y i - \Delta x j$ . The variables inside the brackets are evaluated using the  $N$  and  $P$  control volumes.  $C_{diff}$  is the cross-diffusion term for the common cell face. This term disappears when the nodal distance vector  $D$  is perpendicular to the surface vector  $S$ , and it is small compared with the main term if the non-orthogonality is not severe. Moreover, if a time implicit scheme is used, this type of discretisation leads exactly to the same set of equations obtained by the finite difference method used in MODFLOW.

However, when the mesh is highly non-orthogonal, the cross-diffusion term is significant and thus, should not be neglected. Croft (1998) proposed two correction terms for this aspect of mesh skewness, which affects particularly the diffusion term. The approximation of the derivative along a face using formula such as:

$$\left(\frac{\partial h}{\partial n}\right)_{NP} = \frac{h_N - h_P}{d_{NP}}$$

is no more accurate as the line connecting the two adjacent nodes is no longer parallel to the face normal vector as shown in Figure 4.7. The amended term will be:

$$\left(\frac{\partial h}{\partial n}\right)_{NP} = (v \cdot n)_{NP} \frac{\partial h}{\partial v} + \beta_x \frac{\partial h}{\partial x} + \beta_y \frac{\partial h}{\partial y} \quad (4.16)$$

where  $\beta_x$  and  $\beta_y$  are the Cartesian components of vector  $\beta$  as defined in Figure 4.7. For a fully orthogonal mesh, Equation 4.16 yields:

$$\left(\frac{\partial h}{\partial n}\right)_{NP} = \left(\frac{\partial h}{\partial v}\right)_{NP} = \frac{h_N - h_P}{d_{NP}}$$

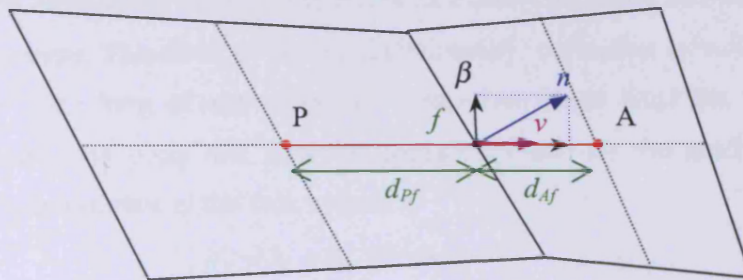


Figure 4.7 Non-orthogonal control volumes.

The estimation of the derivative of  $h$  with respect to the face normal in Equation 4.16 is now reduced to the calculation of the derivative of  $h$  on the control volume faces. Linear interpolation between nodal values, of the derivatives allows the face values to be calculated as:

$$\begin{aligned} \left(\frac{\partial h}{\partial x}\right)_{NP} &= \alpha_{NP} \left(\frac{\partial h}{\partial x}\right)_P + (1 - \alpha_{NP}) \left(\frac{\partial h}{\partial x}\right)_N \\ \alpha_{NP} &= \frac{d_{NF}}{d_{NF} + d_{FP}} \end{aligned} \quad (4.17)$$

In order to calculate the Cartesian derivative of  $h$  at a node the derivative is integrated over the control volume about the node in the following ways:

$$\left(\frac{\partial h}{\partial x}\right)_P = \frac{1}{V_P} \iiint_V \frac{\partial h}{\partial x} dV \quad (4.18)$$

and using the divergence theorem, this reduces to:

$$\iiint_V \frac{\partial h}{\partial x} dV = \iint_S h \cdot n_x dS = \sum_f h_f S_x \quad (4.19)$$

Substituting Equation 4.19 in Equation 4.18 yields:

$$\left(\frac{\partial h}{\partial x}\right)_P = \frac{1}{V_P} \sum_f h_f S_x \quad (4.20)$$

The nodal value of the derivative is now given in terms of the sum of the face values of  $h$ .

The estimated face value of any quantity should be an average value for the whole face. As it is assumed at most stages of the discretisation that variables change linearly between two points, then the face centroid value is the representative average value on this face. The line connecting nodes in the elements either side of the face does not pass through the face centre. Therefore, a ‘non-conjunctionality’ correction term is introduced to represent this other form of skewness. The correction starts from the interpolated value at the intersection point and uses extrapolation based on the gradients of the quantity to obtain an estimate at the face centre:

$$h_f = h_i + \underline{d}_{if} \cdot \underline{grad}h \quad (4.21)$$

Where  $\underline{d}_{if}$  is a vector from the intersection point to the face centre as shown in Figure 4.8.

Substituting Equation 4.21 into Equation 4.20 gives:

$$\left(\frac{\partial h}{\partial x}\right)_P = \frac{1}{V_P} \sum_f A_f s_x (h_I + \underline{d}_{If} \cdot \text{grad} h)_f \quad (4.22)$$

where  $(\text{grad } h)_f$  is calculated using interpolation of its values in the elements either side of face  $f$ . This dependence is resolved by transforming Equation 4.22, and the similar equation for the  $y$  gradient into a 2 by 2 matrix equation for the unknown element gradients. To solve this equation, the gradients are stored and previous iteration values are used on the right hand side of Equation 4.22. The non-conjunctionality correction is not applied to any of the gradient terms, as gradients of gradients would be zero.

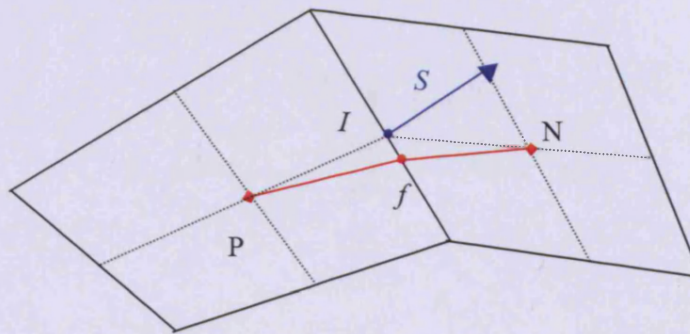


Figure 4.8 Skewness correction through surface  $S_{AP}$  for non-orthogonal mesh.

Croft (1998) showed that for relatively simple problems dominated by diffusion (e.g. heat transfer along a bar), then the use of the orthogonality correction terms on their own causes a deterioration in the accuracy of the simulation results as compared to those results obtained with no correction. For better accuracy, both the conjunctionality and the orthogonality corrections need to be used. However, the use of a Cartesian mesh yields results close to the analytical values than skewed meshes, even when both corrections are applied.

So far no research has been undertaken which definitively establishes the best way to approximate the gradient in the cross-diffusion flux term, the performance of each of the suggested methods being subject to specific boundary conditions, anisotropy ratios and mesh geometries. Jayantha and Turner (2001, 2003, 2005) investigated different strategies for solving the two dimensional diffusion equation in orthotropic medium.



Different gradient approximation techniques and transformations were investigated to calculate the flux at control volume faces. Among these methods is the hybrid control volume finite element method (CV-FE), also called the vertex-centred control volume technique (Ferguson and Turner, 1996), and the flux approximation using decomposed vectors (FADV). In this latter method the gradients at node points are approximated using an interpolation technique, such as: Radial Basis Functions (RBF), Least-Squares Gradient Reconstruction (LSGR), Least-Squares Gradient Polynomial Reconstruction (LSPR), whereas in the hybrid CV-FE method, shape or basis functions are used for interpolations.

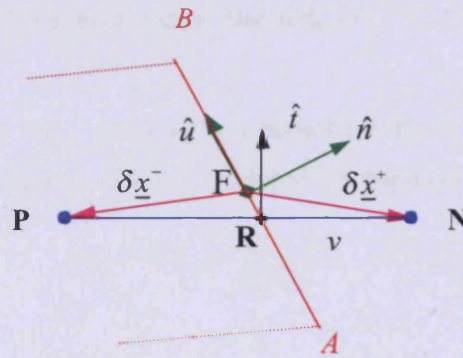


Figure 4.9 Representative control-volume face.

### Model GWFV

In 2003, Jayantha and Turner proposed a high order gradient approximation technique that gives accurate results on coarse meshes. Their method is applicable even for highly anisotropic media, where the  $K$  tensor is not necessarily diagonal. In this study, a model based on the high order flux approximation technique proposed by Jayantha and Turner (2003a, 2003b) has been developed, and will be termed hereinafter the GWFV model. The principle used in this method is to decompose the flux using vectors  $u$  and  $v$  in Figure 4.9, and then introducing corrections for mesh skewness using an improved Least Squares Gradient Reconstruction (ILSGR).

In the first step, the term  $(K\nabla h)\hat{n}$  of Equation 4.6 can be written as or  $\nabla h \cdot w = \nabla h \cdot (K^T \hat{n})$  which is decomposed as follows:

$$\begin{aligned} (\nabla h) \cdot w &= \alpha \nabla h \cdot v + \beta (\nabla h \cdot \hat{u}) \\ &= \alpha (h_N - h_P) + \beta (\nabla h \cdot \hat{u}) \end{aligned} \quad (4.23)$$

where the constants  $a$  and  $\beta$  depend on the tensor  $K$  and the geometry of the CV mesh. This decomposition is made at each cell face. To find explicitly terms of Equation 4.23, the vector  $w = K^T \hat{n}$  should be decomposed in terms of the vectors  $v$  and  $\hat{u}$ . The two vector equations  $v = (v \cdot \hat{u}) \hat{u} + (v \cdot \hat{n}) \hat{n}$  and  $w = (w \cdot \hat{u}) \hat{u} + (w \cdot \hat{n}) \hat{n}$  give the following formula:

$$w = (w \cdot \hat{u}) \hat{u} + (w \cdot \hat{n}) \frac{v - (v \cdot \hat{u}) \hat{u}}{v \cdot \hat{n}} \quad (4.24)$$

Therefore, the term  $\nabla h \cdot w$  can be expressed as:

$$(\nabla h) \cdot w = \frac{w \cdot \hat{n}}{v \cdot \hat{n}} \nabla h \cdot v + \left\{ w \cdot \hat{u} - w \cdot \hat{n} \frac{v \cdot \hat{u}}{v \cdot \hat{n}} \right\} (\nabla h \cdot \hat{u}) \quad (4.25)$$

The primary term  $\nabla h \cdot v$  is evaluated at the midpoint  $F$  of the CV face (see Figure 4.9) by:

$$(\nabla h \cdot v)_F = h_N - h_P$$

In Equation 4.6, this term needs to be evaluated at point  $R$ , so that errors due to mesh skewness will be corrected. Using a Taylor series expansion of the function  $h$  yields:

$$h(\underline{x}_F + \delta \underline{x}^+) = \sum_{k=0}^m \frac{1}{k!} (\delta \underline{x}^+ \cdot \nabla)^k h(\underline{x}_F) + R^+ \quad (4.26)$$

and

$$h(\underline{x}_F + \delta \underline{x}^-) = \sum_{k=0}^m \frac{1}{k!} (\delta \underline{x}^- \cdot \nabla)^k h(\underline{x}_F) + R^- \quad (4.27)$$

where the remainder  $R$  has the *Lagrange form*. Subtracting Equation 4.27 from Equation 4.26 and assuming  $R^+ - R^- \approx 0$  yields:

$$(\nabla h \cdot v)_F \approx (h_N - h_P) - \varepsilon_{np} \quad (4.28)$$

where

$$\varepsilon_{np} \approx \sum_{k=2}^m \frac{1}{k!} \left\{ (\delta \underline{x}^+ \cdot \nabla)^k - (\delta \underline{x}^- \cdot \nabla)^k \right\} h(\underline{x}_F) \quad (4.29)$$

and  $m$  is the order of the Taylor expansion. In this study, the accuracy will be limited to second order. Thus, correction term in Equation 4.29 becomes:

$$\varepsilon_{np} \approx \frac{1}{2} \left\{ (\delta \underline{x}^+ \cdot \nabla)^2 - (\delta \underline{x}^- \cdot \nabla)^2 \right\} h(\underline{x}_F) \quad (4.30)$$

Substituting Equation 4.28 in Equation 4.25, yields:

$$\{(K \nabla h) \hat{n}\}_F^{n+1} = \frac{w \cdot \hat{n}}{v \cdot \hat{n}} (h_N^{n+1} - h_P^{n+1}) + \left\{ w \cdot \hat{u} - w \cdot \hat{n} \frac{v \cdot \hat{u}}{v \cdot \hat{n}} \right\} (\nabla h \cdot \hat{u})_F^{n+1} - \frac{w \cdot \hat{n}}{v \cdot \hat{n}} (\varepsilon_{np})_F^{n+1} \quad (4.31)$$

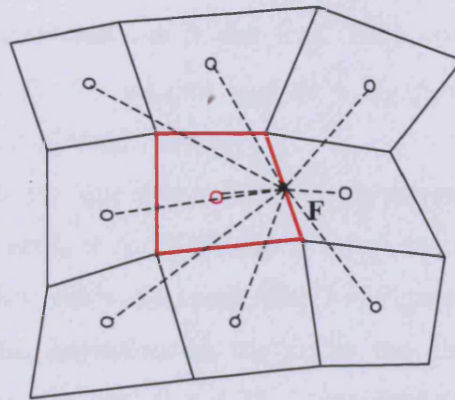


Figure 4.10 Neighbouring nodes involved in surface flux calculation.

**(iv) Direct Surface Interpolation Techniques:**

Other methods used to approximate gradients through cell faces deploy simple interpolations of the function values at particular points (nodes or vertices). Two cases of these interpolations techniques will be developed and tested for accuracy and comparison purpose with the previously developed model.

**Model V**

An alternative to approximate the gradient over control volume faces is merely to use the arithmetic average scheme using flux at the vertices defining the surface (Wasantha Lal, 1998). This method seems to be the choice when polygons, not triangles, are used in the discretisation. Therefore, in Figure 4.9, the gradient on face  $AB$  will be approximated by:

$$(\text{grad}h)_{AB} = \frac{1}{2}[(\text{grad}h)_A + (\text{grad}h)_B]$$

In Cartesian co-ordinates, the approximation is written as follows:

$$\left(\frac{\partial h}{\partial x}\right)_{AB} = \frac{1}{2}\left[\left(\frac{\partial h}{\partial x}\right)_A + \left(\frac{\partial h}{\partial x}\right)_B\right] \quad (4.35-a)$$

$$\left(\frac{\partial h}{\partial y}\right)_{AB} = \frac{1}{2}\left[\left(\frac{\partial h}{\partial y}\right)_A + \left(\frac{\partial h}{\partial y}\right)_B\right] \quad (4.35-b)$$

For a cell-centred finite volume method, Equations 4.35-a and 4.35-b provide straightforward approximations to the flux. They correspond to the application of a trapezium formula for the integral  $\int_{AB} f dy = (f_A + f_B)(y_B - y_A)/2$ . This approximation is second order accurate (Hirsch, 1988).

The fluxes through cell face approximations are therefore reduced to an average of the fluxes at the cell vertices A, B, C and D when summing the contribution of all the integrals over the four sides of the cell ABCD of Figure 4.5.

Computation of the derivatives at the nodes has already been discussed in Croft's method and is given by Equation 4.28. These derivatives need to be approximated at each of the four vertices of the control volume. The integral method is applied once more, but this time on an auxiliary control volume around each vertex point (Liu and Jameson, 1993). In Figure 4.11 the vertex *A* is considered in a two-dimensional mesh, with the index notation for a structured mesh being as in MODFLOW, the auxiliary cell is formed by connecting nodes  $(i, j)$ ,  $(i, j+1)$ ,  $(i+1, j)$  and  $(i+1, j+1)$  and the midpoints  $(i+1/2, j)$ ,  $(i+1, j+1/2)$ ,  $(i+1/2, j+1)$  and  $(i, j+1/2)$  of the cell faces.

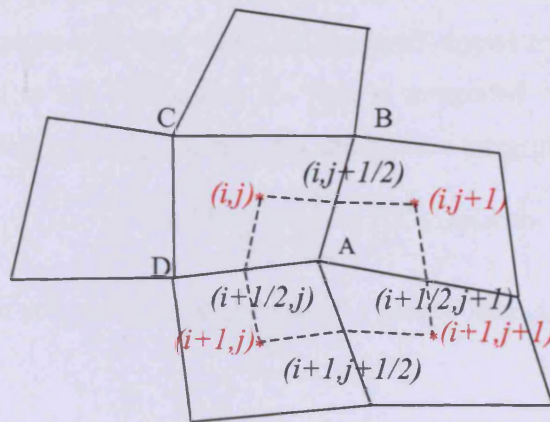


Figure 4.11 Auxiliary cell used to calculate diffusive balance in model V.

The derivatives at the vertex *A* can now be approximated by summing the flux balances over the eight faces of the auxiliary cell to give:

$$\left(\frac{\partial h}{\partial x}\right)_A \cong \frac{1}{S_A} \oint h x dS = \frac{1}{S_A} \sum_{m=1}^8 h_m \Delta y_m \quad (4.36-a)$$

$$\left(\frac{\partial h}{\partial y}\right)_A \cong \frac{1}{S_A} \oint h y dS = \frac{1}{S_A} \sum_{m=1}^8 h_m \Delta x_m \quad (4.36-b)$$

where  $h$  in each edge of the auxiliary surface accounts for the head nodal value at the cell centre belonging to it, for example:

$$(h\Delta y)_{(i,j);(i,j+1/2)} = h_{i,j} \Delta y_{(i,j);(i,j+1/2)} \quad (4.37)$$

The derivatives at the other vertices can likewise be computed in the same manner. Substituting Equations 4.35-4.37 in Equation 4.6 yields an approximation of the diffusive term in cell  $(i,j)$  using the nodal values of  $h$  at the nine adjacent nodes. This model will be called model V hereinafter.

### Model S

Faille (1992) proposed another conservative control volume scheme with a consistent approximation of the fluxes over a face  $S$ . Denoting the approximation of a surface integral over a side  $S$  by  $L_S(h)$  gives:

$$L_S(h) = \iint_S (K \text{grad } h \cdot n_S) dS = (K \text{grad } h)_S \iint_S n_S dS \quad (4.38)$$

In this equation, the gradient component along sides can be computed using the integral method. A staggered grid, also called the diamond-shaped region, surrounding the side is created (Elmahi et al., 1999), and the flux is integrated over the surface of the new staggered grid. For example, for side  $AB$ , the surface integral is written as:

$$(K \text{grad } h)_{AB} \cong \frac{1}{V_{S_{AB}}} \iiint_{V_{S_{AB}}} K \text{grad } h \, dv \quad (4.38)$$

where  $V_{S_{AB}}$  is the volume of the staggered grid around face  $AB$ , as shown in Figure 4.12.

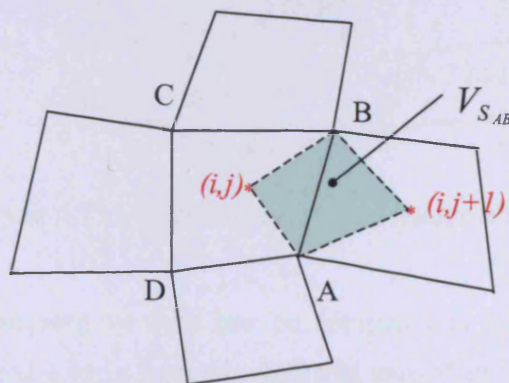


Figure 4.12 Staggered grid for face  $AB$  in model S.

Applying the Gauss formula in Equation 4.38 yields:

$$(K \text{ grad } h)_{AB} \cong \frac{1}{V_{S_{AB}}} \sum_{m=1}^4 \iint_{S_m} (K \text{ grad } h \cdot n_m) dS_m = \frac{1}{V_{S_{AB}}} \sum_{m=1}^4 h_m \cdot K'_m \cdot S_m \quad (4.39)$$

where  $m$  refers to the four surfaces of the staggered grid  $V_{S_{AB}}$ . The head required at the diamond-shaped co-volume faces is computed using the values of the data on the nodes and the vertex sharing this grid (Elmahi et al., 1999). Thus, Equation 4.39 is written as follows:

$$(K \text{ grad } h)_{AB} \cong \frac{1}{V_{S_{AB}}} \sum_{m=1}^4 h_m \cdot K'_m \cdot S_m = \frac{1}{V_{S_{AB}}} \sum_{m=1}^4 \frac{1}{2} (h_{N_1}^m + h_{N_2}^m) K'_m \cdot S_m \quad (4.40)$$

where  $N_1$  and  $N_2$  are the nodes of an edge  $m$  of the staggered grid surface  $S$ . The estimation of the head value at each vertex of the control volume is determined by a weighted average of the surrounding cell-centred solution quantities (Frink, 1992). As it is assumed that the known values of the solution are concentrated at the cell centres, the contribution to a vertex from the surrounding cells is inversely proportional to the surface between the vertices and each cell centre, as shown in Figure 4.13.

$$h_A = \frac{1}{\sum_{k=1}^4 \frac{1}{V_k^A}} \left[ \frac{h_1}{V_1^A} + \frac{h_2}{V_2^A} + \frac{h_3}{V_3^A} + \frac{h_4}{V_4^A} \right] \quad (4.41)$$

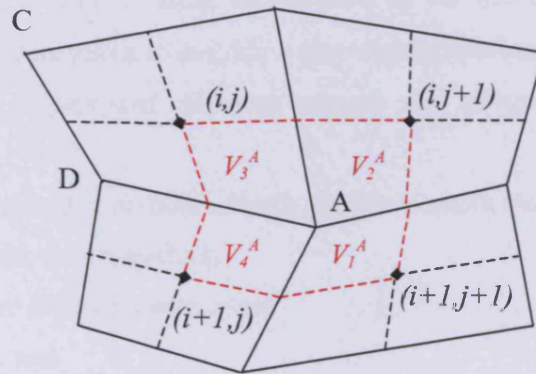


Figure 4.13 Volumes used in head interpolation at vertex  $A$ .

Heads at the remaining vertices can be computed in the same manner. Substituting Equations 4.40 and 4.41 in Equation 4.39 and expanding this formulation to the surface integrals over other faces of cell  $(i,j)$ , in Equation 4.6, yields an approximation of the diffusion term involving nodal variables at the eight cells surrounding cell  $(i,j)$ .

The choice of the appropriate scheme is based upon accuracy, consistency, and adaptability to MODFLOW. In this sense, second-order accuracy is a minimum requirement. The method results also have to achieve a high level mesh-independence for reasonable mesh resolution. The adaptability to MODFLOW was already initiated by the choice of mesh structure. The following step would be to seek a matrix that has possibly the same features as the one solved in MODFLOW, especially since the latter has ideal properties which should be sought after in any finite volume discretisation. This is a more difficult task as the non-orthogonal feature of the cells, the type of interpolations used, and the number of nodes involved in the discretisation for each cell are determinant differences that dictate the elements of the new system matrix. If the matrix doesn't have one of the following properties: sparse, five non-zero diagonals, symmetric, positive definite and diagonally dominant, then new solvers have to be used and thus, added to the MODFLOW programme as a new package. Other choice criteria such as storage, computational time, convergence and stability are left to a second selection level.

So far three discretisation methods out of the different techniques mentioned above have been developed to solve the groundwater flow equation. Ultimately, the choice of the best discretisation method is made on the basis of the accuracy, consistency, and the computational effort required to provide a converging solution. As stated by Morel et al. (1998), the ideal cell-centred diffusion scheme for 2D quadrilateral meshes would require:

- second-order accuracy on both smooth and non-smooth meshes either with or without material discontinuities;
- only cell-centre intensity unknowns;
- a local stencil; and
- a symmetric positive-definite matrix representation for the diffusion matrix.

The ideal method would achieve at least a second order spatial accuracy, produce a symmetric positive definite and diagonally dominant matrix when the time formulation is implicit, and would not require strongly restrictive conditions to ensure stability and convergence of the solver as in explicit schemes.

In this study comparisons have been undertaken to compare the performance of each of the approximation techniques for the flux at cell faces discussed above, with the particular aim of choosing the most suitable scheme to be implemented in MODFLOW. The assessment criteria used have been based on the performance of the selected method as well as the input and programme changes related to mesh consideration, the resulting diffusion matrix and the solver that have to be introduced into the MODFLOW programme. Therefore, a number of performance tests for the three methods have been carried out and these are detailed in the next chapter, together with a comparison of their relevant features. The properties of these methods are detailed in the following sections.

#### 4.3.1.2 Approximating the Permeability on a Control Volume Face

As Equation 4.6 shows it, the permeability coefficient  $K$  has also to be evaluated at cell faces. In MODFLOW this is achieved implicitly by introducing a new term combining grid dimensions and hydraulic conductivity into a single constant, called 'conductance'. For two adjacent cells (see Figure 4.14) and using MODFLOW index notation, the conductance in row  $i$  and layer  $k$  between nodes  $(i,j-1,k)$  and  $(i,j,k)$  is written as:

$$CR_{i,j-\frac{1}{2},k} = KR_{i,j-\frac{1}{2},k} \frac{\Delta c_i \Delta v_k}{\Delta r_{j-\frac{1}{2}}} \quad (\text{L}^2\text{T}^{-1}) \quad (4.42)$$

where  $KR_{i,j-\frac{1}{2},k}$  is the hydraulic conductivity along row  $i$  between nodes  $(i,j-1,k)$  and  $(i,j,k)$ ,  $\text{LT}^{-1}$ ;  $\Delta c_i \Delta v_k$  is the area of the cell face normal to the row direction,  $\text{L}^2$ ; and  $\Delta r_{j-\frac{1}{2}}$  is the distance between nodes  $(i,j-1,k)$  and  $(i,j,k)$ . The index  $k$  will be dropped from MODFLOW formulations as only two-dimensional considerations are cited here. It is also assumed that all of the examples are given for a one-layer domain with a unit thickness.

Given that the nodes are considered to be at the centre of the cells and the transmissivity, in case of a confined aquifer, is uniform over each cell, then the horizontal conductance between the nodes is the equivalent horizontal conductance of two half cells in series, so that:

$$CR_{i,j-\frac{1}{2}} = \frac{\frac{TR_{i,j-1}\Delta c_i}{\Delta r_{j-1}/2} \frac{TR_{i,j}\Delta c_i}{\Delta r_j/2}}{\frac{TR_{i,j-1}\Delta c_i}{\Delta r_{j-1}/2} + \frac{TR_{i,j}\Delta c_i}{\Delta r_j/2}} = 2\Delta c_i \frac{TR_{i,j-1}TR_{i,j}}{TR_{i,j-1}\Delta r_j + TR_{i,j}\Delta r_{j-1}} \quad (4.43)$$

where  $TR$  is the transmissivity in the row direction, ( $L^2T^{-1}$ );  $\Delta r$  is the grid width along a row,  $L$ ; and  $\Delta c$  is the grid width along a column,  $L$ .

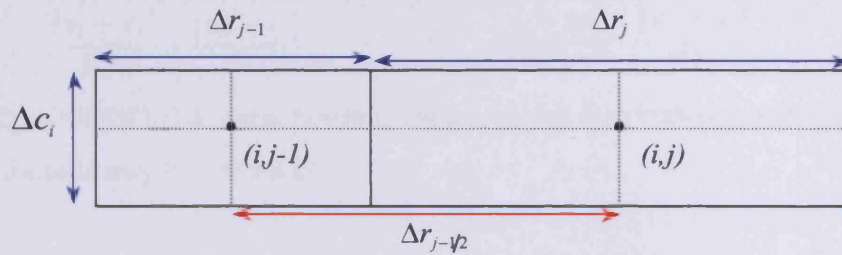


Figure 4.14 Geometrical weight factors for permeability interpolation in MODFLOW.

The same process is applied to compute the equivalent horizontal conductance in a column direction. For an unconfined layer the transmissivity is replaced by the product of the hydraulic conductivity and the saturated thickness. Expression 4.43 will be equal to zero - and thus allow zero flux - when one of the hydraulic conductivities is null (i.e. a no flux boundary) or the saturated thickness is null (i.e. a dewatered cell); this would be the expected value for either of these conditions. Two other alternatives for calculating the horizontal branch conductance, based on different assumptions about specific flow systems, were proposed by Goode and Apple (1992). They are used in the MODFLOW program as options to compute the interblock conductance when the above mentioned specific conditions apply.

In a finite volume discretisation, an equivalent hydraulic permeability has to be assessed at the face between two adjacent quadrilateral cells that are not necessarily orthogonal. Croft (1998) proposed the use of a harmonic mean value to describe the variation of such a coefficient between nodes. Therefore, for the same two adjacent cells, as in Figure 4.4, the equivalent permeability will be:

$$K_f = \frac{K_N K_P}{\alpha_f K_P + (1 - \alpha_f) K_N} \quad \text{with} \quad \alpha_f = \frac{d_{Nf}}{d_{Nf} + d_{Pf}} \quad (4.44)$$

As the line connecting nodes  $N$  and  $P$  does not necessarily lay along the normal face  $f$ , nor does it pass through the centre of the face, then another approximation is made to take into account these types of skewness (i.e. non-orthogonality and non-conjunctionality). In Figure 4.8 for instance, the permeability [ $L^2T^{-1}$ ] along face  $f$  can be estimated by using the formula:

$$KX_f = \frac{\frac{|x_I - x_P| + |x_N - x_I|}{|x_I - x_P|} + \frac{|x_N - x_I|}{|x_N - x_I|}}{\frac{KX_P}{|x_I - x_P|} + \frac{KX_N}{|x_N - x_I|}} \quad \text{and} \quad KY_f = \frac{\frac{|y_I - y_P| + |y_N - y_I|}{|y_I - y_P|} + \frac{|y_N - y_I|}{|y_N - y_I|}}{\frac{KY_P}{|y_I - y_P|} + \frac{KY_N}{|y_N - y_I|}} \quad (4.45)$$

In terms of the MODFLOW index notation, for a common face between cells  $(i,j-1)$  and  $(i,j)$ , these formula may be written as:

$$KX_{i,j-\frac{1}{2}} = \left( \frac{|x_{i,j-\frac{1}{2}} - x_{i,j}| + |x_{i,j-1} - x_{i,j-\frac{1}{2}}|}{|x_{i,j-\frac{1}{2}} - x_{i,j}|} + \frac{|x_{i,j-1} - x_{i,j-\frac{1}{2}}|}{|x_{i,j-1} - x_{i,j-\frac{1}{2}}|} \right) \frac{KX_{i,j-1}KX_{i,j}}{KX_{i,j-1}|x_{i,j-\frac{1}{2}} - x_{i,j}| + KX_{i,j}|x_{i,j-1} - x_{i,j-\frac{1}{2}}|} \quad (4.46)$$

$$KY_{i,j-\frac{1}{2}} = \left( \frac{|y_{i,j-\frac{1}{2}} - y_{i,j}| + |y_{i,j-1} - y_{i,j-\frac{1}{2}}|}{|y_{i,j-\frac{1}{2}} - y_{i,j}|} + \frac{|y_{i,j-1} - y_{i,j-\frac{1}{2}}|}{|y_{i,j-1} - y_{i,j-\frac{1}{2}}|} \right) \frac{KY_{i,j-1}KY_{i,j}}{KY_{i,j-1}|y_{i,j-\frac{1}{2}} - y_{i,j}| + KY_{i,j}|y_{i,j-1} - y_{i,j-\frac{1}{2}}|}$$

where the permeability coefficients are now written with respect to the Cartesian coordinate and not the row and column directions as in MODFLOW, since the orthogonality is no longer verified. These formulations give the same results as in MODFLOW when the same conditions apply (i.e. no flow boundaries and dewatered cells). If the mesh is orthogonal, that is line  $P$  in Figure 4.8 is orthogonal to face  $f$ , and  $I$  lies along this line, then the equivalent permeability in the  $y$  direction will vanish according to Equation 4.46 and the equivalent permeability in the  $x$  direction will be:

$$KX_{i,j-\frac{1}{2}} = KR_{i,j-\frac{1}{2}} = (\Delta r_{j-1} + \Delta r_j) \frac{KR_{i,j-1}KR_{i,j}}{KR_{i,j-1}\Delta r_{i,j} + KR_{i,j}\Delta r_{i,j-1}}$$

The flow coming into cell  $(i,j)$  from cell  $(i,j-1)$  in the row direction is given by Darcy's law as:

$$q_{i,j-\frac{1}{2}} = TR_{i,j-\frac{1}{2}} \Delta c_i \frac{h_{i,j-1} - h_{i,j}}{\Delta r_{j-\frac{1}{2}}} = 2\Delta c_i \frac{TR_{i,j}TR_{i,j-1}}{TR_{i,j}\Delta r_{j-1} + TR_{i,j-1}\Delta r_{i,j}} (h_{i,j-1} - h_{i,j}) \quad \text{-----MODFLOW}$$

$$q_{i,j-\frac{1}{2}} = TR_{i,j-\frac{1}{2}} \Delta c_i \left( \frac{\partial h}{\partial x} \right)_{j-\frac{1}{2}} = (\Delta r_{j-1} + \Delta r_j) \frac{TR_{i,j-1}TR_{i,j}}{TR_{i,j-1}\Delta r_j + TR_{i,j}\Delta r_{j-1}} \Delta c_i \frac{h_{i,j-1} - h_{i,j}}{\Delta r_{j-\frac{1}{2}}} \quad \text{-----Finite volume}$$

As  $\Delta r_{j-\frac{1}{2}} = \frac{\Delta r_{j-1} + \Delta r_j}{2}$ , the finite volume approximation yields exactly the same expression as in MODFLOW discretisation when the mesh is fully orthogonal.

### 4.3.2 Implementation of Boundary Conditions

One of the advantages of the cell-centred control volume technique is the ease with which the boundary conditions can be accommodated within the scheme (Turner, 1995). For control volumes that have a face coincident with the domain boundary, information is introduced into the equation to complete the formulation and enable it to be solved. In groundwater flow, the appropriate boundary conditions are: specified head boundaries (Dirichlet conditions), specified flow boundaries (Neumann conditions) and head dependent flow boundaries (Cauchy conditions). To simulate these types of boundaries, the three boundary categories that have been defined in MODFLOW are:

- 'constant-head' cells: these give the Dirichlet condition in which the head is specified in advance, and is held constant for all time steps of the simulation;
- 'inactive' or 'no flow' cells: no flow into or out of these cells is permitted at any time step of the simulation. This type of boundary is a special case Neumann condition. The specified flow boundary for which the flux across a boundary is known and differs from zero is simulated within the third category; and
- 'variable-head' cells: for all of the remaining cells of the mesh. The Cauchy and Neumann conditions, in which the specified flow is not zero are simulated through the use of external source terms. Packages like River (RIV), Drain (DRN), Evapotranspiration (EVT) and General Head Boundaries (GHD) are used in MODFLOW for this purpose.

In the three new discretisations, the same conditions are simulated in a similar way to those used in MODFLOW. However, in the model GWFV, the heads at surrounding cells of the stencil are needed to calculate the flux at faces of cells at boundaries, see Figure 4.15. Nine point values are required to write the matrix Equation 4.33. Thus, values at cells that cannot appear at boundaries are replaced with existing adjacent cells (empty circles), and associated vectors are extended only to the centre of the boundary face, as shown with filled circles in Figures 4.15.

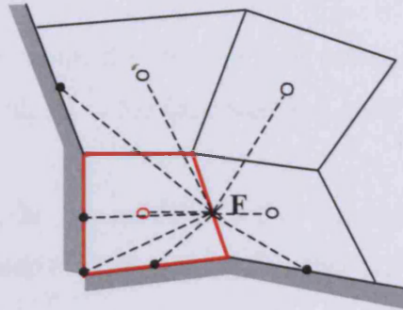


Figure 4.15 Typical boundary control volume and related point values.

### 4.3.3 Source Term

In equation 4.4, the source term can be written as:

$$\iiint W dV = W_{i,j} V_{i,j} = QS_{i,j}$$

where  $V_{i,j}$  is the volume (with unit depth) of node  $(i,j)$ , and  $W_{i,j}$  is the volumetric flux per unit volume,  $T^{-1}$ , accounting for flows into or out of cell  $(i,j)$  from processes external to the aquifer, such as streams, drains, areal recharge, evaporation, wells and sinks,. For most of these physical processes, the source term  $QS_{i,j}$  can generally be linearised<sup>1</sup> giving:

$$QS_{i,j} = Q_{i,j} + P_{i,j} h_{i,j} \quad (4.47)$$

where  $QS_{i,j}$  is the sum of the flows from all external sources affecting the cell  $(i,j)$ ,  $L^3T^{-1}$ ; and  $P_{i,j}$  and  $Q_{i,j}$  are constants,  $L^2T^{-1}$  and  $L^3T^{-1}$ . The coefficient  $P_{i,j}$  must always be less than or equal to zero to ensure that the final head coefficient at node  $(i,j)$  is always positive (Patankar, 1980). If a source is non-linear in  $h$  then it can be appropriately linearised, and cast into the format of equation (4.47), where the values of  $P_{i,j}$  and  $Q_{i,j}$  are to prevail over the irregular control volume.

### 4.3.4 Transient Term – Temporal Discretisation

In Equation 4.4, the transient term is approximated using the backward substitution as in MODFLOW, thus:

$$\iiint_V S_s \frac{\partial h}{\partial t} .dV = S_{S_{i,j}} \frac{h_{i,j}^{m+1} - h_{i,j}^m}{t^{m+1} - t_m} V_{i,j} \quad (4.48)$$

where the superscript  $m$  denotes the old-time step value,  $V_{i,j}$  is the volume of the control volume defined by node  $(i,j)$ ,  $t$  is the time step and  $h_P$  denotes value of  $h$  at the centroid of the cell  $P$ .

It is worth noting that, in the model GWFV, the matrix equation (4.33) is solved explicitly. At each time step  $m+1$ , the vector  $X_D$ , that provides the function value and its derivatives at each CV face, is required to compute  $\nabla h \hat{u}$  and  $\varepsilon_{np}$  in equation (4.31) with the vector values being available from the previous time step  $m$ . A fully implicit treatment of these equations is possible, but this solution leads to a nine-unknown equation for each cell for models S and V, whereas in the GWFV model as in MODFLOW, only five unknowns exist for each cell at each time step.

#### 4.4 Formulation of Linear Equations

In the models V and S, the substitution of approximation terms into Equation 4.4 gives the finite volume approximation for cell  $(i,j)$  as:

$$\begin{aligned} & A'_{i,j} (h_{i-1,j-1} - h_{i,j}) + B'_{i,j} (h_{i-1,j} - h_{i,j}) + C'_{i,j} (h_{i-1,j+1} - h_{i,j}) + D'_{i,j} (h_{i,j-1} - h_{i,j}) \\ & + F'_{i,j} (h_{i,j+1} - h_{i,j}) + G'_{i,j} (h_{i+1,j-1} - h_{i,j}) + H'_{i,j} (h_{i+1,j} - h_{i,j}) + I'_{i,j} (h_{i+1,j+1} - h_{i,j}) \\ & + P'_{i,j} h_{i,j} + Q_{i,j} = S_{i,j} \frac{\Delta h_{i,j}}{\Delta t} V_{i,j} \end{aligned} \quad (4.49)$$

where the coefficients  $A'$ ,  $B'$ ,  $C'$ ,  $D'$ ,  $F'$ ,  $G'$ ,  $H'$  and  $I'$  depend upon the space discretisation method used.

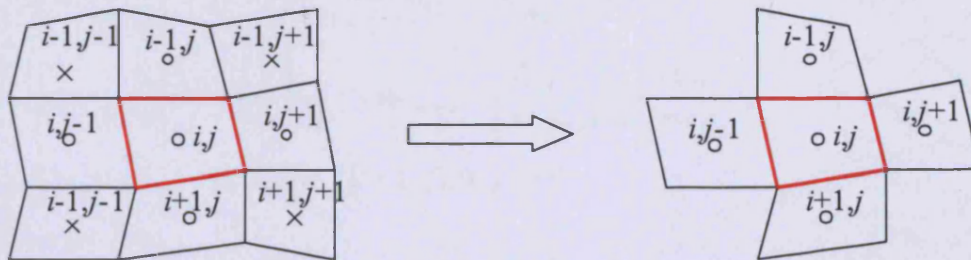


Figure 4.16 A nine-node stencil reduced to five-node stencil.

In the GWFV model, as in MODFLOW, only five nodes of the cross stencil (Figure 4.16) are required. In order to reduce the nine-node computational stencil of models V and S to a five-node stencil, an interpolation method of second order accuracy is used to express the nodes at the four corners of the stencil at node  $(i,j)$ . This method is described herein. For the known values of a function at the four nodes presented in Figure 4.17, linear interpolation between point C and the other nodes gives:

$$f_1(C) \approx \omega_1 f(1) + (1 - \omega_1) f(3) \quad \text{where } \omega_1 = \frac{[C,3]}{[1,3]}$$

$$f_2(C) \approx \omega'_1 f(2) + (1 - \omega'_1) f(4) \quad \text{where } \omega'_1 = \frac{[C,4]}{[2,4]}$$

As  $f_1(C) \approx f_2(C)$  then

$$f(1) \approx \frac{\omega'_1}{\omega_1} f(2) + \frac{(1 - \omega'_1)}{\omega_1} f(4) - \frac{(1 - \omega_1)}{\omega_1} f(3) \tag{4.50}$$

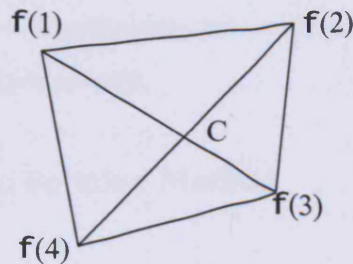
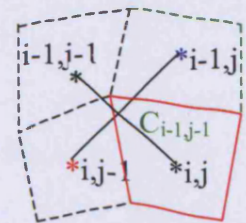


Figure 4.17 Estimation of a function at one corner of a quadrilateral in terms of the function values at remaining corners.

According to Equation 4.50, approximation at any of the corner nodes, for instance node  $(i-1,j-1)$ , can be written as:

$$\left\{ \begin{array}{l} h_{i-1,j-1} \approx \frac{\omega'_{i-1,j-1}}{\omega_{i-1,j-1}} h_{i-1,j} + \frac{(1 - \omega'_{i-1,j-1})}{\omega_{i-1,j-1}} h_{i,j-1} - \frac{(1 - \omega_{i-1,j-1})}{\omega_{i-1,j-1}} h_{i,j} \\ \omega_{i-1,j-1} = \frac{[C_{i-1,j-1}, (i, j)]}{[(i-1, j-1), (i, j)]} \quad \omega'_{i-1,j-1} = \frac{[C_{i-1,j-1}, (i, j-1)]}{[(i-1, j), (i, j-1)]} \\ C_{i-1,j-1} = [(i-1, j-1), (i, j)] \cap [(i-1, j), (i, j-1)] \end{array} \right.$$



(4.51)



In the GWFV model, discretisation leads to a symmetric  $A$  matrix. This property is also satisfied in the model V and model S matrices if the grid is orthogonal and the medium is isotropic and homogeneous. When non-orthogonality, heterogeneity and/or anisotropy occur, this property is no longer satisfied. However, the difference between the diagonal terms that should be symmetric can be quantified, and thus controlled, in terms of the grid geometry and medium heterogeneity. If  $K$  is isotropic the banded system will be well conditioned if the grid is near-orthogonal. However, for the general case of a non-orthogonal grid, the presence of strong variations in  $K$  can lead to poor conditioning (Hyman et al., 2001). Nevertheless, the banded system is always positive definite. Also, the mesh technique, such as rezoning and remapping the grid if the grid is too distorted, can be used as explained by Margolin and Shashkov (2003). Generally, the stability of finite difference methods is satisfied when the interpolation operators are symmetric and positive definite (Hymann and Shashkov, 1999). Therefore these properties should be sought in the current schemes to guarantee stability. The GWFV model shows more similarities in the matrix properties with MODFLOW, and is closer to the ideal criteria of matrix resulting from discretisation on a quadrilateral grid. The matrix is symmetric, positive definite and diagonally dominant and a specific analysis of the model accuracy is considered further.

#### 4.5.2 Solution Technique

The system of the form of the Equations 4.53 can be solved by direct methods. However, a great deal of computer memory and time may be required, in addition to round-off errors that may become unacceptably large. The classic direct solvers do not enable the advantage of the sparse feature of the system matrix to be taken into account, as many non-zero elements arise while factoring the matrix into a lower triangular and upper triangular matrices. Iterative solutions appear to provide a more appropriate solution option. A similar set of algebraic equations for various FV discretisations have been solved using different packages in different models. These include: Maple (Abell & Braselton, 1994) and Math-cad (Mathcad7, 1997).

For the GWFV model, the iterative procedure used to solve the system of algebraic equations is the Strongly Implicit Procedure, as included in the MODFLOW programme (i.e. the SIP solver). This method proved to be the best for large systems (Patankar, 1980). Also, it provides accurate solutions if the proper combination of the SIP solver parameters is chosen. A comparison of this method with the Slice Successive Overrelaxation (SSOR) and the Preconditioned Conjugate-Gradient2 (PCG2) solvers in MODFLOW can be found in Osiensky and Williams (1997).

For the models V and S, the coefficients in Equation 4.52 show a non-symmetric behaviour in non-orthogonal cases, and treating this equation implicitly requires appropriate solvers to be chosen. Many solvers can be found in the literature or are available in public or private domains for such matrices, for example: SLAP (Seager, 1988), PetSc (Smith et al., 1995), Itpack (Kincaid et al., 1989), DSLUGM in SLATEC (Brown et al., 1992). However, except the LMG package, all of the other MODFLOW solvers are restricted to symmetric matrices. Thus, at this stage, an explicit formulation in models S and V is sufficient to achieve a primary comparison of their accuracy with the GWFV model. The cells are chosen in such a way that computations are carried out within time steps restricted by the stability limit.

The explicit formulation of Equation 4.49 is:

$$B_{i,j}h_{i-1,j}^m + D_{ii,j}h_{i,j-1}^m + \left( E_{i,j} + P_{i,j} + \frac{S_{S_{i,j}}V_{i,j}}{t^{m+1}-t^m} \right) h_{i,j}^m + F_{i,j}h_{i,j+1}^m + H_{i,j}h_{i+1,j}^m + Q_{i,j} = \frac{S_{S_{i,j}}V_{i,j}}{t^{m+1}-t^m} h_{i,j}^{m+1} \quad (4.54)$$

where  $E_{i,j} = -B_{i,j} - D_{ii,j} - F_{i,j} - G_{i,j} - H_{i,j}$

This system is solved by starting from the initial distribution of piezometric heads  $h_{i,j}^0$ , and then  $h_{i,j}^1$  are calculated directly from Equation 4.54 for all nodes of the mesh. Recursive use of Equation 4.54 leads up to the solution at any desired time level. This solution procedure is relatively easy to program, but has a great disadvantage with regard to the time step having to be restricted to ensure computational stability and accuracy.

## 4.6 Accuracy Issues of the Selected Scheme

The use of the midpoint rule in the finite volume technique can maintain second order accuracy only if the flux approximation at the CV face is at least second-order accurate (Murthy and Marthur, 1998). The approximation of the gradient component along the line joining two nodes, used in both the MODFLOW finite difference method, and in the finite volume method expressed in Equation 4.31, is the first order Taylor approximation. The error in the flux estimation is mainly dominated by the approximation of this term.

At the level of Equation 4.5, no approximation has been made, and thus, it is exact (Tukel, 1985). In the following steps, Equations 4.6 and 4.7 are second order in space if the flux approximation at the midpoint of the CV faces is at least second order accurate (Jayantha and Turner, 2003 (a) and (b)).

### 4.6.1 Numerical errors in the discretisation procedure

In the finite volume discretisation, sources of errors can be divided into two groups, namely: errors caused by discretisation of the solution domain and errors caused by equation discretisation (Jasak, 1996). The first category includes insufficient mesh resolution, mesh skewness and non-orthogonality. The second category is represented through numerical diffusion when a second-order finite volume method is used. This type of error is derived from the convection term and temporal discretisation. For the model considered herein, only numerical diffusion arising from temporal discretisation is of concern, and emphasis will be focused on the first type of error. Analysis of the two types of errors induced in this scheme are presented.

#### 4.6.1.1 Numerical Diffusion from Temporal Discretisation

Considering the time integral from  $n\delta t$  to  $(n+1)\delta t$ , the discrete form of Equation 4.4 can be written as:

$$\begin{aligned} \lambda \left[ \sum_{A=1}^4 K_{i,A} \left( \frac{\partial h}{\partial x_i} \right)_A^{(n+1)} x_i S_A + P_{i,j} h_{i,j}^{(n+1)} \right] + (1-\lambda) \left[ \sum_{A=1}^4 K_{i,A} \left( \frac{\partial h}{\partial x_i} \right)_A^{(n)} x_i S_A + P_{i,j} h_{i,j}^{(n)} \right] + Q_{i,j} \\ = S_{i,j} \frac{V_{i,j}}{\Delta t} (h_{i,j}^{(n+1)} - h_{i,j}^{(n)}) \end{aligned} \quad (4.55)$$

The parameter,  $\lambda = 1$  gives a fully implicit scheme,  $\lambda = 0$  leads to a fully explicit scheme and  $\lambda = 1/2$  provides a semi-implicit scheme or what is called the Crank-Nicholson method, which gives a fully second-order accurate discretisation in time. This latter represents a reference to which any other temporal discretisation scheme is compared to in order to derive its numerical diffusion (Jasak, 1996).

$$E_i = -\frac{1}{2} \left[ \sum_{A=1}^4 K_{i,A} \left( \frac{\partial h}{\partial x_i} \right)_A^{(n+1)} x_i S_A - \sum_{A=1}^4 K_{i,A} \left( \frac{\partial h}{\partial x_i} \right)_A^{(n)} x_i S_A \right] - \frac{1}{2} (P_{i,j} h_{i,j}^{(n+1)} - P_{i,j} h_{i,j}^{(n)}) \quad (4.56)$$

Using the Taylor expansion:

$$h^{n+1} = h^n + \frac{\partial h}{\partial t} \Delta t \text{ and } (\nabla h)^{n+1} = (\nabla h)^n + \frac{\partial(\nabla h)}{\partial t} \Delta t$$

then Equation 4.56 can be written as:

$$E_i = -\frac{\Delta t}{2} \sum_{A=1}^4 K_A \frac{\partial(\nabla h)_A}{\partial t} S_A - \frac{\Delta t}{2} P_{i,j} \left( \frac{\partial h}{\partial t} \right)_{i,j} \quad (4.57)$$

where  $E_i$  includes two errors namely:

- Diffusion error:  $D_D = -\frac{\Delta t}{2} \sum_{A=1}^4 K_A \frac{\partial(\nabla h)_A}{\partial t} S_A$  (4.58)

- Source term error:  $D_S = -\frac{\Delta t}{2} P_{i,j} \left( \frac{\partial h}{\partial t} \right)_{i,j}$  (4.59)

To analyse these two terms, it is first necessary to express the temporal derivative of  $h$  as a combination of spatial terms. To do so, Equation 4.2 is used giving:

$$S_s \frac{\partial h}{\partial t} = \nabla(K \nabla h) - W$$

Thus, the error terms given in equations 4.58 and 4.59 can be written as:

$$D_D = -\frac{\Delta t}{2} \sum_{A=1}^4 \left( \nabla \cdot \nabla \left( \frac{K}{S_s} \nabla h \right) \right)_A S_A + \frac{\Delta t}{2} \sum_{A=1}^4 \left( \nabla \left( \frac{W}{S_s} \right) \right)_A S_A \quad (4.60)$$

$$D_S = -\frac{\Delta t}{2} P_{i,j} \left[ \nabla \left( \frac{K}{S_s} \nabla h \right) \right]_{i,j} + \frac{\Delta t}{2} P_{i,j} \left( \frac{W}{S_s} \right)_{i,j} \quad (4.61)$$

The first terms in  $D_D$  and  $D_S$  include higher derivatives of  $h$  and are therefore neglected. The second terms cannot be further analysed as they depend on the distribution of the source (Jasak, 1996).

#### 4.6.1.2 Mesh-Induced Errors

##### (i) Non-Orthogonality Error:

The non-orthogonal correction potentially creates unboundness and the corresponding non-orthogonality error for the GWFV model has the following form:

$$E_d = \sum_A \beta_A (\nabla h \cdot u)_A S_A = \sum_A (\Gamma_D \nabla h)_A \quad (4.62)$$

where  $\Gamma_D = \beta \cdot u \cdot S$ . This coefficient depends on the non-orthogonality angle of the mesh (angle between  $u$  and  $S$ ).

##### (ii) Skewness Error:

When the line joining two nodes does not pass through the middle of the vertical face between the nodes then interpolation is needed to give the value of the parameter at the middle of the face using its value at the intersection point. Therefore, accuracy of face integrals is reduced to first order. For the GWFV model, this skewness error has the form:

$$E_S = \sum_A \alpha_A \varepsilon_A S_A \quad (4.63)$$

The magnitude of his error depends on the importance of  $\varepsilon_A$ , which involves the vectors  $\delta \underline{x}^-$  and  $\delta \underline{x}^+$  given in Equation 4.29. For meshes of reasonable quality, then the vertical component of the difference between the two vectors is smaller than the horizontal difference, which is equal to  $\|\underline{v}\|$ . The influence of this term is expected to be smaller than the non-orthogonality error, except on highly distorted meshes where it can have significant influence.

### 4.6.2 Error Estimation

The field of error estimation in the finite volume method is still in the stage of development and researchers are still improving the accuracy of the error estimators. This is particularly important since the estimation of the solution domain discretisation errors forms the basis of appropriate mesh generation, and what is more recently known as automatic resolution control or adaptive mesh refinement (Jasak and Gosman, 2000). Many authors used this estimation as a tool to assess the consistency and accuracy of the numerical method that they have developed (Croft, 1998). The most famous methods for error estimation are Taylor Series Error Estimate, Moment Error Estimate, Residual Error Estimate, and Element Residual Error Estimate, with each method having its strengths and deficiencies (Jasak and Gosman, 2000 and 2003, Ilinca et al., 2000). For the model reported herein, a Taylor series expansion based method has been used to assess the accuracy of the numerical scheme.

Most of the truncation error analyses for the FVM reported in literature is made for uniform rectangular grids. Botte et al. (2000) showed that the truncation error ( $T.E$ ) was the same for the approximations of the second and first derivatives using central nodes in the FDM or internal control volumes in the FVM. MODFLOW uses a two-point central difference approximation for the first derivative at a cell face, which yields an accuracy of order  $(\Delta x_i)^2$  in each  $x_i$  direction. When reduced to  $(x,y)$  space, then the MODFLOW expression for the flux through a cell face, for instance  $(i,j+1/2)$  in Figure 4.9, is written as:

$$q_{i,j+1/2} = KR_{i,j+1/2} \Delta c_i \frac{h_{i,j+1} - h_{i,j}}{\Delta r_{j+1/2}} \quad (4.64)$$

In the GWFV model Taylor series expansion has been limited to second order as shown in Equation 4.30. The first term of the equation represents the discretised form of the first derivative along the line joining nodes  $P$  and  $N$  (or  $(i,j),(i,j+1)$ ). When this line is orthogonal to the face, the expression used for the first derivative in the GWFV model is the same as that used in MODFLOW; therefore, the accuracy and truncation errors must be the same when the mesh is orthogonal. For a general mesh, the expansion for the

points  $h_p$  and  $h_n$  around the face  $AB$  represented by midpoint  $F$  (see Figure 4.9) gives the following expression for the truncation error  $(T.E)_F$ :

$$(T.E)_F = (R^+ - R^-) \frac{\nu}{\|\mathbf{v}\|^2} = \frac{\nu}{\|\mathbf{v}\|^2} \frac{1}{6} \left\{ (\delta \underline{x}^+ \cdot \nabla)^3 h(\underline{x}_F + \theta \delta \underline{x}^+) - (\delta \underline{x}^- \cdot \nabla)^3 h(\underline{x}_F + \theta \delta \underline{x}^-) \right\} \quad (4.65)$$

Using the  $(i,j)$  notation, the Taylor expansion of heads at adjacent nodes is:

$$h_{i,j} = h_{i,j+\nu_2} + \Delta x^- \frac{\partial h}{\partial x} \Big|_{i,j+\nu_2} + \Delta y^- \frac{\partial h}{\partial y} \Big|_{i,j+\nu_2} + \frac{1}{2} \left[ (\Delta x^-)^2 \frac{\partial^2 h}{\partial x^2} \Big|_{i,j+\nu_2} + 2\Delta x^- \Delta y^- \frac{\partial^2 h}{\partial x \partial y} \Big|_{i,j+\nu_2} + (\Delta y^-)^2 \frac{\partial^2 h}{\partial y^2} \Big|_{i,j+\nu_2} \right] + R^-$$

$$h_{i,j+1} = h_{i,j+\nu_2} + \Delta x^+ \frac{\partial h}{\partial x} \Big|_{i,j+\nu_2} + \Delta y^+ \frac{\partial h}{\partial y} \Big|_{i,j+\nu_2} + \frac{1}{2} \left[ (\Delta x^+)^2 \frac{\partial^2 h}{\partial x^2} \Big|_{i,j+\nu_2} + 2\Delta x^+ \Delta y^+ \frac{\partial^2 h}{\partial x \partial y} \Big|_{i,j+\nu_2} + (\Delta y^+)^2 \frac{\partial^2 h}{\partial y^2} \Big|_{i,j+\nu_2} \right] + R^+$$

Therefore, the explicit form of Equation 4.65 can be written as:

$$(T.E)_{i,j+\nu_2} = \frac{\nu}{\|\mathbf{v}\|^2} \frac{1}{6} \left\{ \begin{aligned} & \left[ (\Delta x^+)^3 - (\Delta x^-)^3 \right] \frac{\partial^3 h}{\partial x^3} \Big|_{i,j+\nu_2} + 2 \left[ (\Delta x^+)^2 \Delta y^+ - (\Delta x^-)^2 \Delta y^- \right] \frac{\partial^3 h}{\partial x^2 \partial y} \Big|_{i,j+\nu_2} \\ & + 2 \left[ \Delta x^+ (\Delta y^+)^2 - \Delta x^- (\Delta y^-)^2 \right] \frac{\partial^3 h}{\partial x \partial y^2} \Big|_{i,j+\nu_2} + \left[ (\Delta y^+)^3 - (\Delta y^-)^3 \right] \frac{\partial^3 h}{\partial y^3} \Big|_{i,j+\nu_2} \end{aligned} \right\} \quad (4.66)$$

### 4.6.3 Accuracy Analysis

The finite volume method has the advantage of being conservative across each control volume, as well as being able to solve the flow equation on a non-rectangular mesh, without alteration to the formulation (Ferguson, 1998). Thus its stability is assured. Yet, currently there are no theories that predict the accuracy of the method on non-uniform grids. Generally, in grid-based numerical models, a loss of accuracy is unavoidable for strongly distorted meshes, and discontinuous mesh size variations should be avoided, when possible. Therefore, the question arises regarding the proper level of discretisation for accurate solutions. In numerically investigating the accuracy, particularly the accuracy of the fluxes (velocities), this is found to depend on the space and time discretisation and this will be considered in more detail in the next chapter. In his discussion, Patankar (1980) presented four basic rules that the discretisation equation should obey to ensure physical realism and overall balance. They are: consistency, positive coefficients, negative slope linearisation of the source term and the sum of the neighbour coefficients being equal to zero. The third and fourth rules are already

checked in sections 4.3.3 and 4.5.2 (i.e. Equations 4.47 and 4.54). In the different methods developed above, it can easily be shown that the same expression is used to approximate the gradient of  $h$  at a cell face from the adjacent cell sharing the same face (i.e. Equations 4.23, 4.35, and 4.38). The expression of equivalent permeability on a common face remains also invariant as it depends only on the permeabilities of the two adjacent cells. Therefore, the flux of water at a common face between two adjacent control volumes is represented by the same expression in the discretisation equation; thus, the model is rigorously consistent.

For steady state flow, the discretised equation for groundwater flow has the form:

$$B_{i,j}h_{i-1,j} + D_{i,j}h_{i,j+1} + (E_{i,j} + HCOF_{i,j})h_{i,j} + F_{i,j}h_{i,j+1} + H_{i,j}h_{i+1,j} = RHS_{i,j} \quad (4.67)$$

The positive coefficients rule states that the coefficients B, D, F, H and  $-E$  must always be positive. In the GWFV model these coefficients are:

$$B_{i,j} = S_{i-\nu_2,j} \alpha_{i-\nu_2,j}; \quad D_{i,j} = S_{i,j-\nu_2} \alpha_{i,j-\nu_2}; \quad F_{i,j} = S_{i,j+\nu_2} \alpha_{i,j+\nu_2}; \quad H_{i,j} = S_{i+\nu_2,j} \alpha_{i+\nu_2,j}$$

$$\text{and } E_{i,j} = -B_{i,j} - D_{i,j} - F_{i,j} - H_{i,j}$$

Since  $S$  and  $\alpha$  are always positive, then the rule is satisfied.

The accuracy of the three models with regard to their sensitivity to mesh shape and size, and boundaries, is investigated using numerical tests in the next chapter.

# Chapter 5

## Numerical Tests

### 5.1 Introduction

The numerical model GWFV has been compared to model S and model V. The three models have been tested and evaluated by running a suite of test cases that include the results generated by analytical solutions and by MODFLOW. The main feature of the programmes relating to the use of an irregular mesh has been assessed by analysing strengths and weaknesses of this particular aspect. Particularly in using an orthogonal grid, the new models have been assessed to confirm that the same formulation of the flow equation is used as in MODFLOW. Five examples were selected to test the codes performance. The accuracy of the methods has been examined for unsteady flow to a discharging well in a 2D confined aquifer well using the Theis analytical solution for this problem. The sensitivity of the models to the mesh size was tested using different random mesh resolutions for a simple Laplace equation. The same equation has been used with a 2D Kershaw mesh to examine the effects of the grid non-orthogonality and skewness on the overall performance of these procedures. The accuracy at irregular boundaries has also been examined using a benchmark example. Finally, a heterogeneity test has been carried out to check the effectiveness of the selected equivalent permeability formulation. A comparison of the test results for the different selected schemes is provided.

## 5.2 Model Testing and Evaluation

### 5.2.1 Numerical Tests Selection

The accuracy and performance of the new code first needed to be checked. According to the USEPA, the tests used to meet this task generally reputed to address five categories (Van der Heijde and Kanzer, 1997, p. 52) as cited below:

- 1- Conceptual problems in a theoretical framework,
- 2- Mathematical (non-coding) issues related to the formulation of the equations, the solution technique, etc.;
- 3- Implementation of the algorithms in code logic and code structure;
- 4- Input/output handling (e.g. file interaction, keyboard/screen interaction);
- 5- Internal data handling (e.g., argument handling in subroutines, common blocks, equivalencies, etc.)

The final objective of the development of the GWFV was to produce an additional process to the existing MODFLOW-2000, allowing the option of using the finite volume method within this programme to generate a more flexible mesh. Therefore, the identification of concerns relating to code correctness was based on this objective. The selected tests did not aim to check the existing MODFLOW functionality, performance or applicability issues, but to verify the correctness and compatibility of the new method within MODFLOW-2000. The tests have been particularly focused on the efficiency of the grid design in calculating groundwater heads. The testing methodology in this analysis used a two-level approach including analytical solutions and field validation tests.

### 5.2.2 Evaluation Methods

The exact solutions for the homogeneous isotropic case, and the corresponding numerical models results computed on very fine meshes for the anisotropic and heterogeneous cases, where analytical solutions are not available, were first used to assess the accuracy of the proposed schemes in tests 1 and 5. A comparison between the results for the new

numerical schemes and the exact solution, or benchmark solution, were performed for certain selected points of the overall domain. For transient simulations, the variations in results through time have been assessed at selected points. Indeed, to gauge the accuracy of the numerical method relative to the exact solution, the errors were calculated overall nodes at the selected  $n$  nodes using the following root-mean-squared error (*RMSE*) formula:

$$RMSE = \sqrt{\frac{\sum_{k=1}^n (h_{k,exact} - h_{k,calculated})^2}{n}} \quad (5.1)$$

### 5.3 Numerical Tests

The three models, GWFV, model S and model V were tested for accuracy by applying them to a number of test problems having known solutions. The first test was used to check the ability of the finite-volume method to solve the diffusion equation accurately in time. A comparison between the three different approaches was carried out for a 2D groundwater flow scenario. The second test was carried out to check the result of the new models against benchmark results and MODFLOW results.

#### 5.3.1 Test 1: Accuracy

In order to test the ability of the new finite-volume methods to solve the diffusion equation accurately, a problem with an analytic solution was first studied. The selected problem was a ground-water example from Wang and Anderson (1982). A well discharged at a constant rate of  $2000 \text{ m}^3 \text{ day}^{-1}$  from the centre of a confined aquifer of  $4000 \text{ m} \times 4000 \text{ m}$ , and having a constant transmissivity  $T$  of  $300 \text{ m}^2 \text{ day}^{-1}$ . The potentiometric surface was initially horizontal and set to 10 m. The quadrilateral discretisation used within the two models is shown in Figure 5.1 with 1681 ( $41 \times 41$ ) cells and volumes varying within a range of  $4 \times 10^3$  to  $2 \times 10^4 \text{ m}^2$ . No-flow boundaries were assigned along the domain borders and a storage coefficient  $S$  of 0.006 was chosen to avoid boundary effects influencing the numerical results. The MODFLOW model was also set up to simulate the same flow conditions. The flow for this test is normally

symmetric and it is therefore common practice to simulate a quarter of the domain, with the well located at one corner. The entire domain was modelled in this study to check that the model kept the symmetry property, even on an asymmetric grid.

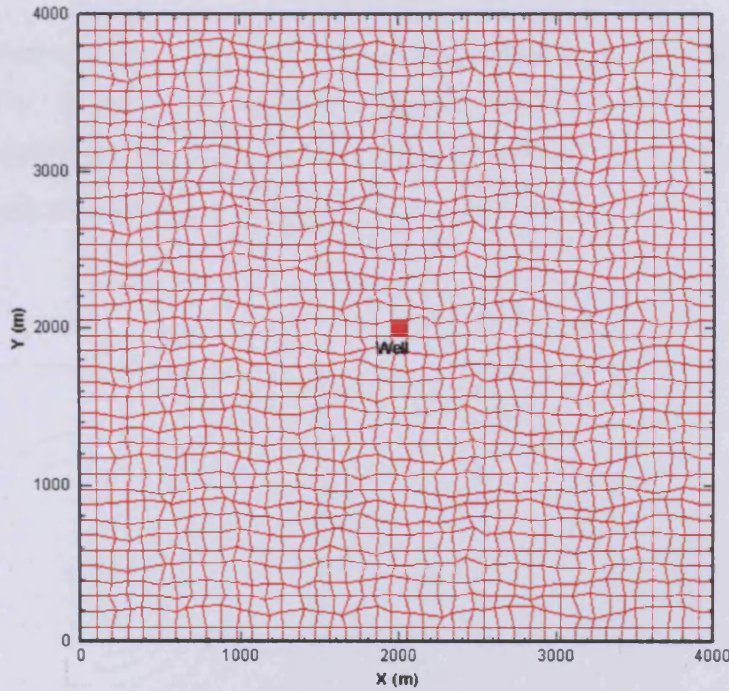


Figure 5.1 The  $41 \times 41$  random quadrilateral mesh used for the three models.

The analytic solution for this problem is the one given by Theis (1935). The drawdown at a radius  $r$  from the well given as:

$$h^0 - h = \frac{Q}{4\pi T} W(u) \quad (5.2)$$

where

$$W(u) = \int_u^\infty \frac{e^{-\psi}}{\psi} d\psi \quad \text{and} \quad u = \frac{r^2 S}{4Tt}$$

$W(u)$  is called the well function and is given by Wang in tabular form. To represent the solution given in Equation 5.2, the Jacob approximation of the Theis solution is used given:

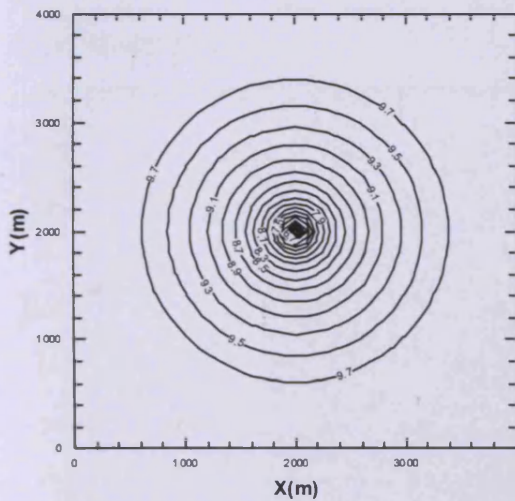
$$h^0 - h = \frac{Q}{2\pi T} \ln\left(\frac{R_L}{r}\right) \quad \text{with} \quad R_L = \sqrt{\frac{2.25Tt}{S}} \quad (5.3)$$

where the well function is approximated by  $W(u) = -0.5772 - \ln u$ , and  $u$  is less than about 0.01. The term  $R_L$  is the radius of influence beyond which the drawdown is zero. The simulation time was taken as 30 days, therefore, the radius of influence at the end of the

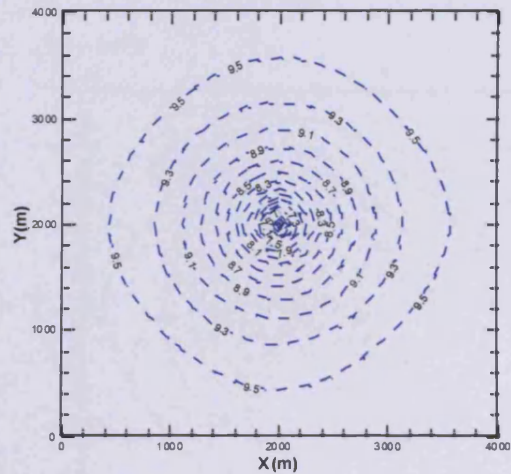
simulation was 1837 m. All models were run for 30 time periods, each period has 1 day length and 100 time steps. The SIP solver was set up with a 0.01 m head change criterion for convergence, a number of iteration parameter set to 5 and an acceleration factor set to 1.

The water level contours at the end of the 30 day simulations, as obtained for the three models GWFV, S and V, are shown in Figures 5.2(c), (d) and (e) respectively. The analytical solution and the finite difference model MODFLOW results obtained for this problem are presented in Figure 5.2(a) and (b) respectively.

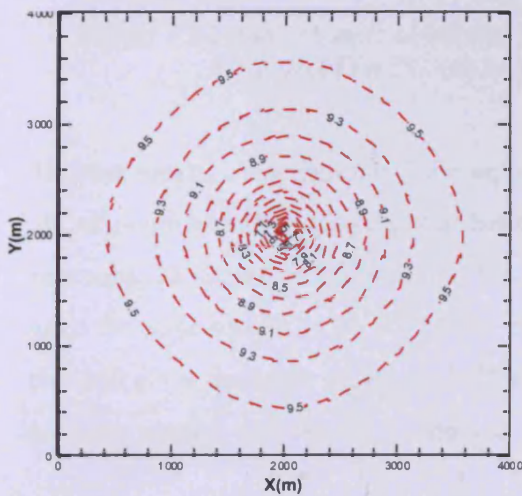
(a) Analytic



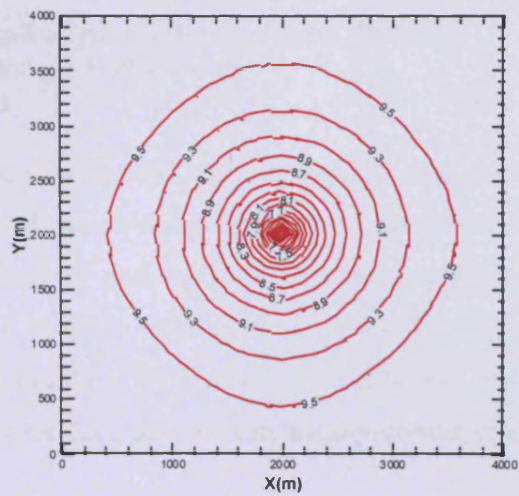
(b) MODFLOW



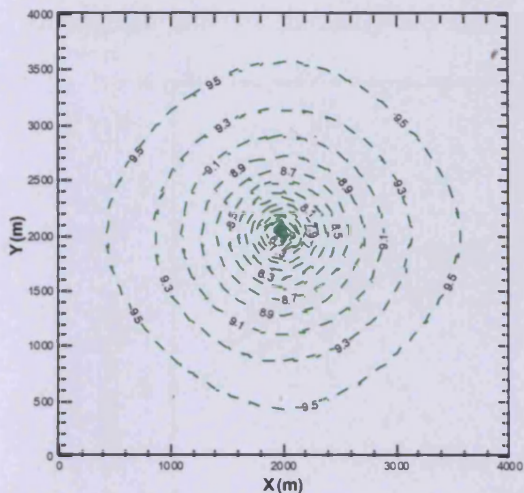
(c) GWFV: Orth



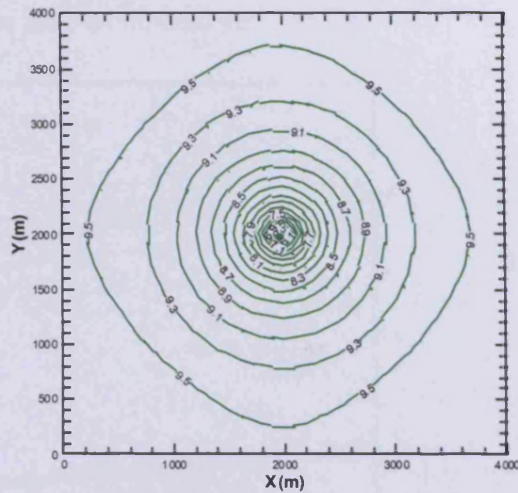
Non-orth



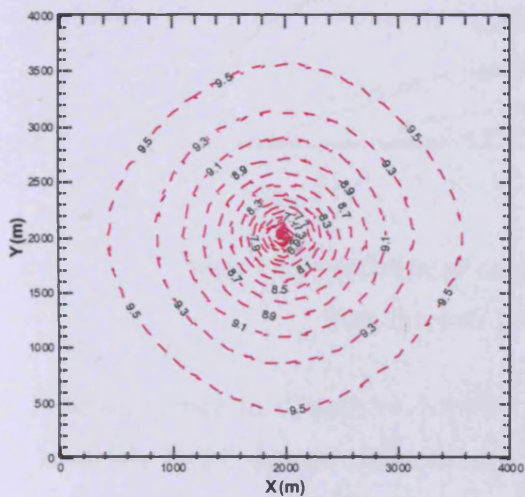
(d) Model S: Orth



Non-orth



(e) Model V: Orth



Non-orth

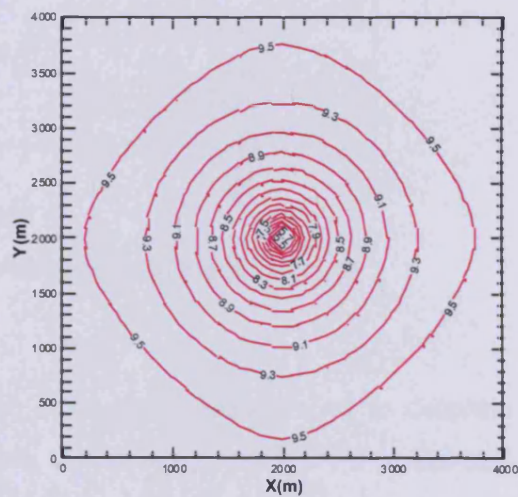


Figure 5.2 Head contours obtained using: (a) analytical solution; (b) MODFLOW; (c) model GWFV; (d) model S; and (e) model V.

The test results show that the finite volume models with 1681 cells, of average surface of  $10^4 \text{ m}^2$ , exhibit radial convergence behaviour and can produce accurate and symmetrical solutions, as shown in Figures 5.2. On an orthogonal grid the three developed schemes gave the same results as MODFLOW. However, on a non-orthogonal grid the only model that still gives the same figures as MODFLOW was the GWFV model. Model S gave less accurate results, and model V showed even lower accuracy for this locally converging

flow. Figure 5.3 illustrates the difference between the four models results on non-orthogonal grid and the analytical solution for the time of simulation.

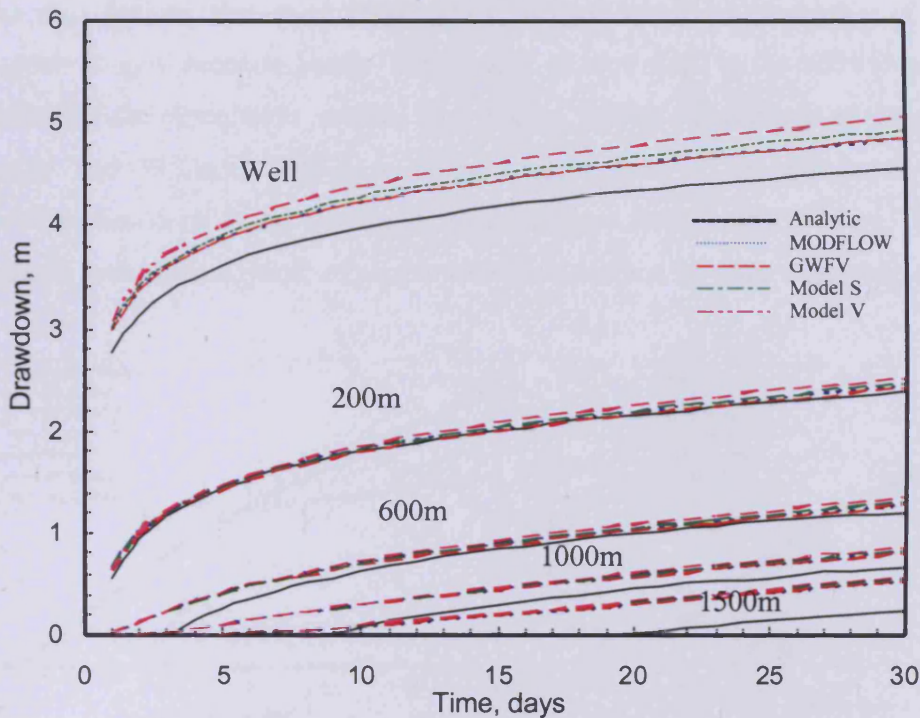


Figure 5.3 Variation of drawdown with time at different distances from the well for Test 1.

The difference in drawdown between the three developed models tended to decrease relatively to the distance from the well. However, it was mostly the GWFV model that compared as well as MODFLOW to the analytic solution on the overall domain. The deviation of the numerical results from the Theis curve at the final time steps was due to the non-infinite nature of the model domain in the analytical solution. The comparison will continue to deteriorate if the models were run for longer time. The mesh resolution may also be a factor in the models accuracy. This issue is particularly investigated in the next test.

The GWFV model gave identical results on non-orthogonal and orthogonal grids. Although it might be considered that the size of the cells was not large enough to assess the effect of the non-orthogonality on the model accuracy, it was clear from the results that the two other models, i.e. S and V, did not provide as high a level of accuracy as the GWFV model, even for this level of discretisation. Therefore, the next test was set up to

address the behaviour of the numerical error in the proposed finite-volume models on meshes of different levels of discretisation.

It was also noticed that even MODFLOW needed specific adjustments of the time parameters to give accurate heads. The number of time steps in the SIP solver changed considerably the simulation results (see Figure 5.4(a)). Therefore, as suggested by Osiensky and Williams (1997), a proper combination of the SIP matrix solution parameters should be found by trial runs to minimise water balance errors. In the case considered here, the analytical solutions were provided and no trials were necessary.

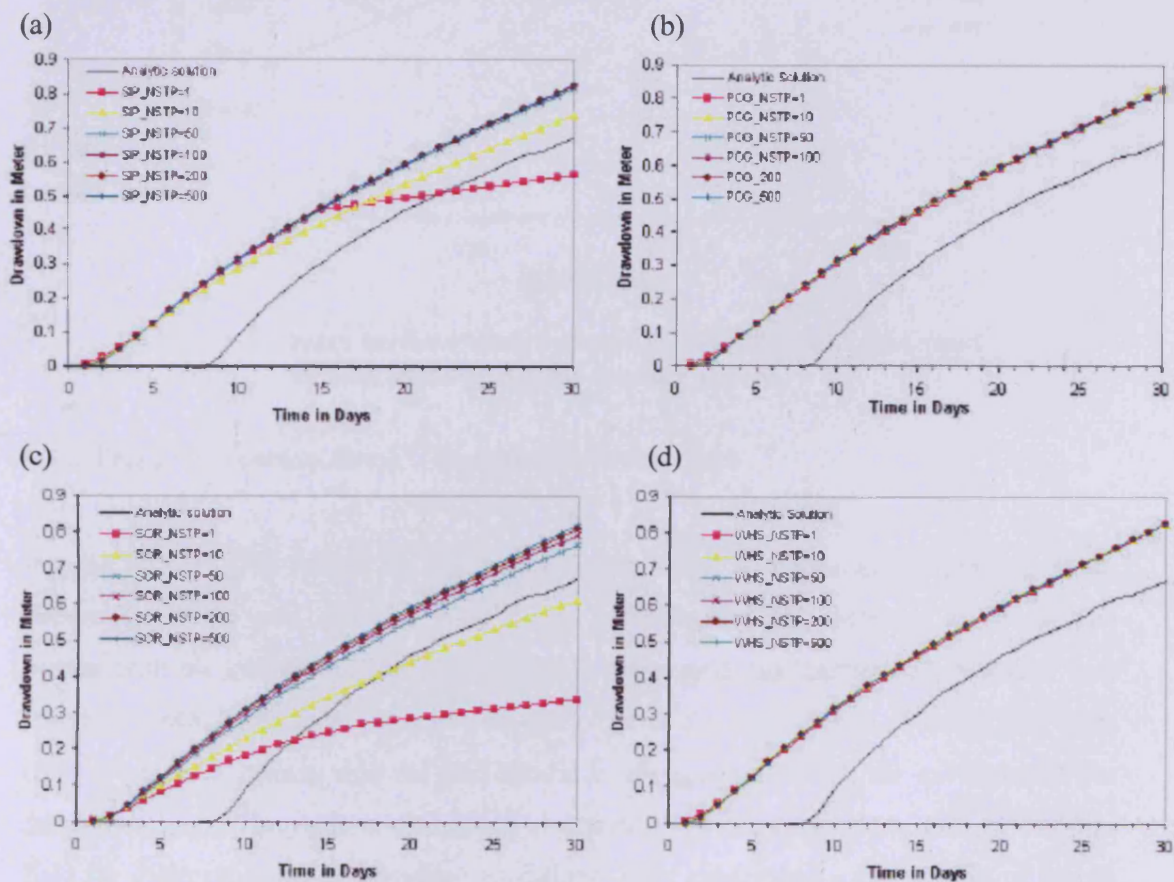


Figure 5.4 Plot of drawdown values versus time for well test, computed using MODFLOW, for different time steps, using various matrix solvers at a distance of 1 km from the pumping well: (a) SIP solver, (b) PCG solver, (c) SOR solver, and (d) WHS solver.

The SIP solver proved to be more accurate than all of other combinations for different matrix solvers when one time step was used, but converged to the same results as the PCG and WHS solvers when the number of time steps in a stress period was bigger than

100 (Figure 5.5). For the general case, the PCG and WHS solvers proved to be the most accurate and least sensitive to the solver parameters. Thus in the test undertaken herein, the SIP solution parameters that gave the same results as the PCG and WHS solvers were the ones that have been considered (NSTP=100).

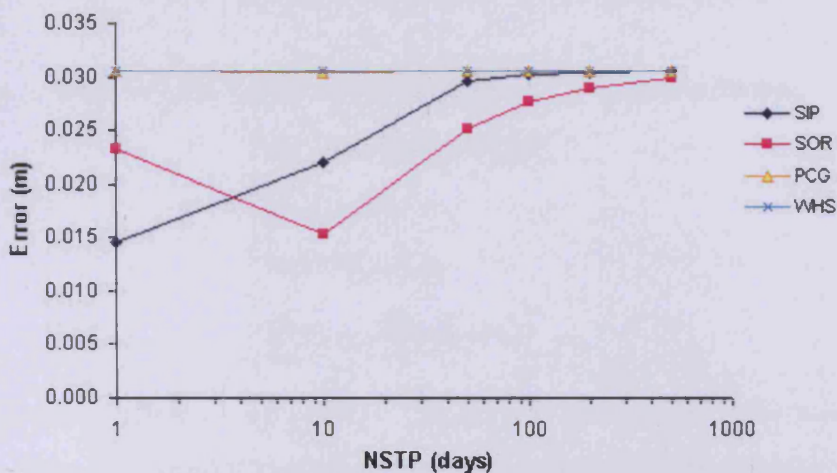


Figure 5.5 Error on the overall test area versus number of time steps in each stress period for the four solvers.

### 5.3.2 Test 2: Numerical Error – Sensitivity to Mesh Size

For the MODFLOW model, the non-orthogonality is not an issue, but the predictions do depend upon the grid size and time steps. Andersen (1993) addressed these specific points, with his general conclusions being that a fine grid can approximate a spatial flow variation much better than a coarse grid, but requires a larger number of nodes and more CPU time. As a general rule the grid should be designed to match the curvature of the drawdown cone. Haitjema et al. (2001) also tested the accuracy of MODFLOW's flow field for different types of boundary conditions. They established a set of rules of thumb for the minimum requirement on the grid resolution for each type of boundary condition to achieve accurate simulations.

In this test the effects of the grid structure, in terms of cell sizes, on the behaviour of numerical error and convergence of the three new schemes have been investigated. A test problem similar to the one used by Morel et al. (1992), has been used to demonstrate the accuracy of the different models as a function of the mesh size for 'random' meshes. A

10 × 10 m square area was used to simulate a two-dimensional flow through a porous media. The domain was meshed with a quadrilateral grid of five different levels of discretisation, as shown in Figure 5.6. Each mesh was generated from a uniform orthogonal mesh by moving each interior node in a random direction, on a circle of radius equal to 20% of the interior-nodal distance and centred about the original position of the corner.

The problem to be solved has the following boundary and internal conditions:

$$\left\{ \begin{array}{l} \Delta h = 0 \text{ in } [0,10] \times [0,10] \\ h(x,0) = 0 \text{ m} \\ h(x,10) = 10 \text{ m} \\ \frac{\partial h}{\partial x}(0,y) = \frac{\partial h}{\partial x}(10,y) = 0 \end{array} \right.$$

the exact solution of which is  $\bar{h}(x,y) = y$ . The relative mean-square norm was used to compute the error. The results from simulating this problem for different mesh sizes are given in Table 5.1. It has to be recalled that these results are dependent on the solver accuracy, which is represented in the SIP solver by the head change criterion for convergence. It was set to  $10^{-4}$  as to the size of cells in the most refined mesh (80 × 80) and the head gradient.

The results from the 5-point models on orthogonal meshes showed similar behaviour. The three new models show even better results than MODFLOW on the most refined grid. However, on non-orthogonal meshes, models GWFV and S performed better than model V especially when results were closer to the solver precision criterion. From these model results it can be seen that the error was reduced by a factor of minimum 2 each time the mesh spacing was reduced by a similar factor, which indicates a second-order accurate method on all grids that have been used. MODFLOW reached its best accuracy level with the mesh resolution 40 × 40 (see Table 5.1), whereas the results from the other models were still improving relatively to higher mesh resolution (i.e. mesh 80 × 80).

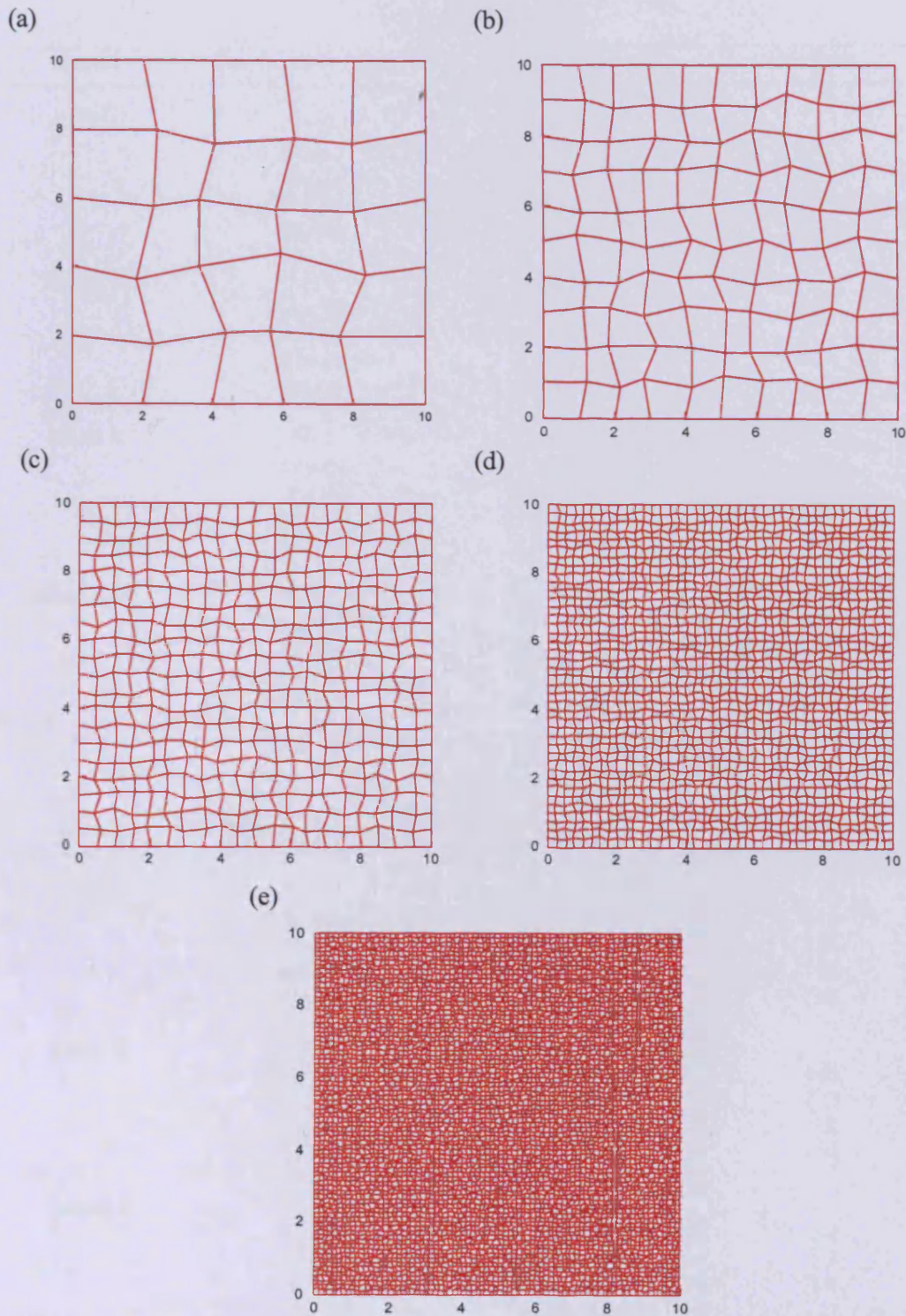


Figure 5.6 Test 2: Random grids, (a)  $5 \times 5$ ; (b)  $10 \times 10$ ;  
(c)  $20 \times 20$ ; (d)  $40 \times 40$ ; and (e)  $80 \times 80$ .

## Orthogonal meshes

Model	Problem Size (cells)	Relative $L_2$ norm	Error Ratio
GWFV	5 × 5	$12.3091 \times 10^{-2}$	
	10 × 10	$5.5348 \times 10^{-2}$	2.22
	20 × 20	$2.6292 \times 10^{-2}$	2.1
	40 × 40	$1.2818 \times 10^{-2}$	2.05
	80 × 80	$6.3456 \times 10^{-3}$	2.02
Model V	5 × 5	$12.3091 \times 10^{-2}$	
	10 × 10	$5.5348 \times 10^{-2}$	2.22
	20 × 20	$2.6292 \times 10^{-2}$	2.1
	40 × 40	$1.2818 \times 10^{-2}$	2.05
	80 × 80	$6.3456 \times 10^{-3}$	2.02
Model S	5 × 5	$12.3091 \times 10^{-2}$	
	10 × 10	$5.5348 \times 10^{-2}$	2.22
	20 × 20	$2.6292 \times 10^{-2}$	2.1
	40 × 40	$1.2818 \times 10^{-2}$	2.05
	80 × 80	$6.3456 \times 10^{-3}$	2.02
MODFLOW	5 × 5	$12.3092 \times 10^{-2}$	
	10 × 10	$5.5346 \times 10^{-2}$	2.22
	20 × 20	$2.6291 \times 10^{-2}$	2.1
	40 × 40	$1.2824 \times 10^{-2}$	2.05
	80 × 80	$6.6505 \times 10^{-3}$	1.93

## Non - Orthogonal meshes

Model	Problem Size (cells)	Relative $L_2$ norm	Error Ratio
GWFV	5 × 5	$13.1917 \times 10^{-2}$	
	10 × 10	$6.1586 \times 10^{-2}$	2.14
	20 × 20	$2.8816 \times 10^{-2}$	2.14
	40 × 40	$1.4000 \times 10^{-2}$	2.05
	80 × 80	$6.7411 \times 10^{-3}$	2.07
Model V	5 × 5	$13.6432 \times 10^{-2}$	
	10 × 10	$6.1241 \times 10^{-2}$	2.23
	20 × 20	$2.8685 \times 10^{-2}$	2.13
	40 × 40	$1.3025 \times 10^{-2}$	2.2
	80 × 80	$9.5796 \times 10^{-3}$	1.36
Model S	5 × 5	$13.0794 \times 10^{-2}$	
	10 × 10	$5.9227 \times 10^{-2}$	2.2
	20 × 20	$2.8090 \times 10^{-2}$	2.1
	40 × 40	$1.3386 \times 10^{-2}$	2.1
	80 × 80	$6.2311 \times 10^{-3}$	2.15

Table 5.1 Test 2: Errors on random grids

### 5.3.3 Test 3: Grid Shape Effect, Non-Orthogonality and Skewness

As discussed in section 4.3.1.1, the cross-diffusion term can significantly affect the accuracy of the models when the mesh is highly non-orthogonal. To test this particular aspect in the proposed models, a common test for the diffusion equation in hydrodynamic codes is the Kershaw test (Kershaw, 1981). This test allows the sensitivity of the model to the mesh shape to be studied, particularly for non-orthogonality and skewness. In this example a  $10 \times 10$  Kershaw mesh was used (Figure 5.7). The unit area was meshed such that the shape of the elements varied from square to extremely skewed quadrilaterals. The area was given a hydraulic conductivity of 300 m/d, constant head boundaries at the upper and lower boundaries, with 1m and 0m respectively, and no flow boundaries along the right and left boundaries.

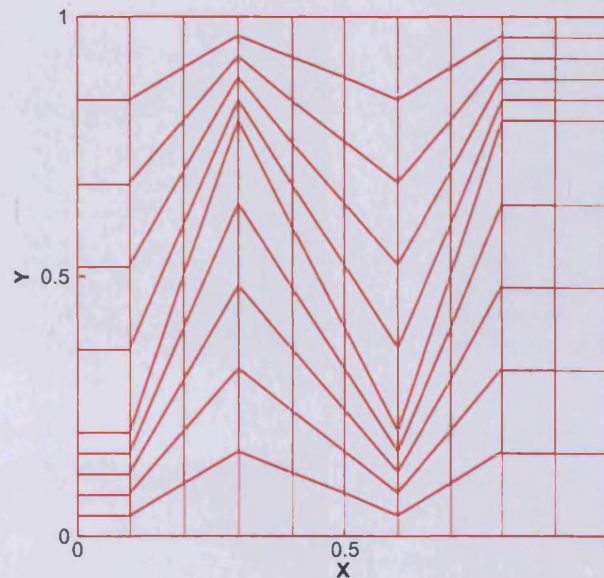
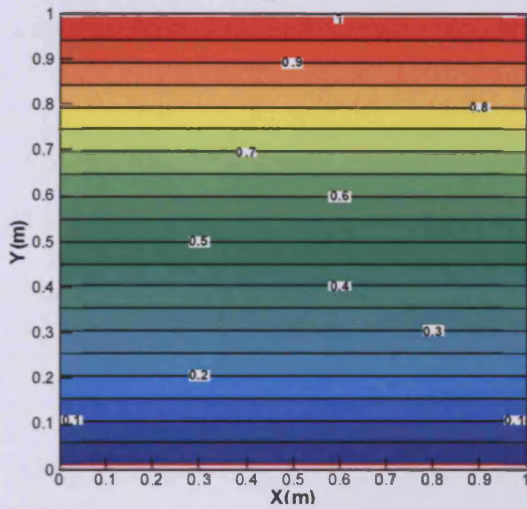


Figure 5.7 The  $10 \times 10$  Kershaw mesh.

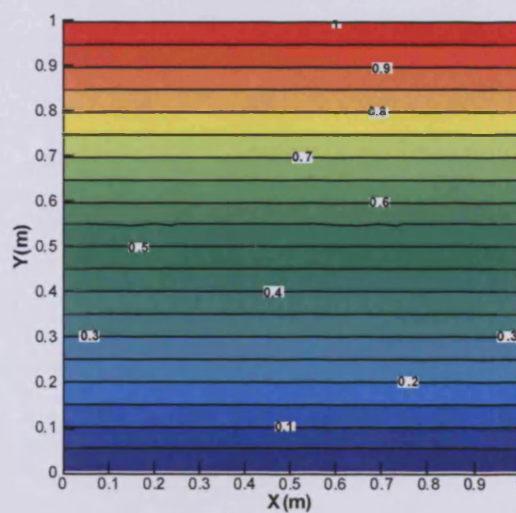
The models were then run to determine a steady state head profile across the area. A tool which correctly calculates the heads will show equally spaced isolines parallel to the constrained sides. Therefore, the head results would not have been expected to be a function of the mesh generated or the shape of the elements. The problem was first solved for an orthogonal mesh. The contour plot of the steady state results gave straight lines for the four models as shown in Figure 5.8 (a). The analytical solution was linear in  $y$ , and the methods reproduced this result exactly, as shown by the straight contour lines. This

was expected because the method reduced to the standard five-point finite difference method for the case of an orthogonal mesh. The head contours for the  $10 \times 10$  Kershaw non-orthogonal mesh are shown for the three models in Figure 5.8. It can be seen from the results that the isolines from the GWFV model are not altered by the distortion of the grid. However, contours from Model S were less straight than the contours from the two other models. Model GWFV showed the best independence from the mesh shape as these contours were the straightest. The same simulation was repeated with a  $20 \times 20$  mesh. The mesh and its corresponding head contours for the steady state results are shown in Figure 5.9.

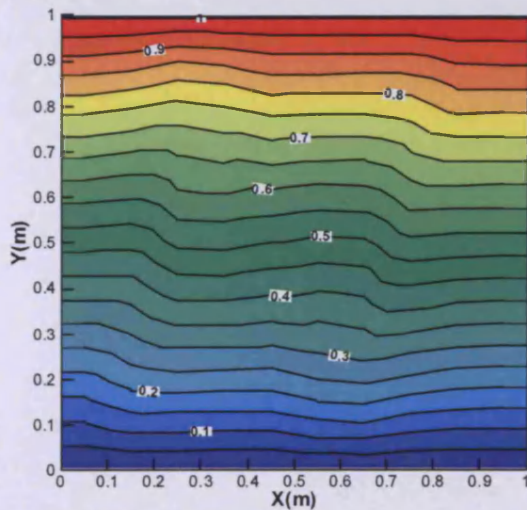
(a) MODFLOW



(b) GWFV: Non-orth



(c) Model S: Non-orth



(d) Model V: Non-orth

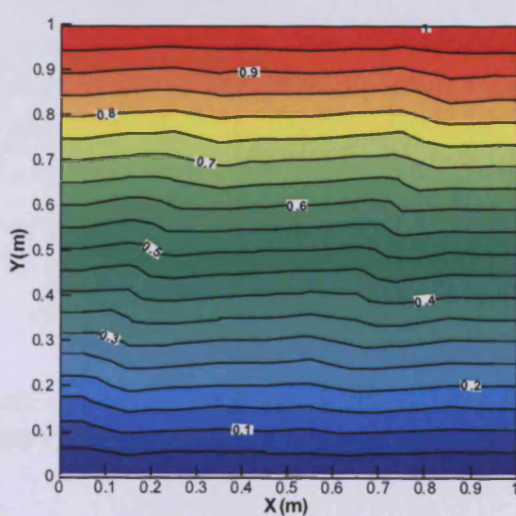
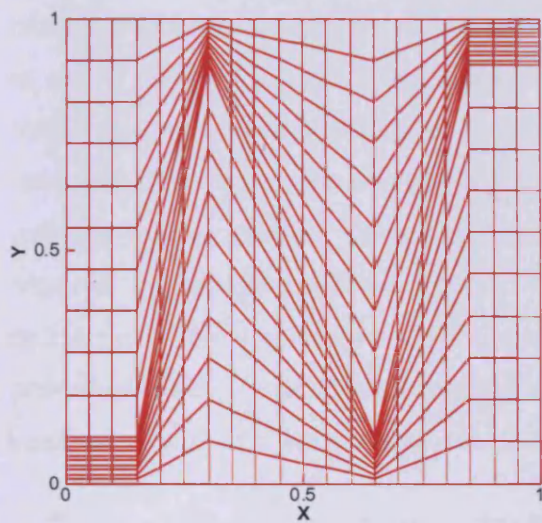


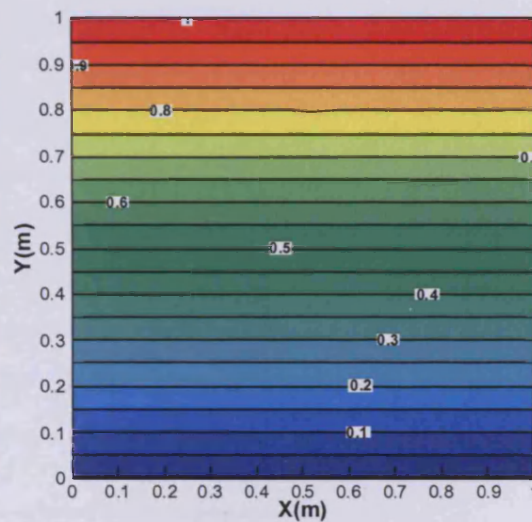
Figure 5.8 Isolines on the  $10 \times 10$  Kershaw mesh for the four models.

The isolines in Figure 5.9 remain linear, even though the mesh was more severely skewed. This was particularly true for the model GWFV model as it gave less curvature and more accurate contour for both levels of mesh distortion. Indeed, this model calculations exhibited linearity of the solution down to machine precision.

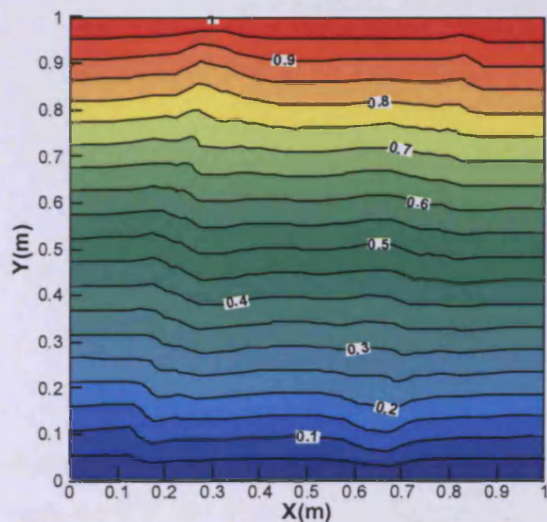
(a) The mesh



(b) GWFV: Non-orth



(c) Model S: Non-orth



(d) Model V: Non-orth

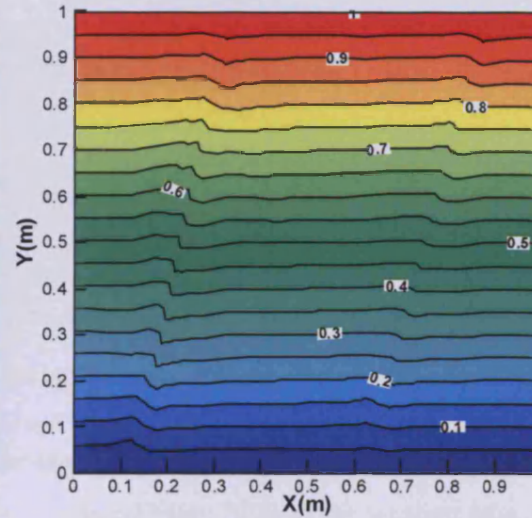


Figure 5.9 The  $20 \times 20$  Kershaw grid, (a) the mesh; (b) (c) and (d) isolines resulting from the three new models.

### 5.3.4 Test 4: Accuracy at Irregular Boundaries

A non-orthogonal mesh overcomes the difficulty of representing irregular boundaries of the physical domain with grid lines normal to each other. To test this new feature, a groundwater application from Kinzelbach (1986), has been used as a benchmark problem. The aquifer shown in Figure 5.10 is phreatic and isotropic. There are constant head boundaries at the western and eastern edges of the modelled region, with heads at 80 m above sea level on the western side and 75 m on the eastern side. The horizontal aquifer bottom is at an elevation of 10 m below the surface elevations. The grid had 10 rows and 15 columns. The permeability had a constant value of 0.0003 m/s. The diffuse recharge by precipitation was on average  $3 \times 10^{-9} \text{ m}^3/\text{s}/\text{m}^2$ . As steady-state results are required, the storage coefficient was set to zero everywhere, except at prescribed head boundaries where a value of  $1 \times 10^{15}$  was chosen. The initial heads were set equal to the prescribed head at prescribed-head-boundaries. At all other nodes an average value was assumed. A well of a water works withdraws water at a constant rate of  $0.1 \text{ m}^3/\text{s}$ .

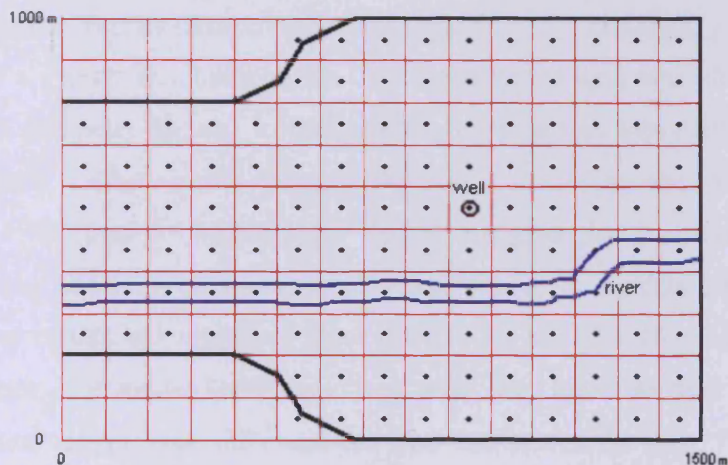


Figure 5.10 Aquifer and grid used in Test 4.

A river is allowed to exchange water with the aquifer. The leakage factors at every river-node were  $5 \cdot 10^{-6} \text{ s}^{-1}$ . The river bottom elevation ranged from 79 m at the western edge to 72 m at the eastern edge. The water surface in the river was 3 m above the river bed everywhere. The orthogonal and non-orthogonal meshes used to model the domain are shown in Figure 5.11 (a) and (b) respectively.

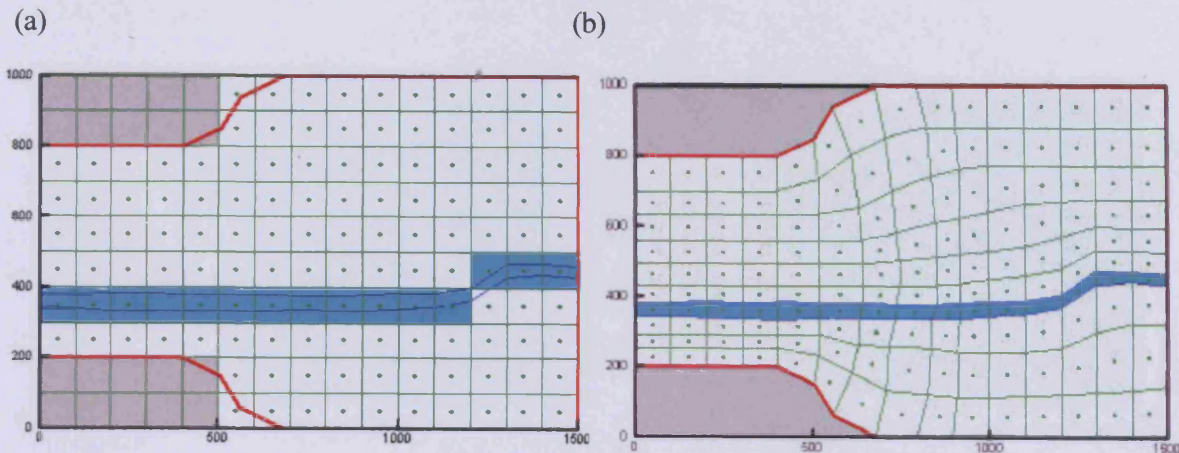
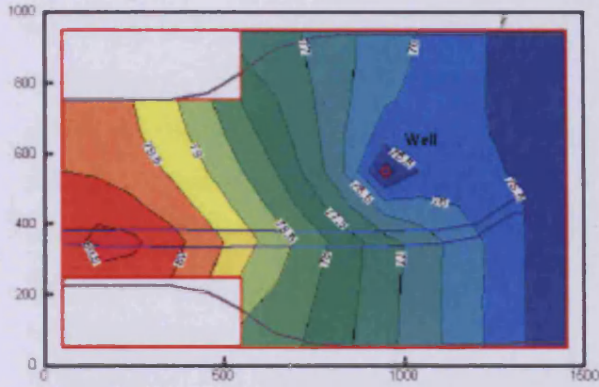


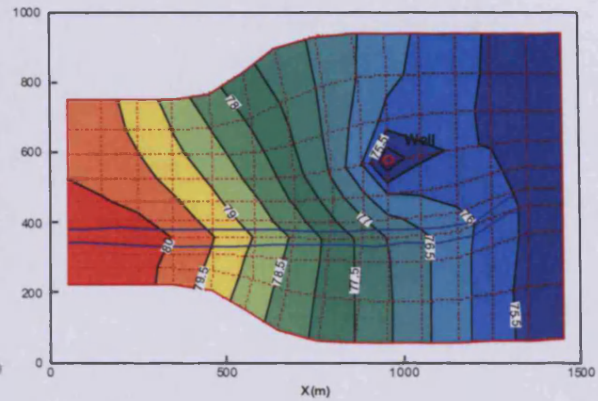
Figure 5.11 Aquifer mesh in Test 4: (a) orthogonal mesh; (b) non-orthogonal mesh.

Results from all of the models show a flow from west to east that slows down when it enters the wide part of the aquifer. A depression cone is formed around the well and the river water infiltrates into the aquifer as the resulting isolines show in Figure 5.12. All models give the same results for the orthogonal grid as MODFLOW (see Figure 5.12 (a)) and the benchmark results (Kinzelbach 1986). For the non-orthogonal grid, the three new models show a greater flexibility at the boundaries as the grid was allowed to fit more accurately the geometry and the isolines are smoother in this area than the MODFLOW finite difference model results. Nearly the same results as the benchmark results (Kinzelbach 1986) and the MODFLOW results are given by the new models, even if some cells show considerable non-orthogonality. Whilst the models GWFV and S gave similar contour results at boundaries, these differed for model V (Figure 5.12 (b), (c) and (d)). In addition, the model GWFV isolines were the closest to those of MODFLOW inside the model region, especially near the river and around the well. The GWFV model was therefore seemed to be the most accurate model with regard to accuracy over the whole domain.

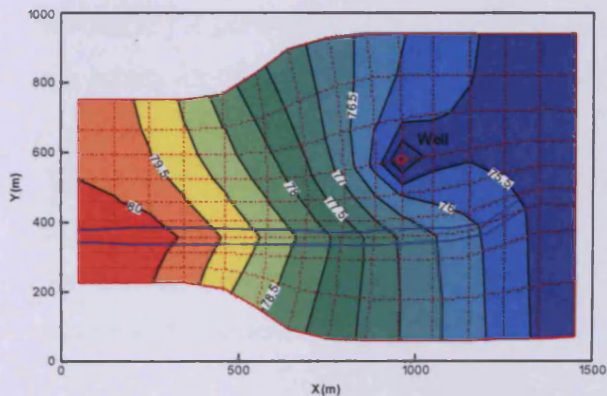
(a) MODFLOW



(b) GWFV



(c) Model S



(d) Model V

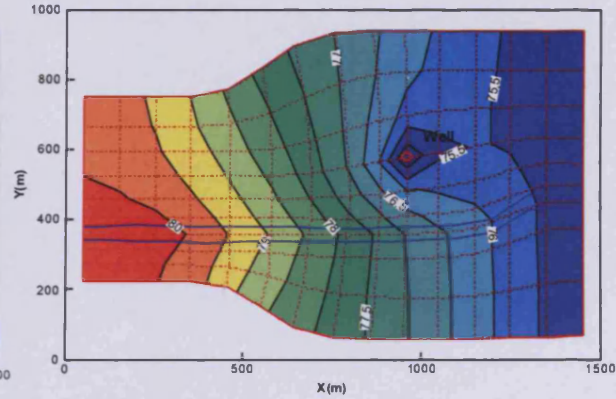


Figure 5.12 Head isolines for Test 4 from application of (a) MODFLOW, (b) GWFV, (c) model S, (d) model V.

### 5.3.5 Test 5: Permeability-Heterogeneity

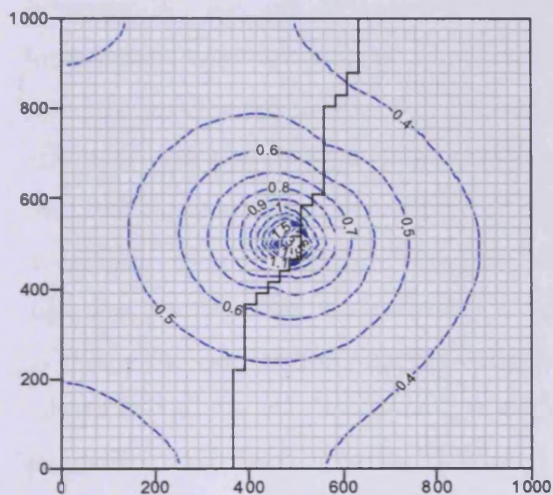
He et al. (2002) have developed a procedure, called the conforming scale up method, for the calculation of equivalent cell permeability tensors appropriate for general two-dimensional control volumes (i.e. non-rectangular quadrilateral and other polygonal cells) in reservoir simulation studies. In this work, as discussed in Chapter 4, the new shape of cells involved a new formulation of equivalent permeability at cell faces. To test this modification, a simple two-data set was constructed with variable hydraulic conductivity and incorporating a single extraction well. Similarly to Test 1, no flow boundaries were assumed along the borders of the model domain. A well discharged at a constant rate of  $1000 \text{ m}^3 \text{ day}^{-1}$  from the centre of a confined aquifer of  $1000 \text{ m} \times 1000 \text{ m}$ . The test runs

were performed with uniform isotropy and benchmarked against MODFLOW results. The results of the transient simulation after 20 days with variable hydraulic conductivity are shown in Figure 5.13. The left hand side of the simulation area had a conductivity coefficient of 90 m/day and a storage coefficient of  $8 \times 10^{-3}$ . Whereas the right hand side of the domain had values of 900 m/day and  $8 \times 10^{-2}$  for the same parameters. The SIP solver was set to run with 20 stress periods, with each period being one day long. The number of time steps in each period was 800. This number was chosen to make sure that the MODFLOW solver would give the same results and thus can be considered as the benchmark result.

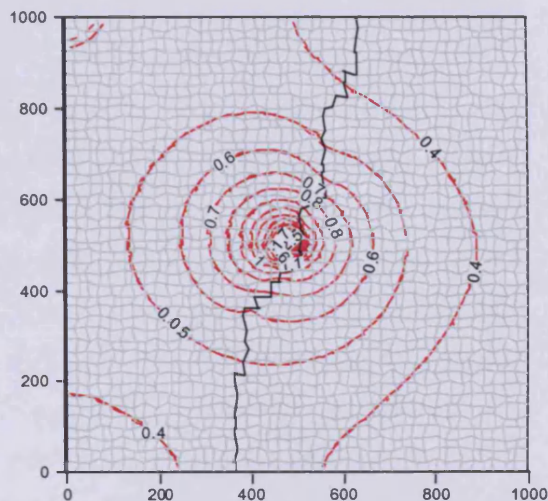
It has been noticed that the new equivalent conductivity formulation and that in MODFLOW gave exactly the same results when implemented in any of the three new models if the grids were orthogonal. However, the MODFLOW results are different from the results for the other models on non-orthogonal grids, as shown in Figure 5.13.

The GWFV model results with the non-orthogonal grid did not differ much from the results obtained with the orthogonal grid. However, the same equivalent permeability formulation gave less accurate results in models S and V in comparison with the GWFV model with the non-orthogonal mesh.

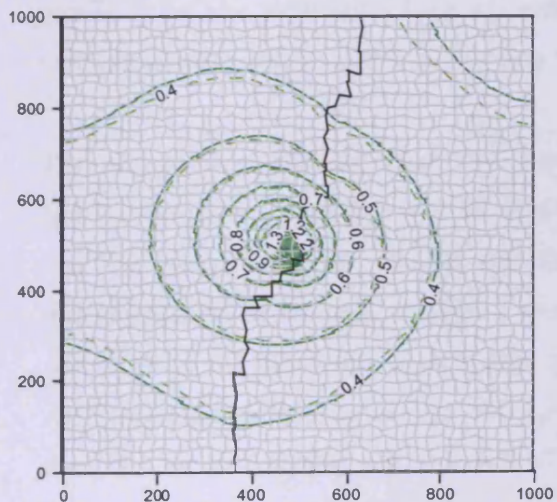
(a) MODFLOW



(b) GWFV: Non-orthogonal



(c) Model S: Non-orthogonal



(d) Model V: Non-orthogonal

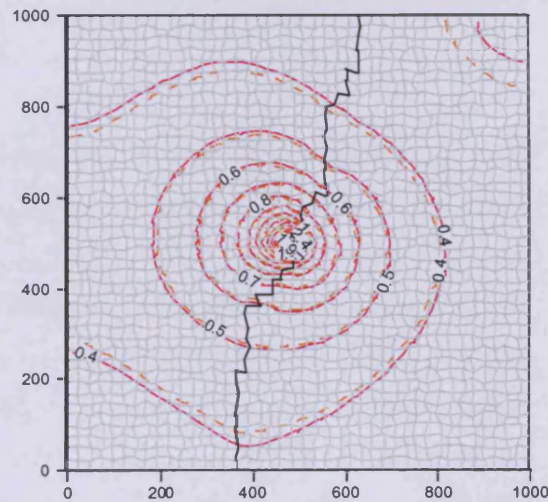


Figure 5.13 Head drawdown for Test 5 from application of (a) MODFLOW, (b) Model GWFV, (c) Model S, and (d) Model V on non-orthogonal grids.

## 5.4 Discussion

The suite of tests used herein is certainly not exhaustive but demonstrates the accuracy of the new models and the changes in comparison with the MODFLOW numerical concept. In particular, the use of non-orthogonal grids and the new equivalent permeability formulations were investigated. The comparative analysis of the tests results showed the strengths in all cases of the GWFV model as compared to the models S and V. The effects of grid non-orthogonality and skewness in the finite volume formulation used in the GWFV model were more absorbed than in the other formulations. The models S and V initially used a 9-stencil molecule associated to cell  $(i,j)$  to formulate the system equation, but then this was reduced to a 5-stencil molecule as described in Equations 4.49 to 4.52. The use of multiple reductions to come up with the five integration points adversely influenced the method accuracy during each reduction. In addition, the parameters associated with the head in each cell in the system equation in the GWFV model (namely  $B_{i,j}$ ,  $D_{i,j}$ ,  $F_{i,j}$ ,  $H_{i,j}$  in Equation 4.52) contained less terms in relation to the geometry of the cells when compared with the models S and V. Therefore, model GWFV proved to be less sensitive to grid non-orthogonality and skewness and more accurate as to heterogeneity and boundary conditions.

The simulations showed also that time stepping considerably affected the head distribution results. This was essentially due to the solver performance. It should be noted that the tests were all carried out with a single solver, namely the SIP. The implementation of the new numerical model in the MODFLOW programme allows the use of all of the other solvers available to be used after making the necessary changes. Additional tests related to the stability and convergence of the new implemented method can also be carried out, but this will place more emphasise on the efficiency of the solvers, rather than on the numerical changes in the new model. The solvers performance in terms of convergence behaviour, computing time and memory requirements are related to the new resulting matrix properties, which have been discussed in the previous chapter. The appropriate choice of solver parameters and initial head distributions were also discussed.

The accurate results obtained from these tests using some analytical or benchmarked conditions have provided a good indication of the correctness of the new model, but are not sufficient to guarantee that results will be accurate for more complex boundary conditions. Therefore, a real field case will be used as an additional test in chapter 6 where observed and predicted hydraulic heads will be compared as one measure of model accuracy.

### **5.5 Finite Volume- Based Changes in MODFLOW**

The GWFV model was based on the same mathematical model as MODFLOW but treated numerically the governing equations with finite volume technique instead of the finite difference method. Consequently, new input data were required for generating the new non-orthogonal structured cells. The discretisation of the equation system included new arrays to be accounted for when solving the generated matrix.

The GWFV code was written as a separate executable version of MODFLOW. The model was implemented as an optional 'process' for MODFLOW. This integration required the use of a separate "name" file that includes names compatible with MODFLOW. Changes affecting the programme from both programmer's and user's perspectives are described in Appendix D. The computer-memory requirement for the new GWFV model was greater than those for the MODFLOW programme. The additional arrays used by the code increased the memory size requirement which was strongly dependent on the number of nodes used in the studied area.

# Chapter 6

## A Field Application: Case Study

### 6.1 Introduction

To validate the new developed model, a two-dimensional field application has been used. The Visual MODFLOW groundwater flow and transport model (see Table B.2 in Appendix B) was set up in the Hydroenvironmental Research Centre of Cardiff University, in co-operation with a private company. This work was undertaken within the Research Centre's European Research Development Fund project 'Provision of Environmental Water Management Software Tools to Small and Medium Enterprises (SMEs) in Industrial South Wales (ISW)'. The site comprised a nickel refinery plant and a landfill area, passed through by a river. The refinery activity was suspected of causing an adverse environmental impact on the river water quality. Investigations indicated the presence of nickel contamination in the surface waters. The numerical model was set up to give a clear insight into the quantity and direction of the groundwater flow beneath the site and therefore to quantify the mass contribution of nickel into the river. Substantial amounts of data were available from many official sources such as the Environment Agency and the Geological Survey of Great Britain) and site investigations and routine monitoring were carried out by the refinery company.

The model was initially set up as a three-dimensional study. The flow simulations in this study area suggested that there was a four-layer aquifer system, drained by a river. In this chapter the three-dimensional flow simulations have been presented. An equivalent unit

layer model was then set up in order to provide a two-dimensional case study to validate the GWFV programme. This was conceptually achieved by generating new flow conditions for the parameters that have uncertainties. The resulting new calibrated parameters were then used to simulate the same field conditions with the new GWFV model. Comparisons between the results from MODFLOW and the GWFV programmes were then undertaken and are reported herein.

This study was chosen as a model-validation field test to establish the accuracy of the final simulations. The available data and flow conditions allowed the dimensionality of the site groundwater flow simulations to be reduced from a three-dimensional to a two-dimensional study, as ideally appropriate for this case.

## **6.2 Site Presentation**

### **6.2.1 Land Description**

The site is located to the southeast section of the town of Clydach in South Wales (see Figure 6.1) in a region of varied topography and diverse landscape character. It is set within the Lliw Valley district, to the north of Swansea and southeast of Clydach, and covers an area of approximately 121 hectares, of which approximately 21.5 hectares are developed. The Ordnance Survey Grid Reference for the site centre is SN 694 012.

The landscape of the area surrounding the site is complex, comprising strong natural landscape elements, such as: the Mynydd Gelliwastad to the west, mixed woodland areas to the northeast, the Lower Clydach Valley to the north and open fields to the south. However, many of these have been overlain or affected by anthropogenic influences.

In close proximity to the refinery site lie: (i) the River Tawe, which flows in a westerly direction immediately south of the works, (ii) the Swansea Canal, which borders the northern boundary of the site, and (iii) the Lower Clydach River. The Swansea canal discharges into the Lower Clydach River to the west of the refinery, prior to its confluence with the River Tawe.

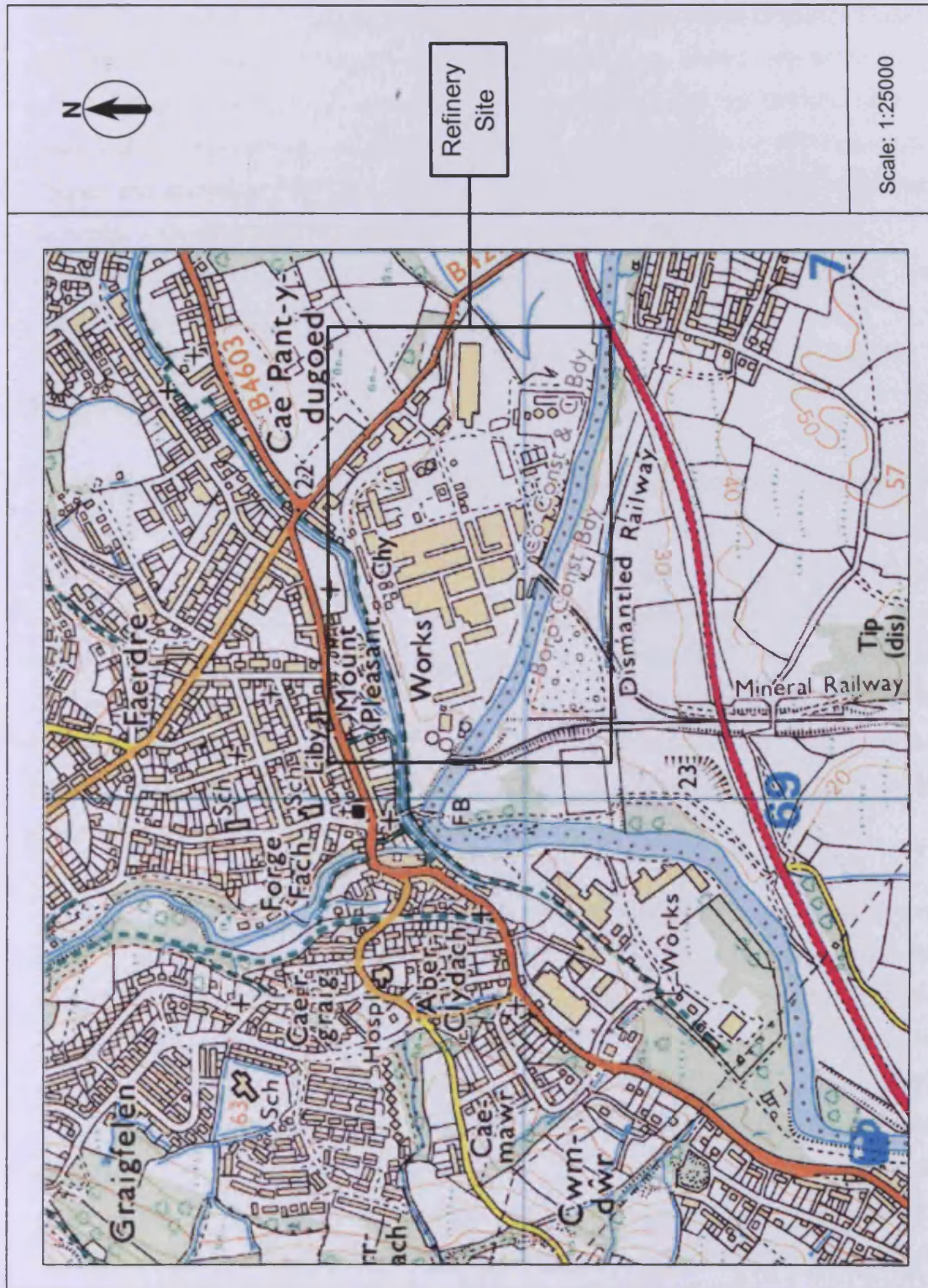


Figure 6.1 Site location plan from Digimap (Digimap, 2004).

The refinery site lies at an approximate elevation of 23 metres above Ordnance Datum (OD). However, the surrounding land lies at a higher elevation. Immediately to the south of the works (i.e. south of the Afon Llynfi and the dismantled railway) the land rises to approximately 53 metres above OD. Located to the north of the works are the town centre Clydach and accompanying residential areas. These areas lie at much higher levels than the works, with settlement of Penydre being at elevations of over 100 m above OD.

To the west, Clydach and the refinery site are bounded by the eastern slopes of the Mynydd Gelliwastad, which rises to approximately 213 m above OD.

### 6.2.2 Site Geology

The Geological Survey of Great Britain Sheet SN 60 SE scale 1:10560 (see Figure 6.2) depicts the site to be directly underlain by an undetermined thickness of alluvial material, consisting of intermixed lenses of sandy, silty clay and coarse gravels. Immediately to the south of the site, across the River Tawe, the Glais Moraine lies east-west across the valley and is shown to be approximately 30 m to 40 m higher than the valley floor. The Moraine generally consists of sands and gravels. Underlying the superficial materials, the Geological Survey plan depicts the solid strata to be the Grovesend Beds of the Carboniferous (UCM), upper Pennant measures. The bedrock in this area typically comprises sandstones.

The ground investigations generally confirmed the existence of the superficial deposits. However, as would be expected of an industrial site, varying depths of made ground were found overlying recent alluvial material. Correlations between the strata of the encountered sands, clays and gravels, recorded in the exploratory boreholes, were problematic as dense and soft materials within the strata were at varying depths, suggesting intermixing of glacial and fluvial deposits. Such strata irregularities could also be indicative of channel systems and possible sediment reworking. In general, sandstone bedrock was not encountered during drilling operations on site. However, some deeper exploratory holes, drilled as part of a structural investigation (records held by the refinery company), suggested that the bedrock might occur at depths between 30 m and 40 m below ground level.

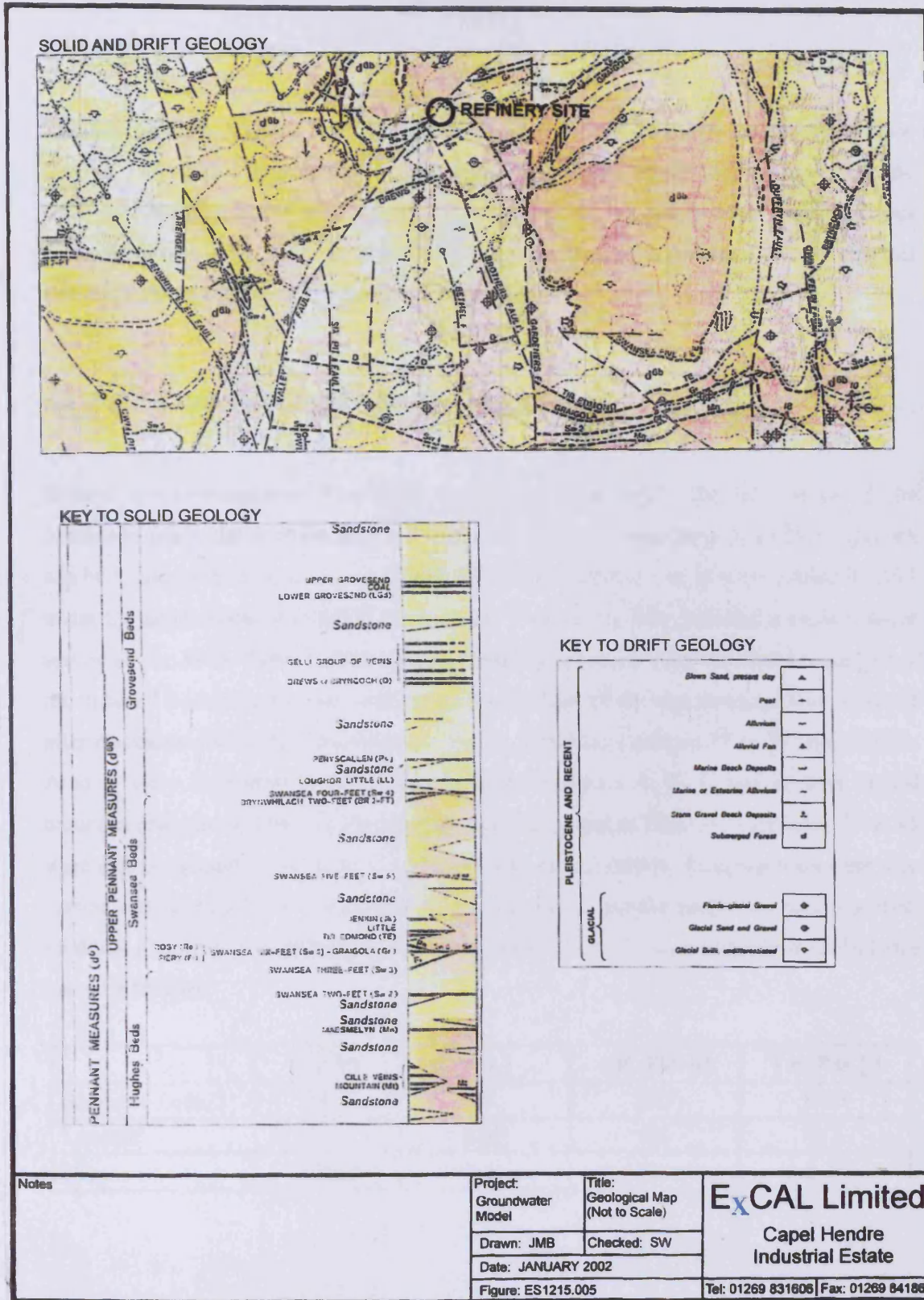


Figure 6. 2 Site geological map (courtesy of ExCal Ltd.).

### 6.2.3 Site Hydrogeology

The Environment Agency classifies the Carboniferous rocks beneath the site as a minor aquifer. The sandstone beneath the site forms a multi-layer aquifer system with separate water bodies in each sandstone horizon. These sandstone formations yield large quantities of water, which vary both spatially and temporally and are important for local supplies and maintaining the base flow of the local rivers.

### 6.3 Data Availability and Site Investigation

Several site investigations have been undertaken since 1993. The location of all the boreholes and wells is illustrated in Figure 6.3. Borehole logs from these investigations can be found in the ExCal Report (2000). Borehole locations 1 to 16 were drilled in 1993 under the supervision of GIBB (UK) Limited. This survey later included a surface water survey of the River Tawe (GIBB Report, 1996) to acquire a more detailed assessment of the material transported to the river. In a second phase of the site investigations, initiated after discussions with the Environment Agency, borehole locations 17 to 27 and trial pits A to Y were excavated in 1997. The borehole locations A, B, C and D were drilled around a chloride building condemned to demolition, and in 2000 the boreholes S1 to S5 were drilled around an old sulphate plan prior to its demolition. Pumping tests were also carried out on two wells during this phase. The initial aquifer properties resulting from field test data (for sand and gravel) and estimated values (for clay lenses and landfill) are given as follows:

	$S_s$ [1/m]	$S_y$ [-]	Eff. Por [-]	Tot. Por [-]
Sand and Gravel	$10^{-4}$	0.1	0.25	0.35
Landfill	$10^{-5}$	0.02	0.1	0.2
Clay	0.0013	0.01	0.4	0.48

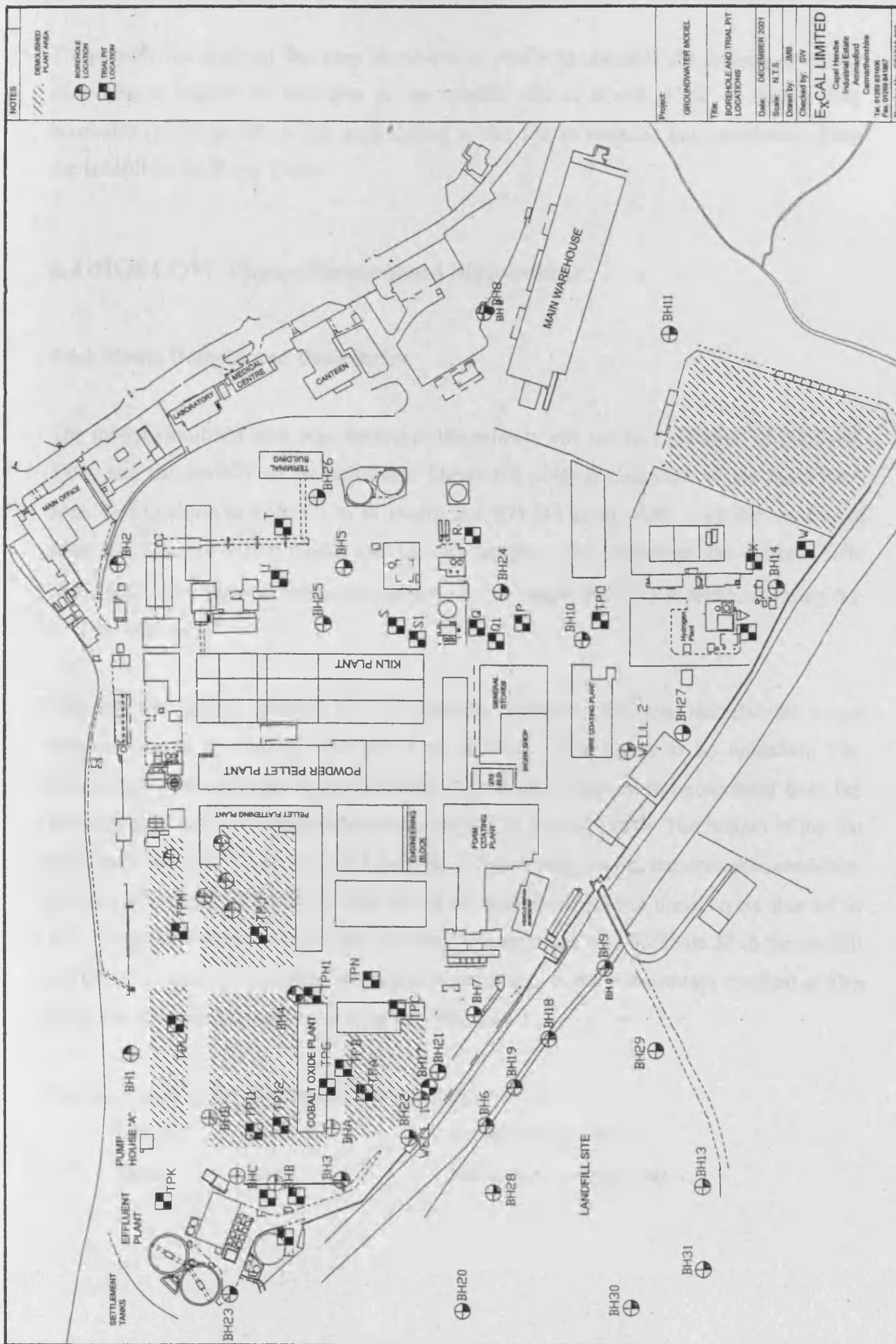


Figure 6. 3 Borehole locations (courtesy of ExCal Ltd.)

To quantify the material that may be needed to profile the landfill, the refinery company excavated a further 18 trial pits in the landfill site in March 2000. A further four boreholes (locations 28 to 31) were drilled at this site to evaluate the contribution from the landfill to the River Tawe.

## 6.4 MOFLOW Three-Dimensional Simulations

### 6.4.1 Model Domain and Boundaries

The model simulated area was limited to the refinery site on the right bank of the River Tawe and the landfill on the left bank. Figure 6.4 gives a plan view of the considered area. The model was 820.575 m in length and 574.743 m in width, with the number of rows and columns being similar and initially assigned 100. Therefore, the uniform cells of the  $100 \times 100$  finite difference mesh were 8.2 m length and 5.75 m width, covering the 47.2 ha total area.

Although the geology beneath the site generally consisted of alluvial material, the model was considered to contain four layers to allow the clay lenses to be modelled. The information related to the layer elevations and the clay lenses were interpolated from the borehole logs and the topographical surveys (ExCal Report, 2000). The bottom of the last layer was assigned as a horizontal surface, corresponding to the impermeable sandstone bedrock at a depth of 80.84 m. The minimum thickness between these layers was set to 1m. The ground surface maximum elevation was recorded near borehole 20 in the landfill at 108.35 m, and the minimum elevation recorded was in the downstream riverbed at 93m while the refinery site covered a relatively flat area.

The units used in the simulations were as follows:

Length:	meters	Conductivity:	m/day
Time:	days	Recharge:	mm/year

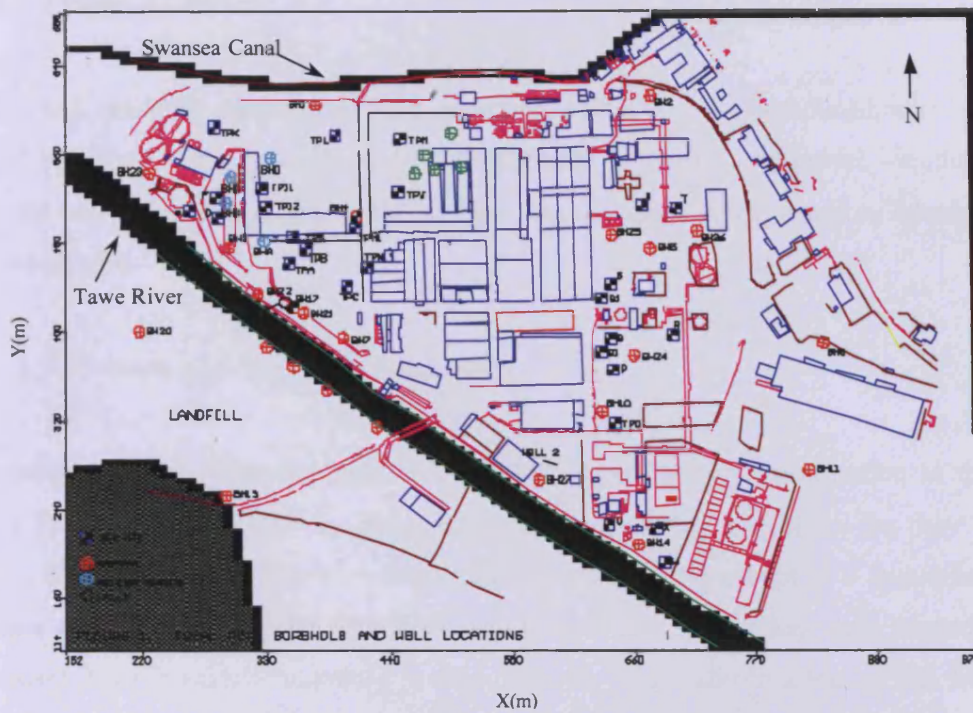


Figure 6.4 Plan view of the model and boundary conditions.

### 6.4.1.1 Northern and Eastern Boundaries

The model area is crossed by River Tawe and the Swansea Canal and is limited to the refinery site and the landfill area. Many scenarios were tested to simulate as accurately as possible boundary conditions. At the beginning of the simulation, data (especially ground levels and the location of the water table) in the landfill site were rare. As the domain of prime interest was the flow to the north east of the river, an approach was adapted to overcome the lack of information at the landfill site and this involved assigning inactive cells all over this area for all of the layers. For this scenario, the river was assigned as a constant head boundary since it was located at the edge of the refinery site. This simulation may have ignored leakage from the river, but it showed that the flow was still coming into the river even without imposing any constant head boundary condition at the eastern corner. The equipotentials for different times also showed a net flow coming along the sides of this corner into the model. Therefore, constant head boundaries were assigned along the half edges, meeting at the upper right corner (see Figure 6.4). No flow boundaries were imposed elsewhere along these sides.

#### 6.4.1.2 Swansea Canal

The canal could be considered to act as a river, with a very low conductance or a general head boundary, since the amount of flow entering, or exiting, the model was dependent on the head at a cell in the model. These two scenarios were also considered for the different runs.

#### 6.4.1.3 Western and Southern Boundaries

It was also shown from the different scenarios simulated that contribution to the river flow from the landfill site was important, and that this may also affect the flow coming from the refinery site. This area was assigned to be active, except at a few cells in the corner which had negligible influence on the flow as long as they were bordered by a constant head boundary imposing a flow into the river. The location of this boundary followed the shape of the initial flow equipotential in this region. No flow boundaries were imposed elsewhere along these sides.

As the calibration process was simulated for each scenario, Figure 6.5 shows the location of the final boundary conditions imposed for the flow simulations.

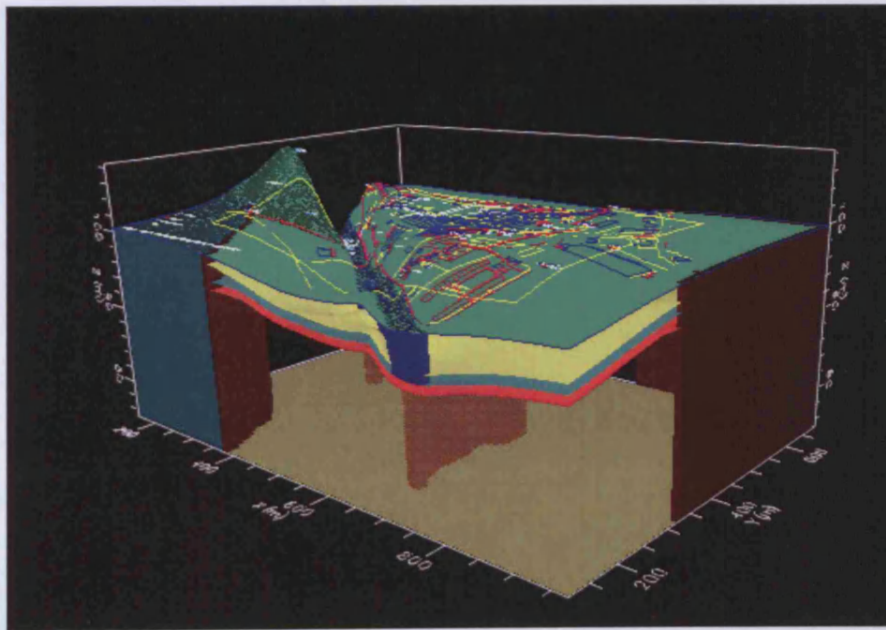


Figure 6.5 Three-dimensional view of the final model input.

#### 6.4.1.4 Tawe River

The riverbed was assumed to be 0.3 m deep and consisted mainly of fine sand gravel and silt, which corresponded to a conductivity of 0.67 m/d. The conductance of the riverbed was then computed from:

$$C = K.L.W/M = 104.38 \text{ m}^2/\text{d}$$

where:  $C$  is the hydraulic conductance ( $\text{m}^2/\text{d}$ ),  $L$  is the length of a reach through a cell (m),  $W$  is the width of the river in the cell (m),  $M$  is the thickness of the river bed (m) and  $K$  is the hydraulic conductivity of the river bed material (m/d).

The average of water level in the river was assumed to be 0.41 m and its stage dropped from 96.509 m to 94.013 m between the most southwesterly point of the river and the northeast extremity. Monthly values of river stage were recorded at station: Ynystanglws, downstream of the refinery site, for the period 01/2000 to 07/2000. Linear interpolations were made to find the related stage of the River Tawe at the refinery site, as shown in Figure 6.6.

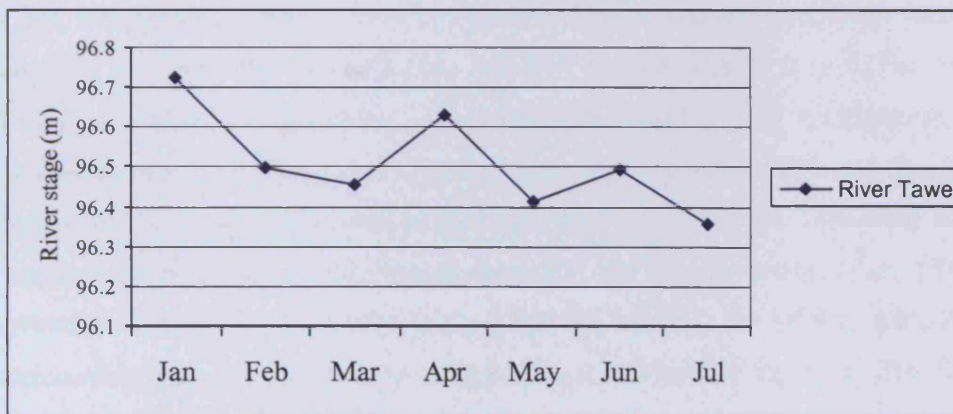


Figure 6.6 River stage upstream River Tawe in year 2000.

#### 6.4.1.5 General Head Boundaries

As the Swansea Canal seemed had been in existence for some considerable time and the flow tranquil and steady, the canal bed was assumed to be covered with old fine sand

deposits. The canal bed was at an elevation of 99 m and the canal stage was set to 99.78 m. The conductivity value of the bed was assumed to be 0.0259 m/d, and the relative conductance was 4.038 m<sup>2</sup>/d. These values have been adjusted with calibration.

#### **6.4.1.6 Constant Head Boundaries**

Constant head boundaries were assigned in the northeast boundary along the model edge, and at the southwesterly corner along the limit of inactive cells. This choice of boundary condition was made mainly on the basis of the initial water table as the equipotentials showed a net flow into the model area along these sides.

#### **6.4.1.7 Recharge Data**

Monthly values of rainfall were available only for year 2000 at the Rhoose station near Cardiff (see Figure 6.7). These data were used in the transient model as they coincide with the availability of the river stage data. The recharge data were also interpolated to represent data related to the study area using the standard annual average rainfall (SAAR) at the site, which was reported to be 1301mm. Not all of the rainfall percolated through to the aquifer. The effective recharge was reduced by the surface runoff, the rational coefficient indicating the percentage share of surface runoff and by evapotranspiration which was assumed to reduce the effective recharge by another 50%. As the rational coefficient for heavy industrial area of this type was 0.6 to 0.9, the remaining 10-40% was reduced by 50% due to the evapotranspiration. Of the remaining value, 10% was considered as recharge to the ground in the industrial area (i.e. the refinery site), 20% to the surrounding housing area, 30% to the landfill site and 50% to the river. Therefore, in steady state simulation, four values were assigned according to the type of ground surface use (see Figure 6.8):

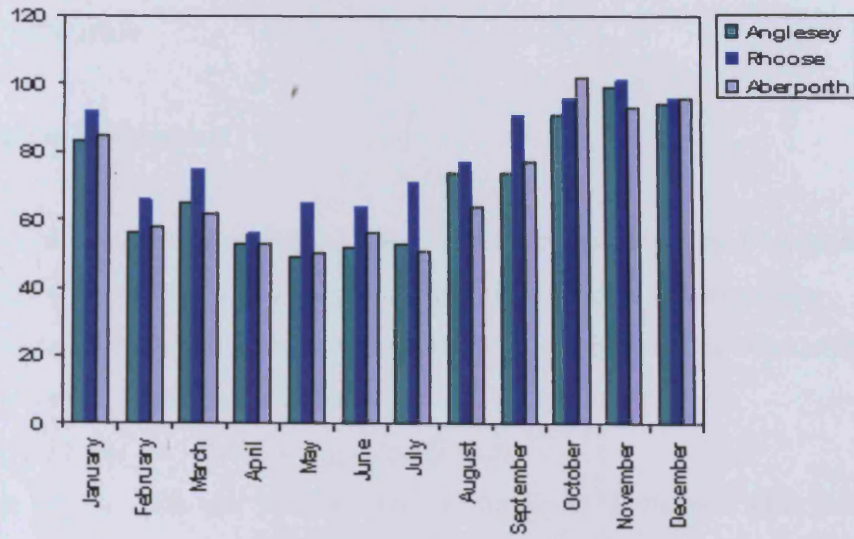


Figure 6.7 Monthly rainfall in mm/year in 2000

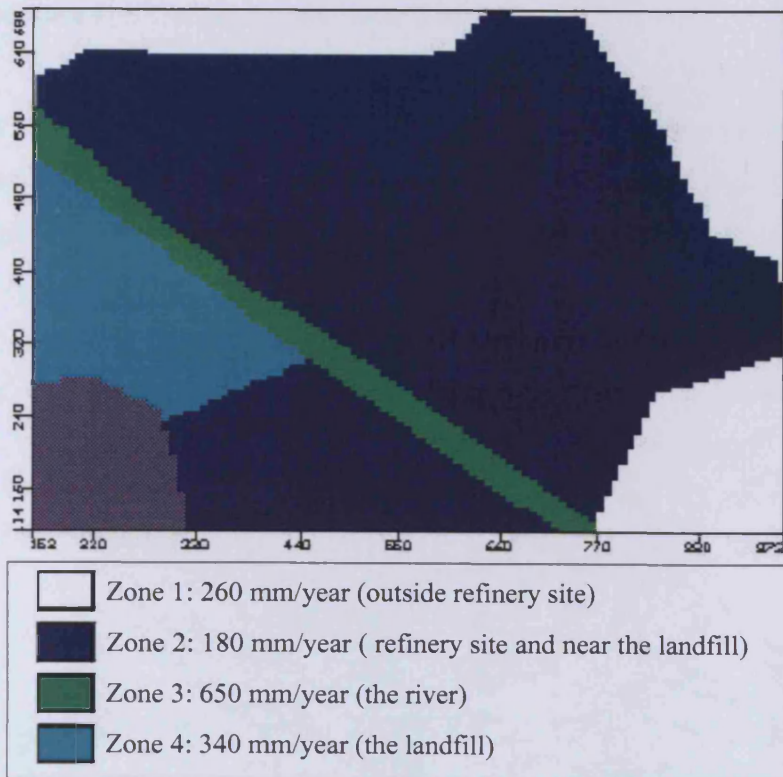


Figure 6.8 Recharge model zone distributions.

## 6.4.2 Model Calibration

### 6.4.2.1 Calibration Programme

The model was calibrated by comparing measured and predicted values of groundwater heads at different observation boreholes. The model was calibrated in two modes:

- steady state, to calibrate the aquifer permeabilities and the hydraulic conductance of the River Tawe and the Swansea Canal, and
- transient, to calibrate the aquifer storage coefficients.

The calibration of the hydraulic conductance of the River Tawe was also achieved through both steady and transient simulations.

### 6.4.2.2 Calibration Results for Steady State Simulations

The observation boreholes that were used in this calibration are shown in Figure 6.9. They were focused around three major groups: the landfill group, the river group and the refinery site group, thereby enabling separate and global calibrations to be undertaken for each site covered by these groups.

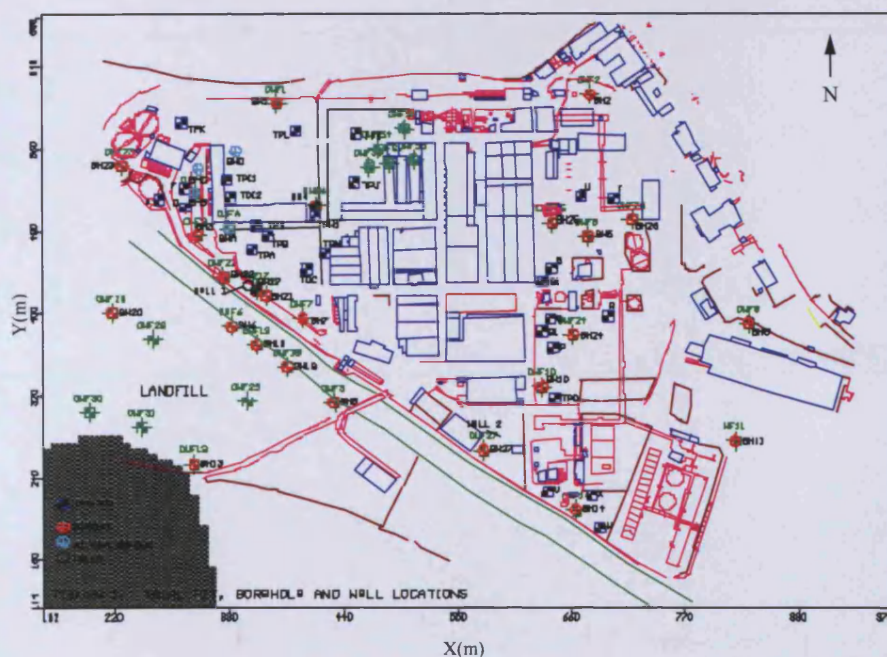


Figure 6.9 Location of observation boreholes used for model calibration.

The observed heads at the boreholes were taken as the average heads recorded during the period 11/1998 to 07/2001. Figure 6.10 shows a statistical measure of the difference between the observed and calculated heads at 95% confidence interval with all observation groups being used. The root mean square error *RMSE* is given by:

$$RMSE = \sqrt{\frac{\sum(O_i - P_i)^2}{n}}$$

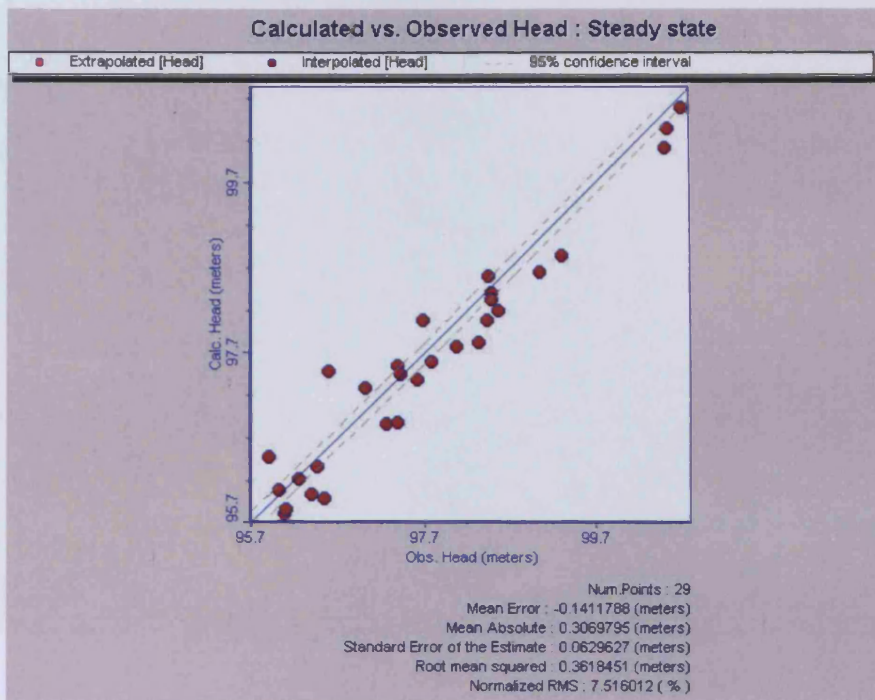
where  $P_i$  are the predicted values and  $O_i$  are the observed values, with the summation being over  $n$  observation points. The *RMSE* is equal to zero when all predicted values are identical to observed values.

In this steady state calibration, the *RMSE* calculated was equal to 0.36 m over the whole model area. This result implies a very good approximation when the range of water levels is in excess of 94 m. The steady state groundwater levels resulting from this simulation are given in Figure 6.11 and can be considered as the average water levels over the last four years over the model area. It was clear from these results that the river drains the aquifer system from both sides. The model water balance for the steady state conditions is given in table 6.1.

Table 6.1 Steady state water balance

Component	Flow m <sup>3</sup> /d
Constant Head	539.41
General Head Boundary	42.27
Recharge	286.36
River Leakage	867.835
	Inflow – Outflow = 0.008667

(a)



(b)

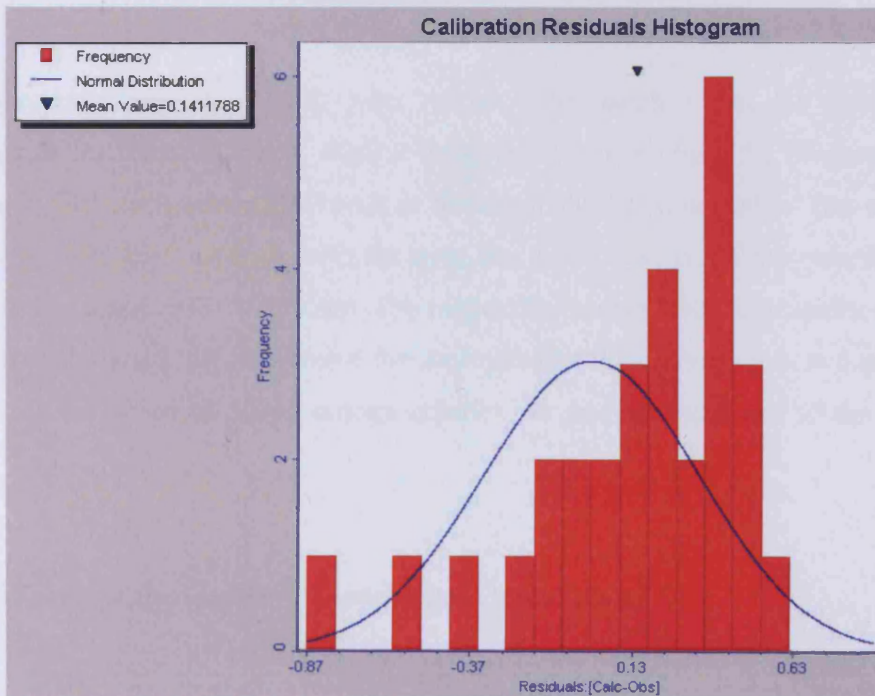


Figure 6.10 Steady state calibration results: (a) Statistical measure of predictions, and (b) calibration residuals histogram.

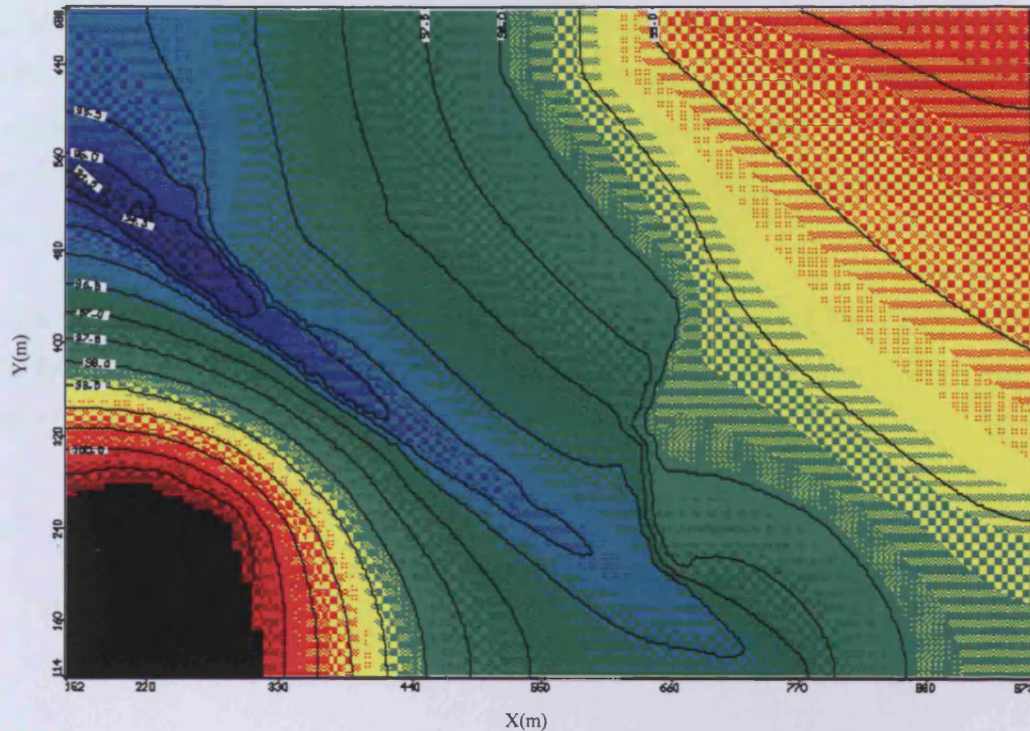


Figure 6.11 Predicted steady state groundwater levels (equipotentials at 0.5 m intervals).

It was apparent from the steady state model water balance that the aquifer was discharging to the River Tawe. A small leakage was predicted from the Swansea Canal, due to the difference between the heads in the canal and the water table. The estimated flow coming from the refinery site to the river was  $84 \text{ m}^3/\text{day}$ , while the contribution of the landfill was found to be  $10 \text{ m}^3/\text{day}$ . The model discrepancy was calculated to be zero, which provided a good match between the approximated flow coming into and out of the system when the precision (head change criterion for convergence) was of the order of  $10^{-2}\text{m}$ .

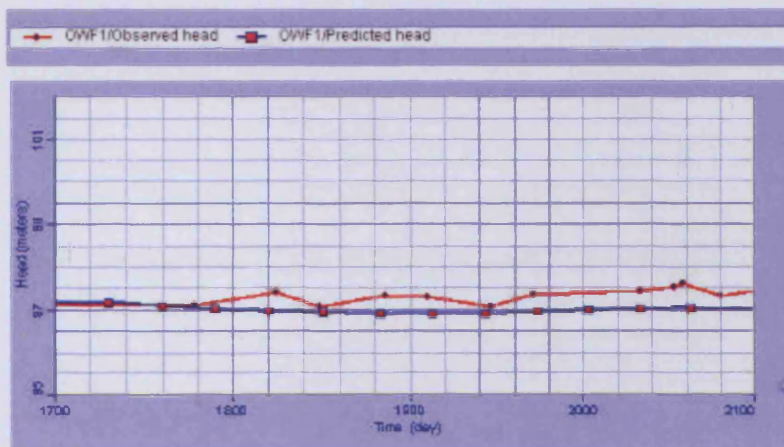
#### 6.4.2.3 Calibration Results for Transient State Simulations

The groundwater model was then run for year 2000, using the steady state groundwater levels as initial conditions. This was the only year for which data were available, for both the recharge and river discharge. The time reference was fixed at April 1995. The

calculated heads were compared with the time dependent monitoring results available for all of the observation wells shown in Figure 6.9. Comparisons of the groundwater levels were provided in Figure 6.12 at Borehole 1 near the Swansea Canal, Borehole 21, next to the river from the landfill side, Borehole 6 near the river from the refinery side, Borehole 25 for the refinery site and Borehole 13 for the landfill.

These results generally show good agreement between the observed and predicted levels. The *RMSE* for all of the well groups and time steps varied from 0.37 to 0.46 m which is similar to the error obtained for the steady state simulations.

(a)



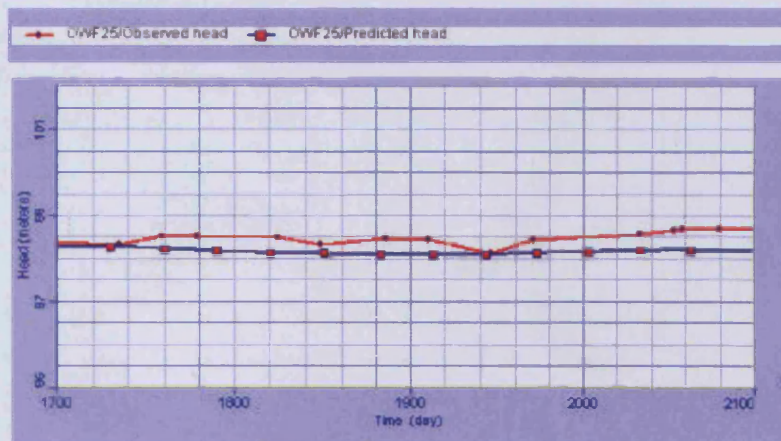
(b)



(c)



(d)



(e)

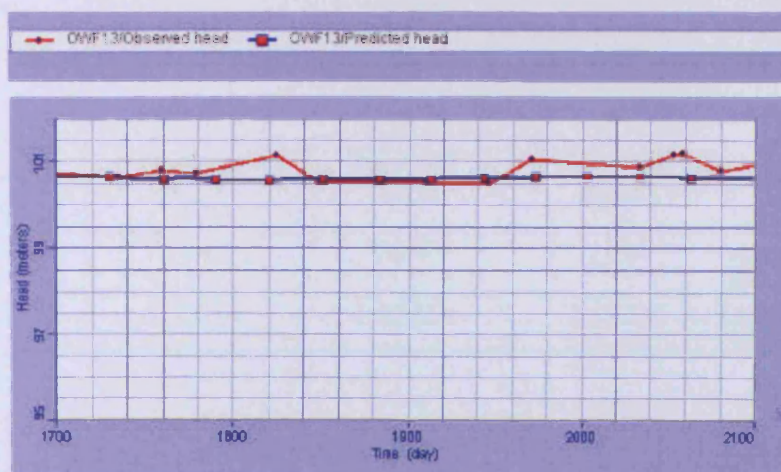


Figure 6.12 Observed and predicted groundwater levels for transient simulation at different boreholes: (a) BH1, (b) BH6, (c) BH21, (d) BH 25, (e) BH13.

6.4.2.4 The Calibrated Conceptual Model

The final conceptual model was arrived at after running many scenarios of the aquifer system and then calibrating each. The final calibrated aquifer permeabilities are shown in Figure 6.13.

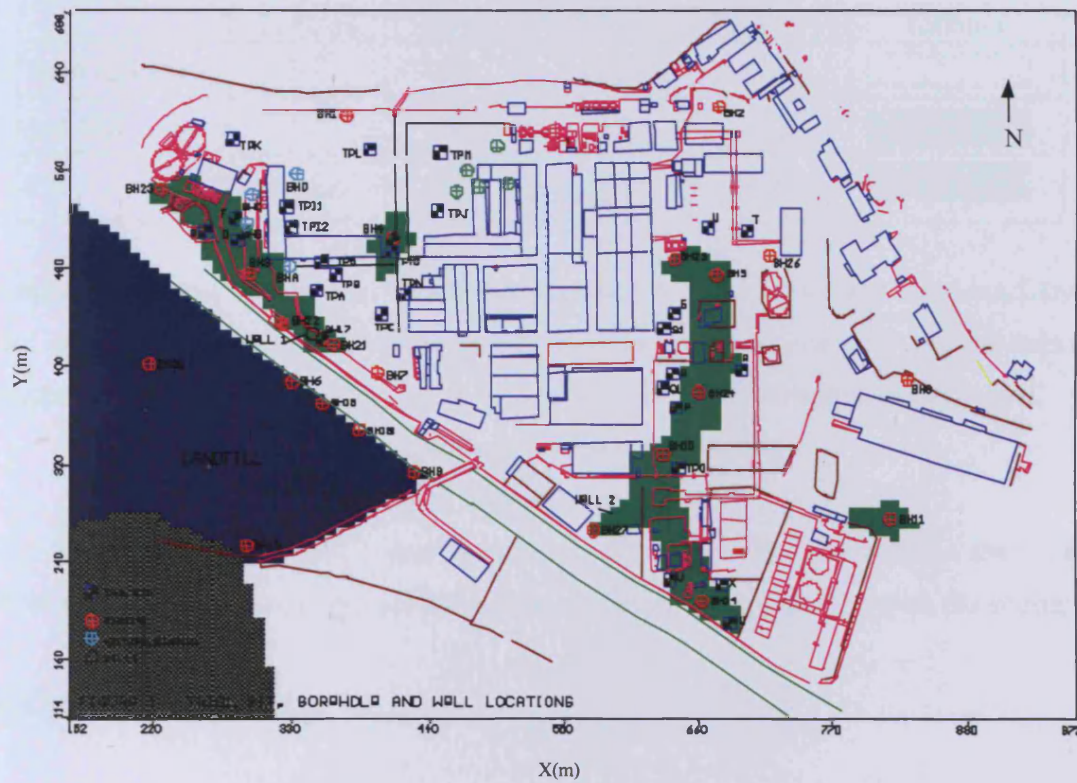
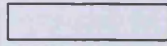
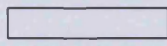
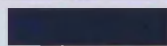


Figure 6.13 Calibrated model permeability distribution in layer 2.

	$K_x$ [m/d]	$K_y$ [m/d]	$K_z$ [m/d]	Colours
Sand and gravel	3.024	3.024	0.3024	
Landfill	0.147	0.147	0.025	
Clay	0.00864	0.00864	0.00777	

These values are within the range of the expected values given in literature. The low permeability at the landfill was due to the nature of the waste buried in the landfill. The resulting value was consistent with the pumping test result in Borehole 28 (see GIBB, 1996). The same distribution was used for the storage coefficient in all layers with the calibrated values being as given below:

	$S_s$ [1/m]	$S_y$ [-]	Eff.Por [-]	Tot.Por [-]	Colours
Sand and gravel	$10^{-4}$	0.1	0.25	0.35	
Landfill	$10^{-5}$	0.02	0.1	0.2	
Clay	0.0013	0.01	0.4	0.48	

Uniform hydraulic conductance values were applied to River Tawe and Swansea Canal and calibrated by matching groundwater levels in the upper and lower parts of the stream respectively using specific observation well groups. The final calibrated values were:

$$\text{River Tawe conductance} = 104.38 \text{ m}^2/\text{d}$$

$$\text{Swansea Canal conductance} = 2.048 \text{ m}^2/\text{d}.$$

The larger value for the River Tawe was entirely consistent with it being below the water table and draining the aquifer, while the canal exchanged very little flow with the aquifer.

### 6.4.3 Sensitivity Analysis

In order to evaluate calibration errors, a number of sensitivity runs were undertaken. The model parameters were varied from the calibrated set and the corresponding predictions compared. As the measured data available for comparison were long term averaged groundwater levels for monthly sets for the period 98-2000, the model was run for both the steady and transient states. The results have been compared with measurements using the root mean square error as an indicator of the overall degree of model fit. The results are presented in Table 6.2.

Table 6.2 Root mean squared error for sensitivity runs.

Model parameter variation	RMSE (m)
The calibrated model	0.36
Permeability increased 40%	0.43
Storage increased 40%	0.46
Storage decreased 40%	0.68
Recharge decreased 40%	0.42
River Tawe level increased 40%	0.41
River Tawe level decreased 40%	0.362
River Tawe hydraulic conductance increased 40%	0.365
River Tawe hydraulic conductance decreased 40%	0.38
Swansea Canal level increased 40%	0.361
Swansea Canal level decreased 40%	0.365
Swansea Canal hydraulic conductance increased 40%	0.362
Swansea Canal hydraulic conductance decreased 40%	0.37

As a permeability test had been carried out in the landfill area at Borehole 28 (GIBB, 1996), a uniform value of the permeability was assigned to this area. The remaining values for the refinery site and the clay lenses were varied over a realistic range, within typical interval values. It was noticed that the model was more sensitive overall to the sand and gravel conductivity. This can be explained by the fact that this area had the largest surface areas and more boreholes than other areas, therefore its impact in error calculations was more significant. When this value was increased then the *RMSE* increased, since the water table dropped and thereby leaving many cells dry within the first layer. The value given to the permeability of sand and gravel was the lowest plausible, based on typical values. The clay lenses permeability affected the model predictions much less than the sand and gravel formation.

In transient mode, it was noticed that the model was very sensitive to both the storage coefficient and the effective porosity at the beginning and end of the simulations, affecting the solver run time (number of iterations and time). As the river stage was fluctuating and the recharge values were variable, an increase in the storage and porosity

raised the water table above observed values and a decrease meant that more water flowed into the river. The calibrated values were optimal, as the data available for this transient simulation were given for a relatively short period, thereby making the model more sensitive to any change in the input. A general decrease of the recharge values gave under-estimated predictions of the water heads. Specifically, a decrease in the refinery site recharge lowered the water table, as this was the dominant surface in the modelled area. The final value of the recharge was assigned the highest possible value regarding the average rainfall over 10 years recorded in this area.

The model was more sensitive to changes in the River Tawe data than Swansea Canal since the river basin size, location and number of observation boreholes available in the locality were larger than for the canal. When raising the river stage it was noted that the calculated heads were lower than the observed ones. The same effect was noticed when the river conductance was increased. Finally, the flow velocities were found to increase towards the river, as shown in Figure 6.14.

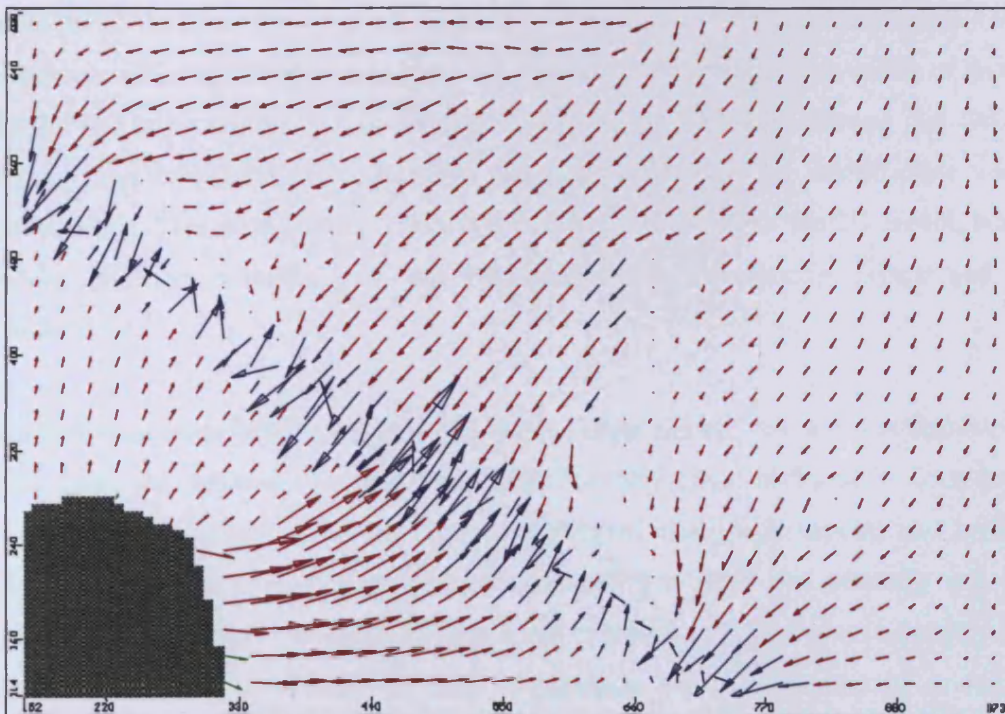


Figure 6.14 Increasing flow velocities towards the river.

## 6.5 MODFLOW Two-Dimensional Simulation

Producing two-dimensional simulations instead of a three-dimensional model was achieved by considering a unit thickness in the  $z$  direction, starting from the horizontal bottom of the last layer of the model. From an aquifer viewpoint, this unit layer is confined and the flow is strictly horizontal through this layer, with leakage going into and up to the river, as may be seen in the fourth layer of the area three-dimensional simulation (see Figure 6.15). The hydraulic approach normally consists of averaging the flow conditions in the vertical dimension in a depth integrated model. However, neither the aquifer geometry nor the vertical flow components could justify this simplification. Indeed for this case the aquifer was  $820.6 \text{ m} \times 574.7 \text{ m}$  to  $27.5 \text{ m}$  in depth, and induced a net flow to the river; this scenario did not allow the vertical flow components to be neglected relatively to the horizontal components. Appropriate flow conditions had to be chosen for the new two-dimensional conceptual model. Many parameters were specified according to their values from the three-dimensional calibrated model. The distribution of the clay lenses in this layer and the hydraulic parameters of each formation were kept the same as for the three-dimensional model. The river surface was projected in this layer as water was still drained from this layer too. However, the conductance values of this new feature had to be adjusted. Also the flow budget in the 3D model showed that flow was coming into this layer from the upper layers, especially at the landfill zone and the refinery site. This incoming flow was simulated as a recharge in the 2D model, but with values adjusted according to the thickness of the overlaying layers and their conductivities.

The flow was essentially horizontal. The water budget showed that the contribution to the flow from the refinery site and the landfill basically came horizontally from layer 3 through the riverbanks, whereas layer 4 contributed from both vertical and horizontal directions. Also, the geological formation showed that there was basically one major geological set, namely the sand and gravel, where layers only arose due to the clay lenses distributions. The uncertainty in their distribution allowed the use of a one-layer conceptual model in these regions.

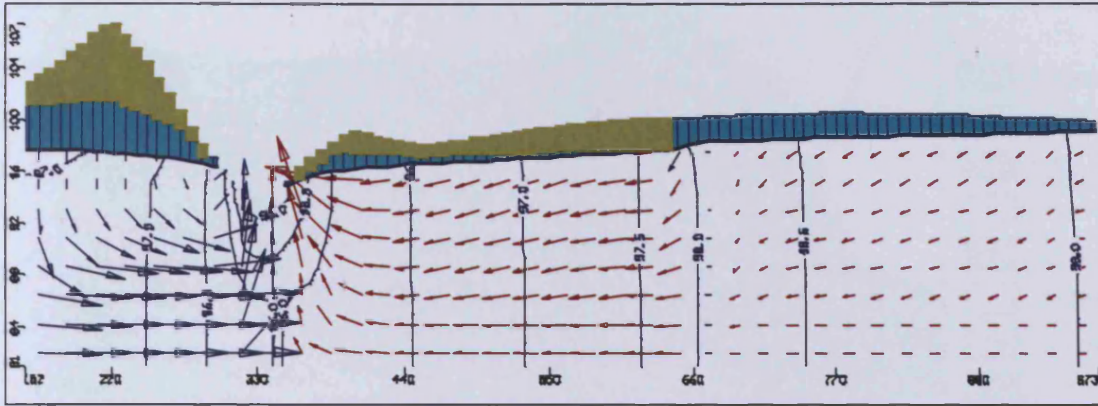


Figure 6.15 Flow direction in the fourth layer in the three-dimensional 100×100 MODFLOW simulation in vertical cut along row 50.

In the new two-dimensional model, the distribution of the clay lenses was reflected in the three layers containing the lenses in the original three-dimensional model. The permeability of all geological formations was kept to the same values as used in the initial calibrated model. However, the recharge was modified. The unit layer was assumed to be flat, and the clay lenses appeared at the surface, whereas in the 4-layers model the clay lenses started from the second layer and the recharge was applied only to the highest active cell in each vertical column. Therefore the recharge values were reduced by factors based on the original elevations of the surface and the geological nature of the terrain (see Figure 6.16). The initial layer bottom was located at 94 m and was coincident with the average elevation of the riverbed. The Swansea Canal was omitted from this layer as it did not affect the flow at these elevations. Many scenarios were run to find the final recharge values relative to their distribution. The steady state groundwater levels resulting from the 2D simulation are shown in Figure 6.17. The calibrated 2D model has 7.11 % normalised *RMSE* on the overall domain, and 12.75 % over the river (see Figure 6.18).

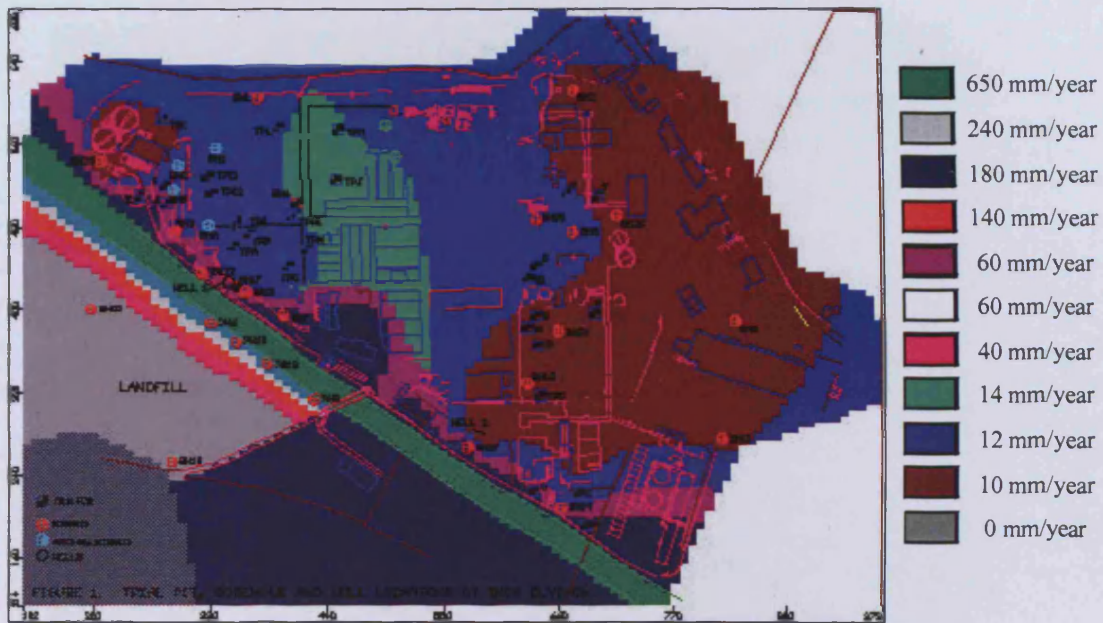


Figure 6.16 Recharge input for two-dimensional simulation of MODFLOW.

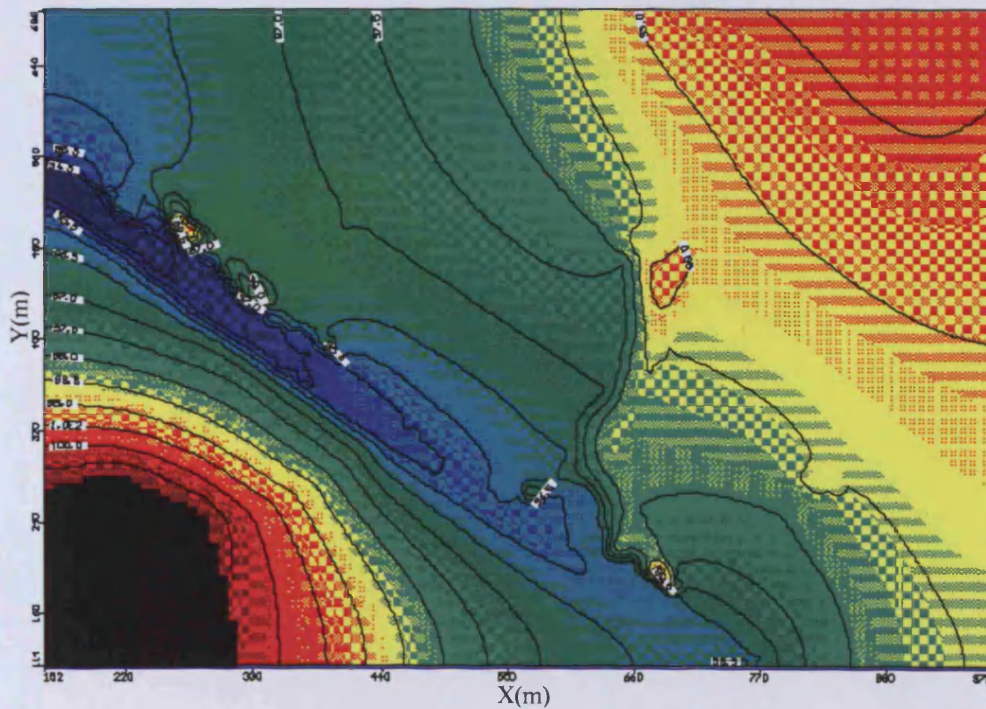
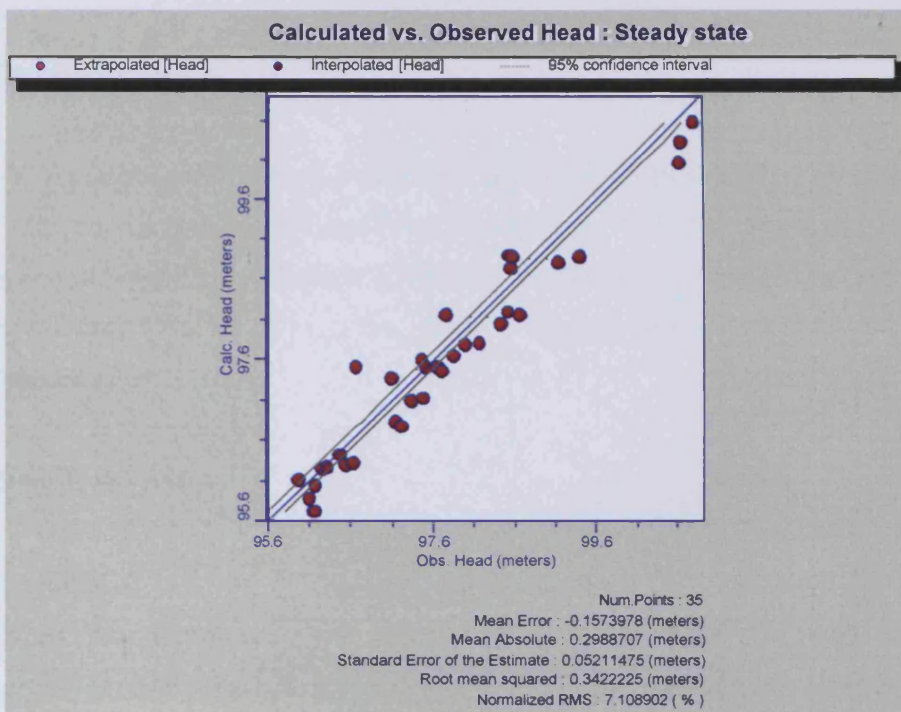


Figure 6.17 Predicted hydraulic heads from the 2D steady state MODFLOW simulation on the  $100 \times 100$  mesh (equipotentials at 0.5 m intervals).

(a)



(b)

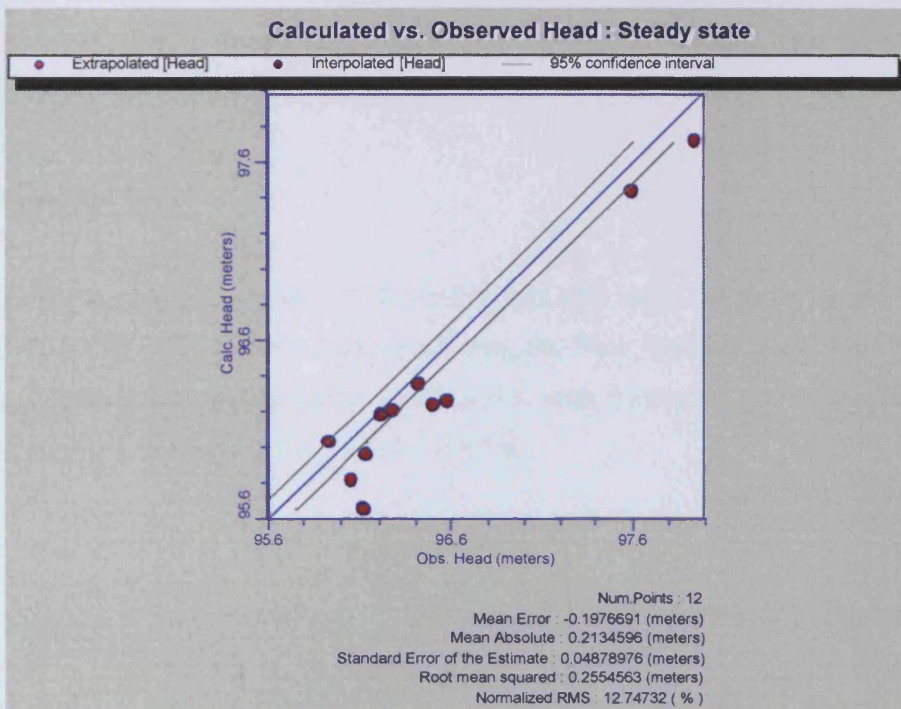


Figure 6.18 Calibration of the two-dimensional MODFLOW simulation  
 (a) error for the overall observation boreholes  
 (b) error for the river observation boreholes.

## 6.6 GWFV Two-Dimensional Simulation

### 6.6.1 Discretisation

The new non-orthogonal grid was generated using the Tecplot Mesh Generator (Amtec, 1999). The model rectangular area was divided into 50 rows and 50 columns on an algebraic structured mesh. The row direction was chosen to be parallel to the riverbanks and the columns were drawn in such a way that fitted the flow direction towards the river (see Figure 6.19).

### 6.6.2 Data Generation

The quadrilateral cell coordinates were generated using the write mesh file option of Tecplot and then reconverted to a format adapted within the GWFV programme input. Another file gave the equivalent cell indices ( $i, j$ ) for each orthogonal cell from the non-orthogonal generated mesh. This basic file allowed the translation of all the MODFLOW input parameters (e.g. permeability, recharge, boundary conditions, etc.) into properties file adapted to the GWFV programme for the structured non-orthogonal grid.

### 6.6.3 Program Run

The GWFV model was run for the non-orthogonal grid using the same run parameters as for MODFLOW. For a steady state simulation, the Slice Implicit Procedure (SIP) solver was used with a user-defined seed equal to 0.1, with 5 iteration parameters and a head change criterion for convergence equal to  $10^{-2}$ m.

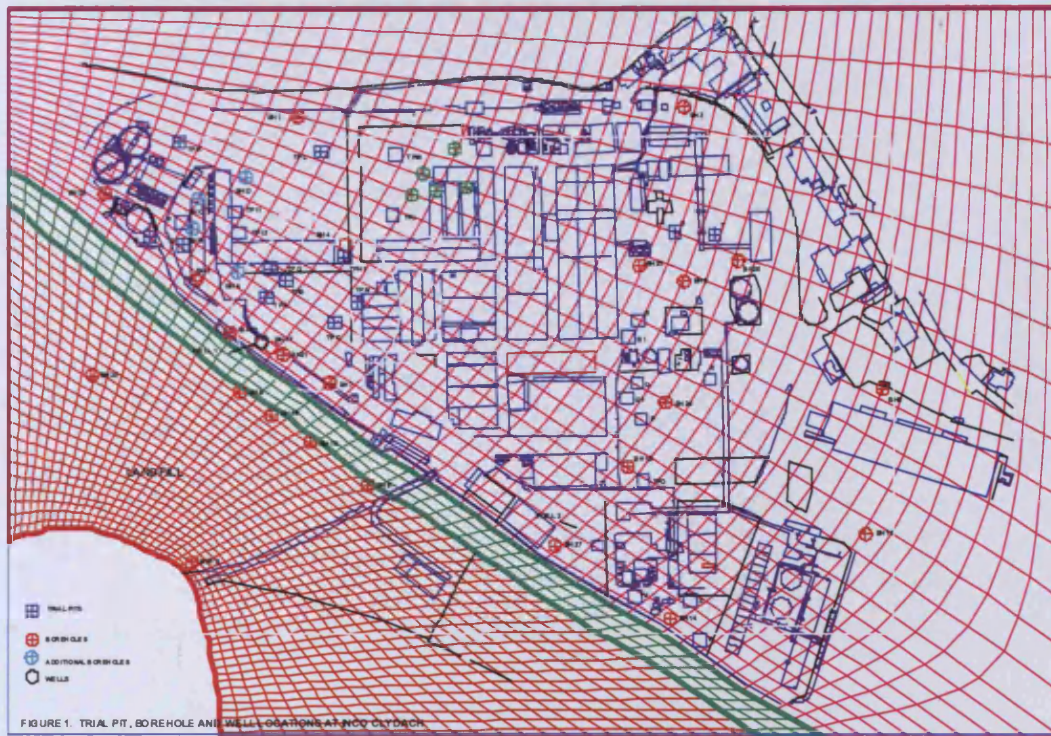


Figure 6.19 The non-orthogonal 50 × 50 mesh.

### 6.7 Comparison and Discussion

For an orthogonal grid, model GWFV gave the same results as MODFLOW. The heads contour map is shown in Figure 6.20. For the non-orthogonal mesh, Figure 6.21 illustrates the contour map for the heads calculated from the GWFV simulation. From both models, it can be seen that the river is still draining into the one-layer aquifer. However, differences between the heads arose at a few borehole sites. To assess the accuracy and correctness of the two models, a comparison was undertaken with the observed heads for the existing.

Table 6.3 Root mean squared error results comparison.

RMSE (m)	Refinery well group	River well group	Landfill well group	All groups
MODFLOW	0.31199	0.50776	0.49619	0.42176
GWV	0.28770	0.43227	0.49262	0.381931

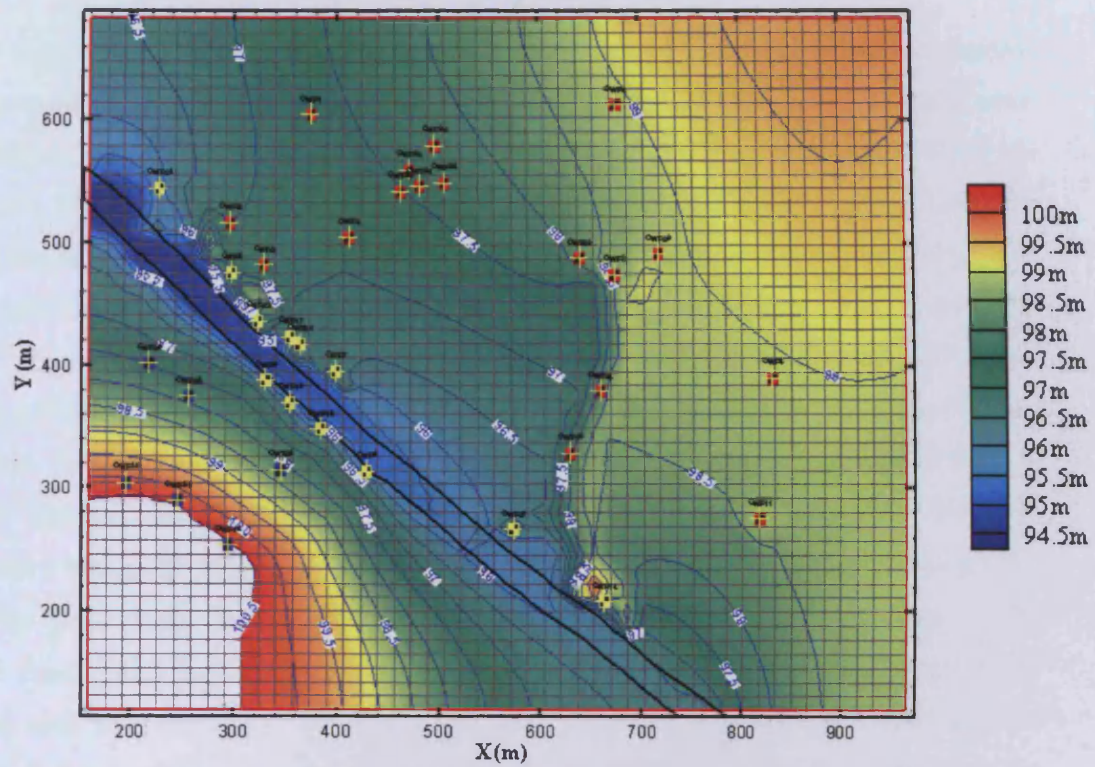


Figure 6.20 Head results from MODFLOW (50 × 50 mesh).

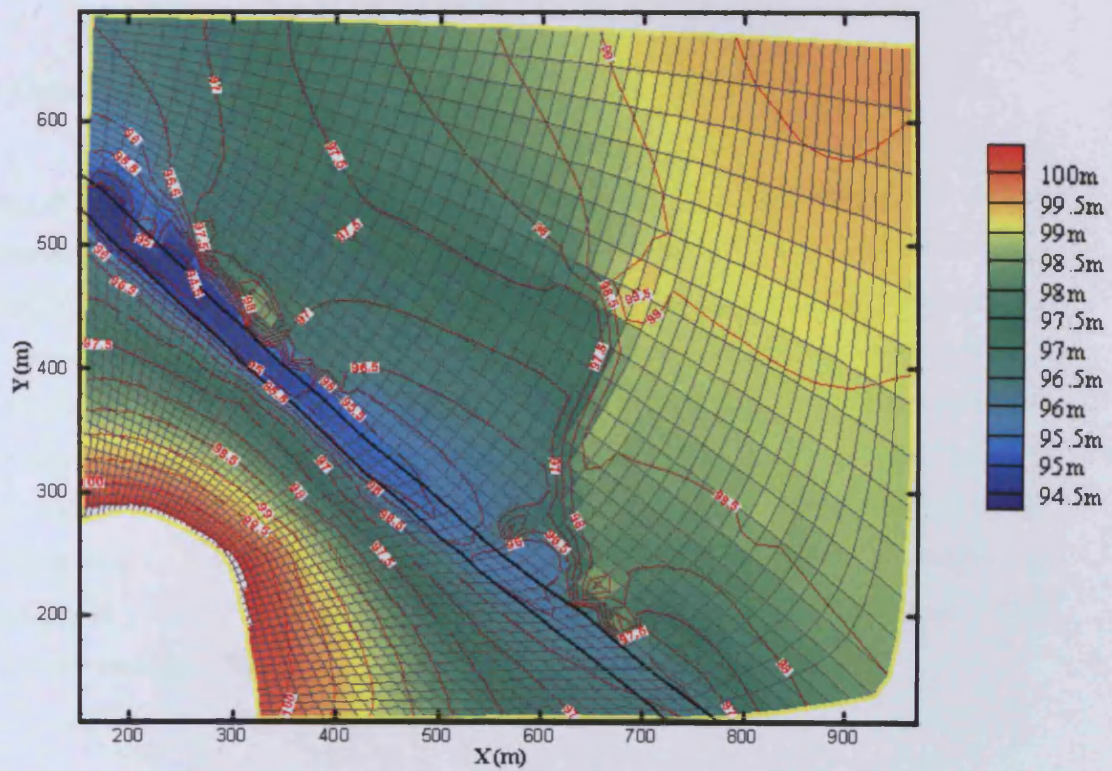


Figure 6.21 Head results from GWFEV on non-orthogonal grid (50 × 50 mesh).

The observation wells were grouped into three groups to make more distinctive comparisons between the accuracy of the two models. The root mean squared error (*RMSE*) of all the groups and the overall area is given in Table 6.3. The basic difference between the models is solely the shape of the mesh used in the GWFV model, and it can be seen that the best improvement in accuracy was noticed at the river well group since the cells fitted exactly to the shape the river and the direction of the flow towards the river. Figure 6.22 emphasises the improved accuracy for this group. Figures 6.23 shows the overall features of the steady state calculated vs. observed head around a line of equal relation. The normalised *RMSE* for MODFLOW was 8.21%, on the orthogonal  $50 \times 50$  mesh whereas the GWFV on the  $50 \times 50$  non-orthogonal mesh gave 7.15%. This accuracy was only reached by MODFLOW when running the model on a mesh refined by two (i.e. a  $100 \times 100$  mesh). The MODFLOW normalised *RMSE* was then 7.11%. This clearly highlighted the higher accuracy of the GWFV relatively to MODFLOW when using non-orthogonal grid that capture the geometry of the river for this particular case. A lower mesh resolution was needed for the GWFV to give the same results as MODFLOW.

## 6.8 Conclusion

Although only a  $50 \times 50$  mesh was used, the results of the GWFV model for a non-orthogonal mesh were compared to the results from the  $100 \times 100$  mesh using MODFLOW and the comparisons showed a high level accuracy. In particular, the agreement was closest near the river, where heads at observation boreholes were close to the predicted heads. Therefore, it can be noted that using a grid that fits closely the geometrical layout of the river with the GWFV model, in this case, reduced the use of mesh nodes by 50% in comparison with MODFLOW, without losing accuracy in the predicted heads. The new model generated from MODFLOW with a non-orthogonal quadrilateral grid can give more accurate results, with a greater flexibility at internal and/or external boundaries.

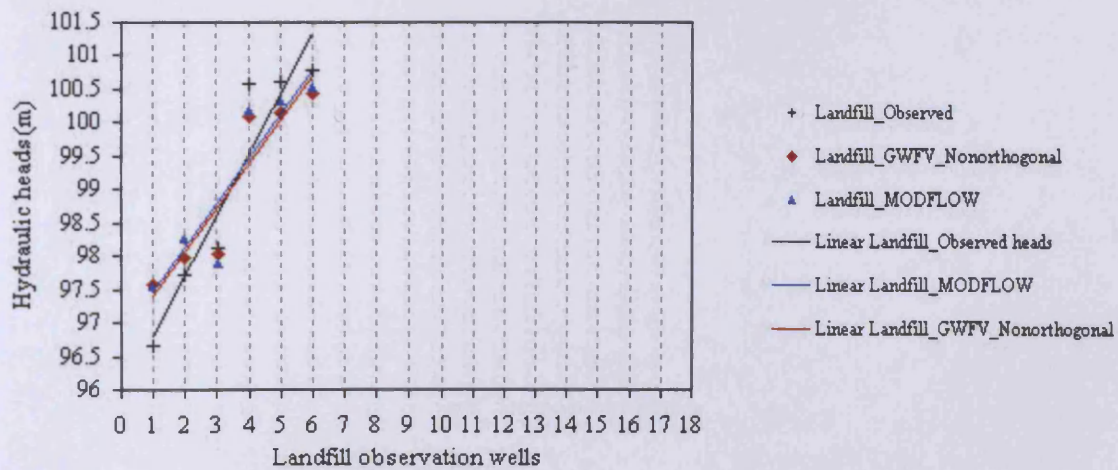
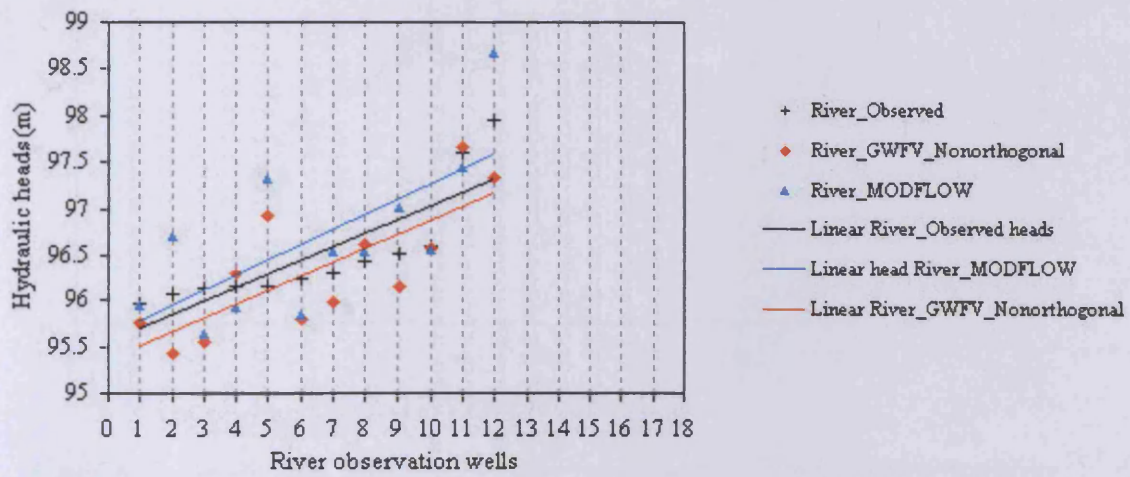
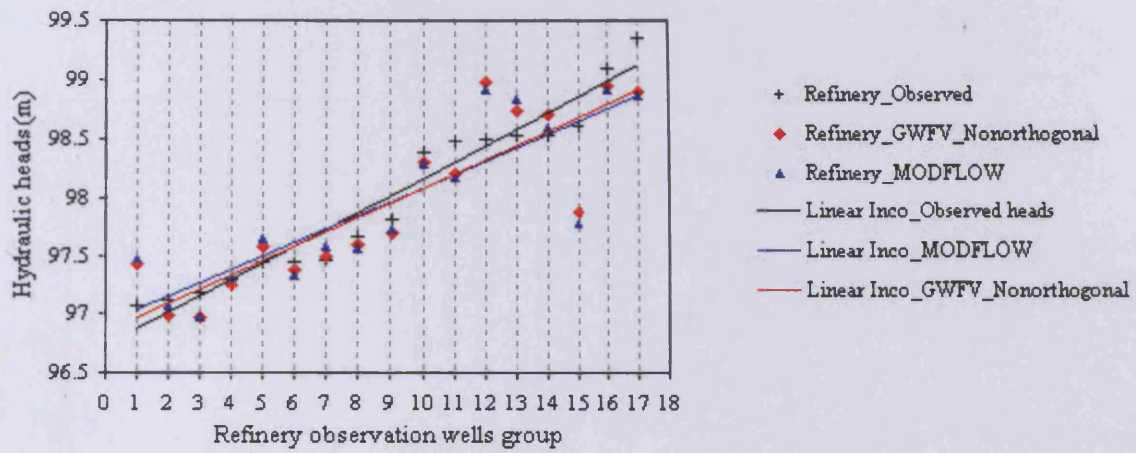


Figure 6.22 Comparison of head results from MODFLOW and the GWFV model for non-orthogonal with observed heads, for different observations well groups.

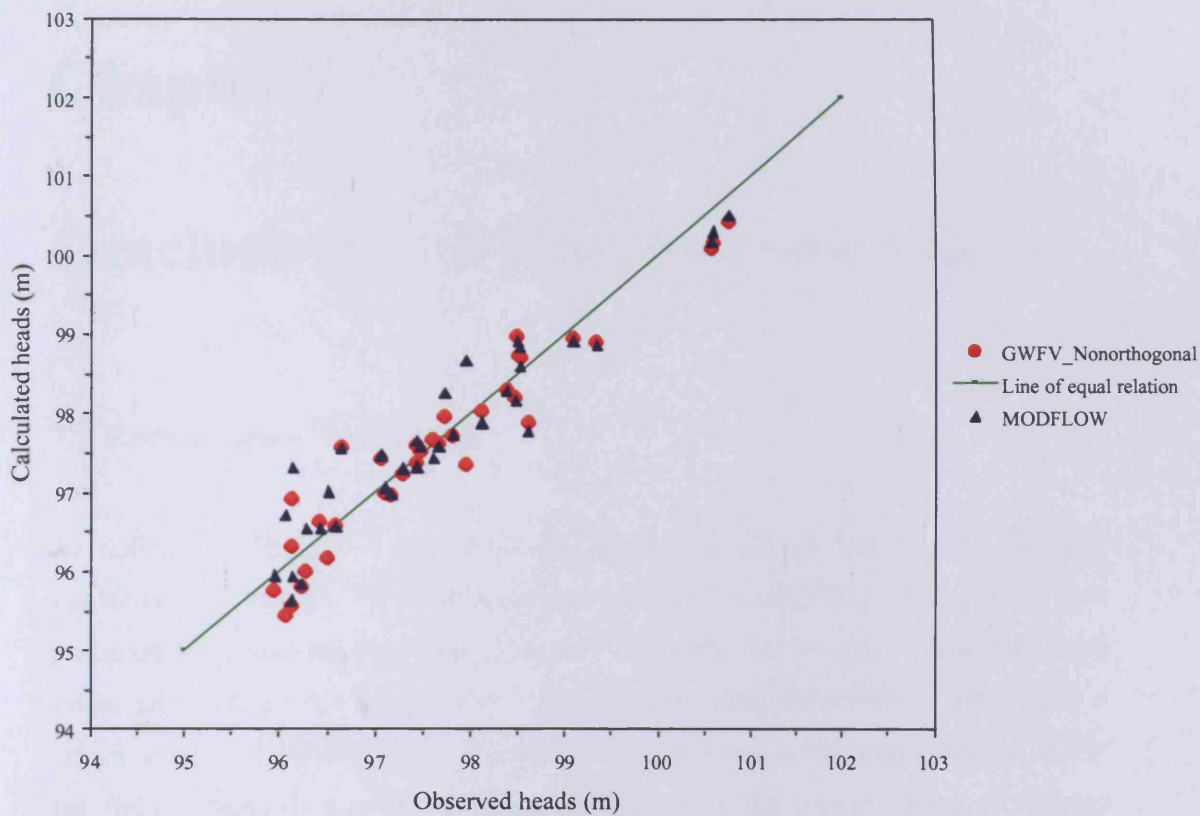


Figure 6.23 Steady state calculated vs. observed heads on 35 observation boreholes.

# Chapter 7

## Conclusions and Recommendations

### 7.1 Review and Conclusions

As outlined in Chapter 1, the main objective of this work has been to develop, implement and verify a 2D finite volume solution within MODFLOW, to predict flow processes in groundwater systems. This new capability was to include non-orthogonal grids, and include the benefits of unconditional mass conservation. Following a critical review of MODFLOW, and recent improvements, it was found that the use of the finite difference method presented limitations in the representation of features with a curved geometry and thus a loss of accuracy in the numerical solutions. To tackle this problem, a new 2D groundwater flow finite volume model, named the GWFV model, was developed in this study as an alternative solution method, within the finite difference-based simulator MODFLOW. The numerical method used to solve the governing equations was aimed at giving broad flexibility for grid shapes in the  $x$  and  $y$  directions. Therefore, when constructing a conceptual model, assumptions related to the geometry of the boundaries could be more realistic and accurate. The changes that were made in developing the new model were made in a consistent manner to the structures of MODFLOW, with popularity-oriented objectives.

The main developments and findings from this study can be summarised as follow:

Firstly, many forms of the approximation of a flux through a surface that can be employed in the discretisation of the groundwater flow equation, using a quadrilateral geometry, were reviewed and evaluated with respect to their suitability for numerical

solution by the finite volume approach and within the MODFLOW objectives. Three different finite volume discretisation methods were selected and developed to solve the groundwater flow equation. The differences between these methods were in the way that the gradient on a control volume face was approximated and, consequently, the generated matrix coefficients.

Secondly, numerical tests were carried out to check the performance of the three constructed methods. Five particular aspects were investigated, namely: accuracy, sensitivity to mesh size, grid shape effects in terms of non-orthogonality and skewness, accuracy at irregular boundaries, and heterogeneity effects. It was found that the model based on the higher order flux approximation technique, termed the GWFV model, gave the most accurate results.

Thirdly, a brief description of the implementation of the preferred finite volume method into the existing MODFLOW code, and the consequent changes and requirements were presented. The core of these changes was: (i) the computational grid enabled by the new method, which consisted of structured quadrilateral-shaped control volumes defined by the coordinates of their vertices, and (ii) the calculations needed to approximate the gradient terms at cell faces.

Fourthly, a field case model was set to validate the GWFV model. The model was first set up in 3D in order to have the best choice of parameter estimation and boundary conditions. The calibration process gave good results. The model was then conveniently reduced to a 2D model, for the new GWFV code to be fully validated. The test results indicated that GWFV offers a viable alternative to the finite difference solution method used in MODFLOW. Its use is desirable when accurate simulation of boundary conditions or complex property distributions with a mass balance are required. For the field case of this study, the GWFV model performed better than the MODFLOW model.

When constructing the GWFV model, the primary focus was on finding the best finite volume method to solve the groundwater flow equation, for the same assumptions, and with a more accurate representation of the boundary conditions, giving a similar ease of use as in MODFLOW, and minimal changes to the source code. In this sense,

when developing the three finite volume methods in Chapter 4, the mesh structure was kept constant but the resulting matrix coefficients showed similar properties to the matrix system equations in MODFLOW, with the exception of the GWFV model when using the non-orthogonal grid. The numerical errors of this method and accuracy issues were discussed. Numerical tests showed that the method was second-order accurate and had the lowest non-orthogonality induced error. The changes necessary within MODFLOW, to make it compatible with the new finite volume formulation, mainly affected the input data and the code lines concerned with the equations formulation. The calibrated field model also showed that the GWFV model performed well in simulating flow to a river boundary that was sited diagonally in a near rectangular aquifer. The accuracy improvement from the GWFV model was particularly noticeable near the river and at the landfill site, where the cells were fitted to the boundaries closely. The simulated results, the benchmarked results, and the field observation results are shown to give good agreement.

## **7.2 Recommendations for Further Work**

### **7.2.1 Two-Dimensional Finite Volume Extension to Other Processes**

In this study, the changes inspired by the finite volume implementation were basically made in the MODFLOW-2000 global (GLOBAL) and groundwater flow (GWF) processes. Similar changes can be expanded to the observation and sensitivity processes of MODFLOW 2000. Several packages of these processes involve cell geometry dimensions and thus should be adjusted for compatibility with the new numerical method implemented in the GLOBAL and GWF processes.

The finite volume discretisation used in this study can be adequately used to simulate transport in strongly orthotropic and anisotropic media in two dimensions (see Jayantha and Turner, 2003 (a) and (b)). This method can also be particularly applied to the solute-transport equation, as used by the U.S. Geological Survey MOC3D transport model or the MT3DMS model. The MOC3D model uses the method-of-characteristics to solve the transport equation, on the basis of the hydraulic gradients computed with MODFLOW for a given time step. It is also in the public domain and the code is available from the World Wide Web, within the MODFLOW-2000

process and is called GWT. The MT3DMS model includes the standard finite-difference method, along with three optional solution schemes for transport. This model is private (developed at the University of Alabama for the U.S. Department of Defense). However, recent versions of MODFLOW incorporate the package LMG, linking MODFLOW to the MT3DMS model.

## **7.2.2 Extension to 3D and Implementation in MODFLOW Recommendations**

### **7.2.2.1 Three-Dimensional Finite Volume Discretisation**

Few studies have been undertaken to investigate accurate three-dimensional finite volume discretisations for solving flow and transport problems dominated by diffusion in heterogeneous and anisotropic media. This is due to the fact that these techniques are still being improved in two dimensions. The extension of these methods to three dimensions is a laborious task and the algebra may be quite complicated. Thus, the extension should be made on the basis of an exhaustive investigation of the available techniques in two-dimensions and a rigorous analysis and comparison of their performances.

The study reported herein has presented a thorough investigation of the existing two-dimensional finite volume techniques that are applicable to solve the governing groundwater flow equation as used in MODFLOW. The final selected method was developed after analysing and comparing the performance of a range of investigated techniques. Naturally, the next recommended step in this work would be to develop the finite volume model in three dimensions. This could be achieved by adding a vertical discretisation (i.e. along the  $z$  direction) to the groundwater equation used in MODFLOW, as expressed in Equation 3.1. The vertical discretisation concepts used in MODFLOW would no longer be needed, as the flexibility of the non-orthogonal grid would enable the model to fit the layers stratification. This method would provide a good foundation upon which the three-dimensional extension of the finite volume model, developed within MODFLOW, could be made. The method has proved to perform well throughout the numerical and field tests in this study comparatively to the analytical and/or MODFLOW solutions, with the solution not requiring any new solvers to treat the generated system of equations. Furthermore, extending the scheme

to 3D applications would be less costly than using the other methods considered in terms of computational effort and storage requirements. However, the increase in computer memory requirements due to the introduction of additional arrays in the 3D model code should be investigated. Tests should also be carried out to assess the performance of the existing solvers with the newly generated matrix, as well as their sensitivity to the new 3D cell shapes and number. The computational effort would be analysed by a CPU time measurement.

### 7.2.2.2 Implementation in MODFLOW

The traditional process of discretisation, consisting of manually calculating appropriate parameter values to assign to each finite-difference cell, would no longer be necessary with a 3D finite volume solution. Assigning a non-orthogonal and structured mesh to an aquifer system to be modelled, and its related parameters, is a task that could be achieved by using a graphical tool. For MODFLOW-2000, the recently developed USGS programme MFI2K (Harbaugh, A.W., 2002) helps in preparing model input-data by interactively entering the data through a series of display screens. However, the program does not allow any space visualisation or mesh generation of the modelled area.

A link to visualisation software tools and a mesh generator will be needed, particularly for discretising the aquifer system to be modelled into a three dimensional mesh. Robins et al. (2005) have pointed out the main role of visualisation tools as a foundation for a conceptual model. They also presented 3D visualisation software to facilitate the development of a conceptual model and allow data held within it to be directly accessed by Visual Modflow. This will help the modeller in fitting more precisely the grid to the hydrogeological features of the aquifer in 2D and 3D. An interface with a Geographical Information System (GIS) could also be considered. A combination of a 3D visualisation software tool and a GIS would provide a more valuable tool for displaying and analysing data. In this sense, software tools such as MDR (Modflow Data Reader) or GW Modeler (see Table B.2) should be modified to account for the new MODFLOW finite volume process GWFV input requirements.

Finally, an interface with a mesh generator that can discretise the geometric domain of the aquifer into quadrilateral (in 2D) or hexahedra (in 3D) fitting with the spatial distribution of boundaries, geologic formations and hydraulic constraints could be included. Mesh generators such as Easymesh (2D) and LaGriT (3D) give an insight as to how a suitable MODFLOW-GWFV linked-mesh generator should be. An interface between Tecplot Mesh Generator ('Mesh file' format ASCII) and the GWFV programme as the MODFLOW free format-reading programme can also be suggested.

### 7.2.2.3 Three-Dimensional Finite Volume Model Testing

The numerical model could be validated for a 3D flow situation by comparison with laboratory experimental observations. For example, a 3D sand model (see section 2.1.1) could be set up to check the accuracy of the numerical model, particularly with respect the representation of irregular geometries of specific hydraulic features. Complex flow situations could be studied, such as uniform flow in a heterogeneous medium with an irregular interface shape either vertically (layers) or horizontally (adjacent geological formations), or a semi-phreatic flow between two channels with a curved pattern in a homogeneous aquifer with uniform recharge. The model could replicate groundwater flow using a container with dry glass beads of known shape, and therefore hydraulic conductivity, and the tests could be constructed at an appropriate laboratory scale.

Analytical solutions could also be used and developed further for specific conditions of 1D, 2D and 3D flow cases (see section 2.4.1). The cross section cases, such as flow to a pumped well in a confined, unconfined, or leaky aquifer (e.g. Theis solution, Hantush solution, Moench and Prickett solution), or 2D flows in vertical plane (Toth solution) could be used to check the accuracy of the added vertical discretisation in the new model.

Finally, a field case study that has been extensively investigated would be ideal to validate the 3D model. The case would preferably have a multi-layer aquifer system, curved areal extension, and hydraulic features that could highlight the adaptability of the non-orthogonal grid to the geometry for the surface and/or vertical dimensions

(e.g. river, different areal recharges, stream, wetlands). Most importantly, if not already modelled and calibrated, this study would ideally have enough monitoring data in space and time to build a realistic conceptual model, with a minimum of uncertainties, and offering reliable field observations data to enable comparison with the numerical model predicted results.

# **APPENDIX A**

Table A.1 Compilation of few analytical groundwater flow models.

Name of Software	Model Description/ Process simulations	Type of solution	Site Conditions for Model Application	References/ Sources
<b>3DFLOW*</b>	3-D groundwater flow	Analytic Element Method	Steady flow to horizontal wells, partially or fully penetrating wells in a regional field of uniform flow. Bounded horizontal, semi-infinite or infinite aquifer can be simulated.	Steward, D. Kansas State University
<b>ANALYT</b>	2 and 3-D groundwater flow with recharge/discharge	Superposition	Isotropic or anisotropic, homogeneous water-table aquifer with an impermeable or semi-pervious layer; different boundary conditions and geometry; and several independent recharge or discharge sources of different geometry, operational time, and flux rate.	Kolesov, A.A. Production and Research Institute for Engineering Construction Survey (PNIIS), RUSSIA
<b>AQTESOLV</b>	Aquifer test analysis	Exact / approximate analytical	Confined, unconfined, leaky or fractured aquifers, one or two-aquifer systems, single or multiple pumping wells, partially or fully penetrating wells.	Duffield, G.M. HydroSOLVE, Inc
<b>AquiferTest Pro</b>	Pumping Test Analysis	Exact / approximate analytical	Confined, unconfined, leaky aquifers and fractured rock aquifers.	Waterloo Hydrogeologic, Inc.
<b>AquiferWellTest</b>	Aquifer test analysis	Exact / approximate analytical	Single well test data with solutions for: slug, constant discharge, variable discharge, step drawdown and recovery tests.	BOSS International
<b>AquiferWin 32</b>	Aquifer test analysis	Exact / approximate analytical solution and analytic elements	Confined, unconfined or leaky aquifers with completely or partially penetrating pumping wells, fissured groundwater reservoir with fracture skin.	Scientific Software Group
<b>BEAVERSOFT</b>	2-D groundwater flow and pollution	Analytic solutions	Steady and unsteady 2-D flow in nonhomogeneous aquifers, flow through dams.	Verruijt, A., and Bear, J. Delft University of Technology
<b>CAPZONE</b>	2-D groundwater flow	Exact / approximate analytical	Isotropic and homogeneous confined, leaky-confined, or unconfined flow conditions with up to 100 wells.	Bair, E.S., et al. IGWMC
<b>GFLOW2000*</b>	3-D local flow, 2-D regional flow	Analytic Element Method	Confined and unconfined, homogeneous or heterogeneous aquifers, streams, lakes, wetlands, areal recharge and drains can be simulated.	Haitjema, H.M. Haitjema Software, LLC
<b>GWFLOW</b>	7 groundwater flow problems	Exact / approximate analytical	Homogeneous, isotropic aquifers, confined, unconfined or leaky aquifer, fully penetrating single well, circular recharge area.	Van der Heijde, P.K.M. IGWMC
<b>MLPU</b>	3-D groundwater flow	Analytic Element Method	Multi-aquifer system, wells, line-sinks, infiltration ponds and transient wells, confined and leaky aquifers, aquifer assumed to be of infinite extent, laterally homogeneous and isotropic, but aquifers can be composed of up to 3 layers with distinct permeability, porosity and thickness.	Nienhuis, P.R. The Netherlands
<b>ModAEM*</b>	3-D regional groundwater flow	Analytic Element Method	Partially penetrating well in confined/unconfined and stratified aquifers.	Haitjema, H.M. Wittman Hydro Planning Associates (W.H.P.A. Inc.)
<b>PhreFlow*</b>	3-D groundwater flow and advective transport	Analytic Element Method	Single layer groundwater flow, unconfined with partially penetrating wells and inhomogeneities.	Jankovic, I., and Barnes, R. University at Buffalo

Name of Software	Model Description/ Process simulations	Type of solution	Site Conditions for Model Application	References/ Sources
<b>PRINCE</b>	2-D groundwater flow 1, 2 and 3-D solute transport	Exact / approxiamte analytical	Confined, unconfined or leaky, isotropic or anisotropic aquifer of finite, semi-finite and infinite lateral extent, single or multiple injection and extraction wells. Simple treatment of recharge/barrier boundary conditions can be used.	Cleary, R., and Unga, M. Waterloo Hydrogeologic, Inc.
<b>QuickFlow</b>	2-D groundwater flow	Semi-analytical	Confined and unconfined aquifers, wells, uniform recharge, circular recharge/discharge areas, line sources and sinks.	Rumbaugh, J.O. Rockware, Inc.
<b>RBCA Tier 2 Analyzer</b>	2-D groundwater flow and contaminant transport simulation	Superposition	Complex boundary conditions and 'leaky' boundary conditions representing pumping wells and injection wells, flow boundaries, rivers and lakes with complex geometries, and regional hydraulic gradients.	Scientific Software Group
<b>SATEM 2002</b>	Aquifer test analysis	Exact / approxiamte analytical	Unconsolidated, confined, leaky confined or phreatic aquifers, fully or partially penetrating wells.	Boonstra, J. International Institute for Land Reclamation and Improvement (ILRI)
<b>Single Well Solutions</b>	Pumping test analysis	Exact / approxiamte analytical	Single well pump, constant or variable discharge, fully or partially penetrating in confined or unconfined aquifers.	Streamline Groundwater Applications
<b>SLAEM/MLAEM</b>	2 and 3-D regional groundwater flow	Analytic Element Method	Confined, unconfined, and leaky heterogeneous aquifers, single or multi-layers, streams, lakes, rivers, extraction or infiltration and leakage can be represented.	Strack, O.D.L. Strack Consulting, Inc.
<b>SLUGC/SLUGT</b>	Aquifer test analysis	Exact / approxiamte analytical	Simulates traditional manual curve fitting. In addition, SLUGT can estimate effects due to air entrapped in the completion region of a piezometer.	Van der Heijde, P.K.M. / Mills, A. IGWMC
<b>SPLIT*</b>	2-D groundwater flow	Analytic Element Method	Single-layer groundwater flow in heterogeneous aquifers with particle tracking, capture-zone delineation, and parameter estimation.	Jankovic, I. University at Buffalo
<b>THCVFIT</b>	Pumping test analysis	Exact / approxiamte analytical	Nonsteady state Theis equation for radial flow.	Van der Heijde, P.K.M. IGWMC
<b>THEISFIT</b>	2-D groundwater flow	Exact / approxiamte analytical	Isotropic homogeneous nonleaky confined aquifer (Theis assumptions).	McElwee, C.D. IGWMC
<b>THWELLS</b>	Pumping / injection test Analysis	Exact / approxiamte analytical	Isotropic, homogeneous confined, leaky confined or unconfined aquifer of infinite extent. Up to 100 pumping and/or injection wells can be used.	Van der Heijde, P.K.M. IGWMC
<b>TimSL/TimML*</b>	Groundwater flow	Analytic Element Method	Single aquifer steady-state and transient groundwater flow. Multi-aquifer steady-state groundwater flow with analytic elements.	Bakker, M., et al. The University of Georgia
<b>TIMELAG</b>	Single-well test analysis	Exact / approxiamte analytical	Estimates hydraulic conductivity from single-well test.	Thompson, D.B. IGWMC
<b>TWODAN</b>	2-D groundwater flow model	Analytic Element Method	Unconfined and confined aquifers, stratified aquifers, heterogeneities, thin barriers, local and global infiltration or leakage. Uniform regional flow, wells and sinks, resistant and impermeable elements.	Fitts, C. Fitts Geosolutions
<b>VERTPAK*</b>	Groundwater flow and solute transport	Exact / approxiamte analytical	Fractured and unfractured porous media, homogeneous, isotropic confined aquifer of infinite lateral extent, fully or partially penetrating well.	Lester, B., et al. Nuclear Energy Agency

Name of Software	Model Description/ Process simulations	Type of solution	Site Conditions for Model Application	References/ Sources
<b>Visual BLUEBIRD*</b>	2-D groundwater flow	Analytic Element Method	Single-layer heterogeneous aquifers. Rivers, lakes, wells, recharge, leakage, horizontal wells can be represented.	Craig, J. University at Buffalo
<b>WALTON 35</b>	2 and 3-D groundwater flow, solute and heat transport	Exact / approximate analytical	Confined/leaky confined/water-table aquifer, steady/non-steady state, multiple fully penetrating wells, recharge and steam depletion.	Walton, M.W.C IGWMC
<b>WELLTEST</b>	Pump test and slug test analysis	Exact / approximate analytical	Homogeneous, isotropic, confined, leaky confined and water table aquifers, partially or fully penetrating wells.	IGWMC.
<b>WhAEM 2000*</b>	Capture zone delineation and protection area mapping	Analytic Element Method	Confined/unconfined, homogeneous/heterogeneous aquifers, hydrological boundaries such as rivers, recharge, and no-flow contacts.	Strack, O.D.L., and Haitjema, H.M. USEPA
<b>WHPA*</b>	2-D groundwater flow capture zone delineation	Semi-analytical	Homogeneous confined, unconfined, and/or leaky aquifers. multiple pumping and injection wells, barrier or stream boundary conditions can be used.	Blandford, T.N., and Huyakorn, P.S. USEPA
<b>WinFlow</b>	2-D groundwater flow	Analytic Element Method	Homogeneous confined, unconfined, and/or leaky aquifers with multiple wells, uniform recharge, circular recharge/discharge areas, and line sources or sinks.	Rumbaugh, J. Environmental Simulations Inc.

\* can be found in a public domain version

**USEPA** United State Environment Protection Agency  
**USNRC** United State Nuclear Regulatory Commission  
**USACE** United State Army Corps of Engineers  
**USDOE** United State Department of Energy  
**IGWMC** International Ground Water Modeling Center

Table A.2 Compilation of few numerical groundwater flow models.

Name of Software	Model Description/ Process simulations	Type of solution	Site Conditions for Model Application	References/ Sources
<b>3DFATMIC*</b>	3-D subsurface flow, transport and fate	FE	Transient or steady-state density-dependent flow field in heterogeneous and anisotropic media with variable boundary conditions.	Yeh, G.T., USEPA
<b>3DFEMFAT</b>	3-D flow groundwater and transport	FE	Saturated/unsaturated media, heterogeneous and anisotropic, transient or steady-state, variable boundary conditions.	Yeh, G.T., Scientific Software Group
<b>ABCFEM</b>	2-D groundwater flow and transport	FE	Steady state or transient flow, pumping or injection wells. Variety of boundary conditions. Confined/ unconfined systems.	Brown, A., and Hertzman, R. Adrian Brown Consultants Inc.
<b>AQUA3D</b>	3-D groundflow, heat and solute transport	FE	Inhomogeneous and anisotropic flow conditions, variable boundary conditions, steady or transient flow.	Scientific Software Group
<b>AQUIFEM</b>	2 and 3-D groundwater flow	FE	Anisotropic, heterogeneous, phreatic or confined, leaky or non-leaky aquifers under transient or steady state conditions.	Townley, L.R., et al., Scientific Software Group
<b>BEAVERSOFT</b>	2-D groundwater flow and transport	FD and FE	Steady and unsteady 2-D flow in nonhomogeneous aquifers, flow through dams.	Verruijt, A., and Bear, J. Delft University of Technology
<b>BEMPLAP</b>	2 or 3-D Laplace problems	BEM	Steady state, homogeneous and isotropic media, subject to any type of the domain boundary conditions, no sources/sink can be considered.	Kirkup, S. Integrated Sound Software
<b>BIGFLOW</b>	3-D groundwater flow	FD or FV	Saturated/unsaturated, heterogeneous and anisotropic media, transient and/or steady-state, variable boundary conditions.	Ababou, R. U.S.Nuclear Regulatory Commission
<b>BioF&amp;T</b>	3-D biodegradation, groundwater flow and transport	FE	Saturated/unsaturated, heterogeneous, anisotropic porous media or fractured media, variable boundary conditions, steady or transient flow.	Scientific Software Group
<b>BIOSLURP</b>	2-D groundwater flow and vapor transport	FE	Multiphase flow in saturated/unsaturated zones, heterogeneous, anisotropic porous media or fractured media, 1st and 2nd type boundary, source/sink boundary.	Scientific Software Group
<b>CFEST*</b>	2 and 3-D coupled fluid, energy and solute transport	FE	Accounts for heterogeneity and anisotropy, steady and transient -state flow, multilayered system and time-dependent or constant source/sinks.	Gupta, S.K., and Cole, C.R. USDOE
<b>DSTRAM</b>	3-D groundwater flow and transport	FE	Density-dependent flow and transport in fully saturated porous media, steady/transient simulations, heterogeneous and anisotropic media, a wide range of boundary conditions	Huyakorn, P.S. HydrGeoLogic, Inc.
<b>DYNFLOW</b>	3-D groundwater flow	FE	Transient and/or steady-state flow, heterogeneous anisotropic saturated media, confined-unconfined flow conditions, allows a wide range of stresses and boundary conditions.	Riordan, P.J., et al. Camp Dresser &McKee
<b>FACT</b>	3-D groundwater flow and contaminant transport	FE	Saturated/unsaturated, porous media, highly heterogeneous, multi-layer aquifer system with different options for boundary conditions implementation.	Aleman, S. USDOE
<b>FEFLOW</b>	2 and 3-D groundwater flow and transport	FE	Transient or steady-state flow, density-dependent flow, variable boundary conditions.	Durbin, T.J., and Bond, L.D. Waterloo Hydrogeologic, Inc.
<b>FEMWATER*</b>	3-D saturated/unsaturated groundflow	FE	Heterogeneous and anisotropic media, transient and/or steady-state, variable boundary conditions.	Yeh, G. T. USEPA and USNRC
<b>FLONET</b>	2-D groundwater flow	FE	Steady-state, confined or unconfined aquifer, heterogeneous and anisotropic porous media with complex boundary.	Frind, E., et al. Waterloo HydroGeologic Software

Name of Software	Model Description/ Process simulations	Type of solution	Site Conditions for Model Application	References/ Sources
<b>FLOWPATH</b>	2-D groundwater flow	FD	Steady-state, confined, leaky or unconfined flow in heterogeneous and anisotropic porous media. variable boundaries.	Franz, T., and Guiguer, N. Waterloo HydroGeologic Software
<b>FTWORK</b>	1, 2 and 3-D groundwater flow and solute transport	FD	Steady-state and transient flow in saturated media under confined and unconfined conditions. The model handles heterogeneities and anisotropy for flow.	Faust, C.R., et al. GeoTrans, Inc.
<b>GGU-SS FLOW2D</b> <b>GGU-TRANSIENT</b> <b>GGU-SS FLOW 3D</b>	2 -D groundwater flow  3 -D groundwater flow	FE	Steady state. Considerations of seepage lines and unsaturated zones apply. The transient state flow model. Steady state only.	GGU-Software
<b>Golder Groundwater Computer Package</b>	2 and 3-D groundwater flow and solute transport	FE	Steady-state or transient simulation, in anisotropic, heterogeneous, multi-layered aquifer systems, for confined, leaky-confined and unconfined flow problems.	Miller, I., and Marlon-Lambert, J. Golder Associates, Inc.
<b>HMS (SHM, THM, GHM, CGI)</b>	3-D hydrologic model system	FD	The sub-model GHM simulates saturated flow for confined-unconfined aquifers, restrictions on boundary conditions.	Yu, Z. Earth System Science Center, Penn State University
<b>HST3D*</b>	3-D groundwater flow, heat and solute transport	FD	Saturated groundwater flow, onfined or unconfined aquifer, heterogeneous and anisotropic with variable boundary conditions.	Kipp, J.K.L. USGS
<b>JDB2D/3D*</b>	2-D groundwater flow quasi-3D flow	FD	2D, single-aquifer (JDB2D) and quasi-3D, multi-aquifer (JDB3D), transient flow for confined and leaky-confined aquifer systems.	Bredehoeft, J.D. USGS
<b>MARS</b>	2 or 3-D groundwater flow and solute transport	FE	Multiphase flow in unconfined heterogeneous, anisotropic aquifers, in saurated or unsaturated zones.	Scientific Software Group
<b>MicroFEM</b>	2-D groundwater flow	FE	Confined, leaky and unconfined conditions, heterogeneous aquifers and aquitards steady-state and transient flow, anisotropic aquifers, spatially and temporally - varying wells and boundary conditions, Precipitation, evaporation, drain, rivers, saturated single-density flow, multiple-aquifer systems and stratified aquifers.	Hemker, C J and Boer, R.G. Scientific Software Group
<b>MikeSHE</b>	2 or 3-D groundwater flow and hydrologic processes	FD	Saturated/unsaturated zones, heterogeneous and isotropic media, steady/unsteady state confined/unconfined aquifer, variables boundary conditions, link to surface water models.	DHI Software
<b>MODFE*</b>	2-D groundwater flow	FE	Transient or steady state conditions; nonhomogeneous and anisotropic flow, confined and unconfined, the three types of boundary conditions.	Torak, L.J., et al. USGS
<b>MODFLOW*</b>	3-D groundwater flow	FD	Transient or steady state conditions; nonhomogeneous and anisotropic flow, confined and unconfined, variable boundary conditions.	McDonald, M.G., and Harbaugh, A.W. USGS
<b>MOFAT*</b>	2-D groundwater flow and solute transport	FE	Multiphase flow in variably-saturated porous media, heterogeneous, anisotropic porous media, boundary type 1 and 2 can be simulated.	Katyal. A.K., et al. USEPA
<b>MOTIF</b>	1, 2 or 3-D groundwater flow, heat and solute transport	FE	Variably saturated flow in fractured, deformable or porous media, steady/transient state, heterogeneous and anisotropic media.	Guvanasen V., et al. Atomic Energy of Canada, Ltd.
<b>MOVER</b>	2-D groundwater flow	FE	Multiphase flow, saturated/unsaturated zones, heterogeneous, anisotropic porous or fractured flow systems, with specified head and flux conditions and source/sink.	Scientific Software Group

Name of Software	Model Description/ Process simulations	Type of solution	Site Conditions for Model Application	References/ Sources
<b>PLASM</b>	2-D groundwater flow	FD	Nonsteady flow of ground-water in heterogeneous anisotropic aquifers under water table, nonleaky, and leaky confined conditions, Includ pumpage from wells.	Prickett, T.A., and Lonquist, C.G. Thomas A. Prickett & Associates, Inc.
<b>PORFLOW</b>	2 or 3-D groundwater flow, heat and mass transport	FV	Multiphase fluid flow, variably saturated, fractured or porous media, anisotropic and heterogeneous, arbitrary sources of sinks and varied boundary conditions	Runchal, A.K. Analytic & computational research Inc.
<b>ROCKFLOW*</b>	2-D groundwater flow heat and mass transport	FE	Variable density flow, porous or fractured media, confined/unconfined aquifers, anisotropy and heterogeneity, variable boundary conditions.	Krohn, K.P., et al. Institute of Fluid Mechanics, Hannover.
<b>SEEP2D</b>	2-D groundwater flow	FE	A steady state, confined or unconfined, saturated and unsaturated flow model with non-homogeneous and anisotropic soil. It is designed to compute seepage on profile models.	Tracy, F. USACE
<b>SEEP/W</b>	2-D groundwater flow	FE	Saturated/unsaturated conditions, steady/transient state flow, wells, a variety of boundary conditions, confined/phreatic heterogeneity and anisotropy may be analysed.	Krahn, J., et al. GeoSlope International, Inc.
<b>SUTRA*</b>	2 and 3-D groundwater flow, solute or energy transport	FE and IFD	Saturated/unsaturated, constant or variable-density fluid flow, steady-state or transient flow, variables flowboundary conditions.	Voss, C.I., USGS
<b>SWICHA</b>	3-D groundwater flow and solute transport	FE	Simulates variable density fluid flow and solute transport processes in fully-saturated porous media, steady-state or transient field problems.	Huyakorn, P.S., et al. GeoTrans, Inc.
<b>SWIFT</b>	3-D groundwater flow and transport	FD	Flow and transport of fluid, heat, brine, and radionuclide chains in porous and fractured geologic media. Heterogeneity, anisotropy and a variety of boundary condition and sources may be modeled.	Cranwell, R.M., et al. GeoTrans, Inc.
<b>TARGET</b>	2, 3-D groundwater flow and chemical-species transport	IFD	2-D confined/unconfined, transient ground-water flow, 3-D saturated, density coupled, transient ground-water flow.	Sharma, D., et al. IGWMC
<b>VS2DT</b>	1 and 2-D groundwater flow and solute transport	FD	Variable saturated flow, confined/unconfined aquifers, anisotropy and heterogeneity may be modeled, varied boundary conditions.	Healy, R.W. USGS

\* can be found in a public domain version

**USEPA** United State Environment Protection Agency  
**USNRC** United State Nuclear Regulatory Commission  
**USACE** United State Army Corps of Engineers  
**USDOE** United State Department of Energy  
**IGWMC** International Ground Water Modeling Center

## **APPENDIX B**

Table B.1 Current MODFLOW compatible pre and post-processors (February 2003).

	Description	Developer	Web Reference
<b>Pre-processors</b>			
<b>MapIt</b>	A software tool that rapidly produces code specific flow and transport modeling (ex. MODFLOW, MT3D) input files. It can read a variety of model independent 1, 2 and 3-D data sources, provides interpolation and extrapolation control, as well as extensive mesh editing capabilities with an easy-to-use graphical interface.	Lawrence Livermore National Laboratory, USA.	<a href="http://www.llnl.gov">http://www.llnl.gov</a>
<b>MFI2K*</b>	A data input programme for MODFLOW-2000 and MODPATH. Data are entered interactively through a series of display screens.	USGS	<a href="http://water.usgs.gov/">http://water.usgs.gov/</a>
<b>MODELGIS</b>	A menu-driven GIS-based interface for MODFLOW running on Unix workstations, which helps to prepare data sets with separate menus for each of the MODFLOW packages.	HIS GeoTrans, USA.	<a href="http://www.hsigeotrans.com">http://www.hsigeotrans.com</a>
<b>MODLMAKR</b>	A graphical interactive pre-processor for flow and solute transport models (MODFLOW and MOC).	Microcode Inc. USA.	NA
<b>MODPORT</b>	A graphical-based pre-processor for MODFLOW. It uses two different screens ( the foreground and background) to modify existing arrays of data and to build MODFLOW input files.	SDI Environmental Services, Inc. USA.	<a href="http://www.isgw.com/modport.html">http://www.isgw.com/modport.html</a>
<b>PREMOD</b>	An interactive user friendly programme used to create new input data files and editing existing ones for MODFLOW. Array data entry is facilitated by six different algorithms that eliminate repetitive data	IGWMC, USA.	<a href="http://typhoon.mines.edu/software/igwmcsoft/">http://typhoon.mines.edu/software/igwmcsoft/</a>
<b>RADMOD*</b>	A pre-processor to the programme MODFLOW for simulation of axisymmetric problems, calculating the conductances and storage capacity.	USGS	<a href="http://water.usgs.gov/">http://water.usgs.gov/</a>
<b>Post-processors</b>			
<b>3D Groundwater Explorer (or 3D Master Explorer)</b>	A software that provides three-dimensional visualization and animation of data from groundwater flow and transport models. It uses MODFLOW 88/96/2000 input files or models created by PMWIN.	Scientific Software Group, USA.	<a href="http://www.scisoftware.com">http://www.scisoftware.com</a>
<b>CONTOUR*</b>	A basic contouring programme for gridded data designed for use with finite difference models. It can use as input data formatted data from most models or unformatted data from MODFLOW.	USGS	<a href="http://water.usgs.gov/">http://water.usgs.gov/</a>
<b>GW_Chart*</b>	A utility programme developed in conjunction with the MODFLOW-GUI and is used for postprocessing of the output of MODFLOW creating specialized graphs (calibration plots, water budget plots, hydrographs, lake plots and piper diagrams).	USGS	<a href="http://water.usgs.gov/">http://water.usgs.gov/</a>
<b>GMPP (Groundwater Modeler's Productivity Pak )</b>	A programme that converts MODFLOW, SUTRA and MOC output to a variety of file formats for graphical display of model results.	Saguaro Software Inc. USA.	<a href="http://www.saguarosoft.com">http://www.saguarosoft.com</a>
<b>Model Viewer*</b>	A computer programme that displays the results of 3-D groundwater models (including MODFLOW). It can display colorful isosurfaces, vectors, pathlines, cells or nodes that represent model features, auxiliary graphical objects, and animation.	USGS	<a href="http://water.usgs.gov/">http://water.usgs.gov/</a>
<b>MODPATH* and MODPATH-PLOT*</b>	A particle-tracking post-processor model for MODFLOW which computes 3D flow paths and MODPATH-PLOT displays results graphically.	USGS	<a href="http://water.usgs.gov/">http://water.usgs.gov/</a>
<b>MODTOOLS*</b>	A set of computer programmes that translates data arrays input to or output by a MODFLOW simulation, and data from MODPATH into the GIS software ARC/INFO.	USGS	<a href="http://water.usgs.gov/">http://water.usgs.gov/</a>

<b>PATH3D</b>	A general particle tracking programme for calculating groundwater flow paths and travel times using input and resulting head files solution of MODFLOW. It is a DOS-based code with a menu-driven shell.	S.S. Papadopoulos & Associates, Inc. USA	<a href="http://www.sspa.com/products/Path3d.htm">http://www.sspa.com/products/Path3d.htm</a>
<b>pmod_ada*</b>	A MODFLOW post-processor added to MT3D software package. It creates 2D head/drawdown ASCII files using the binary output from MODFLOW. The resulting files can be used in SURFER or any software for contour plots.	USEPA	<a href="http://www.epa.gov/ada/csmos.html">http://www.epa.gov/ada/csmos.html</a>
<b>POSTMOD</b>	A MODFLOW post-processor that reformats the model output of head, drawdown, and cell-by-cell flow terms. The reformatted output is compatible with graphical contouring packages such as	IGWMC, USA.	<a href="http://typhoon.mines.edu/software/igwmcsoft/">http://typhoon.mines.edu/software/igwmcsoft/</a>
<b>Visual Groundwater</b>	A graphical tools for 3-D visualization, animation and interpretation of site characterization data and modeling results. It provides a direct import of Visual MODFLOW groundwater modeling projects. SURFER.	Waterloo Hydrogeologic, Inc. Canada.	<a href="http://www.flowpath.com/">http://www.flowpath.com/</a>
<b>ZONEBDGT*</b>	A post-processor to calculate subregional water budgets from MODFLOW simulation results. A separate budget is computed for each user-specified zone.	USGS	<a href="http://water.usgs.gov/">http://water.usgs.gov/</a>
<b>Pre and post-processors</b>			
<b>CADSHLL</b>	AutoCAD-based graphical pre-processor and post-processor for the simulation programmes MODFLOW, MODPATH and MT3D.	IHU GmbH, Germany	<a href="http://www.ihu-gmbh.com">http://www.ihu-gmbh.com</a>
<b>Graphic Groundwater *</b>	A graphical interface for MODFLOW and MODPATH wich simplifies model development and data input, helps to develop maps and diagrams, and provides graphic and text files which can be processed outside Graphic Groundwater.	Southern Illinois University, USA	<a href="http://bear.geo.siu.edu/">http://bear.geo.siu.edu/</a>
<b>Groundwater Data Utilities</b>	A set of nearly 40 programs designed for data preparation, translation and formatting tasks required in groundwater modeling and data analysis. It can be used with MODFLOW, PEST, and PMWIN, and for interfacing with countouring packages (ex. GRAPHER, SURFER).	Scientific Software Group, USA.	<a href="http://www.scisoftware.com">http://www.scisoftware.com</a>
<b>GW Modeler (GWM)</b>	An ArcView 3.1 extension that assists pre and post-processing for MODFLOW by creating and passing parameter input files to MODFLOW and interactively displays output.	University of Wyoming, USA.	<a href="http://www.wygisc.uwyo.edu/gwmodeler/">http://www.wygisc.uwyo.edu/gwmodeler/</a>
<b>ModelCad* and TMR Wizard*</b>	Pre- and post-processing capabilities for the groundwater flow and solute transport models MODFLOW, MODPATH, MT3D, and MODFLOWT. TMR Wizard is a telescopic mesh refinement programme for ModelCad.	Stonemont Solutions Inc. USA	<a href="http://www.hydrotrak.com">http://www.hydrotrak.com</a>
<b>MODFLOW-GUI*</b> (Graphical User Interface with Arqus ONE)	GIS -based pre and post-processor graphical-user interfaces for preparing MODFLOW-2000, MODFLOW-96, MOC3D, MODPATH, and ZONEBDGT input data and viewing model output for use within Argus Open Numerical Environments (Argus ONE).	USGS	<a href="http://water.usgs.gov/">http://water.usgs.gov/</a> <a href="http://www.argusone.com">http://www.argusone.com</a>
<b>MODFLOWwin32</b>	An advanced pre and post-processing version of MODFLOW developed specifically for Microsoft Windows (Win32s) and Windows NT.	Environmental Simulations, Inc. USA.	<a href="http://www.groundwatermodels.com/">http://www.groundwatermodels.com/</a>

<b>MODIME</b>	A user-friendly, DOS-based graphical interface for preparation of input files and analysis of simulation results for the MODFLOW, PATH3D and MT3D programs.	S.S. Papadopoulos & Associates, Inc. USA	<a href="http://www.sspa.com/products/Modime.htm">http://www.sspa.com/products/Modime.htm</a>
<b>MMSP</b> (Modular Model Statistical Processor)	A statistical pre- and post-processor for analyzing MODFLOW input data and output results. It allows to easily read data input to and output from the Modular Model, calculates descriptive statistics, generates histograms, performs logical tests, calculates data arrays, and calculates flow vectors for use in a graphical-display program.	USGS	<a href="http://ok.water.usgs.gov/abstracts/wrir89-4159.html">http://ok.water.usgs.gov/abstracts/wrir89-4159.html</a>
<b>PMDIS</b>	A countouring program that works with PMWIN, or independently, to assign cell values using Kriging or other interpolation (extrapolation) methods.	Scientific Software Group, USA.	<a href="http://www.scisoftware.com">http://www.scisoftware.com</a>

\* can be found in a public domain version

<b>IGWMC</b>	International Ground Water Modeling Center
<b>USEPA</b>	United State Environment Protection Agency
<b>USGS</b>	United State Geological Survey

Table B.2 Up-to-date MODFLOW related programmes (February 2003).

	Description	Developer	Web Reference
<b>Groundwater transport modelling</b>			
<b>BIOMOD 3-D</b>	A finite-element fate and multicomponent transport model that is linked to MODFLOW. It simulates convection, dispersion, diffusion, adsorption, desorption, and some microbial processes.	Draper Aden Environmental Modeling, Inc.	<a href="http://www.techstuff.com/draper.htm">http://www.techstuff.com/draper.htm</a>
<b>MF2K_GWT*</b>	An enhanced version of MODFLOW-2000 that incorporates the additional capability to simulate solute-transport processes (advection, hydrodynamic dispersion, retardation, decay, matrix diffusion, and mixing with multiple fluid sources) based on MOC3D model.	USGS	<a href="http://water.usgs.gov/">http://water.usgs.gov/</a>
<b>MOC3D*</b> (with <b>ELLAM</b> algorithm)	A 3-D transport model that uses the method-of-characteristics to solve the transport equation on the basis of the hydraulic gradients computed with MODFLOW for a given time step. It also gives the alternative of using a finite volume Eulerian-Lagrangian localised adjoint method (ELLAM) to solve the transport equation.	USGS	<a href="http://water.usgs.gov/">http://water.usgs.gov/</a>
<b>MODFLOWT</b>	A contaminant transport model which is fully compatible with previous MODFLOW versions (88/96). It simulates advection, dispersion, adsorption and first-order decay using fully implicit finite difference method.	Hydrosolve, Inc. USA.	<a href="http://www.hydrosolveinc.com/">http://www.hydrosolveinc.com/</a>
<b>MT3DMS*</b> (Modular 3-D Transport packages)	A contaminant transport model that was developed for use with any block-centered finite-difference flow model such as MODFLOW. The simulated transport processes include advection, dispersion, diffusion, and single-species basic chemical reactions, with various types of boundary conditions and sources or sinks.	The University of Alabama, USA.	<a href="http://hydro.geo.ua.edu/mt3d/">http://hydro.geo.ua.edu/mt3d/</a>
<b>RT3D</b> (Reactive Transport in 3-D)	An add-on MT3DMS bioremediation transport package for simulating 3D multi-species, reactive transport in groundwater. It can accommodate multiple sorbed and aqueous phase species with any reaction framework.	PNL, USA.	<a href="http://www.pnl.gov/">http://www.pnl.gov/</a>
<b>SEAM3D</b> (Sequential Electron Acceptor Model 3-D)	An add-on MT3DMS bioremediation transport package for modelling aerobic and sequential anaerobic biodegradation (includes biodegradation, NAPL dissolution, dechlorination and cometabolism packages).	Virginia Tech university, USA.	<a href="http://gms.watermodeling.org/html/seam3d.html">http://gms.watermodeling.org/html/seam3d.html</a>
<b>Variable density flow modelling</b>			
<b>SEAWAT*</b>	A programme that combines MODFLOW and MT3DMS to simulate 3-D variable-density groundwater flow in porous media.	USGS	<a href="http://water.usgs.gov/">http://water.usgs.gov/</a>
<b>MODCALIF</b> (MODflow and CALibration with Front limitation)	A program based on MODFLOW and MT3D for modelling flow and density-dependent transport. It solves the equations according to the front limitation algorithm. It also performs parameter calibration using the sensitivity method, and is compatible with VISUAL MODFLOW.	Institute of Drilling Engineering and Fluid Mining, Germany.	<a href="http://www.tu-freiberg.de">http://www.tu-freiberg.de</a>
<b>Multiphase and unsaturated zone modelling</b>			
<b>AIR3D*</b>	An adaptation of MODFLOW code to simulate three dimensional air-flow induced through dry wells or trenches, as in vapor-extraction remediation caused by atmospheric-pressure variations in unsaturated zones.	USGS	<a href="http://water.usgs.gov/">http://water.usgs.gov/</a>
<b>MODAIR</b>	A software for modeling airflow in the unsaturated zone, including airflow to an extraction well. It is based on MODFLOW, AIRGEN, a preprocessor for preparing the input files for MODFLOW; and PMAIR, a post-processor to plot two-dimensional air-pressure distributions. Supported MODFLOW packages are BAS, BCF, WEL, CHD, SIP and output control utilities.	Scientific Software Group, USA.	<a href="http://www.scisoftware.com">http://www.scisoftware.com</a>
<b>P3DAIR</b>	It uses the input files and pressure solution of MODAIR to simulate air movement and the advective transport of vapor in unsaturated soils. It is particularly useful for delineating contaminant capture zones and evaluating the effectiveness of vapor extraction wells.		

Surface water/groundwater modelling				
<b>DAFLOW*</b>	An integrated surface water/groundwater model that couples the Diffusion Analogy Surface-water flow model to MODFLOW to compute water exchange between channel branches and aquifers.	USGS	<a href="http://water.usgs.gov/">http://water.usgs.gov/</a>	
<b>MODBRNCH*</b>	It is the coupled BRANCH (branch-network dynamic flow model) and MODFLOW-96 models to simulate surface and groundwater interactions, specifically open-channel/aquifer leakage.	USGS	<a href="http://water.usgs.gov/">http://water.usgs.gov/</a>	
<b>IHM</b> (Integrated Hydrologic Model)	An integrated surface water/ground water model which couples Hydrologic Simulation Programme–Fortran HSPF(version 12) and MODFLOW-96 to simulate the full hydrologic cycle.	INTERA , Inc. USA.	<a href="http://www.intera.com/">http://www.intera.com/</a>	
<b>MODHMS</b>	A MODFLOW-based integrated hydrologic model that includes additional modules to simulate overland flow, channel flow, and solute transport.	HydroGeoLogic, Inc. USA.	<a href="http://www.hgl.com">http://www.hgl.com</a>	
<b>MODNET</b>	A model that couples MODFLOW with UNET (Flow through a Full NETWORK of Open Channels model) developed by USACE. UNET is coupled with MODFLOW through channel bed flux interaction.	West Consultants, Inc.		
<b>MODRET</b> ( Model to design RETention ponds)	A program that calculates unsaturated and saturated infiltration losses from stormwater retention/detention ponds in unconfined shallow aquifers. The saturated infiltration is calculated using MODFLOW.	Scientific Software Group, USA.	<a href="http://www.scisoftware.com">http://www.scisoftware.com</a>	
Local/Regional groundwater modelling				
<b>MODTMR*</b>	A program for telescopic mesh refinement using MODFLOW. It allows construction of local-model data sets that specify perimeter boundary conditions of local models embedded within regional models constructed with MODFLOW-96.	USGS	<a href="http://water.usgs.gov/">http://water.usgs.gov/</a>	
<b>TMRDIFF*</b>	A program which provides a means of comparing computed head or drawdown in a local model and those in its corresponding area in the regional model.	USGS	<a href="http://water.usgs.gov/">http://water.usgs.gov/</a>	
<b>RIVGRID*</b>	A program to construct MODFLOW data sets for head-dependent boundaries (river, drain, general-head boundary , stream) using grid-independent data sets. It can also be used in applications of MODTMR.	USGS	<a href="http://water.usgs.gov/">http://water.usgs.gov/</a>	
<b>GFLOW2000*</b>	A groundwater flow model based on analytic element method and particularly suitable for modeling regional horizontal flow. It supports a MODFLOW-extract option to automatically generate MODFLOW files in a user defined area to facilitate detailed local flow modeling.	Haitjema Consulting, Inc. USA.	<a href="http://www.haitjema.com/">http://www.haitjema.com/</a>	
GIS linking				
<b>GW Modeler</b>	An ArcView 3.1 extension that was developed to assist pre-processing and post-processing for MODFLOW. It creates and passes parameter input files to MODFLOW and interactively displays output.	University of Wyoming, USA.	<a href="http://www.wygisc.uwyo.edu/gwmodeler/">http://www.wygisc.uwyo.edu/gwmodeler/</a>	
<b>MODFLOWARC*</b>	A modified version of MODFLOW which can read and write files used by a geographic information system .	USGS	<a href="http://oregon.usgs.gov/projs_dir/modflowarc/">http://oregon.usgs.gov/projs_dir/modflowarc/</a>	
<b>IDRISMOD</b>	A software that translates between regular images from IDRISI Geographical Information System files and MODFLOW array-images.	IGWMC, USA.	<a href="http://typhoon.mines.edu/software/igwmcsoft/">http://typhoon.mines.edu/software/igwmcsoft/</a>	
<b>MDR (MODFLOW Data Reader)</b>	An ArcView® GIS Software extension that imports MODFLOW input data sets into ArcView shape files. The optional version of the MDR can contour MODFLOW output data into lines and/or shaded model grid cells. The shape files created with the MDR are available for further processing in the ArcView Software environment.	GeoTrans, Inc. USA.	<a href="http://www.geotransinc.com">http://www.geotransinc.com</a>	

### Optimization, management and Remediation with MODFLOW

<b>AQMAN3D</b>	A mathematical programming system dataset generator for aquifer management using MODFLOW.	USGS	<a href="http://water.usgs.gov/">http://water.usgs.gov/</a>
<b>MODMAN*</b> (MODflow MANagement)	Adds optimization capability to MODFLOW-96. When it is used in conjunction with the Lindo® optimisation software, it can determine where pumping and injection wells should be located, and at what rate water should be extracted or injected at each well.	GeoTrans. Inc. USA.	<a href="http://www.geotransinc.com">http://www.geotransinc.com</a>
<b>ModGA</b>	A model for optimal design of groundwater hydraulic control and remediation systems under general field conditions. The model couples genetic algorithms technique with modflow and MT3D .	The University of Alabama, USA.	<a href="http://hydro.geo.ua.edu/mt3d/modga.htm">http://hydro.geo.ua.edu/ mt3d/modga.htm</a>
<b>ModGA_P</b>	The version of ModGA for aquifer parameter estimation.		
<b>ASAP</b> (Adaptive Simulated Annealing Package)	The software provides optimised engineering designs for surface water and groundwater management problems. It also combines MODFLOW and MT3DMS with artificial neural network (ANN) and adaptive simulated annealing (ASA) techniques for groundwater remedial design and water resource planning optimisation .	Waterstone Inc. USA.	<a href="http://www.waterstoneinc.com/">http://www.waterstoneinc. com/</a>
<b>MODOFC*</b>	It determines optimal pumping solutions for groundwater flow control problems by coupling MODFLOW simulation program with an internal implementation of the simplex algorithm.	University of Massachusetts, USA.	<a href="http://www.ecs.umass.edu/modofc/">http://www.ecs.umass.edu/ modofc/</a>
<b>Parameter estimation and calibration</b>			
<b>PEST-ASP*</b> (Advanced special parameterisation)	A parameter estimation software which can be used in both groundwater and surface water model calibration. It can be used to calibrate MODFLOW-2000 models for special complex situations.	Watermark Numerical Computing, Australia.	<a href="http://members.ozemail.com.au/">http://members.ozemail. com.au/</a>
<b>MODFLOW-ASP*</b>	A special version of MODFLOW-2000, modified for optimal use with PEST. It provides a MODFLOW2000-to-PEST translator which converts input dataset for MODFLOW-2000's PES process to a MODFLOW/PEST input dataset.		<a href="http://www.sspa.com/pest/">http://www.sspa.com/pest/</a>
<b>MODINV</b>	3-D transient inverse model which performs a non-linear weighted least squares parameter value optimisation for MODFLOW to modify parameters to obtain the best fit between observed and calculated heads.	Scientific Software Group, USA.	<a href="http://www.scisoftware.com">http://www.scisoftware.com</a>
<b>MODPUMP</b> (MODflow simulated PUMPing test)	A computer program that allows calculation of aquifer parameters for a single or multiple (up to three) layer aquifer systems by simulating field pumping test data using the MODFLOW model. The aquifer parameters are calculated by trial and error using graphical data matching techniques.	Scientific Software Group, USA.	<a href="http://www.scisoftware.com">http://www.scisoftware.com</a>
<b>UCODE*</b>	A general purpose parameter estimation utility using a modified Gauss-Newton method to minimise the objective function . Its interface in GMS can be used to perform automated parameter estimation for MODFLOW.	IGWMC, USA.	<a href="http://www.mines.edu/igwmc/">http://www.mines.edu/ igwmc/</a>

<b>MODFLOW-SURFACT</b>	An extension of MODFLOW capabilities for subsurface flow calculations and contaminant transport simulation accommodating up to 5 contaminant species in a simulation.	HydroGeoLogic, Inc. USA.	<a href="http://www.hgl.com">http://www.hgl.com</a>
<b>MS-VMS</b> (MODFLOW-SURFACT Visual Modeling System)	MODFLOW-SURFACT based ground-water flow and contaminant transport modeling system which provides a modeling environment for visual data preparation and interpretation using Groundwater Vistas, graphics and animations of model data and results using a Tecplot Interface (TIF).		
<b>PMWIN</b> (Processing MODFLOW)	A simulation system with graphical user interface for modeling groundwater flow and transport processes with MODFLOW2000, MT3D, MT3DMS, MOC3D, RT3D, PMPATH, PEST, and UCODE	Chiang, W.-H, and W. Kinzelbach	<a href="http://www.pmwin.net/">http://www.pmwin.net/</a>
<b>GMS</b> (Groundwater Modeling System)	A graphical user environment for numerical subsurface flow and contaminant transport modeling. It supports FEMWATER, MODFLOW2000, MODPATH, MT3D, RT3D, ART3D (analytical multi-species reactive transport model), SEAM 3D, NUFT(Nonisothermal, Unsaturated Flow and Transport model), UTCHEM* (multi-phase flow and transport model), FACT (subsurface flow and contaminant transport model), SEEP2D, PEST and UCODE codes.	DOD, USA.	<a href="http://chl.wes.army.mil/software/gms/stochastic.htm">http://chl.wes.army.mil/ software/gms/stochastic.htm</a> <a href="http://www.emrl.byu.edu/gms.htm">http://www.emrl.byu.edu/ gms.htm</a> <a href="http://www.ems-i.com/">http://www.ems-i.com/</a>
<b>Visual MODFLOW</b>	A modeling platform designed for groundwater flow and contaminant transport modeling using MODFLOW, MODPATH, and MT3DMS and RT3D programs. Professional version includes parameter estimation with winPEST, more graphical capabilities with 3-D explorer, and support for MODFLOW-SURFACT programme.	Waterloo Hydrogeologic, Inc. Canada.	<a href="http://www.flowpath.com/">http://www.flowpath.com/</a>
<b>Groundwater Vistas</b>	A Windows graphical user interface and modeling environment for MODFLOW2000, MT3D99, GFLOW, MODPATH, MT3DMS, RT3D, PATH3D, MODFLOWT, MODFLOW-SURFACT, PEST ASP, MODOFC, and UCODE. Advanced version of the software allows risk assesment using Monte Carlo versions of MODFLOW (Stochastic MODFLOW), MODPATH and MT3D.	Environmental Simulations, Inc. USA.	<a href="http://www.groundwater-vistas.com/">http://www.groundwater- vistas.com/</a> <a href="http://www.esinternational.com">http://www.esinternational. com</a>
<b>MIKE SHE</b>	An integrated modeling environment for simulating major hydrological processes of the land phase (saturated /unsaturated flow, channel flow, overland flow, solute transport, particle tracking, geo-chemistry, micro-biology). It supports MODFLOW2000 and MODFLOW-SURFACT.	DHI Software Danemark	<a href="http://www.dhisoftware.com/mikeshe/">http://www.dhisoftware.com /mikeshe/</a>

\* can be found in a public domain or freeware version

<b>DOD</b>	United State Department of Defense
<b>IGWMC</b>	International Ground Water Modeling Center
<b>PNL</b>	Battelle Pacific Northwest National Laboratory
<b>USACE</b>	United State Army Corps of Engineers
<b>USGS</b>	United State Geological Survey

# **APPENDIX C**

---

**MODFLOW FUNCTIONALITY DESCRIPTION**


---

MODEL NAME: MODFLOW-2000  
 VERSION: 1.15.01  
 RELEASE DATE: April 2005

AUTHOR(S): Harbaugh, et al.  
 INSTITUTION OF DEVELOPMENT: U.S. Geological Survey

CONTACT ADDRESS: U.S.G.S Office of Ground Water, Reston, VA  
 PHONE: (703) 648-5615  
 FAX: (703) 648-5644

PROGRAMME LANGUAGE: FORTRAN77  
 COMPUTER PLATFORM (S): DOS, UNIX,

LEGAL STATUS: Public domain  
 PREPROCESSING OPTIONS: Not included

POSTPROCESSING FACILITIES: RESAN-2000, YCINT-2000, BEAL-2000

---

**MODEL TYPE**

- |   |   |  |
|---|---|--|
| <input checked="" type="checkbox"/> single phase saturated flow                     | <input type="checkbox"/> parameter ID unsaturated flow (analytical/numerical) | <input type="checkbox"/> sediment transport            |
| <input type="checkbox"/> single phase unsaturated flow                              | <input type="checkbox"/> parameter ID solute transport (numerical)            | <input type="checkbox"/> surface water runoff          |
| <input type="checkbox"/> vapor flow/transport                                       | <input type="checkbox"/> aquifer test analysis                                | <input type="checkbox"/> stochastic simulation         |
| <input checked="" type="checkbox"/> solute transport                                | <input type="checkbox"/> tracer test analysis                                 | <input type="checkbox"/> geostatics                    |
| <input type="checkbox"/> virus transport  | <input type="checkbox"/> flow of water and steam                              | <input type="checkbox"/> multimedia exposure           |
| <input type="checkbox"/> heat transport   | <input type="checkbox"/> fresh/salt water interface                           | <input type="checkbox"/> pre-/postprocessing           |
| <input type="checkbox"/> matrix deformation   | <input type="checkbox"/> twophase flow three phase flow                       | <input type="checkbox"/> expert system                 |
| <input type="checkbox"/> geochemical  | <input type="checkbox"/> phase transfers                                      | <input type="checkbox"/> data base                     |
| <input type="checkbox"/> optimization   | <input type="checkbox"/> chemical transformations                             | <input type="checkbox"/> ranking/screening             |
| <input checked="" type="checkbox"/> groundwater and surface water hydraulics        | <input type="checkbox"/> biochemical transformations                          | <input checked="" type="checkbox"/> water budget       |
| <input checked="" type="checkbox"/> parameter ID saturated flow (inverse numerical) | <input type="checkbox"/> watershed runoff                                     | <input type="checkbox"/> heat budget                   |
|   |   | <input type="checkbox"/> chemical species mass balance |

**UNITS**

- |                                       |   |                                       |
|---------------------------------------|---|---------------------------------------|
| <input type="checkbox"/> SI system    | <input type="checkbox"/> US customary units               | <input type="checkbox"/> user-defined |
| <input type="checkbox"/> metric units | <input checked="" type="checkbox"/> any consistent system |                                       |

**PRIMARY USE**

- |                                    |   |   |
|------------------------------------|---|---|
| <input type="checkbox"/> research  | <input checked="" type="checkbox"/> general use | <input type="checkbox"/> policy-setting |
| <input type="checkbox"/> education | <input type="checkbox"/> site-dedicated         |   |
-

---

**GENERAL MODEL CHARACTERISTICS**


---

Parameter discretisation

- lumped
  - mass balance approach
  - transfer function (s)
- distributed
- deterministic
- stochastic

Spatial orientation

## saturated flow

- 1D horizontal
- 1D vertical
- 2D horizontal (areal)
- 2D vertical (cross-sectional profile)
- 2D axi-symmetric (horizontal flow only)
- fully 3D
- quasi-3D (layered; Dupuit approx.)
- 3D cylindrical or radial (flow defined in horizontal and vertical directions)

## unsaturated flow

- 1D horizontal
- 1D vertical
- 2D horizontal
- 2D vertical
- 2D axi-symmetric
- fully 3D
- 3D cylindrical or radial

Restart capability – types of updates possible

- dependent variables (e.g., head, concentration, temperature)
- fluxes
- velocities
- parameter values
- stress rates (pumping, recharge)
- boundary conditions

Discretisation in space

- no discretization
- uniform grid spacing
- variable grid spacing
- movable grid (relocation of nodes during run)
- maximum number of nodes/cells/elements
  - modifiable in source code (requires compilation)
  - modifiable through input
- maximum number of nodes (standard version):
- maximum number of cells/elements (standard Version):

## Possible cell shapes

- 1D linear
  - 1D curvilinear
  - 2D triangular
  - 2D curved triangular
  - 2D square
  - 2D rectangular
  - 2D quadrilateral
  - 2D curved quadrilateral
  - 2D polygon
  - 2D cylindrical
  - 3D cubic
  - 3D rectangular block
  - 3D hexaedral (6 sides)
  - 3D tetrahedral (4 sides)
  - 3D spherical
-

---

 FLOW SYSTEM CHARACTERISATION
 

---

## Saturated zone

## Hydrogeologic zoning

- confined
- semi-confined (leaky-confined)
- unconfined (phreatic)
- hydrodynamic approach
- hydraulic approach (Dupuit-Forcheimer assumption for horizontal flow)
- single aquifer
- single aquifer/aquitard system
- multiple aquifer/aquitard systems
- max. number of aquifers:
  - discontinuous aquifers (aquifer pinchout)
  - discontinuous aquitards (aquitard pinchout)
- storativity conversion in space (confined-unconfined)
- storativity conversion in time
- aquitard storativity

## Hydrogeologic medium

- porous medium
- fractured impermeable rock (fracture system, fracture network)
- discrete individual fractures
- equivalent fracture network approach
- equivalent porous medium approach
- dual porosity system (flow in fractures and optional in porous matrix, storage in porous matrix and exchange between fractures and porous matrix)
- uniform hydraulic properties (hydraulic conductivity, storativity)
- anisotropic hydraulic conductivity
- nonuniform hydraulic properties (heterogeneous)

## Flow characteristics

- single fluid, water
- single fluid, vapor
- single fluid, NAPL
- air and water flow
- water and steam flow
- moving fresh water and stagnant salt water
- moving fresh water and salt water
- water and NAPL
- water, vapor and NAPL
- incompressible fluid
- compressible fluid
- variable density
- variable viscosity
- linear laminar flow (Darcian flow)
- non-Darcian flow
- dewatering (desaturation of cells)
- dewatering (variable transmissivity)
- rewatering (resaturation of dry cells)
- delayed yield from storage

## Boundary conditions

- infinite domain
- semi-infinite domain
- regular bounded domain
- irregular bounded domain
- fixed head
- prescribed time-varying head
- zero flow (impermeable barrier)
- fixed cross-boundary flux
- prescribed time-varying cross-boundary flux
- cross-boundary flux
- areal recharge:
  - constant in space
  - variable in space
  - constant in time
  - variable in time

## Boundary conditions -continued

- induced recharge from or discharge to a source bed aquifer or a stream in direct contact with ground water
  - surface water stage constant in time
  - surface water stage variable in time
  - stream penetrating more than one aquifer
- induced recharge from a stream not in direct contact with groundwater
- evapotranspiration dependent on distance surface to water table
- drains (gaining only)
- free surface
- seepage face
- springs

## Sources/Sinks

- point sources/sinks (recharge/pumping wells)
    - constant flow rate
    - variable flow rate
    - head-specified
    - partially penetrating
    - well loss
    - block-to-radius correction
    - well-bore storage
    - multi-layer well
  - line source/sinks (internal drains)
    - constant flow rate
    - variable flow rate
    - head-specified
  - collector well (horizontal, radially extending screens)
  - mine shafts (vertical)
    - water-filled
    - partially-filled
  - mine drifts, tunnel (horizontal)
    - water-filled
    - partially filled
-

---

 FLOW SYSTEM CHARACTERISATION - continued
 

---

Dependent variable (s)

- |  |   |
|--|---|
| <input checked="" type="checkbox"/> head     | <input type="checkbox"/> potential        |
| <input checked="" type="checkbox"/> drawdown | <input type="checkbox"/> moisture content |
| <input type="checkbox"/> pressure            | <input type="checkbox"/> stream dunction  |
| <input type="checkbox"/> suction             | <input type="checkbox"/> velocity         |

Solution methods - Flow

- |  |  |
|--|--|
| <input type="checkbox"/> Analytical <ul style="list-style-type: none"> <li><input type="checkbox"/> single solution</li> <li><input type="checkbox"/> superposition</li> <li><input type="checkbox"/> method of images</li> </ul> <input type="checkbox"/> Analytic element method <ul style="list-style-type: none"> <li><input type="checkbox"/> point sources/sinks</li> <li><input type="checkbox"/> line sinks</li> <li><input type="checkbox"/> ponds</li> <li><input type="checkbox"/> uniform flow</li> <li><input type="checkbox"/> rainfall</li> <li><input type="checkbox"/> layering</li> <li><input type="checkbox"/> inhomogeneities</li> <li><input type="checkbox"/> doublets</li> <li><input type="checkbox"/> leakage through confining beds</li> </ul> <input type="checkbox"/> Semi-analytical <ul style="list-style-type: none"> <li><input type="checkbox"/> continuous in time, discrete in space</li> <li><input type="checkbox"/> continuous in space, discrete in time</li> <li><input type="checkbox"/> approximate analytical solution</li> </ul> <input type="checkbox"/> Solving stochastic pdes <ul style="list-style-type: none"> <li><input type="checkbox"/> Monte Carlo simulations</li> <li><input type="checkbox"/> spectral methods</li> <li><input type="checkbox"/> small perturbation expansion</li> <li><input type="checkbox"/> self-consistent or renormalization technique</li> </ul> | <input checked="" type="checkbox"/> Numerical<br><br>Spatial approximation <ul style="list-style-type: none"> <li><input checked="" type="checkbox"/> finite difference method             <ul style="list-style-type: none"> <li><input checked="" type="checkbox"/> block-centred</li> <li><input type="checkbox"/> node-centred</li> </ul> </li> <li><input type="checkbox"/> integrated finite difference method</li> <li><input type="checkbox"/> boundary elements method</li> <li><input type="checkbox"/> particle tracking</li> <li><input type="checkbox"/> pathline integration</li> <li><input type="checkbox"/> finite element method</li> </ul> Time-stepping scheme <ul style="list-style-type: none"> <li><input checked="" type="checkbox"/> fully implicit</li> <li><input type="checkbox"/> fully explicit</li> <li><input type="checkbox"/> Crank-Nicholson</li> </ul> Matrix-solving technique <ul style="list-style-type: none"> <li><input checked="" type="checkbox"/> Iterative             <ul style="list-style-type: none"> <li><input checked="" type="checkbox"/> SIP</li> <li><input type="checkbox"/> Gauss-Seidel (PSOR)</li> <li><input type="checkbox"/> LSOR</li> <li><input checked="" type="checkbox"/> SSOR</li> <li><input type="checkbox"/> BSOR</li> <li><input type="checkbox"/> ADIP</li> <li><input type="checkbox"/> Iterative ADIP (IADI)</li> <li><input type="checkbox"/> Predictor-corrector</li> </ul> </li> <li><input checked="" type="checkbox"/> Direct             <ul style="list-style-type: none"> <li><input checked="" type="checkbox"/> Gauss elimination</li> <li><input type="checkbox"/> Cholesky decomposition</li> <li><input type="checkbox"/> Frontal method</li> <li><input type="checkbox"/> Doolittle</li> <li><input type="checkbox"/> Thomas algorithm</li> </ul> </li> <li><input type="checkbox"/> Point Jacobi</li> </ul><br><input checked="" type="checkbox"/> Iterative methods for nonlinear equations <ul style="list-style-type: none"> <li><input checked="" type="checkbox"/> Picard method</li> <li><input type="checkbox"/> Newton-Raphson method</li> <li><input type="checkbox"/> Chord slope method</li> </ul> <input checked="" type="checkbox"/> Semi-iterative <ul style="list-style-type: none"> <li><input checked="" type="checkbox"/> conjugate-gradient</li> </ul> |
|--|--|
-

---

 FLOW SYSTEM CHARACTERISATION - continued
 

---

Inverse Modelling/Parameter Identification for flow
Parameters to be identified

- hydraulic conductivity
- transmissivity
- storativity/storage coefficient
- leakance/leakage factor
- areal recharge
- cross-boundary fluxes
- boundary heads
- pumping rates
- soil parameters/coefficients
- streambed resistance

User input

- prior information on parameter (s) to be identified
- constraints on parameters to be identified
- instability conditions
- non-uniqueness criteria
- regularity conditions

Parameter Identification method

- aquifer tests (based on analytical solutions)
- numerical inverse approach

Direct method (model parameters treated as dependent variable)

- energy dissipation method
- algebraic approach
- inductive method (direct integration of PDE)
- minimising norm of error flow (flatness criterion)
- linear programming (single- or multi-objective)
- quadratic programming
- matrix inversion
- Marquardt

Indirect method (iterative improvement of parameter estimates)

- linear least-squares
  - non-linear least-squares
  - quasi-linearization
  - linear programming
  - quadratic programming
  - steepest descent
  - conjugate gradient
  - non-linear regression (Gauss-Newton)
  - Newton-Raphson
  - influence coefficient
  - maximum likelihood
  - (co-) kriging
  - gradient search
  - decomposition and multi-level optimization
  - graphic curve matching
  - Marquardt algorithm
-

---

 FLOW SYSTEM CHARACTERISATION - continued
 

---

## Output Characteristics – Flow

## Echo of input (in ASCII text format)

- grid (nodal coordinates, cell size, element connectivity)
- initial heads/pressures/potentials
- initial moisture content/saturation
- soil parameters/function coefficients
- aquifer parameters
- flow boundary conditions
- flow stresses (e.g., recharge, pumping)

## Simulation results – form of output

- dependent variables in binary format
- complete results in ASCII text format
- spatial distribution of dependent variable for post-processing
- time-series of dependent variable for post-processing
- direct screen display – text
- direct screen display – graphics
- direct hardcopy (printer)
- direct plot (pen-plotter)
- graphic vector file
- graphic bitmap/pixel/raster file

## Simulation results – type of output

- head/pressure/potential
  - areal values (table, contours)
  - temporal series (table, x-t graphs)
- saturation/moisture content
  - areal values (table, contours)
  - temporal series (table, x-t graphs)
- head differential/drawdown
  - areal values (table, contours)
  - temporal series (table, x-t graphs)
- moisture content/saturation
  - areal values (table, contours)
  - temporal series (table, x-t graphs)

## Type of output – continued

- internal (cross-cell) fluxes
  - areal values (table, vector plots)
  - temporal series (table, x-t graphs)
- infiltration fluxes
  - areal values (table, vector plots)
  - temporal series (table, x-t graphs)
- evapo(transpi)ration fluxes
  - areal values (table, vector plots)
  - temporal series (table, x-t graphs)
- cross boundary fluxes
  - areal values (table, vector plots)
  - temporal series (table, x-t graphs)
- velocities
  - areal values (table, vector plots)
  - temporal series (table, x-t graphs)
- stream function values
- streamlines/pathlines (graphics)
- capture zone delineation (graphics)
- traveltimes (table of arrival times; tics on pathlines)
- isochrones (i.e., lines of equal travel times; graphics)
- position of interface (table, graphics)
- location of seepage faces
- water budget components
  - cell-by-cell
  - global (main components for total model area)
- calculated flow parameters
- uncertainty in results (i.e., statistical measures)

## Computational information

- iteration progress
  - iteration error
  - mass balance error
  - CPU time use
  - memory allocation
-

# Appendix D

## Data Input Instructions for GWFV

The finite volume simulation can be activated by introducing a new file type (Ftype) called "FV" in the MODFLOW name file to link to the GWFV name file.

The GWFV name file specifies the files to be used when simulating groundwater flow with the finite volume method. This file includes basically the same files as the MODFLOW name file, with exceptions in the Basic, Block Centered Flow and Output control files.

### GWFV Name File (GWFV)

FOR EACH SIMULATION

Data:            FTYPE            NUNIT            FNAME

FTYPE:           contains the same file type as in MODFLOW, except for the following character strings:

<b>BASFV</b>	new Basic input data for GWFV
<b>OCFV</b>	output for GWFV
<b>BCFV</b>	new Block Centered Flow input data for GWFV

**1-Input:**

All the input packages are similar to the ones used by the MODFLOWW GWF process , except for the discretisation file where input data DELR and DELC are no longer required. The input data that are needed instead are XV and YV, which refer to the vertices coordinates along the  $x$  and  $y$  directions respectively. The indexing notation  $(i,j,k)$  used in MODFLOW was kept the same, with the difference being the  $k$  index equal to 1 as one-unit layer was assumed at all of the model development steps. The array dimensions of the two new variables are also different from those removed outlined below:

DELR—is the cell width along rows. One value is read for each of the NCOL columns.

XV—is the  $x$ -coordinate of a vertex of the mesh. One value is read for each of the  $(NCOL+1) \times (NROW+1)$  vertices.

DELC—is the cell width along columns. One value is read for each of the NROW rows.

YV—is the  $y$ -coordinate of a vertex of the mesh. One value is read for each of the  $(NCOL+1) \times (NROW+1)$  vertices.

**2-Code:**

- The cell non-orthogonality has induced new expressions for calculating cell faces and volumes. DELR and DELC are no longer used in the programme, instead a new subroutine that accounts for the cell geometry has been added. The output of this subroutine was two face surfaces (vertical right-hand side face and horizontal lower face), the volume (the cell surface times unit vertical depth) and the node location  $(XN,YN)$  for each cell  $(i,j,1)$ . Consequently, appropriate changes were made to the subroutines calling variables DELR and DELC. The changes were executed in:

The GLO1BAS6 package to:

- allocate space for the new arrays (variable ISUM) (AL);
- read and prepare the XV and YV arrays,
- compute new cell entries (RP).

The GWF1BCF package to:

- compute equivalent permeabilities at cell faces (instead branch conductance) using the new formulation (SGWF1BCF6C in RP),
- add storage capacity conformingly to the new mathematical formulation through HCOF and RHS, (SGWF1BCF6N in FM),
- new subroutine to add the new finite volume decomposition - related terms on the RHS of Equation 4.31,
- print out node locations (XN,YN) (OT).

The GWFV1WEL6, GWF1RECH6 packages to:

- add recharge/discharge rates to RHS (FM).

The SIP5 package to:

- assign new formulae for the coefficients of Equation system 4.54 (i.e. B, D, F, G, H, E) (in AP).

### **3-Output:**

The indexing system used in MODFLOW is the only indication used when writing calculated heads at nodes in the LIST file or GLOBAL output files. As the grid used in MODFLOW is orthogonal, node locations can be easily deduced. In the GWFV model, this indexing system can still be used, but finding the node locations is no longer a simple task. Thus, the output procedure of the GWF1BCF package was changed to allow the user to print out the node locations if needed. UTL (ULAPRS for SGWF1BAS6H called from GWF1BAS6OT) package was changed.

# Bibliography

Abell, M.L., & Braselton, J.P., 1994. The Maple V Handbook. New York: AP Professional.

Ahmadi, A., Aigueperse, A., Quintard, M., 2001. Calculation of the Effective Properties Describing Active Dispersion in Porous Media: From Simple to Complex Unit Cells. *Advances in Water Resources* 24 (3-4), 423-438.

Alley, W.M., Emery, P.A., 1986. Groundwater Model of the Blue River Basin, Nebraska - Twenty Years Later. *Journal of Hydrology* 85 (3-4), 225-249.

American Society for Testing and Materials (ASTM), 1984. Standard Practices for Evaluating Environmental Fate Models of Chemicals. *Annual Book of ASTM Standards*, E978-84, American Society for Testing and Materials, Philadelphia, Pennsylvania.

American Society for Testing and Materials (ASTM), 1997. Standard Guide for Documenting a Ground-Water Modeling Code. *ASTM Book of Standards*, Vol. 04.09, D6171-97(2004), American Society for Testing and Materials, Philadelphia.

Amtec, 1999. Tecplot Mesh Generator, Version 1.0. User's Manual. Amtec Engineering, Inc., Bellevue, Washington, USA. <http://www.tecplot.com>

Anderson, M.P., Woessner, W.W., 1992. *Applied Groundwater Modeling: Simulation of Flow and Advective Transport*. Academic Press, San Diego.

Andersen, P.F., 1993. A Manual of Instructional Problems for the U.S.G.S. MODFLOW Model. EPA/600/R-93/010.

Appel, C.A., Reilly, T.E., 1994. Summary of Selected Computer Programs Produced by the U.S. Geological Survey for Simulation of Ground-Water Flow and Quality. U.S. Geological Survey Circular 1104.

Archer, R.A., 2000. Computing Flow and Pressure Transients in Heterogeneous Media Using Boundary Element Method. PhD thesis, Stanford university.

- Babu, D.K., 1976. Infiltration Analysis and Perturbation Methods, 2. Horizontal Absorption. *Water Resources Research* 12 (5), 1013-1018.
- Bakker, M., Kraemer, S.R., De Lange, W.J., Strack, O.D.L., 2000. Analytic Element Modeling of Coastal Aquifers. EPA/600/SR-99/110.
- Bakker, M., Strack, O.D.L., 2003. Analytic Elements for Multiaquifer Flow. *Journal of Hydrology* 271 (1-4), 119-129.
- Barrash, W., Dougherty, M.E., 1997. Modeling Axially Symmetric and Nonsymmetric Flow to a Well with MODFLOW, and Application to Goddard2 Well Test, Boise, Idaho. *Ground Water* 35 (4), 602-611.
- Basak, P., Murty, V.V.N., 1981. Groundwater Quality Improvement through Nonlinear Diffusion. *Journal of Hydrology* 53 (1-2), 151-159.
- Batelaan, O., De Smedt, F., Triest, L., 2003. Regional Groundwater Discharge: Phreatophyte Mapping, Groundwater Modelling and Impact Analysis of Land-Use Change. *Journal of Hydrology* 275 (1-2), 86-108.
- Bear, J., 1972. *Dynamics of Fluids in Porous Media*. American Elsevier, New York.
- Bear, J., 1979. *Hydraulics of Groundwater*. McGraw-Hill, New York, New York.
- Bear, J., Verruijt, A., 1987. *Modeling Groundwater Flow and Pollution*. D. Reidel Publishing Company, Dordrecht, Holland.
- Bedard, A.H., Day, M.J., Johnson, R.H., Ritter, K.J., Stancel, S.G., Thomson, J.A.M., 1997. Intrinsic Bioremediation Modeling to Support Superfund Site Closure. *Proceedings of the American Power Conference*, 59 (1), 536-540.
- Beljin, M.S., Murdoch, L., 1994. Analytical Models for Interceptor Trenches and Drains. GWMI 94-07, International Ground Water Center, Colorado School of Mines, Golden.
- Benett, D., Kontis, A.L., Lason, S.P., 1982. Representation of Multiaquifer Well Effects in Three-Dimensional Ground-Water Flow Simulation, *Ground Water* 20 (3), 334-341.
- Blum, V.S., Israel, S.M., Larson, S.P., 2001. Adapting MODFLOW to Simulate Water Movement in the Unsaturated Zone. *MODFLOW 2001 and Other Modeling Odysseys*, Proceeding, 60-65, Golden, Colorado.
- Boonstra, J., Kselik, R.A.L., 2001. SATEM 2002: Software for Aquifer Test Evaluation. International Institute for Land Reclamation and Improvement, ILRI publication 57, The Netherlands.
- Botte, G.G., Ritter, J.A., White, R.E., 2000. Comparison of Finite Difference and Control Volume Methods for Solving Differential Equations. *Computers and Chemical Engineering* 24 (12), 2633-2654.

Bouwer, H., 1989. Bouwer and Rice Slug Test - an Update. *Ground Water* 36 (3), 304-309.

Braun, C., Hassanizadeh, M., Helmig, R., 1998. Two-Phase Flow in Stratified Porous Media - Effective Parameters and Constitutive Relationships. *International Conference on Computational Methods in Water Resources, CMWR, Vol. 2*, 43-50.

Brebbia, C.A., 1980. *The Boundary Element Method for Engineers*. 2d ed., Pentech Press, London.

Brebbia, C.A., Wrobel, L.C., 1991. Review of Recent Advances of the Boundary Element Method in Water Resources. Meeting: Proceedings 2: *International Conference on Computational Methods in Water Resources*.

Bredehoeft, J.D., Betzinski, P., Villanueva, C.C., De Marsily, G., Konoplyantsev, A.A., Uzoma, J.U., 1982. *Ground-Water Models. Volume I. Concepts, Problems, and Methods of Analysis with Examples of their Application*. The Unesco Press, France.

Brown, P., Hindmarsh, A., Seager, M.K., 1992. Subroutine DSLUGM in the SLATEC Common Mathematical Library, version 4.1. [www.netlib.org/slatec/slatecsrc.tgz](http://www.netlib.org/slatec/slatecsrc.tgz).

Bumb, A.C., Mitchell, J.T., Gifford, S.K., 1997. Ground-Water Extraction/Reinjection System at a Superfund Site Using MODFLOW. *Ground Water* 35 (3), 400-408.

Burns, L.A., 1983. Validation of Exposure Models: The Role of Conceptual Verification, Sensitivity Analysis, and Alternative Hypotheses. In: *Sixth Symposium on Aquatic Toxicology and Hazard Assessment, STP 802*, American Society for Testing and Materials (ASTM), Philadelphia, Pennsylvania, 255-281.

Cai, Z., Jones, J.E., McCormick, S.F., Russell, T.F., 1997. Control-Volume Mixed Finite Element Methods. *Computational Geosciences* 1 (3-4), 289-315.

Capilla, J.E., Gomez-Hernandez, J.J., Sahuquillo, A., 1998. Stochastic Simulation of Transmissivity Fields Conditional to Both Transmissivity and Piezometric Head Data - 3. Application to the Culebra Formation at the Waste Isolation Pilot Plan (WIPP), New Mexico, USA. *Journal of Hydrology* 207 (3-4), 254-269.

Carrera, J., Melloni, G., 1987. *The Simulation of Solute Transport: An Approach Free of Numerical Dispersion*. SAND86-7095, Sandia National Laboratories, Albuquerque, NM.

Carslaw, H.S., Jaeger, J.C., 1959. *Conduction of Heat in Solids*. 2d ed., Oxford University Press, Oxford.

Castelli, F., 1996. Simplified Stochastic Model for Infiltration into a Heterogeneous Soil Forced by Random Precipitation. *Advances in Water Resources* 19 (3), 133-144.

- Celia, M.A., Russel, T.F., Herrera, I., Ewing, R.E., 1990. Eulerian-Lagrangian Localized Adjoint Method for the Advection-Diffusion Equation. *Advances in Water Resources*, 13 (4), 187-206.
- Chen, Z., Huang, G.H., Chakma, A., 2003. Hybrid Fuzzy-Stochastic Modeling Approach for Assessing Environmental Risks at Contaminated Groundwater Systems. *Journal of Environmental Engineering* 129 (1), 79-88.
- Cheng, A.H-D., Ouazar, D., 1993. Groundwater Flow. Chapter 8 of *Boundary Element Techniques in Geomechanics*. Edited by G.D. Manolis and T.G. Davies, Elsevier.
- Chow, P., Cross, M., Pericleous, K., 1996. A Natural Extension of the Conventional Finite Volume Method into Polygonal Unstructured Meshes for CFD Application. *Applied Mathematical Modelling* 20 (2), 170-183.
- Chowdhury, A. K. M. M., Canter, L.W., 1998. Expert Systems for Ground Water Management. *Journal of Environmental Systems* 26 (1), 89-110.
- Chung, T.J., 1978. *Finite Element Analysis in Fluid Dynamics*. McGraw-Hill, London.
- Connor, J. J., Brebbia. C.A., 1976. *Finite Element Techniques for Fluid Flow*. Newnes-Butterworths, London.
- Cooley, R.L., 1971. A Finite Difference Method for Variably Saturated Porous Media: Application to a Single Pumping Well. *Water Resources Research* 7 (6), 1607-1625.
- Courtois, N., Burghoffer, P., Gerbaux-Francois, O., Getto, D., 2000. Measurement of Groundwater Flow by the Dilution Method Using Dye Tracing Under Natural Hydraulic Gradient Conditions. *IAHS Publication (262)*, 219-224.
- Crank, J., 1956. *Mathematics of Diffusion*. Oxford University Press, New York and London.
- Croft, T.N., 1998. *Unstructured Mesh-Finite Volume Algorithms for Swirling, Turbulent, Reacting Flows*. Ph.D. Thesis, University of Greenwich, UK.
- De Lange, W.J., 1991. *A Groundwater Model of the Netherlands*. Report 90.066. National Institute for Inland Water Management and Waste Water Treatment (RIZA), Lelystad, the Netherlands.
- De Marsily, G., 1986. *Quantitative Hydrogeology: Groundwater Hydrology for Engineers*. Academic Press, Orlando, Florida.
- De Wiest, R.J.M., 1965. *Geohydrology*. John Wiley & Sons, New York.
- Di Giammarco, P., Todini, E., Lamberti, P., 1996. A Conservative Finite Elements Approach to Overland Flow: the Control Volume Finite Element Formulation. *Journal of Hydrology* 175 (1-4), 267-291.

- Digimap, 2004. University of Edinburgh. <http://www.edina.ac.uk/digimap/>
- Doherty, J., 2001. Improved Calculations for Dewatered Cells in MODFLOW, Ground Water 39 (6), 863-869.
- Driscoll, F.G., 1986. Groundwater and Wells. 2d ed., Johnson Division, St. Paul, Minnesota.
- Durlofsky, L.J., 1994. Accuracy of Mixed and Control Volume Finite Element Approximations to Darcy Velocity and Related Quantities. Water Resources Research 30 (4), 965-973.
- EasyMesh, University of Trieste. <http://www-dinma.univ.trieste.it/~nirftc/research/easymesh/>
- Edelman, J.H., 1972. Groundwater Hydraulics of Extensive Aquifers. Bulletin 13, International Institute for Land Reclamation and Improvement (ILRI), Wageningen, The Netherlands.
- El Harrouni, K., Ouazar, D., Walters, G.A., Cheng, A.H.D., 1996. Groundwater Optimization and Parameter Estimation by Genetic Algorithm and Dual Reciprocity Boundary Element Method. Engineering Analysis with Boundary Elements 18 (4), 287-296.
- Elmahi, I., Benkhaldoun, F., Vilsmeier, R., Gloth, O., Patschull, A., Hanel D., 1999. Finite Volume Simulation of a Droplet Flame Ignition on Unstructured Meshes. Journal of Computational and Applied Mathematics 103 (1), 187-205.
- ExCAL Limited, December 2001. Groundwater Flow and Contamination Transport Computer Model. ES1215/KKE.
- Faille, I., 1992. A Control Volume Method to Solve Elliptic Equation on a Two-Dimensional Irregular Mesh. Computer Methods in Applied Mechanics and Engineering, 100, 275-290.
- Ferguson, W.J., Turner, I.W., 1996. A Control Volume Finite Element Numerical Simulation of the Drying of Spruce. Journal of Computational Physics 125 (1), 59-70.
- Ferguson, W.J., 1998. The control volume finite element numerical solution technique applied to creep in softwoods. International Journal of Solids and Structures 35 (13), 1325-1338.
- Ferraresi, M., Marinelli, A., 1996. An Extended Formulation of the Integrated Finite Difference Method for Groundwater Flow and Transport. Journal of Hydrology 175 (1-4), 453-471.
- Fetter, C. W., 1994. Applied Hydrogeology. Englewood cliffs, New Jersey: Prentice-Hall, Inc.

Figueiredo, M.M., Pacheco, R.L., Lemos, J.M.P.F., 2000. Simultaneous Estimation of Transmissivity (or Conductivity), Storage Coefficient (or Porosity) and Effective Recharge, in a Stochastic Framework. IAHS Publication (International Association of Hydrological Sciences), 265, 124-130.

Fitts, C.R., Strack, O.D.L., 1996. Analytic Solutions for Unconfined Groundwater Flow over a Stepped Base. *Journal of Hydrology* 177 (1-2), 65-76.

Fletcher, C.A.J., 1984. *Computational Galerkin Methods*. Springer-Verlag New York.

Forsythe, G.E., Wasow, W.R., 1960. *Finite-Difference Methods for Partial Differential Equations*. John Wiley and Sons, New York.

Fredrick, K.C., Becker, M.W., Flewelling, D.M., Silavisesrith, W., Hart, E.R., 2004. Enhancement of Aquifer Vulnerability Indexing Using the Analytic-Element Method. *Environmental Geology* 45 (8), 1054-1061.

Freeze, G.A., Reeves, M., 1996. Deterministic Sensitivity Analysis Method to Aid Conceptual Model Development. IAHS Publication (International Association of Hydrological Sciences), 237, 503-510.

Frink, N.T., 1992. Upwind Scheme for Solving the Euler Equations on Unstructured Tetrahedral Meshes. *AIAA Journal* 30 (1), 70-77.

Fryar, A.E., Schwartz, F.W., 1998. Hydraulic-Conductivity Reduction, Reaction-Front Propagation, and Preferential Flow within a Model Reactive Barrier. *Journal of Contaminant Hydrology* 32 (3-4), 333-351.

Gau, H.S., Liu, C.W., 2000. Estimation of the Effective Precipitation Recharge Coefficient in an Unconfined Aquifer using Stochastic Analysis. *Hydrological Processes* 14 (4), 811-830.

Ghanem, R., Dham, S., 1998. Stochastic Finite Element Analysis for Multiphase Flow in Heterogeneous. *Transport in Porous Media* 32 (3), 239-262.

Geistlinger, H., Eisermann, D., Schirmer, M., Mayer, U., Clement, P., 2003. Development of New Modeling Tools for Simulating and Designing Reactive Gas Walls. *Groundwater Quality Modeling and Management Under Uncertainty: Proceedings of the Probabilistic Approaches and Groundwater Modeling Symposium*, Philadelphia, Pennsylvania, 192-203.

Geraghty and Miller Software Newsletter, 1992. Geraghty and Miller survey results 4(summer), pp. 1-2.

Giacobbo, F., Zio, E., Marseguerra, M., 2002. Solving the Inverse Problem of Parameter Estimation by Genetic Algorithms: The Case of a Groundwater Contaminant Transport Model. *Annals of Nuclear Energy* 29 (8), 967-981.

GIBB Report, January 1996. River TAWÉ Water Quality Study. J59345A.

Goode, D.J., Appel, C.A., 1992. Finite-Difference Interblock Transmissivity for Unconfined Aquifers and for Aquifers Having Smoothly Varying Transmissivity. U.S. Geological Survey Water-Resources Investigations Report 92-4124.

Gottardi, G., Venutelli, M., 1994. One-Dimensional Moving Finite-Element Model of Solute Transport. *Ground Water* 32 (4), 645-649.

Grannemann, N.G, Hunt, R.J., Nicholas, J.R., Reilly, T.E., Winter, T.C., 2000. The Importance of Ground Water in The Great Lakes Region. U.S. Geological Survey Water-Resources Investigation Report 00-4008.

Guan, J., Aral, M.M., 2004. Optimal Design of Groundwater Remediation Systems Using Fuzzy Set Theory. *Water Resources Research* 40 (1), 1-20.

Haitjema, H.M, 1995. Analytic Element Modeling of Groundwater Flow. Academic Press, San Diego.

Haitjema, H.M, Kelson, V.A., Luther, K.H., 2000. Analytic Element Modeling of Ground-Water Flow and High Performance Computing. U.S. Environmental Protection Agency, EPA/600/S-00/001.

Haitjema, H.M., Kelson, V.A., de Lange, W., 2001. Selecting MODFLOW Cell Sizes for Accurate Flow Fields. *Ground Water* 39 (6), 931-938.

Halford, K.J., Hanson, R.T., 2002. User Guide for the Drawdown-Limited, Multi-Node Well (MNW) Package for the U.S. Geological Survey's Modular Three-Dimensional Finite-Difference Ground-Water Flow Model, Versions MODFLOW-96 and MODFLOW-2000. U.S. Geological Survey Open-File Report 02-293.

Hall, H.P., 1955. An Investigation of Steady Flow Toward a Gravity Well. *La Houille Blanche* 10, 8-35.

Hantush, M.S., 1960. Modification of Theory of Leaky Aquifers. *Journal of Geophysical Research* 65, 3713-3725.

Harbaugh, A.W., 1995. Direct Solution Package Based on Alternating Diagonal Ordering for the U.S. Geological Survey Modular Finite-Difference Ground-Water Flow Model, U.S. Geological Survey Open-File Report 95-288.

Harbaugh, A.W., McDonald, M.G., 1996a. User's Documentation for MODFLOW-96, an Update to the U.S. Geological Survey Modular Finite-Difference Ground-Water Flow Model. U.S. Geological Survey Open-File Report 96-485.

Harbaugh, A.W., McDonald, M.G., 1996b. Programmer's Documentation for MODFLOW-96, an Update to the U.S. Geological Survey Modular Finite-Difference Ground-Water Flow Model. U.S. Geological Survey Open-File Report 96-486.

Harbaugh, A.W., Banta, E.R., Hill, M.C., McDonald, M.G., 2000. MODFLOW-2000, the U.S. Geological Survey Modular Ground-Water Model -- User Guide to Modularization Concepts and the Ground-Water Flow Process. U.S. Geological Survey Open-File Report 00-92.

Harbaugh, A.W., 2002. A Data Input Program (MFI2K) for the U.S. Geological Survey Modular Ground-Water Model (MODFLOW-2000). U.S. Geological Survey Open File Report 02-41.

Harter, T., and Yeh, T.C.J., 1998. Flow in Unsaturated Random Porous Media, Nonlinear Numerical Analysis and Comparison to Analytical Stochastic Models. *Advances in Water Resources* 22 (3), 257-272.

Haverkamp, R., Vauclin, M., Touma, J., Wierenga, P.J., Vauchaud, G., 1977. A Comparison of Numerical Simulation Models for One-Dimensional Infiltration. *Soil Science Society of America Journal* 41, 285-294.

He, C., Edwards, M.G., Durlofsky, L. J., 2002. Numerical Calculation of Equivalent Cell Permeability Tensors for General Quadrilateral Control Volumes, *Computational Geosciences* 6 (1), 29-47.

Heberton, C.I., Russel, T.F., Konikow, L.F., Hornberger, G.Z., 2000. A Three-Dimensional Finite Volume Eulerian-Lagrangian Localized Adjoint Method (ELLAM) for Solute-Transport Modeling. U.S. Geological Survey Water-Resources Investigations Report 00-4087.

Heebner, D., Toran, L., 2000. Sensitivity Analysis of Three-Dimensional Steady-State and Transient Spray Irrigation Models. *Ground Water* 38 (1), 20-28.

Hill, M.C., 1990. Preconditioned Conjugate-Gradient 2 (PCG2), a Computer Program for Solving Ground-Water Flow Equations. U.S. Geological Survey Water-Resources Investigations Report 90-4048.

Hill, M.C., Banta, E.R., Harbaugh, A.W., Anderman, E.R., 2000. MODFLOW-2000, the U.S. Geological Survey Modular Ground-Water Model -- User Guide to the Observation, Sensitivity, and Parameter-Estimation Processes and Three Post-Processing Programs. U.S. Geological Survey Open-File Report 00-184.

Hill, M.C., 2002. The U.S. Geological Survey Modular Ground-Water Flow Model. A MARGINS Education and Planning Workshop: Developing a Community Sediment Model. The Institute of Arctic and Alpine Research (INSTAAR), Boulder, Colorado.

Hirsch, C., 1988. Numerical Computation of Internal and External Flows. Volume 1: Fundamentals of numerical discretisation. John Wiley & Sons, Chichester.

Hoopes, J.A., Harleman, D.R.F., 1967. Waste Water Recharge and Dispersion in Porous Media. *ASCE Journal of the Hydraulics Division* 93 (HY5), 51-71.

- Huisman, L., 1972. *Ground-Water Recovery*. The McMillan Press Ltd., London.
- Hunt, B., 1983. *Mathematical Analysis of Groundwater Resources*. Butterworths, London.
- Hunt, R.J., Anderson, M.P., Kelson, V.A., 1998. Improving a Complex Finite-Difference Ground Water Flow Model Through the Use of an Analytic Element Screening Model. *Ground Water* 36 (6), 1011-1017.
- Hunt, R.J., Steuer, J.J., 2001. Evaluating the Effects of Urbanization and Land-Use Planning Using Ground-Water and Surface-Water Models. U.S.Geological Survey Fact Sheet FS-102-01.
- Hutson, J., Dillon, P.L., Miller, M., Fallowfield, H., 2002. The Potential of Riverbank Filtration for Drinking Water Supplies Relation to Microsystin Removal in Brackish Aquifers. *Journal of Hydrology* 266 (3-4), 209-221.
- Huyakorn, P.S., Pinder, G.F., 1983. *Computational Methods in Subsurface Flow*. Academic Press, New York.
- Hyman, J.M., Shashkov, M., 1999. Mimetic Discretizations for Maxwell's Equations. *Journal of Computational Physics* 151 (2), 881-909.
- Hyman, J., Shashkov, M., Steinberg, S., 2001. The Effect of Inner Products for Discrete Vector Fields on the Accuracy of Mimetic Finite Difference Methods. *Computers & Mathematics with Applications* 42 (12), 21527-1547.
- Hyman, J., Morel, J., Shashkov, M., Steinberg, S., 2002. Mimetic Finite Difference Methods for diffusion equations. *Computational Geosciences*, 6 (3-4), 333-352.
- Ilinca, C., Zhang, X.D., Trépanier, J.-Y., Camarero, R., 2000. A Comparison of Three Error Techniques for Finite-Volume Solutions of Compressible Flows. *Computer Methods in Applied Mechanics and Engineering* 189 (4), 1277-1294.
- Isaacs, L.T., Hunt, B., 1981. Integral Equation Formulation for Ground-Water Flow. *ASCE Journal the Hydraulics Division* 107 (10), 1197-1209.
- Ishaq, A.M., Ajward, M.H., 1993. Investigation of Chloroform Plumes in a Porous Media. Meeting: Proceedings of the Symposium on Engineering Hydrology, 970-976.
- Jasak, H., 1996. Error Analysis and Estimation for the Finite Volume Method with Applications to Fluid Flows. PhD Thesis, Mechanical Engineering Department, Imperial College of Science, Technology and Medicine.
- Jasak, H., Gosman, A.D., 2000. Automatic Resolution Control for The Finite Volume Method, Part 1: A-Posteriori Error Estimates. *Numerical Heat Transfer* 38 (3), 237-256.

- Jasak, H., Gosman, A.D., 2003. Element Residual Error Estimate for the Finite Volume Method.. *Computers and Fluids* 32 (2), 223-248.
- Javandel, L., Doughty, C., Tsang, C.F., 1984. *Ground Water Transport: Handbook of Mathematical Models*. Water Resources Monograph 10, American Geophysical Union, Washington, D.C.
- Jayantha, P.A., Turner, I.W., 2001(a). Generalised Finite Volume Strategies for Simulating Transport in Strongly Orthotropic Porous Media. *Australian & New Zealand Industrial and Applied Mathematics Journal* 44 (E), C443-C463.
- Jayantha, P.A., Turner, I.W., 2001(b). A Comparison of Gradient Approximations for Use in Finite-Volume Computational Models for two-Dimensional Diffusion Equations. *Numerical Heat Transfer, Part B* 40 (5), 376-390.
- Jayantha, P.A., Turner, I.W., 2003(a). A Second Order Finite Volume Technique for Simulating Transport in Anisotropic Media. *International Journal of Numerical Methods for Heat and Fluid Flow* 13 (1), 31-56.
- Jayantha, P.A., Turner, I.W., 2003(b). On the Use of Surface Interpolation Techniques in Generalised Finite Volume Strategies for Simulating Transport in Highly Anisotropic Porous Media. *Journal of Computational and Applied Mathematics* 152 (1-2), 199-216.
- Jayantha, P.A., Turner, I.W., 2005. Second Order Control-Volume Finite-Element Least-Squares Strategy for Simulating Diffusion in Strongly Anisotropic Media. *Journal of Computational Mathematics* 23 (1), 1-16.
- Jones, M.A., 1997. NCF: a Finite-Element Computer Program to Simulate Ground-Water Flow within the U.S. Geological Survey Modular Ground-Water Flow Model (MODFLOW). *Ground Water* 35 (4), 721-723.
- Jones N.L., Budge, T.J., Lemon, A.M., Zundel, A.K., 2002. Generating MODFLOW Grids from Boundary Representation Solid Models. *Ground Water* 40 (2), 194-200.
- Jones, N.L., Green, J.I., Walker, J.R., 2003. Stochastic Inverse Modeling for Capture Zone Analysis. *Groundwater Quality Modeling and Management Under Uncertainty: Proceedings of the Probabilistic Approaches and Groundwater Modeling Symposium*, Philadelphia, Pennsylvania, 1-12.
- Karakostas, C.Z., Manolis, G.D., 1998. Stochastic Boundary Element Solution Applied to Groundwater Flow. *Engineering Analysis with Boundary Elements* 21 (1), 9-21.
- Katsifarakis, K.L., Karpouzou, D.K., Theodossiou, N., 1999. Combined Use of BEM Genetic Algorithms in Groundwater Flow and Mass Transport Problems. *Engineering Analysis with Boundary Elements* 23 (7), 555-565.
- Kelson, V.A., 2002. Using MODFLOW as an Analytic Element Preprocessor. *The Geological Society of America, Denver Annual Meeting*, Paper No. 44-6.

- Kershaw, D.S., 1981. Differencing of the Diffusion Equation in Lagrangian Hydrodynamic Codes. *Journal of Computational Physics* 39, 375-395.
- Keys, W.S., MacCary, L.M., 1971. Application of Borehole Geophysics to Water-Resources Investigations. U.S. Geological Survey Techniques of Water-Resources Investigation, 02-E1, U.S. Government Printing Office, Washington DC.
- Kincaid, D.R., Respass, J.R., Young, D.M., Grimes, R.G., 19. Itpack 2c: A Fortran Package for Solving Large Sparse Linear Systems by Adaptive Accelerated Iterative Methods. <http://www.netlib.org/itpack/> or <http://www.ma.utexas.edu/CNA/ITPACK/>.
- Kinzelbach, W., 1986. Groundwater Modelling: an Introduction with Sample Programs in BASIC. Elsevier Science, Amsterdam.
- Kladias, M.P., Ruskauff, G. J., 1997. Implementing spatially variable anisotropy in MODFLOW. *Ground Water* 35 (2), 368-370.
- Konikow, L.F., Bredehoeft, J.D., 1992. Ground-Water Models Cannot be Validated. *Advances in Water Resources* 15 (1), 75-83.
- Krohelski, J.T., Anderson, M.P., Chung, K., 2002. Using High Hydraulic Conductivity Nodes to Simulate Seepage Lakes. *Ground Water* 40 (2). 117-122.
- LaGriT-Unstructured Finite Element Grid Generation for Geological Applications, Los Alamos National Laboratory. <http://www.t12.lanl.gov/~lagrit>.
- Lahrman, A., 1992. An Element Formulation for the Classical Finite Difference and Finite Volume Method Applied to Arbitrarily Shaped Domains. *International Journal for Numerical Methods in Engineering* 35 (4), 893-913.
- Lal Wasantha, A. M., 2000. Numerical Errors in Groundwater and Overland Flow Models. *Water Resources Research* 36 (5), 1237-1247.
- LaRue, J., Tyagi, A.K., 1998. Fate/Transport Modeling Using Fuzzy Numbers. *International Water Resources Engineering Conference - Proceedings*, 117-122.
- Leake S.A., Claar D.V., 1999. Procedures and Computer Programs for Telescopic Mesh Refinement Using MODFLOW. U.S. Geological Survey Open-File Report 99-238.
- Lemke, L.D., Barrack II, W.A., Abriola, L.M., Goovaerts, P., 2004. Matching Solute Breakthrough with Deterministic and Stochastic Aquifer Models. *Ground Water* 42 (6), 920-934.
- Li, L., Graham, W.D., 1998. Stochastic Analysis of Solute Transport in Heterogeneous Aquifers Subject to Spatially Random Recharge. *Journal of Hydrology* 206 (1-2), 16-38.
- Liggett, J.A., Liu, P.L.F., 1983. *The Boundary Integral Equation Method for Porous Media Flow*. Allen & Unwin, London.

- Liu, F., Jameson, A., 1993. Multigrid Navier-Stokes Calculations for Three-Dimensional Cascades. *AIAA Journal* 31 (10), 1785-1791.
- Loaiciga, Hugo A., Marino, Miguel A., 1987. Parameter Estimation in Groundwater: Classical, Bayesian, and Deterministic Assumptions and Their Impact on Management Policies. *Water Resources Research* 23 (6), 1027-1035.
- Lohman, S.W., 1972. *Ground-Water Hydraulics*. U.S. Geological Survey Professional Paper 708.
- Mac Neal, R.H., 1953. An Asymmetric Finite Difference Network. *Quarterly of Applied Mathematics* 2, 295-310.
- MacCormack, R.W., Paullay, A.J., 1972. Computational Efficiency Achieved by Time Splitting of Finite Difference Operators. AIAA Paper 72-154, San Diego.
- MacDonald, P.W., 1971. The Computation of Transonic Flow Through Two-Dimensional Gas Turbine Cascades. ASME Paper 71-GT-89.
- Manglik, A., Rai, S.N., Singh, V.S., 2004. Modelling of Aquifer Response to Time Varying Recharge and Pumping from Multiple Basins and Wells. *Journal of Hydrology* 292 (1-4), 23-29.
- Margolin, L.G., Shashkov, M., Smolarkiewicz, P.K., 2000. A Discrete Operator Calculus for Finite Difference Approximations. *Computer Methods in Applied Mechanics and Engineering* 187 (3-4), 365-383.
- Margolin, L.G., Shashkov, M., 2003. Second-Order Sign-Preserving Conservative Interpolation (Remapping) on General Grids. *Journal of Computational Physics* 184 (1), 266-298.
- Marino, M.A., and Luthin, J.N., 1982. *Seepage and Groundwater*. Elsevier Scientific, Oxford.
- Mathcad7, 1997. *User's Guide*. Cambridge: MathSoft Inc.
- Mazzia, A., Putti, M., 2002. Mixed-Finite Element and Finite Volume Discretization for Heavy Brine Simulations in Groundwater. *Journal of Computational and Applied Mathematics* 147(1), 191-213.
- McDonald, M.G., Harbaugh, A.W., 1984. A Modular Three-Dimensional Finite-Difference Ground-Water Flow Model. U.S. Geological Survey Open-File Report 83-875.
- McDonald, M.G., Harbaugh, A.W., 1988. A Modular Three-Dimensional Finite-Difference Ground-Water Flow Model. U.S. Geological Survey Techniques of Water-Resources Investigations, Book 6, Chap. A1.

McMahon, A., Heathcote, J., Carey, M., Erskine, A., 2001. Guide to Good Practice for the Development of Conceptual Models and Selection and Application of Mathematical Models of Contaminant Transport Processes in Subsurface. NC/99/38/2, National Groundwater & Contaminated Land Centre (NGWCL), Environment Agency, U.K.

Meerschaert, M.M., Tadjeran, C., 2004. Finite Difference approximations for fractional Advection-Dispersion Flow Equations. *Journal of Computational and Applied Mathematics* 172 (1), 65-77.

Mehl, S.E., Hill, M.C., 2001. MODFLOW-2000, the U.S. Geological Survey Modular Ground-Water Model -- User Guide to the LINK-AMG (LMG) Package for Solving Matrix Equations Using an Algebraic Multigrid Solver. U.S. Geological Survey Open-File Report 01-177.

Mehl, S., Hill, M.C., 2002. Development and Evaluation of a Local Grid Refinement Method for Block-Centered Finite-Difference Groundwater Models Using Shared Nodes. *Advances in Water Resources* 25 (5), 497-511.

Mehl, S., Hill, M.C., 2004. Three-Dimensional Local Grid Refinement Method for Block-Centered Finite-Difference Groundwater Models Using Iteratively Coupled Shared Nodes: a New Method of Interpolation and analysis of Errors. *Advances in Water Resources* 27 (9), 497-511.

Merritt, M.L., Konikow, L.F., 2000. Documentation of a Computer Program to Simulate Lake-Aquifer Interaction using the MODFLOW Ground-Water Flow Model and the MOC3D Solute-Transport Model. U.S. Geological Survey Water-Resources Investigations Report 00-4167.

Moltyaner, G. L., 1988. Approximate Analytical Method for Groundwater Modelling. Atomic Energy of Canada Limited (AECL), Report No. 9254.

Morel, J. E., Dendy, Jr., Hall, M. L., White, S. W., 1992. A Cell-Centered Lagrangian-Mesh Diffusion Differencing Scheme. *Journal of Computational Physics* 103 (2), 286-299.

Morel, J.E., Roberts, R. M., Shashkov, M. J., 1998. A Local Support-Operators Diffusion Discretization Scheme for Quadrilateral  $r$ - $z$  Meshes. *Journal of Computational Physics* 144 (1), 17-51.

Murthy, J.Y., Marthur, S.R., 1998. Computation of Anisotropic Conduction Using Unstructured Meshes. *Journal of Heat Transfer* 120 (3), 583-591.

Narasimhan, T.N. Witherspoon, P.A., 1976. An Integrated Finite Difference Method for Analyzing Fluid Flow in Porous Media. *Water Resources Research*, 12 (1), 57-64.

National Research Council, 1990. Ground Water Models: Scientific and Regulatory Applications. National Research Council Committee on Ground Water Modeling Assessment, Water Science and Technology Board, Commission on Physical Sciences, Mathematics, and Resources, National Research Council, Washington, D.C.

National Groundwater & contaminated Land Centre (NGWCL), 2001. Guidance on Assigning Values to Uncertain Parameters in Subsurface Analytical Contaminant Fate and Transport Models. NGWCLC Report NC/99/38/3, Environment Agency, U.K.

Neuman, S.P., 1984. Adaptive Eulerian-Lagrangian Finite Element Method for Advection-Dispersion. International Journal for Numerical Methods in Engineering, 20 (2), 321-337.

Neville, C.J., Tonkin, M.J., 2004. Modeling Multiaquifer Wells with MODFLOW. Ground Water 42 (6), 910-919.

Ollivier-Gooch, C.F., 1996. A New Class of ENO Schemes Based on Unlimited Data-Dependent Least-Squares Reconstruction. AIAA-34<sup>th</sup> Aerospace sciences meeting and exhibit, Reno, NV. AIAA paper 96-0887.

Osiensky, J. L., Williams, R. E., 1997. Potential Inaccuracies in MODFLOW Simulations Involving the SIP and SSOR Methods for Matrix Solution. Ground Water 35 (2), 229-232.

Osman, Y.Z, Bruen, M.P, 2002. Modelling Stream–Aquifer Seepage in an Alluvial Aquifer: an Improved Loosing-Stream Package for MODFLOW. Journal of Hydrology, 264 (1-4), 69-86.

Osnes, H., Langtangen, H.P., 1998. An Efficient Probabilistic Finite Element Method for Stochastic Groundwater Flow. Advances in Water Resources 22 (2), 185-195.

Oswald, S.E., Kinzelbach, W., 2000. Three-Dimensional Physical Model for Verification of Variable-Density Flow Codes. IAHS Publication (International Association of Hydrological Sciences) 265, 399-404.

Ouazar, D., Cheng, A.H.D., Kizamou, A.D., 1996. Object-Oriented Pumping-Test Expert System. Journal of Computing in Civil Engineering 10 (1), 4-9.

Papadopulos, I.S., 1965. Nonsteady Flow to a Well in an Infinite Anisotropic Aquifer. International Symposium on Hydrology of Fractured Rocks, Dubrovnic, Yugoslavia, Proceedings. International Association of Scientific Hydrology, Publication 73 (1), 21-31.

Patankar, S. V., 1980. Numerical Heat Transfer and Fluid Flow, Hemisphere, Washington, DC.

Peaceman, D., 1977. Fundamentals of Numerical Reservoir Simulation. Amsterdam: Elsevier Scientific Publishing Company.

- Pecher, R., Stanislav, J.F., 1997. Boundary Element Techniques in Petroleum Reservoir Simulation. *Journal of Petroleum Science & Engineering* 17 (3-4), 353-366.
- Pinder, G.F., Gray, W.G., 1977. *Finite Element Simulation in Surface and Subsurface Hydrology*. Academic Press, London.
- Polubarinova-Kochina, P.Y., 1962. *Theory of Groundwater Movement*. Princeton University Press, Princeton, New Jersey.
- Pruess, K., 1987. TOUGH User's Guide. Lawrence Berkeley Laboratory (LBL-20700) and Sandia National Laboratory (SAND86-7104) for the U.S. Nuclear Regulatory Commission (NUREG/CR-4645).
- Reed, J.A., 1980. Type Curves for Selected Problems of Flow to Wells in Confined Aquifers. *Techniques of Water Resources Investigations*, the U.S. Geological Survey, Book 3, Chapter B3.
- Remson, I., Hornberger, G.M., Molz, F.J., 1971. *Numerical Methods in Subsurface Hydrology*. Wiley, New York.
- Restrepo, J.I., Montoya, A.M., Obeysekera, J., 1998. Wetland Simulation Module for the MODFLOW Ground Water Model. *Ground Water* 36 (5), 764-770.
- Richardson, L.F., 1910. The Approximate Arithmetical Solution by Finite Differences of Physical Problems Involving Differential Equations with an Application to the Stresses in a Masonry Dam. *Phil. Trans. Royal Soc.*, A210, 307-357.
- Richtmeyer, R.D., Morton K.W., 1967. *Difference Methods for Initial Value Problems*. Interscience, New York.
- Robins, N.S., Rutter, H.K., Dumbleton, S., Peach, D.W., 2005. The Role of 3D Visualisation as Analytical Tool Preparatory to Numerical Modelling. *Journal of Hydrology* 301 (1-4), 287-295.
- Samani, N., Kompani-Zare, M., Barry, D.A., 2004. MODFLOW Equipped with a New Method for the Accurate Simulation of Axisymmetric Flow. *Advances in Water Resources* 27 (1), 31-45.
- Satish, M.G., Zhu, J., 1992. Stochastic Approach for Groundwater Flow in a Semiconfined Aquifer Subject to Random Boundary Conditions. *Advances in Water Resources* 15 (6), 329-339.
- Satish, M.G., Zhu, J., 1994. Stochastic Analysis of Ground-Water Flow in Semiconfined Aquifer. *Journal of Hydraulic Engineering* 120 (2), 147-168.
- Seager, M.L., 1988. SLAP, Sparse Linear Algebra Package 2.0. Lawrence Livermore National Laboratory, Livermore Computing Center, January 1986 Tentacle. <http://www.netlib.org/slap/index.html>

- Ségol, G., 1994. *Classic Groundwater Simulations: Proving and Improving Numerical Models*. PTR Prentice Hall, Englewood Cliffs, New Jersey 07632.
- Selroos, J.O., Walker, D.D., Strom, A., Gylling, B., Follin, S., 2002. Comparison of Alternative Modelling Approaches for Groundwater Flow in Fractured Rock. *Journal of Hydrology* 257 (1-4), 174-188.
- Sewa, R., Chauhan, H.S., 1987. Analytical and Experimental Solutions for Drainage of Sloping Lands with Time-Varying Recharge. *Water Resources Research*, 23 (6), 1090-1096.
- Shashkov, M. J., Steinberg, S., 1995. Support-Operator Finite-Difference Algorithms for General Elliptic Problems. *Journal of Computational Physics* 118 (1), 131-151.
- Shashkov, M. J., Steinberg, S., 1996. Solving Diffusion Equations with Rough Coefficients in Rough Grids. *Journal of Computational Physics* 129 (2), 383-405.
- Simmons, C.T., Fenstemaker, T.R., Sharp, J.M., 2001. Variable-Density Groundwater Flow and Solute Transport in Heterogeneous Porous Media: Approaches, Resolutions And Future Challenges. *Journal of Contaminant Hydrology* 52 (1-4), 245-275.
- Smith, G.D., 1965. *Numerical Solution of Partial Differential Equations*. Oxford University Press, London.
- Smith, B.F, McInne, L.C., Gropp, W.D., 1995. *PETSc 2.0 User Manual*. Argonne National Laboratory, Technical Report No. ANL-95/11. <http://www-unix.mcs.anl.gov/petsc/petsc-2/>
- Spitz, K., Moreno, J., 1996. *A Practical Guide to Groundwater and Solute Transport Modeling*. Wiley Interscience.
- Spitz, F.J., Nicholson, R.S., and Daryll, A.P., 2001. A Nested Rediscrretization Method to Improve Pathline Resolution by Eleminating Weak Sinks Representing Wells. *Ground Water* 39 (5), 778-785.
- Stamos, C.L., Izbicki, J.A., 2002. *Artificial Recharge Through a Thick, Heterogeneous Unsaturated Zone near an Intermittent Stream in the Western Part of the Mojave Desert, California*. U.S. Geological Survey Open-File Report 02-89.
- Strack, O.D.L., Haitjema, H.M., 1981(a). Modeling Double Aquifer Flow Using a Comprehensive Potential and Distributed Singularities - 1. Solution for Homogeneous Permeability. *Water Resources Research*, 17 (5), 1535-1549.
- Strack, O.D.L., Haitjema, H.M., 1981(b). Modeling Double Aquifer Flow Using a Comprehensive Potential and Distributed Singularities - 2. Solution for Inhomogeneous Permeabilities. *Water Resources Research*, 17 (5), 1551-1560.

- Strack, O.D.L., 1989. *Groundwater Mechanics*. Prentice Hall, Englewood Cliffs, New Jersey.
- Stüben, K., 1999. *Algebraic Multigrid (AMG): An Introduction with Applications*, GMD - Forschungszentrum Informationstechnik GmbH, GMD Report 70.
- Stüben, K., 2001. A review of Algebraic Multigrid. *Journal of Computational and Applied Mathematics* 128 (1-2), 281-309.
- Tannehill, J.C., Anderson, D.A., Pletcher, R.H., 1997. *Computational Fluid Mechanics and Heat Transfer*, 2nd ed., Taylor & Francis, London.
- Taylor, J.K., 1985. What is Quality Assurance. In: J.K Taylor and T.W. Stanley (eds.), *Quality Assurance for environmental measurements*, American Society for Testing and Materials (ASTM) special technical publication 867, 5-11.
- Theis, C.V., 1935. The Relation Between the Lowering of the Piezometric Surface and the Rate and Duration of Discharge of a Well Using Groundwater Storage. *Trans. Amer. Geophys. Union*, 16, 519-524.
- Todd, D.K., 1959. *Ground Water Hydrology*. John Wiley, New York.
- Tolikas, P.K., Sidiropoulos, E.G., Tzimopoulos, C.D., 1984. Simple Analytical Solution for the Boussinesq One-Dimensional Groundwater Flow Equations. *Water Resources Research*, 20 (1), 24-28.
- Toth, J., 1962. A Theory of Groundwater Motion in Small Drainage Basins in Central Alberta, Canada. *Journal of Geophysical Research* 67 (11), 4375-4387.
- Turkel, E., 1985. Accuracy of Schemes with Nonuniform Meshes for Compressible Fluid Flows. *Applied Numerical Mathematics* 2 (6), 529-550.
- Turner, I.W., Ferguson, W.J., 1995 (a). An Unstructured Mesh Cell-Centered Control Volume Method for Simulating Heat and Mass Transfer in Porous Media: Application to Softwood Drying, Part I: The isotropic model. *Applied Mathematical Modelling*, 19 (11), 654-667 .
- Turner, I.W., Ferguson, W. J., 1995 (b). An Unstructured Mesh Cell-Centered Control Volume Method for Simulating Heat and Mass Transfer in Porous Media: Application to Softwood Drying - part II: the Anisotropic Model. *Applied Mathematical Modelling*, 19 (11), 668-674.
- Turner, J.R., Volker, R.E., Demetriou, C., Johnston, A.J., 1994. Simulation of Variable Density Flow and Contaminant Transport in Two and Three Dimensions. *National Conference Publication - Institution of Engineers, Australia*, 2(B), 4/14, 755-758.

- U.S. Environmental Protection Agency (USEPA), 1993. *Compilation of Ground-Water Models*. EPA/600/SR-93/118, Environmental Research Laboratory, U.S. Environmental Protection Agency, Ada, Oklahoma.
- U.S. Environmental Protection Agency (USEPA), 1994. *A Technical Guide to Ground-Water Model Selection at Sites Contaminated with Radioactive Substances*. EPA/402/R-94/012, Office of Solid Waste and Emergency Response, U.S. Environmental Protection Agency, Washington, D.C.
- Van der Heijde, P.K.M., and Elnawawy, O.A., 1992. *Quality Assurance and Quality Control in the Development and Application of Ground-Water Models*. EPA/600/R-93/011, Office of Research and Development, U.S. Environmental Protection Agency, Washington, D.C.
- Van der Heijde, P.K.M., 1996. *Compilation of Saturated and Unsaturated Zone Modeling Software*. EPA/600/SR-96/009, National Risk Management Research Laboratory, Ada: U.S. Environmental Protection Agency.
- Van der Heijde, P. K.M., Kanzer, D.A., 1997. *Ground-Water Model Testing: Systematic Evaluation and Testing of Code Functionality and Performance*. EPA/600/R-97/007, National Risk Management Research Laboratory, Ada: U.S. Environmental Protection Agency.
- Van der Veer, P., 1994. *Exact Solutions for Two-Dimensional Ground Water Flow in a Semiconfined Aquifer*. *Journal of Hydrology*, 156 (1-4), 91-99.
- Varga, R.S., 1962. *Matrix Iterative Analysis*. Prentice Hall, Englewood Cliffs, New Jersey.
- Versteeg, H. K., Malalasekera, W., 1995. *An Introduction to Computational Fluid Dynamics*. Longman, London.
- Voss, C.I., 1984. *A Finite-Element Simulation Model for Saturated- Unsaturated, Fluid-Density-Dependent Ground-Water Flow with Energy Transport or Chemically-Reactive Single-Species Solute Transport*. U.S. Geological Survey Water-Resources Investigations Report 84-4369.
- Walton, W.C., 1962. *Selected Analytical Methods for Well and Aquifer Evaluation*. *Illinois State Water Survey Bull.*, 49-81.
- Walton, W.C., 1970. *Groundwater Resource Evaluation*. McGraw-Hill, New York.
- Walton, W.C., 1987. *Groundwater Pumping Tests. Design and Analysis*. Lewis Publishers, National Water Well Association Chelsea, MI. Dublin, OH.
- Walton. W.C., 1989. *Analytical Groundwater Modeling. Flow and Contaminant Migration* Mich. Lewis, Chelsea.

- Wang, H.F., Anderson, M.P., 1982. Introduction to Ground Water Modeling: Finite Difference and Finite Element Methods. W.H. Freeman, San Francisco, California.
- Wang, M., Zheng, C., 1997. Optimal Remediation Policy Selection under General Conditions. *Ground Water* 35 (5), 757-764.
- Wang S.Y., Alonso C.V., Brebbia C.A., Gray W.G. and G.F. Pinder, 1980. Finite Elements in Water Resources. Proceedings of the Third International Conference on Finite Elements in Water Resource. School of Engineering, the University of Mississippi, U.S.A.
- Wang, X., 1997. Conceptual Design of a System for Selecting Appropriate Groundwater Models in Groundwater Protection Programs. *Environmental Management* 21 (4), 607-615.
- Wasantha Lal, A. M., 1998. Weighted Implicit Finite-Volume Model for Overland Flow. *Journal of Hydraulic Engineering* 124 (9), 941-950.
- Wilson, J.D., Naff, R.L., 2004. MODFLOW-2000, The U.S. Geological Survey Modular Ground-Water Model – GMG Linear Equation Solver Package Documentation. U.S. Geological Survey Open-File Report 2004-1261.
- Winston, R.B., 1999. MODFLOW-Related Freeware and Shareware Resources on the Internet. *Computers & Geosciences*, 25 (4), 377-382.
- Wuolo, R.W., Dahlstrom, D.J., Fairbrother, M.D., 1995. Wellhead Protection Area Delineation Using the Analytic Element Method of Ground-Water Modeling. *Ground Water* 33 (1), 71-83.
- Yangxiao, Z., Van Geer, F.C., 1992. KALMOD, a Stochastic-Deterministic Model for Simulating Groundwater Flow with Kalman Filtering. *Hydrological Sciences Journal* 37 (4), 375-389.
- Zheng, C., 1990. MT3D, a Modular Three-Dimensional Transport Model for Simulation of Advection, Dispersion, and Chemical Reactions of Contaminants in Groundwater Systems. Report to the Kerr Environmental Research Laboratory, U.S. Environmental Protection Agency, Ada, Oklahoma.
- Zienkiewicz, O.C., 1977. The Finite Element Method. 3<sup>rd</sup> ed., McGraw-Hill, New York.
- Zimmerman, R.W., Bodvarsson, G.S., 1989. Integral Method Solution for Diffusion into a Spherical Block. *Journal of Hydrology* 111 (1-4), 213-224.

